INVESTIGATION OF DEFLECTION BASINS TO IDENTIFY STRUCTURAL DISTRESSES WITHIN FLEXIBLE PAVEMENTS

by

Michael Charles Vrtis

A dissertation submitted to the Graduate Faculty of
Auburn University
in partial fulfillment of the
requirements for the Degree of
Doctor of Philosophy

Auburn, Alabama
May 6, 2017

Approved by

David Timm, Chair, Brasfield and Gorrie Professor, Civil Engineering
Carolina Rodezno, Assistant Research Professor, National Center for Asphalt Technology
Rod Turochy, James Madison Hunnicutt Associate Professor, Civil Engineering
Randy West, Director, National Center for Asphalt Technology
April Simons, Assistant Professor, Building Science

ABSTRACT

Cracking in pavements is often considered a random phenomenon that is difficult to predict and diagnose. It would be beneficial to pavement managers to identify pavements that are likely to have cracking in the near future for planning purposes. The mode of cracking is also an important factor for road managers because the type of distress should dictate maintenance or rehabilitation decisions. The objectives of this work were to utilize falling weight deflectometer (FWD) testing to identify structural changes in flexible pavements prior to cracking and to determine the mode of cracking once cracking has occurred. These objectives were met by comparing FWD deflection basins to theoretical deflection basins of simulated distress modes created using linear-elastic analysis. FWD deflection basins on pavement structures with simulated delamination between asphalt concrete (AC) layers, top-down cracking (TDC), and bottom-up fatigue cracking (BUFC) were simulated using BISAR 3.0. The TDC and BUFC simulations were generated by lowering the AC moduli values for the cracked layers. Deflection basin parameters (DBP) were used to capture changes in the pavement structure without backcalculation. DBPs generated from the simulated cracking modes were compared to DBPs from FWD testing data from the NCAT Test Track. Each section had fixed FWD testing stations and FWD data were scrutinized for 165 unique testing locations within 19 sections. Prior to making the comparison between field and theoretical DBPs, it was essential to determine when a given FWD testing location was cracked. An investigation was conducted to determine the

distance at which a discontinuity (crack) begins to influence the deflection basin measured by the FWD. Based on the results, an FWD station was classified as cracked if cracking was observed within 1 foot on a given date. The comparison of the change in field DBPs to the theoretical change in DBPs was successful for the delamination and BUFC sections. The TDC comparison was not successfully conducted but the methodology showed promise based on a limited amount of TDC in the other sections. Seven DBPs that focused on the AC were utilized and their effectiveness was assessed. D_0 was found to be the most sensitive DBP and AREA and F_1 were the least sensitive. In summary, the assessment of DBPs from deflection basins measured at the same location over time provided the ability to predict when cracking was going to occur and if the cracking was due to an issue in the entire AC structure.

ACKNOWLEDGEMENTS

The author would like to acknowledge the assistance and support that made the completion of this work possible. The committee chair and graduate advisor, Dr. David Timm, has provided technical expertise, research direction, and mentoring – but most importantly, friendship – that has made the process of completing this work enjoyable.

The author would also like to acknowledge the work of the entire team of employees at the National Center of Asphalt Technology. The dedication to sound research practice over the last two decades created reliable databases that were used in this work.

Family and friends have provided much needed encouragement and understanding. In particular, the author's mother and sister were always available to listen and motivate. Fellow graduate students facilitated technical proofing of ideas and will hopefully be lifelong friends.

TABLE OF CONTENTS

LIST OF TABLES

LIST OF FIGURES

CHAPTER 1. INTRODUCTION

1.1 Background

Cracks are often visible on pavement surfaces and although cracked pavements are not aesthetically appealing, the effect of the cracks on the pavement structure is difficult to discern from only surface inspection. Generally speaking, cracks that initiate at the pavement surface require different maintenance strategies than cracking initiating deeper in the structure. State and local agencies are charged with assessing pavement condition to properly allocate and prioritize construction or maintenance funding.

Inaccurate structural assessment of a cracked pavement can lead to significant increases in expenses for the agency/owner and to the general public. A structurally inadequate pavement requires full-depth reconstruction to fix the structure. A structurally adequate pavement with surface cracks requires a maintenance type activity. These activities may include milling of the surface and replacing it with new asphalt concrete (AC) which is a much less costly and less time consuming option than full-depth reconstruction. However, if the pavement assessment is not correct and a maintenance-type activity is applied to a structurally inadequate pavement then the pavement will likely deteriorate quickly, wasting the maintenance activity resources, since the cause of the distress was never mitigated. This scenario would create additional expenses for the agency, which is now paying for the wasted maintenance activity and the reconstruction, and to the general public who uses the roadway by subjecting vehicles to additional wear and tear and work zone activity. Conversely, full-depth reconstruction of all pavements with visible cracking on the surface is not a financially feasible or practically necessary option. Therefore, it is

imperative for the owner/agency to be able to accurately distinguish between structurally adequate and inadequate pavements.

In addition to correctly diagnosing the nature of pavement cracking, for planning and budgeting purposes it would be beneficial for an agency to be able to identify structurally inadequate pavements prior to extensive distresses appearing at the surface. Once a pavement has lost its structural integrity, it often quickly develops surface distress that rapidly progresses to an unacceptable road surface condition forcing the owner/agency to conduct (very costly) full-depth reconstruction with limited notice. If the agency was able to identify pavements that are losing structural integrity prior to significant distresses at the surface, then the agency may be able to implement a lower cost maintenance option to mitigate the problem or at the very least be able to plan for costly reconstruction for a longer period of time.

Destructive testing and nondestructive testing (NDT) are the two primary means of assessing pavement structures in-situ. Destructive testing is done by coring or trenching the pavement to visually identify where the distress begins and determine how it is propagating through the structure. Cutting trenches in pavements requires lane closures for extended periods of time and is a hazard to the general public and the agency personnel responsible for opening the trench, assessing the distress progression, and patching the trench prior to opening the lane back to traffic. Capturing the distress progression with coring is an inexact science because the condition under the pavement surface can be impossible to discern visually. Thus, excessive cores may be taken without yielding conclusive results. Even when trenches and core-holes are carefully patched, there are still discontinuities in the structure that may further decrease the ride quality. In summary, destructive testing is time consuming, cost intensive to the roadway owner and users, can leave the pavement in worse condition, and still may not yield conclusive results.

NDT does not further deteriorate the pavement which allows for a faster speed of testing resulting in less impact to roadway users, reduced safety burden to the owner, and a broader amount of the pavement network that can be covered due to the savings of time and money. The most widely implemented NDT technology for structural assessment is based on surface deflection measurement. Analysis of surface deflections generated from a dynamic load device, commonly the falling weight deflectometer (FWD), has become a useful tool for pavement engineers. Recent research has focused on utilizing other NDT techniques to identify structural conditions of pavements but the technologies are still currently in a developmental stage and have only been implemented on a limited basis (Heitzman et al., 2013). The other NDT technologies currently being investigated for structural assessment fall into the following categories: ground penetrating radar, infrared imaging, and mechanical wave from impact.

The FWD is a NDT tool that is used by many agencies to assess in-situ structural characteristics of pavements. The FWD, shown in Figure 1.1, operates by dropping a weight onto a rubber plate placed on the pavement surface and measuring the subsequent deflections of the pavement with sensors at various distances away from the drop. It is able to accurately replicate the loading from a moving vehicle wheel in magnitude and duration (Huang, 2004). The load level of an FWD drop is a result of the height at which the weight is dropped (i.e., greater drop height results in higher load level). Figure 1.2 schematically shows an FWD setup with nine sensors (D_0 through D_8) at increasing distances away from the center of the load plate. The term "deflection basin" is generally used to describe the deformed area measured by the sensors.

Figure 1.1 – Dynatest Model 8000 FWD.

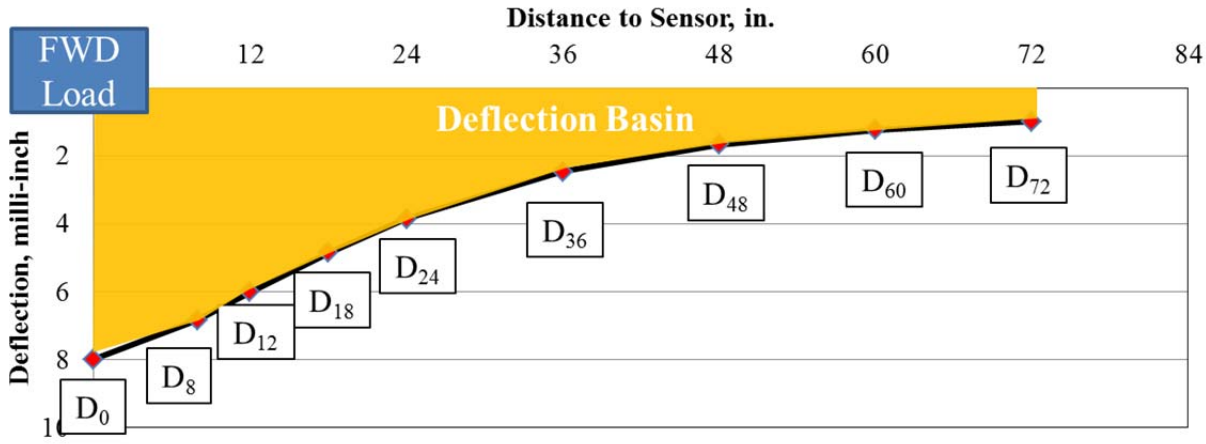

Figure 1.2 – FWD testing schematic.

The resulting deflection basin from an FWD drop is sensitive to the load level, climate (temperature and moisture), and pavement structure/ condition. The spatial variability of pavement structures, or how the structure changes over the distance of a roadway section even when built with the same design, also impacts the resulting deflection basin. Therefore, these factors must be carefully considered when analyzing deflection basins for pavement condition.

FWD-generated deflection basins are commonly used to determine the modulus of each pavement layer through a process known as backcalculation. Given the thickness of each layer in

the pavement structure, a predicted deflection basin is generated using mechanistic modeling and compared to the measured FWD deflection basin. The modulus value of each layer is adjusted during an iterative process until the measured and modeled deflection basins match with reasonable agreement. Numerous computer programs and backcalculation procedures, of varying complexity, have been developed but unreasonable modulus values may still be obtained. A unique solution is not determined in the backcalculation process (i.e., the same deflection basin can be backcalculated to give differing moduli, even with the same computer program (Huang 2004)). Thus, the backcalculated output must be scrutinized for reasonableness.

FWDs are often utilized by agencies to assess pavement structural integrity on a network level and at a project level for overlay design. As a pavement structure deteriorates over time, the deflection basin measured by the FWD will change (Kim, 2001). Although copious research has been conducted on deflection basin analysis and backcalculation, there is still a need to better understand how the measured deflection basin changes as a pavement structure deteriorates, especially prior to distress being visible at the surface. A better understanding of the changes that occur in deflection basins as distresses develop, will allow pavement engineers to diagnose the type of distress that is occurring and then plan maintenance or rehabilitation activities accordingly.

The National Center for Asphalt Technology (NCAT) has a large database of FWD testing results that have been conducted on the same location in full-scale pavement sections subjected to well-documented levels of heavy-vehicle traffic at the NCAT Test Track. Additionally, surface distresses of the sections were closely monitored and recorded. These databases provide a unique opportunity to further investigate deflection basins at a single location in an effort to capture changes in the basin as various distress mechanisms occur within

the pavement structure. Investigating these datasets can lead to the ability to identify the changes in structural response due to different distress mechanisms.

1.2 Objective and Scope of Work

The objectives of this research were to utilize FWD data to identify structural distresses within the AC layers prior to the cracking being visible on the pavement surface and to determine the cracking mechanism once cracking was visible. These objectives were met by comparing FWD data taken from the same location over time with detailed pavement surface distress records from pavement sections with documented layer delamination, bottom-up fatigue cracking (BUFC), and top-down cracking (TDC) failures. A variety of sections were assessed that contain differing rates of distress progression, pavement thicknesses, and failure locations within the pavement structure.

Prior to being able to compare the FWD data with pavement distress at specific locations, it was necessary to determine the distance at which discontinuities (i.e., cracks) begin to influence the FWD deflections with a field investigation. This was done by running a series of FWD tests at different distances away from a vertical, saw-cut discontinuity in the pavement. The results were used throughout this study as a guide to determine when a FWD testing location should be considered “cracked”.

1.3 Organization of Dissertation

This dissertation is organized into seven chapters. Chapter 2 presents a literature review that introduces the cracking mechanisms investigated in this work and discusses studies that have

evaluated the impact of these mechanisms on FWD deflection basins. Chapter 3 outlines the methodology followed in this work to identify changes in the pavement structure that result from cracking. Chapter 3 also presents a sub-investigation that was conducted to determine the distance at which a discontinuity begins to impact the measured FWD deflection basin. Chapter 4 discusses the results from sections that had AC layer delamination. Chapter 5 presents the results from the TDC sections and Chapter 6 presents the results from the BUFC sections. Finally, Chapter 7 summaries the results and provides recommendations.

CHAPTER 2. LITERATURE REVIEW

A thorough literature review was conducted to gather work that has been done on the characterization of deflection basins of distressed pavements. The following literature review summarizes the development of deflection basin parameters (DBP) to characterize the AC, studies that examined DBPs on distressed pavements, and theoretical modeling of FWD testing on distressed pavements. A brief summary of the mechanism behind each distress type investigated is also provided.

2.1 Cracking Mechanisms Assessed

This section will briefly discuss the three cracking mechanisms (BUFC, TDC, and delamination) targeted in this research. The purpose of this section is to provide background for the simulations used in this work and is not intended to be a comprehensive discussion of cracking mechanisms.

2.1.1 BUFC

BUFC, also known as alligator cracking, is a result of repeated traffic loadings that generate tensile stress and strain at the bottom of the AC layer. A schematic of this is shown in Figure 2.1. The cracking originates at the bottom of the AC where the tensile responses are the highest and then propagates towards the surface. The high tensile responses are often a result of heavy-vehicle axle loads on the pavement structure and are exacerbated by saturation of the underlying granular layers (Brown et al., 2009). Since BUFC is a result of repeated traffic loading, it is commonly observed in the wheelpaths. An example of BUFC on a pavement surface is presented in Figure 2.2. For this work, it is important to recognize that BUFC initiates

at the bottom of the AC layers and propagates through the AC to the pavement surface. Thus, at the time cracking is observed on the surface the entire AC structure has been affected.

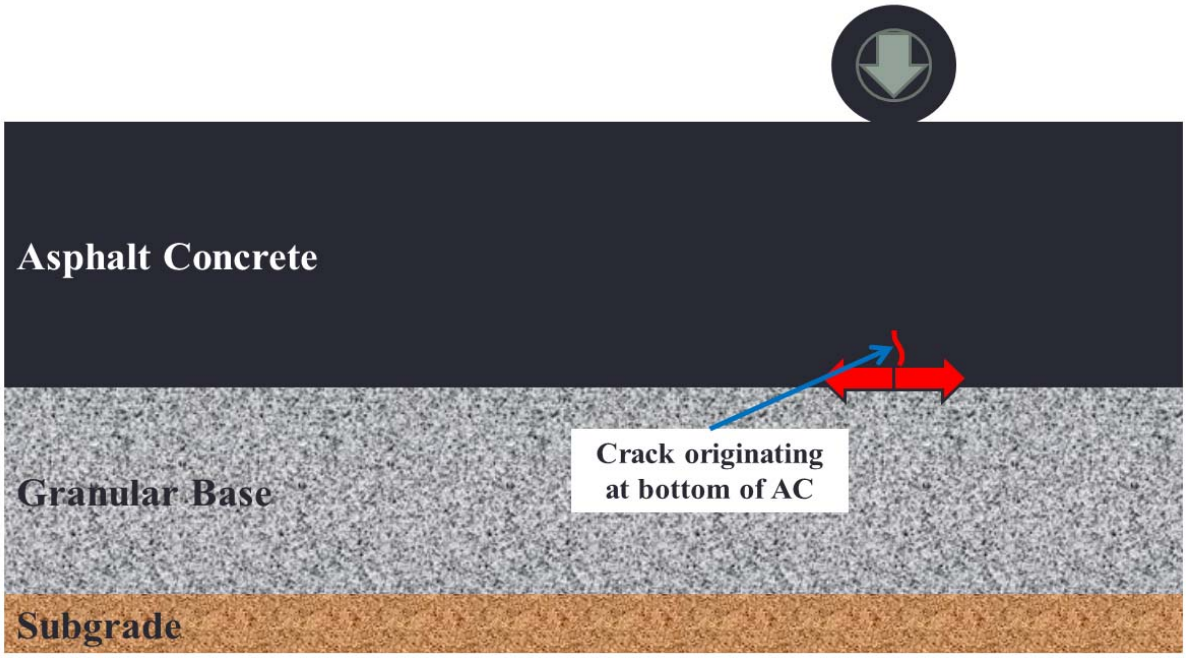

Figure 2.1 – BUFC diagram.

Figure 2.2 – BUFC example.

2.1.2 TDC

The mechanisms behind TDC are not as well understood as BUFC. TDC is a topic that has gained national interest in the United States and there are currently several ongoing research projects aimed at enhancing the understanding of TDC (Moore, 2016; NCHRP 1-52). What is referred to as TDC in this work is also called "near-surface cracking" by some researchers. There is still debate regarding the mechanisms of TDC, but like BUFC, TDC is a result of repeated traffic loading and occurs in, or at the edges of, the wheelpaths of flexible pavements. TDC often results in longitudinal cracks at the edge of the wheelpaths and this type of TDC is believed to be a result of the peak shear stress that occurs at the edge of a tire, as shown in Figure 2.3. However, there have also been documented cases of cracks in the transverse direction that were found to be top-down in nature. Another mechanism that is believed to result in TDC is high tensile strains that occur at the edge of the deflection basin created under a tire load, as shown in Figure 2.4 (Wang et al.2003). The important characteristic of TDC for this work is that the cracking is initially located near the surface while the majority of the pavement structure is still intact.

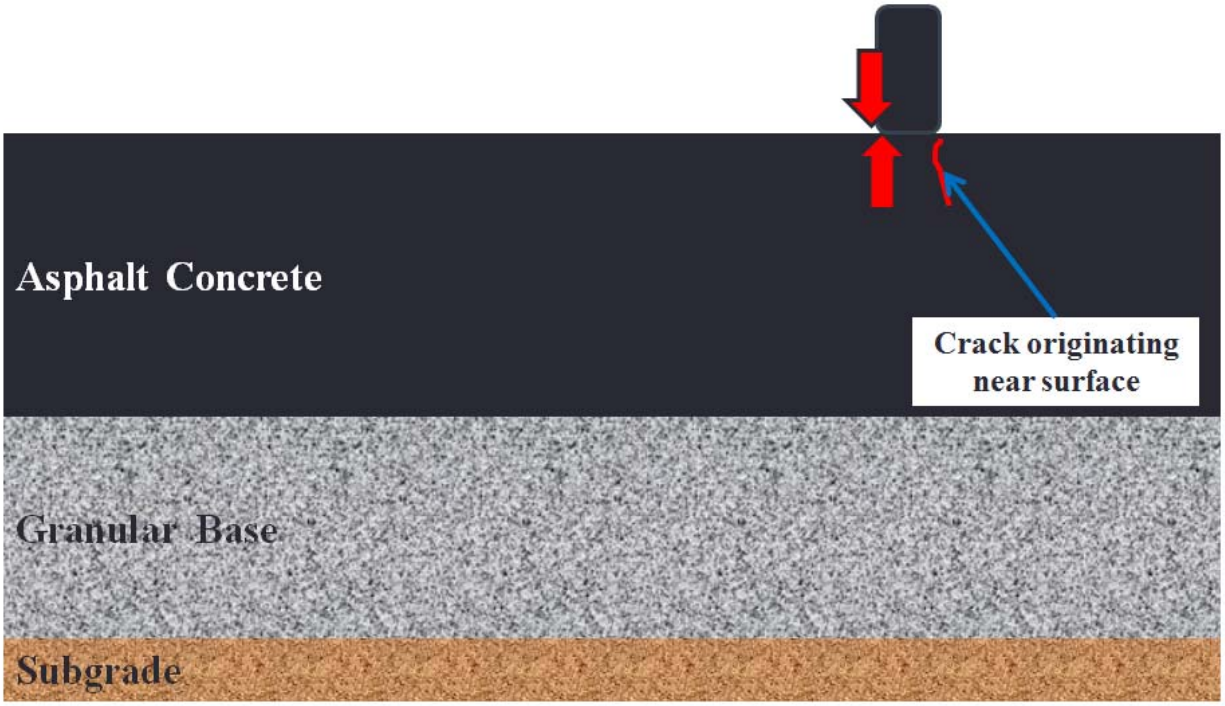

Figure 2.3 – TDC diagram with cracking due to shear stress at edge of tire.

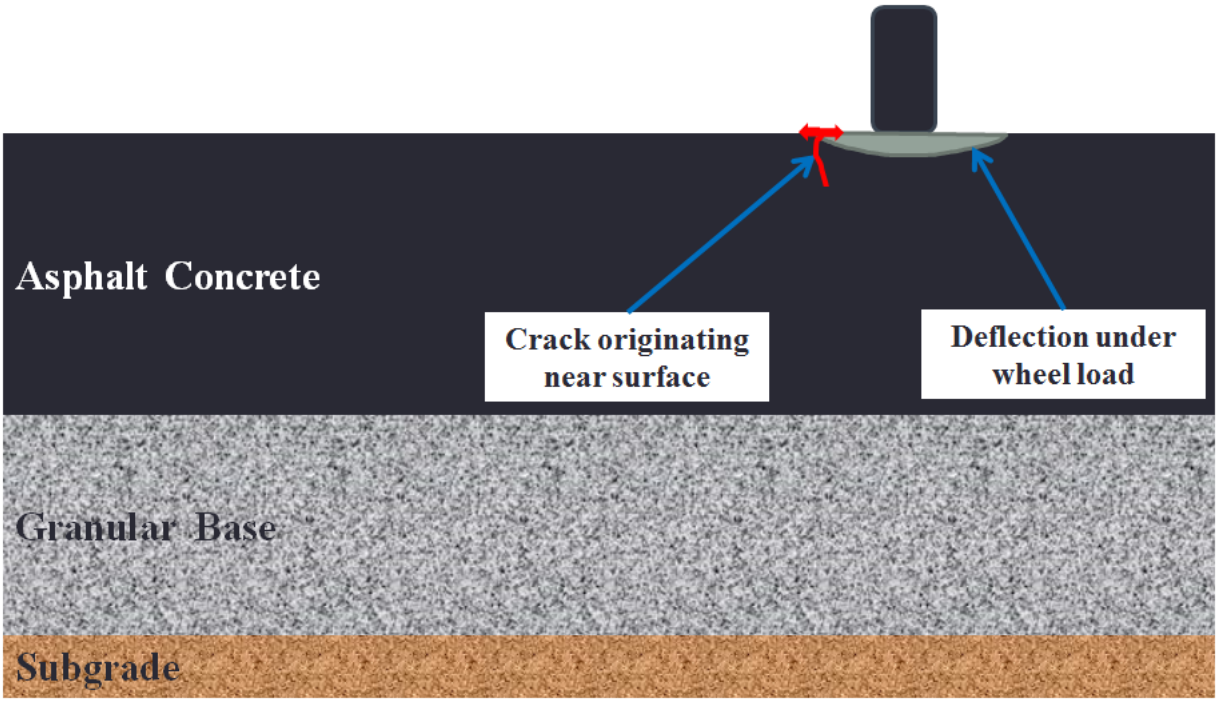

Figure 2.4 – TDC diagram with cracking due to tensile strain at surface.

2.1.3 Delamination

Delamination is a result of shear and tensile forces at the interfaces between AC layers (Mohammad et al. 2012). A schematic of these forces, along with a crack originating from the delamination location, is shown in Figure 2.5. After layer delamination occurs, the pavement layers begin to behave independently instead of acting as a single structure. Delamination often results in rapid failure and requires complete removal of the delaminated layer. If the surface layer is delaminated, tearing and "crescent" shaped cracking is visible on the pavement surface (Brown et al., 2009). In Figure 2.6, it can be seen that the top of the "crescent" is pointing in the direction of traffic. When delamination occurs at AC layer interfaces lower in the structure, the cracking visible on the surface often appears more like fatigue cracking because fatigue cracking is occurring at the bottom of the layer directly above the delaminated interface due to excessive bending under wheel loads.

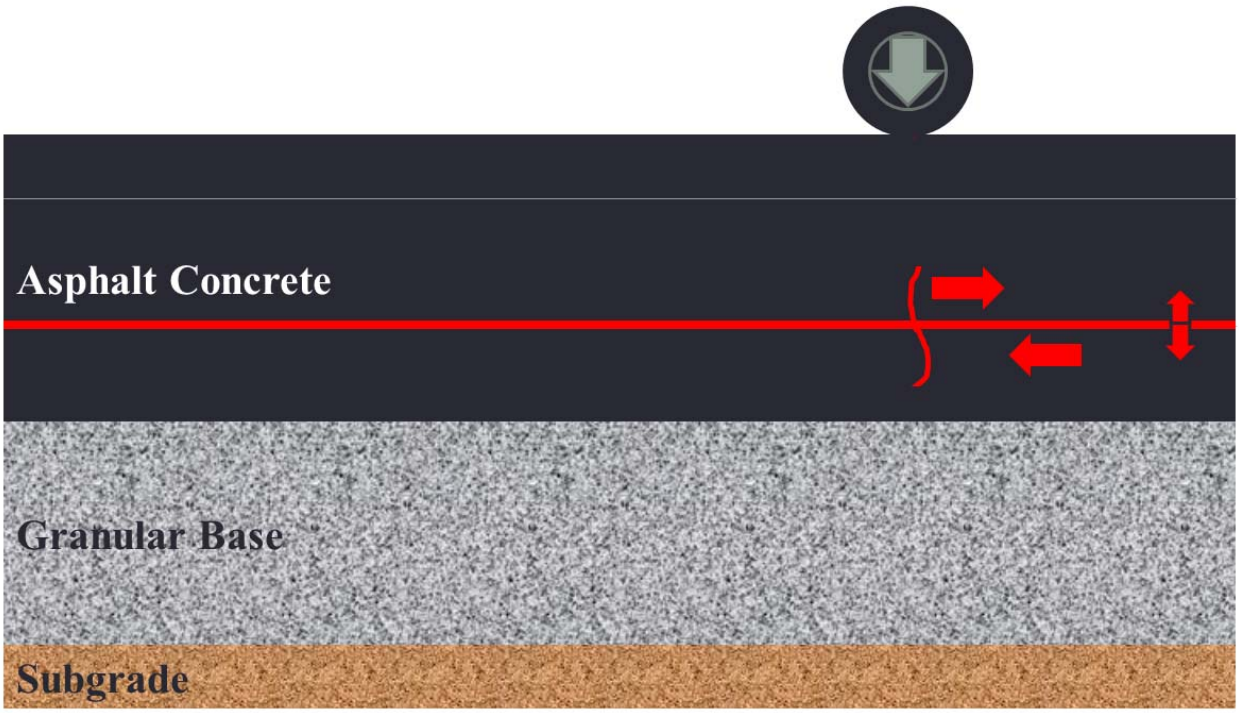

Figure 2.5 – Delamination diagram.

Figure 2.6 – Crescent shaped cracking resulting from delamination of the surface layer.

2.2 Deflection Basin Parameters

Researchers have identified DBPs to characterize FWD deflection basins without directly backcalculating layer moduli. Most researchers have used regression equations to relate DBPs to pavement layer moduli or stress/strain responses at critical locations in the pavement structure (e.g., horizontal strain at the bottom of the AC or vertical stress at the top of the subgrade), to calculate the remaining life of the pavement.

Generally speaking, the deflections measured by sensors closer to the center of the load plate are attributed to the response of the entire pavement structure (AC, base, and subgrade).

Figure 2.7 shows the stress zones under the FWD load plate for each layer in a typical pavement structure (Huang, 2013). The FWD sensors measure the response of the layers with stress zones directly underneath the sensor. Thus, sensors 4 and 5 in Figure 2.7 are only sensitive to the subgrade layer. Therefore DBPs that only consider responses further away from the center of the load are not impacted by distress changes within the AC. This literature review will focus on the development of DBPs that pertain to assessing the entire pavement structure and on studies that investigated FWD deflection basins, both modeled and measured, from pavements with distress.

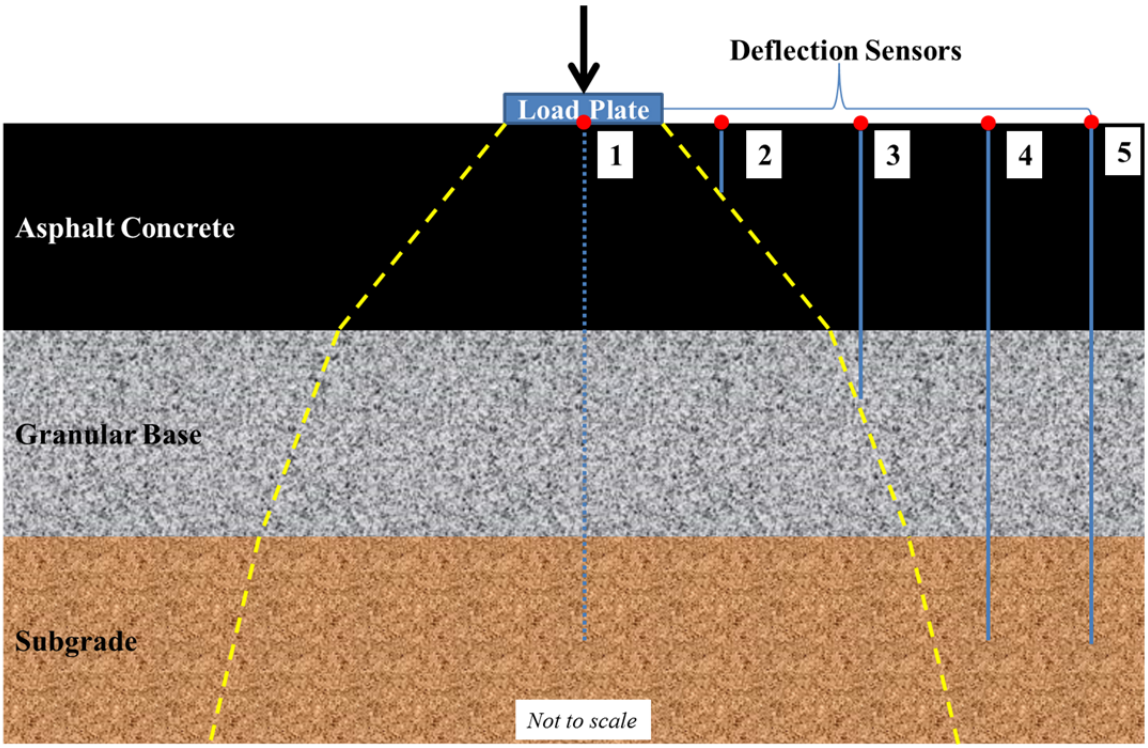

Figure 2.7 – Sensor distance versus response (adapted from Huang, 2004)

Many DBPs were developed prior to the development of the FWD for use with devices such as the Benkelman Beam, Road Rater (RR), or Dynaflect (Hossain and Zaniewski, 1991). The Benkelman Beam was one of the earliest deflection measuring devices and utilized a

measuring probe attached to a 96 inch long support beam for a reference point. Figure 2.8 shows its use during the AASHO Road Test in 1958 (Highway Research Board, 1962). The probe is placed between rear dual-tires of a truck with a back axle weight of 18 kip. The truck slowly drives away and deflection readings are recorded when the truck is at set distances from the measuring probe. The RR and Dynaflect are pictured in Figures 2.9 and 2.10, respectively. They are steady-state vibration devices which apply a sinusoidal dynamic force to the pavement and use accelerometers to measure the resulting deflections at set distance away from the load (Huang, 2004). Although the techniques to generate or measure the deflection basins evolved into the FWD, the DBPs used to evaluate the deflections are still useful.

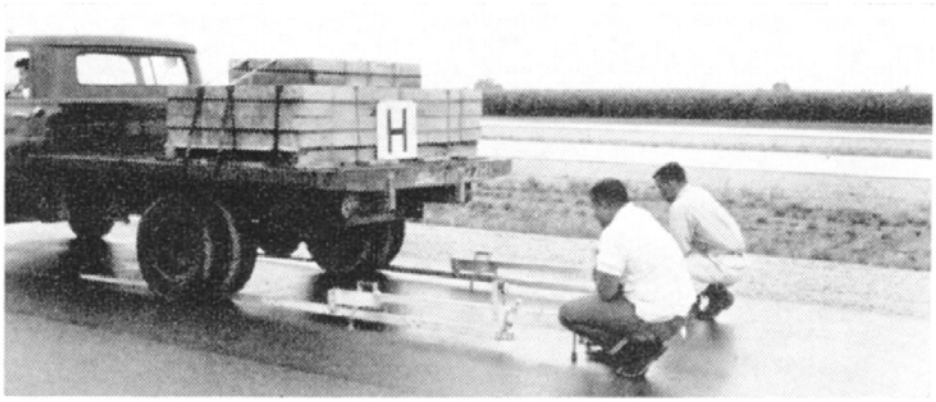

Figure 2.8 – Benkelman Beam being used at AASHO Road Test (Highway Research Board, 1962).

Figure 2.9 – Dynaflect (Rijkswaterstaat, 2017).

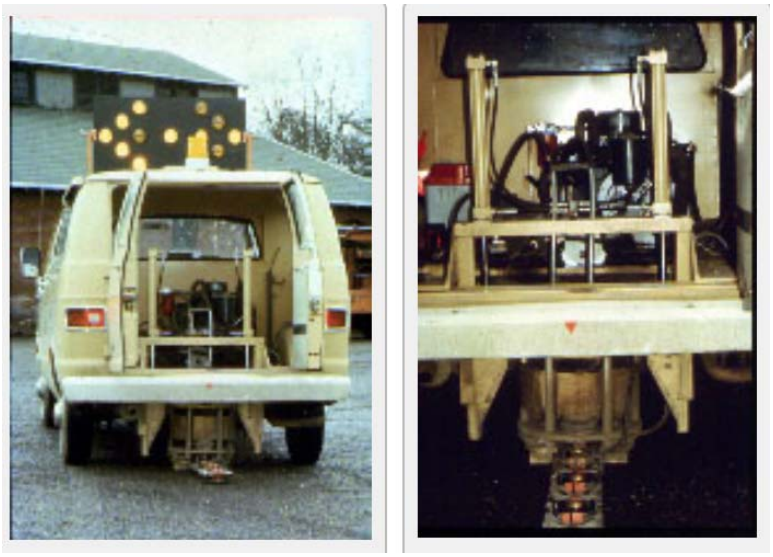

Figure 2.10 – Road Rater (Pavement Interactive, 2017).

The Surface Curvature Index (SCI) was one of the earliest used DBPs as it is simply the difference between the maximum deflection (D_0) and the deflection at a given distance (i) away from the maximum (D_i), as shown in Equation 1. The deflection at 12 inches away from the center of the load (D_{12}) is the most common SCI found in the literature. A lower SCI value

indicates a higher overall pavement stiffness because there is less change over the distance between sensors, thus a stiffer structure.

$$SCI_i = D_0 - D_i \quad [1]$$

where: D_0 = center plate maximum deflection (milli-inch)

D_i = deflection at i distance away from D_0 (milli-inch)

Hoffman and Thompson (1982) were the first to introduce the AREA parameter in a paper describing a non-linear backcalculation procedure. Prior to discussing the backcalculation procedure, deflections, AREA, and other DBPs called shape factors (F_1 and F_2), were used to correlate deflection basins obtained from a RR to FWD deflections. Table 2.1 presents the results of this correlation and shows that deflections closer to the center of the load had the best agreement along with AREA and F_1 parameters, thus providing the most confidence in relating the results from the two devices. The parameters A and B in Table 2.1 are regression coefficients used to correlate the responses and parameters from the RR to FWD.

The AREA parameter assesses the structure by using pavement responses located within 3 feet of the center of the load. As shown in Equation 2, the deflections are normalized back to the center plate deflection (D_0). Theoretically, the AREA can range from 11 to 36, with a stiffer pavement having a higher AREA value. AREA is a measure of the relative stiffness of the upper layer (AC) to the subgrade stiffness. Thus, a softer subgrade or stiffer pavement will increase the parameter. The equations for F_1 and F_2 are shown in Equations 3 and 4, respectively. They also consider deflections measured within 3 feet of the center of the load plate.

Table 2.1 – Correlation between FWD and RR (adapted from Hoffman and Thompson, 1982).

FWD Variable	A	B	R^2	SEE	Mean FWD Value	Mean RR Value
D_0 (mils)	-3.4	1.21	0.94	3.23	24.19	22.85
D_1 (mils)	1.68	0.72	0.92	1.13	12.24	14.62
D_2 (mils)	3.98	0.27	0.54	0.64	6.57	9.71
D_3 (mils)	2.69	0.25	0.48	0.55	4.56	7.52
AREA (in)	-7.59	1.19	0.95	1.14	18.88	22.17
F_1	-0.15	1.73	0.93	0.19	1.29	0.84
F_2	0.03	1.57	0.72	0.26	1.16	0.72

$$AREA = 6(1 + (2\frac{D_{12}}{D_0}) + (2\frac{D_{24}}{D_0}) + \frac{D_{36}}{D_0}) \quad [2]$$

where: D_{12} = deflection measured at 12 inches from load (milli-inch)

D_{24} = deflection measured at 24 inches from load (milli-inch)

D_{36} = deflection measured at 36 inches from load (milli-inch)

$$F_1 = \frac{D_0 - D_{24}}{D_{12}} \quad [3]$$

$$F_2 = \frac{D_{12} - D_{36}}{D_{24}} \quad [4]$$

In a South African study, Horak (1987) analyzed the change of DBPs with loading on four pavement sections by a heavy vehicle simulator. The research summarized commonly used DBPs that were found to be significant. This study developed relationships between DBPs and critical strain values as an alternative to backcalculation of layer modulus and as a verification of the South African design procedure. Regression equations were developed relating the horizontal

strain at the bottom of the AC to several DBPs for flexible pavements with coefficients of correlation (R^2) above 92%. The DBPs that relate directly to the AC identified to be significant by Horak were: AREA, F_1, F_2, and SCI.

Research at the University of Illinois developed the Area Under Pavement Profile (AUPP) parameter. As shown in Equation 5, the deflections within 3 feet of the load center are considered in this parameter. A lower AUPP value represents a higher stiffness pavement. Thompson and Garg (1997) developed a relationship between AUPP and the horizontal tensile strain at the bottom of the AC from FWD data and strain gauge responses at MnROAD.

$$AUPP = \frac{5D_0 - 2D_{12} - 2D_{24} - D_{36}}{2} \quad [5]$$

2.3 Deflection Basins and Pavement Distress

As the FWD was utilized more frequently, researchers had to address the issue of distressed pavements. As distresses occur within the pavement structure, such as cracking, rutting, or stripping, the fundamental assumption of layered elastic continuous homogeneity is violated. This problem has been addressed in various manners that are discussed in this section.

Surface deflections measured by the FWD will theoretically decrease as the distance from the FWD load is increased. If the deflection at a sensor is greater than the deflection at a sensor closer to the load, then there is a violation of linear-elastic theory and likely a discontinuity, testing error, or a shallow depth to a stiff bedrock layer. This theory has been applied by several researchers to identify discontinuities and erroneous data. Jung and Stolle (1992) used the effective surface modulus and the effective subgrade modulus calculated at

increasing distances away from the load to identify pavements with cracked or broken AC. As shown in Figure 2.7, sensors located further away from the center of the load are impacted by less of the pavement structure whereas the centermost deflection is a composite response from the entire pavement structure. Thus, the highest surface modulus should be directly under the FWD load plate (unless a shallow stiff layer is present, then the outermost sensor will have the greatest surface modulus). Figure 2.11 (a) shows that as the distance from the load increases the effective surface modulus will initially drop to a minimum value and then begin to steadily increase at greater distances from the load, called "tail modulus" by the authors. This tail modulus was not apparent in linear-elastic simulations but was explained to be a result of faster dissipation of deflection values in field data than in linear-elastic simulations (smaller than expected deflection values lead to higher effective moduli). For a cracked pavement section, shown in Figure 11 (b), there is not a steady increase in the tail modulus values, thus indicating cracking. This concept was incorporated into a computer program, PROBE, to determine the effective surface and subgrade moduli while accurately characterizing the pavement condition.

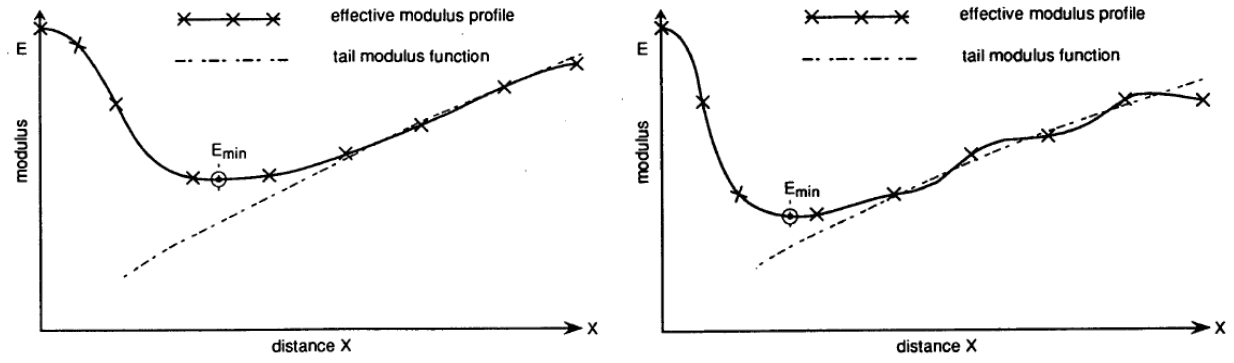

(a) **(b)**

Figure 2.11 – Surface modulus at various distances from load for intact (a) and cracked (b) AC pavements (Jung and Stolle, 1992).

The change in deflection basins generated from a Heavy Weight Deflectometer on pavement sections at the Federal Aviation Administration's National Airport Pavement Test Facility was investigated by Gopalakrishnan and Thompson (2005). The study identified trends in the DBPs with respect to accelerated loading and rut depths. Table 2.2 presents the percent change in DBPs after one inch of rutting (N_1) was measured on various pavement cross-sections. The four pavement cross-sections were comprised of the same AC surface over asphalt stabilized and granular base layers over medium and low strength subgrades, as shown in Figure 2.12. B777 and B747 represent the type of aircraft axle simulated by the accelerated loading. In the table, it can be seen that SCI and AUPP parameters were the most sensitive to rutting and the AREA parameter was the least sensitive.

Table 2.2 – Change in DBPs after 1 inch of Rut Depth (adapted from Gopalakrishnan and Thompson, 2005)

DBP	% Change in DBP from N_0 to $N_{1.0}$							
	MFC		LFC		MFS		LFS	
	B777	B747	B777	B747	B777	B747	B777	B747
AREA	2	5	5	6	-	3	3	3
ISM	20	41	32	36	-	19	25	24
SCI	13	39	37	45	-	25	29	24
AUPP	30	87	61	71	-	40	57	51

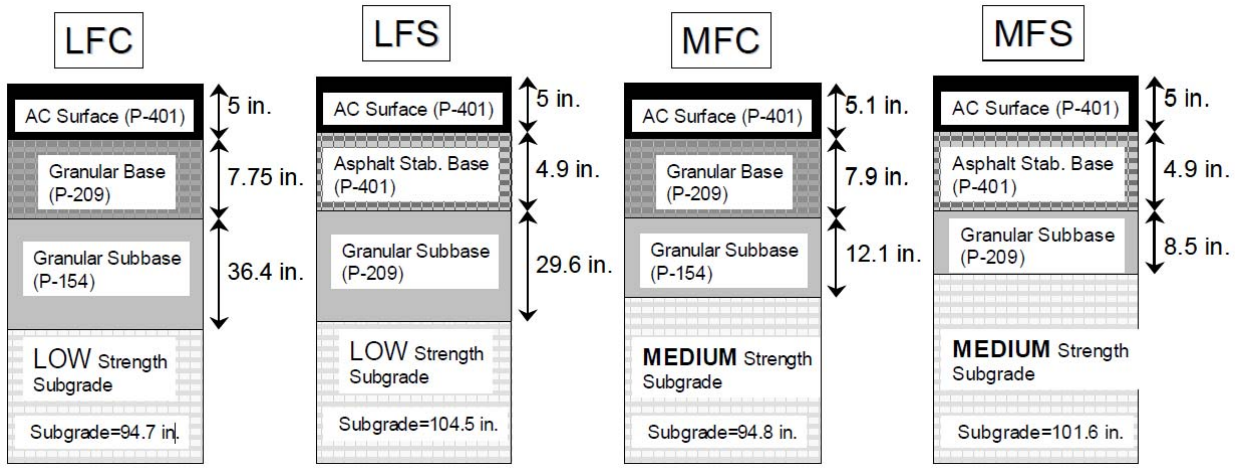

Figure 2.12 – Cross-sections considered by Gopalakrishnan and Thompson (2005).

Significant research, with objectives similar to this dissertation, was conducted at North Carolina State University and was published in several reports (Kim et al., 1999; Kim et al., 2000; Xu et al., 2002 (a); Xu et al., 2002 (b); Xu et al., 2002 (c); Park and Kim, 2003). In this literature review, these reports have been compiled into a single discussion based on the best interpretation of research conducted and therefore are not discussed individually or presented in order of publication date. These works document the development and application of a methodology to estimate pavement layer moduli and layer conditions from dynamic FWD data, without backcalculation. The work culminated in the development of a computer program, APLCAP (Asphalt Pavement Layer Condition Assessment Program). This was accomplished by generating synthetic FWD deflection basins using finite element (FE) modeling of flexible pavements with various combinations of layer moduli, thicknesses, and distress conditions. Analysis of the synthetic deflection database and a limited number of "high quality" field sections led to the identification of "layer condition indicators" that were linked (with regression

equations and artificial neural networks (ANN)) to FWD deflections. Thus, measured deflections could be input into APLCAP and layer moduli and condition would be output.

FE analysis was conducted using ABAQUS software to generate the synthetic deflection basins. Full depth AC pavements (AC over subgrade), aggregate base pavements (AC over aggregate base over subgrade), cement treated base (CTB) pavements (AC over cement treated base over subgrade), and rubblized concrete base pavements (AC over rubblized concrete base over subgrade) were included in the study. In total, 34,000 synthetic deflection basins were created using linear-elastic material models and 10,000 deflection basins were created using non-linear-elastic models. In each simulation, a 9,000 lb. dynamic FWD load was applied and the resulting deflections and critical stress/strain responses were examined. A wide range of typical layer moduli and thicknesses were simulated and the sensitivity of DBPs to these inputs was reported. The percent change of each DBP as the thickness or modulus was independently varied is shown in Table 2.3. It can be seen that SCI and AUPP were found to be the most significant parameters analyzed for changes in the AC modulus and they were also found to be significant for changes in the thickness of the AC. It should be noted that the percentages of change presented in Table 2.3 are very large due to the large range of inputs used (AC modulus 345 – 17,230 MPa; AC thickness 100 mm to 650 mm). Several new DBPs were presented in the report, including a new shape factor and additional area indices; however, they are not presented here because they were not reported to be significant for changes in the AC.

Table 2.3 – DBP Sensitivity to AC Modulus of Flexible Pavements over a Granular Base (Xu et al., 2002 (a))

E_{AC}		H_{AC}	
DBP	**% Change**	**DBP**	**% Change**
SCI	859	BDI	296
AUPP	598	AUPP	256
F_1	271	SCI	252
BDI	248	BDI	177
D_0	209	D_0	122

Discontinuities in the AC from cracking or stripping were also investigated in the FE simulations. Bottom-up cracking was simulated in a FE model by using interface elements to represent cracks in the AC. Simulations were conducted with cracks 152 mm apart and cracks propagating through 75% and 50% of the AC, as shown in Figure 2.13. Stripping was also considered in separate FE models with extents shown in Figure 2.13. The stripped portion of the AC was represented by using a reduced elastic modulus; however, the amount of modulus reduction was not reported (which would have been of particular interest to the modeling conducted in this research). The distressed pavement simulations were compared to intact pavement simulations and the changes in deflection basins due to the simulated distress were investigated but the sensitivity of individual DBPs to simulated distress was not reported (as it was for change in moduli or thickness).

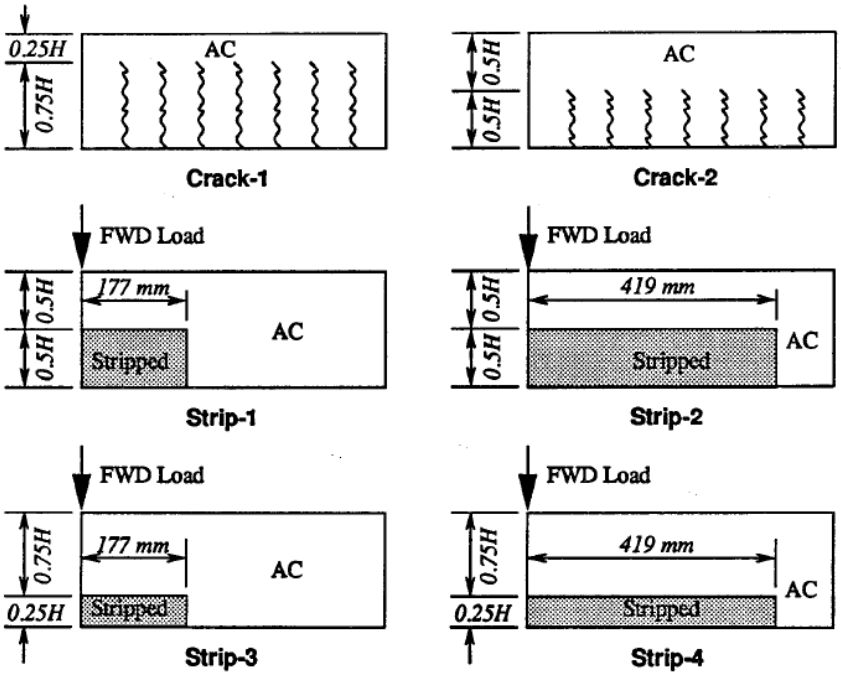

Figure 2.13 – Distress conditions considered in FE modeling (Kim et al., 1999).

High quality field FWD and performance data were used in development of the methodology. The high quality dataset provided by state agencies was reported to be much smaller than anticipated. Field FWD and performance data from the DataPave 2.0 database (from Long Term Pavement Performance (LTPP)) were used only for validation of methodology. Cracking, stripping, and debonding of the AC layers were examined (no simulations of debonding were documented) in the analysis of field measured deflections basins.

Cracking and stripping in the AC were examined by comparing intact to distressed FWD measurements. This was done by using the deflection basins measured from the intact condition to estimate the AC modulus over a range of temperatures. However, the lack of mid-depth pavement temperatures was cited as a reason for "prohibiting a more meaningful comparison" (Kim et al. 2000) on this concept.

Delamination of the AC layers was reported to be difficult to determine for all pavement types examined. This was attributed to larger deflections observed at outer sensors which could be mistakenly attributed to lower subgrade strength. According to Kim et al. (2000) "A single FWD load measurement, therefore, is not sufficient to distinguish between a debonded pavement and an intact pavement with lower subgrade strength." This concept was demonstrated on a limited basis from field data for an aggregate base pavement and the authors emphasized the need to use DBPs sensitive to the lower pavement layers, such as the Base Condition Index (BCI) show in Equation 6.

$$BCI_i = D_{24} - D_{36} \quad [6]$$

The analysis of pavement sections from North Carolina (especially U.S. 421) was documented in greater detail and is worthy of further discussion because it documents some of the challenges encountered working with field data. The distress in the North Carolina sections was characterized based on surface inspection and core logs. Pavement sections were reported as intact, mildly cracked, or severely cracked; however, it is unclear exactly how these classifications were distinguished. Within each pavement section, 10 equally spaced (30.5 m) FWD stations were established for testing but according to Kim et al. 1999 "... a significant station-to-station variation was observed for most cases." Figure 2.14 shows temperature corrected deflection basins measured within a 305 m pavement section (i.e., pavement with the same materials and design thicknesses). The deflections presented in Figure 2.14 are from a target load level of 9,000 lbs. and have been normalized for load by dividing the recorded deflection by the measured load level. Cores taken at each FWD station also showed large

variability within sections but core logs were unable to explain the variation in deflection basins (i.e., the distress level found in the core logs did not match expected FWD deflections for distressed or intact pavements.) The authors indicated that these discrepancies may be attributed to mixture deficiencies such as high asphalt content or low density in the AC layer.

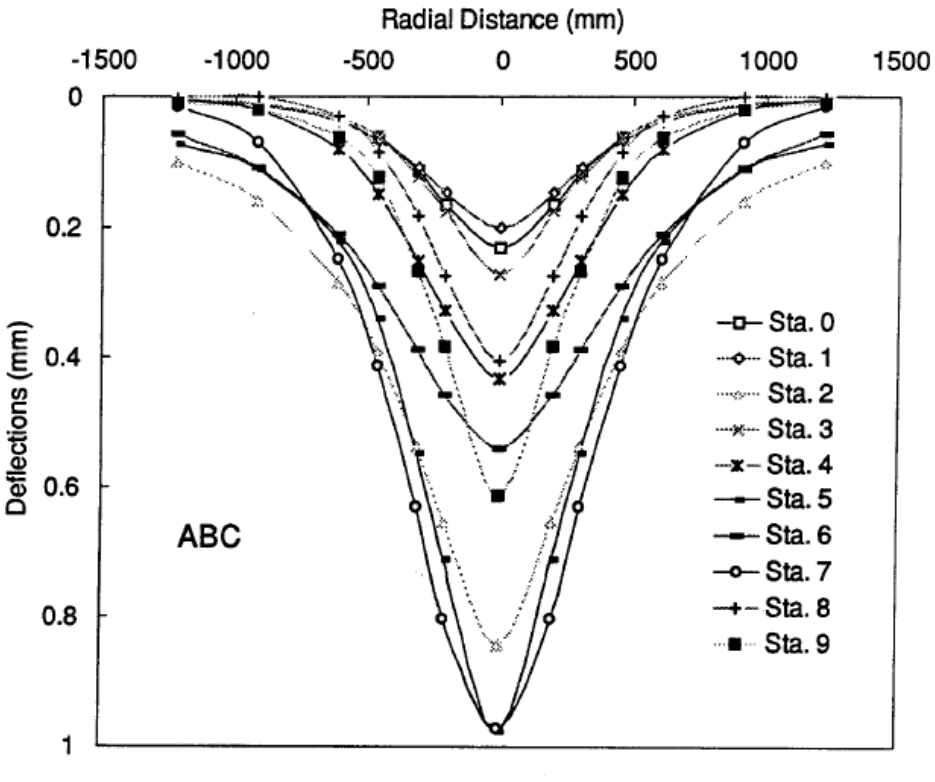

Figure 2.14 – Deflection basin variability within section (Kim et al., 1999).

Due to the variability of the field measured deflection basins, the authors were unable to "extract any definitive correlation" with distress types (Kim et al., 1999). The authors were able to generalize distress conditions for a few sections and reported "representative" deflection basins for different distress types. According to Kim et al. (1999), this was done by "... carefully sorting out the common trends between deflection basins from intact and distressed pavements."

Despite the lack of quantitative statistical analysis used to determine the representative deflection basins, the reported impact of distress types on flexible pavements is noteworthy. Figure 2.15 shows the effect of distress types on deflection basins from a flexible pavement over an aggregate base. It can be seen that the general shape of the deflection basin remained the same between intact and stripped deflection basins but the magnitude of deflection at all sensors increased in the stripped section. The cracked sections resulted in deflection basins that are narrower in shape with large center deflections.

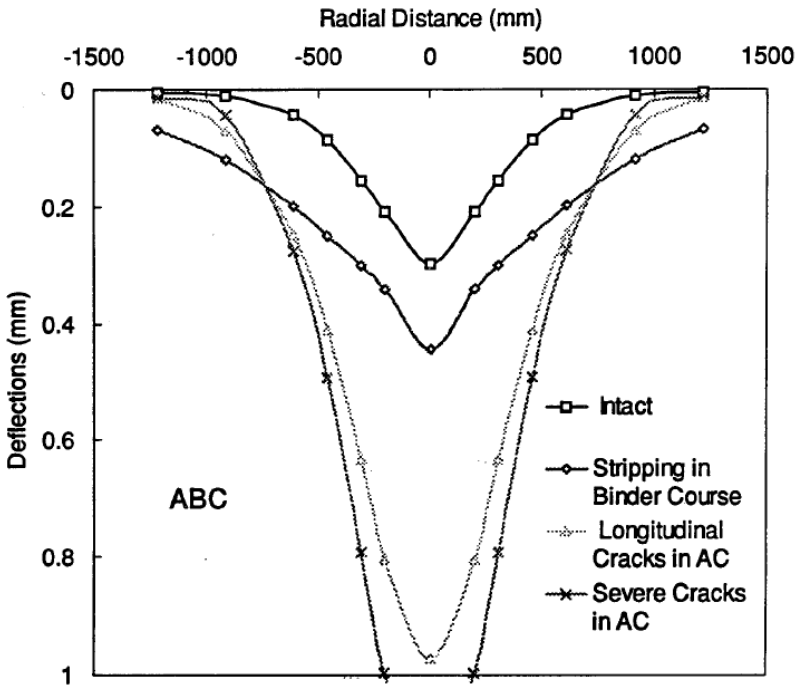

Figure 2.15 – Deflection basins with distress (Kim et al. 1999).

The relationship between AUPP/ BDI and the tensile strain at the bottom of the asphalt layer was estimated with a regression equation (Park and Kim, 2003). Strain levels at the bottom of the AC and were correlated to area of fatigue cracking (FC) based on MnROAD test sections.

This procedure was validated for FC and rutting using LTPP data. It was found that after the precipitation level at the LTPP sites was included in the FC model, the predicted cracking values showed agreement with the LTPP sites in the wet-no freeze region but under predicted cracking in the wet-freeze region, as shown in Figure 2.16. This discrepancy was attributed to low-temperature cracking and spring thaw conditions in the wet-freeze region. Cracking levels from the LTPP sites are reported as total area with FC and there is no indication of whether the FWD testing was conducted on locations with visible surface cracking. The frequency of the FWD testing was irregular and varies between sites but it is estimated from the figures presented that FWD testing was done several times a year at most and as low as once every four years.

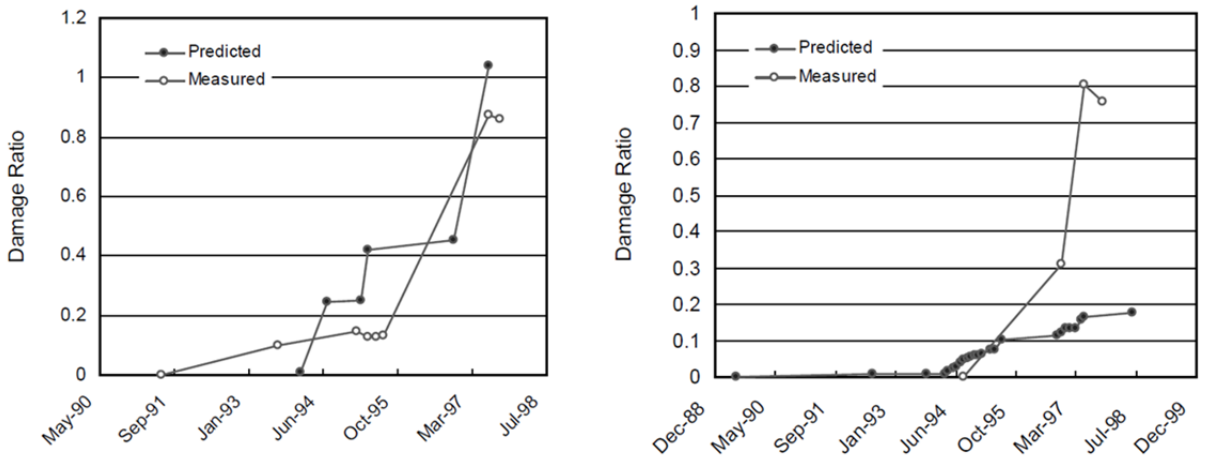

(a) **(b)**

Figure 2.16 – Predicted and measured fatigue cracking from sites (a) in wet- no freeze region and (b) wet – freeze region (Park and Kim, 2003)

Based on this work, the APLCAP computer program was developed. The steps incorporated into APLCAP include prescreening of deflections for abnormalities, prediction and adjustment of condition indicators, and layer condition evaluation based on adjusted condition

indicators. The basic methodology will be presented here for a full-depth AC pavement. The methodology is similar for other flexible pavement types considered but requires additional steps to determine the base layer properties.

Prescreening of field FWD deflections was recommended to identify severe pavement discontinuities in the pavement. This was done by ensuring a monotonic decrease in deflections and effective surface modulus with distance from the FWD load (Kim et al., 2000). As discussed previously, the magnitude of the surface deflection should decrease with distance from the center of the load. If the deflection measured by a sensor is greater than the previous sensor (closer to load) it is an indication of a severe discontinuity in the pavement, a shallow depth to bedrock, or an error in the testing setup. Similarly, if the peak effective surface modulus is located in the middle of the deflection basin then a severe discontinuity exists.

After prescreening, condition indicators were used to determine properties of each layer. The development of condition indicators for AC was documented in Kim et al. (2000) and Xu et al. (2002 (a)). Condition indicators for the subgrade were F_2 and the Base Damage Index (BDI). BDI (Equation 7) is a DBP that is the difference between the deflection at 12 inches away from the center of the load plate (D_{12}) and the deflection at 24 inches away from the load center of the load plate (D_{12}).The modulus of the subgrade (E_{SG}) was estimated based on F_2 and the BDI using an ANN trained from the synthetic database. After finding E_{SG}, the modulus of the AC layer is estimated by using another ANN with inputs of layer thicknesses, E_{SG}, the deflection under the center of the load (D_0), AREA, and the Base Curvature Index (BCI).

$$BDI_i = D_{12} - D_{24} \quad [7]$$

The AC modulus and horizontal strain at the bottom of the AC were determined to be condition indicators for the AC layer based on the synthetic deflection database. These indicators were adjusted to a reference structure (from a synthetic database) and temperature using regression equations. Mid-depth pavement temperature was estimated based on the recorded surface and air temperatures. Distress in the AC layer was classified when the AC modulus was determined to be less than 70% of the value for an intact pavement structure. Figure 2.17 shows the application of this procedure from an aggregate base pavement in Arizona. It can be seen that the modulus is significantly lower in 1995 and 1998 than was originally determined in 1994. Stripping was reported on this section after 1995.

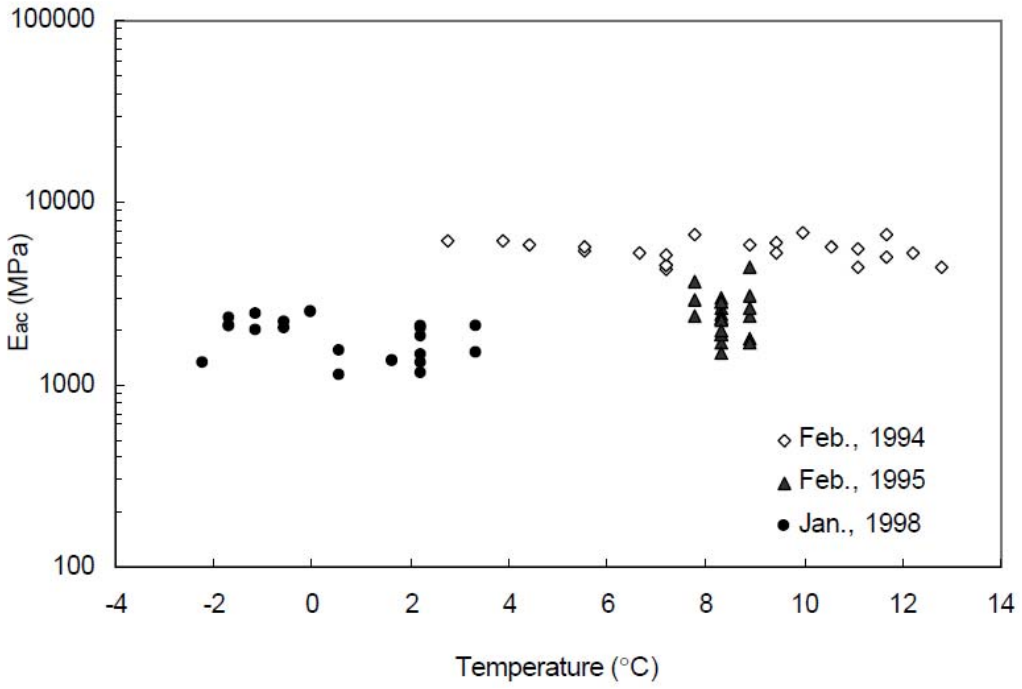

Figure 2.17 – AC Modulus from aggregate base pavement in Arizona (Xu et al., 2003)

APLCAP describes the condition of the AC layer as intact, slightly distressed, or severely distressed. APLCAP was further validated in several case studies used to assess its ability to estimate the AC modulus, critical stress/ strain values, and subgrade strength (Xu et al., 2003). The APLCAP program worked well for three case-studies presented but was unable to accurately estimate the compressive strain in the aggregate base layer, which may limit the ability to assess rutting potential.

This study illustrates the large variability that is encountered in field measured pavement responses and the discrepancies that can arise in visual surface distress surveys, core logs, and deflection measurements. Discussion on the complex nature of pavement systems and the random nature of distress was provided. The authors recommended that the general trends with distress presented in this work be validated by more extensive studies. The limited amount of FWD testing over time, consistent performance monitoring, and pavement temperatures restricted the development and validation of the extensive modeling conducted.

Several researchers have shown through modeling that deflection basins change when AC layers are delaminated (Al Hakim et al., 1999; Romanischi and Metcalf, 2002). Further studies found, through different modeling and interface simulation techniques, that the remaining pavement life is reduced from 20-80% for delaminated pavements (Khweir and Fordyce, 2003; Kruntcheva et al., 2005; Hu and Walubit, 2010). The large variation is attributed to various fatigue transfer functions used, type, thickness, and moduli of the pavement layers, and the location and degree of the delamination within the AC layers. Regardless of the actual percent reduction for a particular scenario, previous modeling research has shown that there is a substantial reduction in pavement life once delamination occurs.

Al Hakim et al. (1999) used FE modeling to generate deflection basins of flexible pavements with debonded layer interfaces. These theoretical deflection basins were then used to develop a two-step backcalculation process to determine the interface bond condition between AC layers. The two-step backcalculation process was validated on a limited amount of FWD generated deflection basins with promising results; however, the method struggled in identifying delamination in relatively thin HMA layers. Al Hakim et al. (1999) recommended further investigation on trial pavement sections with controlled bonding conditions where FWD testing can be used to better understand bonding development.

Several studies have also documented a reduction in pavement life in the field or at accelerated testing facilities once delamination has occurred (Gomba et al., 2005; Willis and Timm, 2007; Chen, 2009; Vrtis and Timm, 2015). Using FWD data from the Federal Aviation Administration's National Airport Pavement Test Facility, Gomba et al. (2005) attempted to quantify the level of interlayer bonding achieved in asphalt pavements that had unintentional delamination. The authors reported higher deflection values for delaminated pavements resulting in lower backcalculated moduli for the AC layers. Based on the backcalculated moduli for individual layers within the AC, several parameters were proposed from the differences in moduli or simulated strain of AC layers. Due to the inexact nature of the backcalculation process (especially between layers AC layers with moduli in the same order of magnitude), this method may be difficult to apply in a blind validation. The work done by Willis and Timm (2007) and Vrtis and Timm (2015) was based on structural test sections at the NCAT Test Track and will be discussed in more detail later in this research.

2.4 Summary of Literature Review

This literature review has shown that DBPs can be used to assess the pavement condition without backcalculation, modeling software can simulate FWD testing on distressed pavements, and that there is a significant reduction in pavement life once distress occurs. Based on this literature review, there is still a need to compare FWD deflections and simulated distress mechanisms with more detailed field performance sections where FWD testing was conducted in the same location over time and surface performance was closely monitored. This comparison will facilitate a better understanding of distresses within the pavement structure and their effect on FWD deflections for use in distress diagnosis and provide guidance in repair decisions.

CHAPTER 3. METHODOLOGY

The methodology to scrutinize deflection basins on flexible pavements that developed cracking is summarized in Figure 3.1 and fully described in the following subsections. Modeling and field data from the NCAT Test Track were used for each section analyzed. The field data for each section consisted of FWD testing, cracking surveys, section properties from construction quality control and laboratory testing, and the failure mechanism documented in previous reports. The FWD testing data were normalized using regression equations to account for the effect of load and pavement temperature. Each section was modeled in BISAR 3.0 (BItumen Stress Analysis in Roads), using laboratory measured moduli and surveyed layer thicknesses, to determine the theoretical effect of the documented cracking type on the FWD deflection basins. Delamination, top-down cracking (TDC), and bottom-up fatigue cracking (BUFC) were the cracking mechanisms considered. The level of cracking at each FWD station over time was quantified based on a sub-investigation that was conducted to determine the horizontal distance at which a discontinuity began to affect the measured deflections. Finally, the DBPs calculated from the BISAR simulations were compared to DBPs from normalized FWD data.

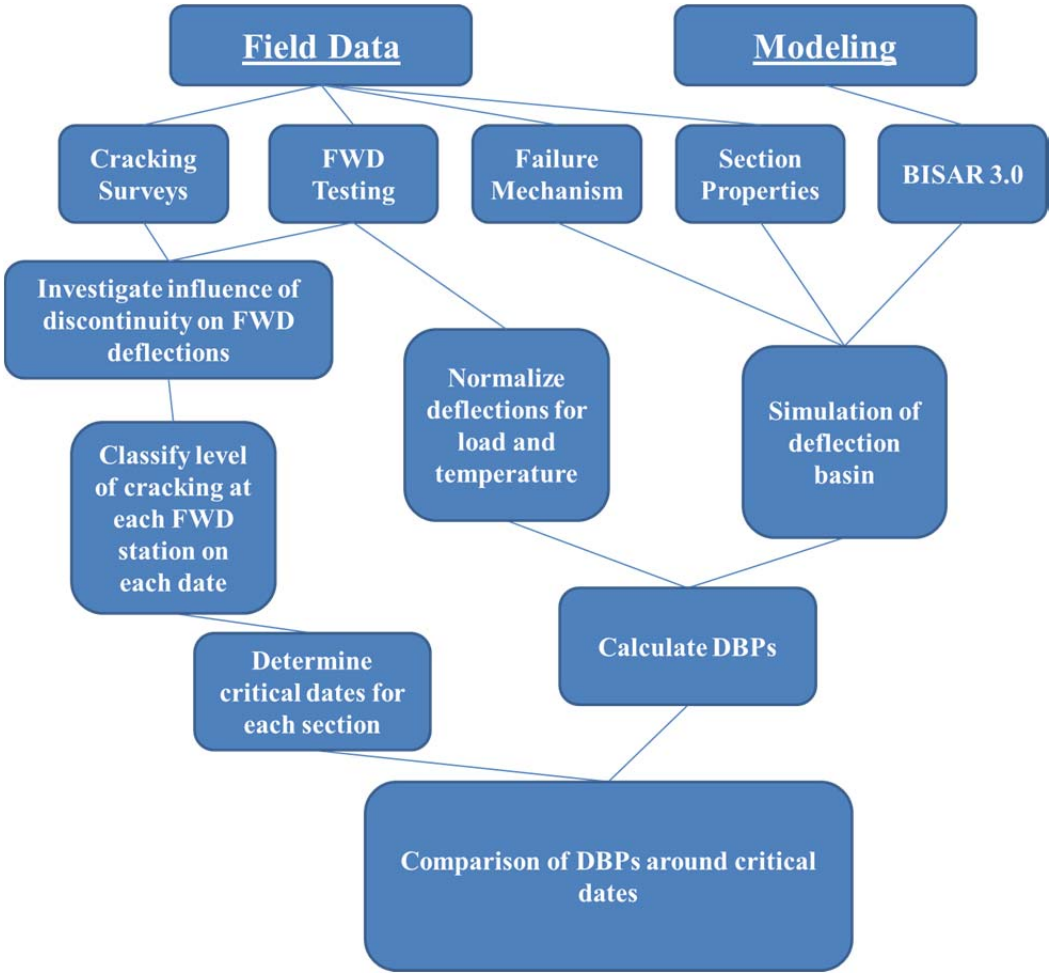

Figure 3.1 – Flowchart of methodology.

3.1 Modeling

Each of the pavement sections selected for analysis in this study were modeled as a multi-layer linear-elastic system using BISAR 3.0, developed by Shell Research. BISAR was selected for this analysis because it is capable of simulating various levels of partial slip between AC layers. The fundamental assumptions in BISAR are that each horizontal layer is homogeneous and isotropic with uniform thickness that extends infinitely in the horizontal direction (BISAR, 1998).

A typical pavement cross-section and the required BISAR inputs for each layer are shown in Figure 3.2. The material properties shown in Figure 3.2 are the properties used in the simulations shown in this chapter. For the simulations of actual Test Track sections, laboratory measured moduli and surveyed layer thicknesses (t) were used. Laboratory dynamic modulus (E) values, obtained following AASHTO TP 79-13 taken at 68° F and 10 Hz, were used to characterize the AC. Granular base and subgrade moduli were obtained from triaxial testing conducted in previous Test Track research on unbound material properties (Taylor, 2008). Poisson's ratios of 0.35, 0.40, and 0.45 (default values in BISAR) were used for the AC, granular base, and subgrade layers, respectively. The AC comprised multiple layers. Each interface between AC layers will be referred to by the upper layer over the lower layer (e.g., Interface 2/3), as shown in Figure 3.2.

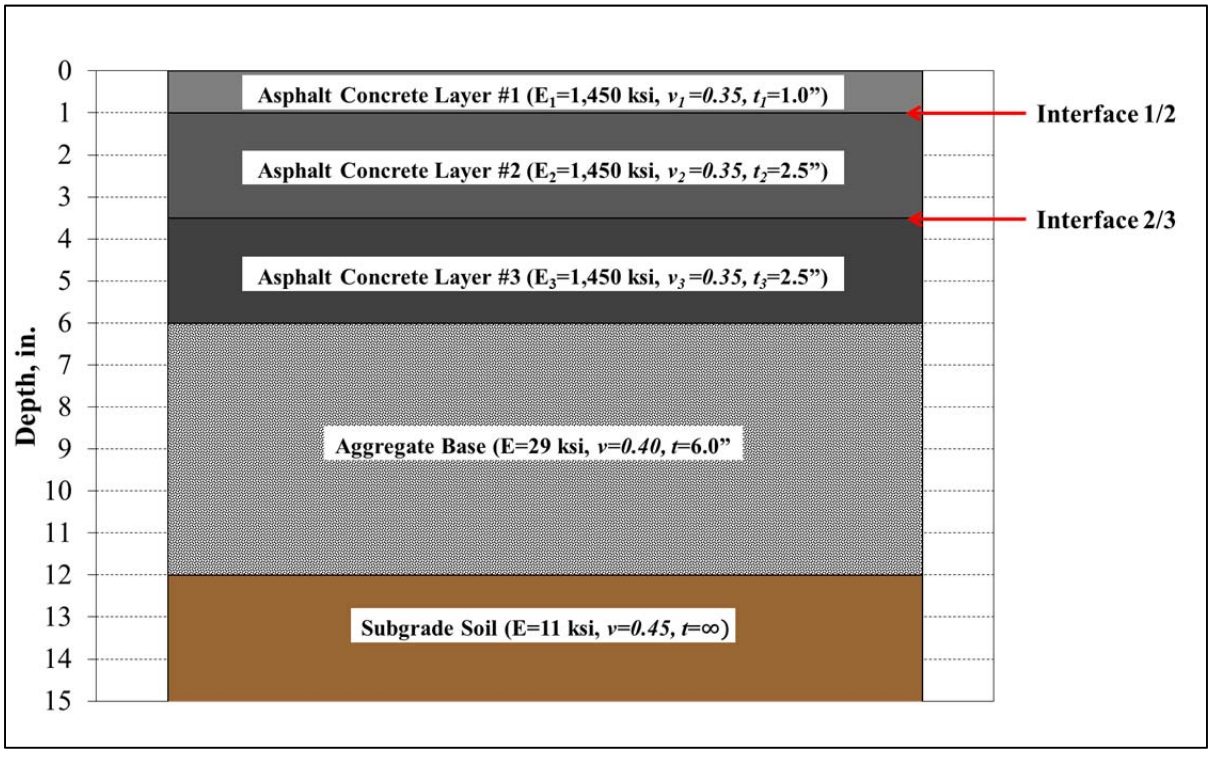

Figure 3.2 – Pavement cross-section and modeling inputs.

The FWD was simulated in BISAR by applying a static 9,000 lb. load to the pavement structure. The resulting surface deflections were determined at the same distance from the loads as the FWD sensors, shown previously in Figure 1.2. Thus, theoretical deflection basins were generated.

3.1.1 Modeling of Delamination

Various degrees of delamination of the AC layers and delamination locations were simulated in BISAR. Within BISAR, an infinitely thin inter-layer characterized by a shear spring compliance (AK) is used to simulate the layer interfaces. AK, shown in Equation 8, is defined as the relative horizontal displacement of layers divided by the stresses acting at the interface. The parameter α, Equation 9, is used to mathematically characterize this relationship considering the radius of the applied load (a) and material properties (E and *v*) from the layer above the interface. The α parameter can range from 0 to 1, with zero representing a full bond condition and 1 representing a full slip condition. By setting α at intermediate values between 0 and 1, various levels of layer slip can be simulated. However, it must be pointed out that α is not a classic coefficient of friction because it is dependent on the radius of the load and is not an independent material property (BISAR, 1998).

$$AK = \frac{relative\ horizontal\ displacement\ of\ layers}{stresses\ acting\ at\ the\ interface} \quad [8]$$

$$\alpha = \frac{AK}{AK + \frac{1+v}{E} * a} \quad [9]$$

where: AK= shear spring compliance, m^3/N

α= friction parameter, with $0 \leq \alpha \leq 1$ (α=0 means full friction; α=1 means complete slip)

a= radius of the load, m

E= modulus of the layer above the interface, Pa

v= Poisson's Ratio of layer above the interface

Figures 3.3 and 3.4 are examples of the theoretical effect that delamination location and severity have on the deflection basins, respectively. It can be seen in Figure 3.3 that there is a greater change in the deflection basin when the 2/3 interface is slipped compared to the 1/2 interface. The greatest change is when both 1/2 and 2/3 are slipped, which conceptually makes sense because the structure is now comprised of 3 thinner AC layers bending independently instead of one thicker AC layer. Figure 3.4 shows the effect of varying α for the 2/3 interface. The change in deflection is not linear with changing α, as there are greater deflections when the interface is completely slipped (α=0.99).

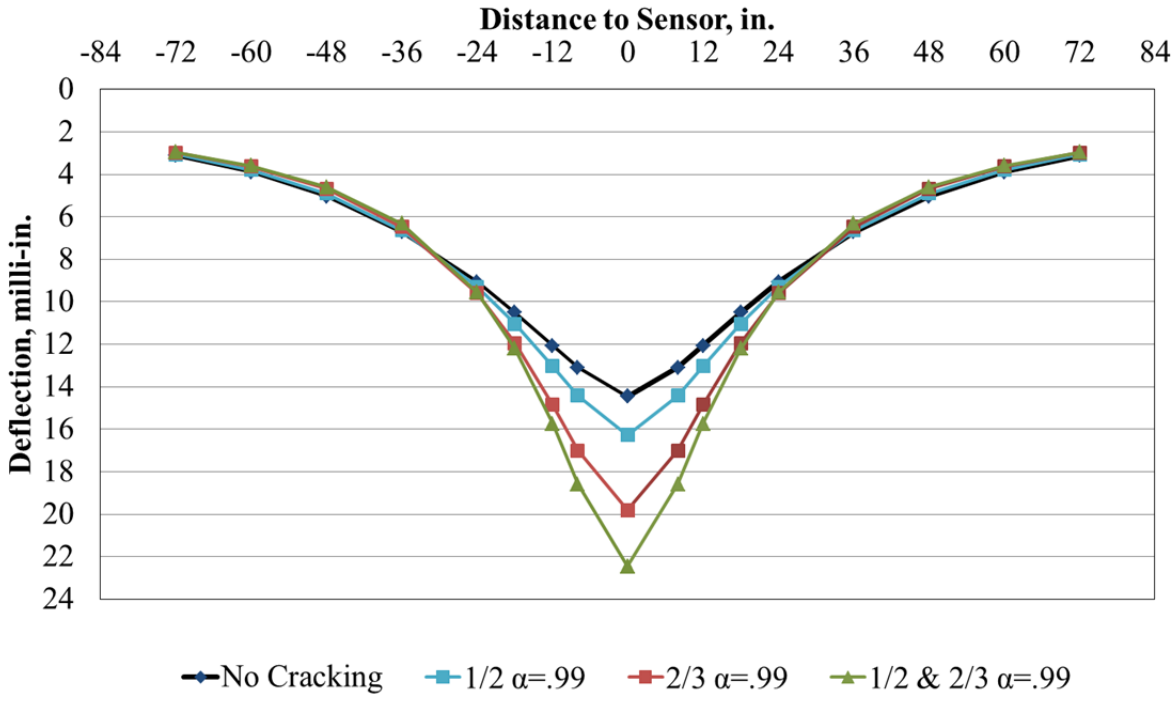

Figure 3.3 – BISAR simulated deflection basin with varying interfaces slipped.

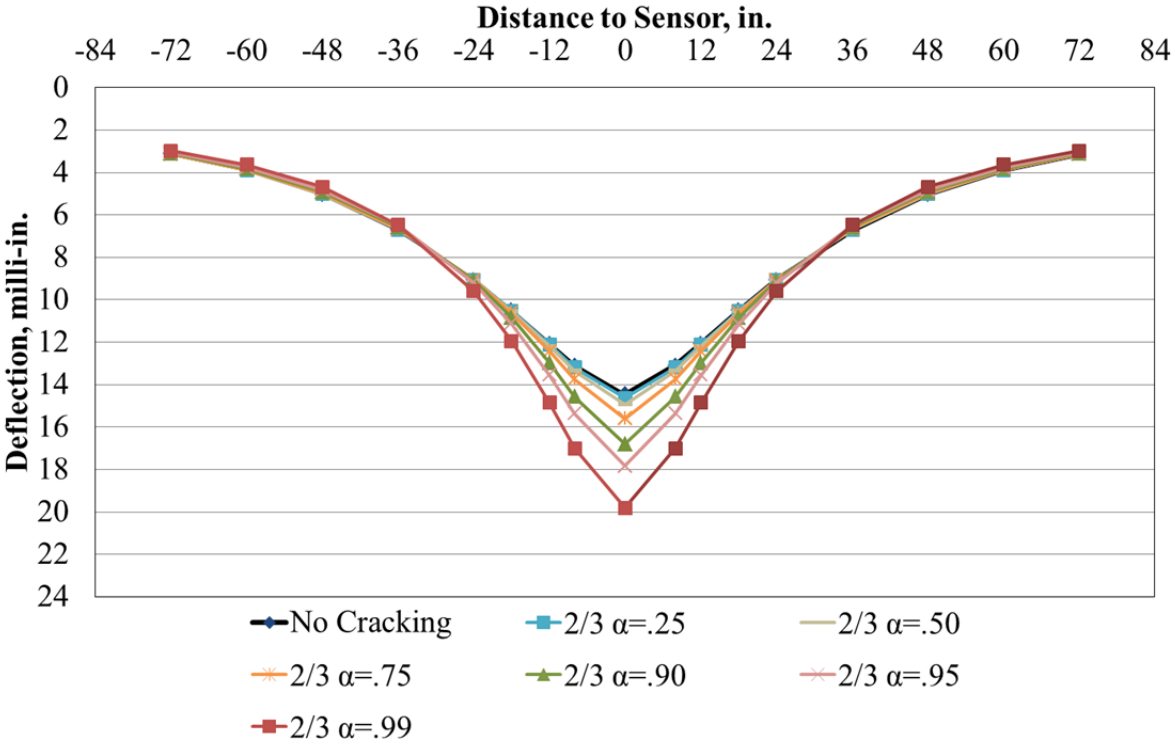

Figure 3.4 – BISAR simulated deflection basin with varying slip at interface 2/3.

3.1.2 Modeling of Bottom-up Fatigue Cracking

Figure 3.5 shows the simulations used to model BUFC in BISAR. Although the discontinuities in the pavement created by cracking directly violate the underlying assumption of homogeneity in linear-elastic modeling, it is still useful to estimate how the deflection basin will change as a result of BUFC. This was simulated by lowering the moduli (E_{AC}) of the "cracked" layers in BISAR. The AC moduli were reduced to 25 and 50% of their original value. The "cracked" layer was increased in 1 inch increments to simulate the impact on the deflection basin as BUFC propagates toward the surface. A modulus reduction to 25% was initially modeled, shown in Figure 3.6, because it was believed that there is a significant reduction in modulus with cracking but since the material is still confined, the modulus should still be on the same magnitude as the intact state. Additionally, a modulus reduction of 50% was tried and is shown in Figure 3.7. A 50% modulus reduction was utilized because it has been used as a failure threshold in laboratory bending beam fatigue testing (AASHTO T321-07). The BUFC model was further refined in the Fatigue Cracking Developmental Group (Chapter 6) when DBPs from sections with BUFC were scrutinized. It can be seen in Figure 3.6 and 3.7 that, as expected, the deflections at sensors within 18 inches of the load increase as the thickness of the simulated fatigue cracking increases.

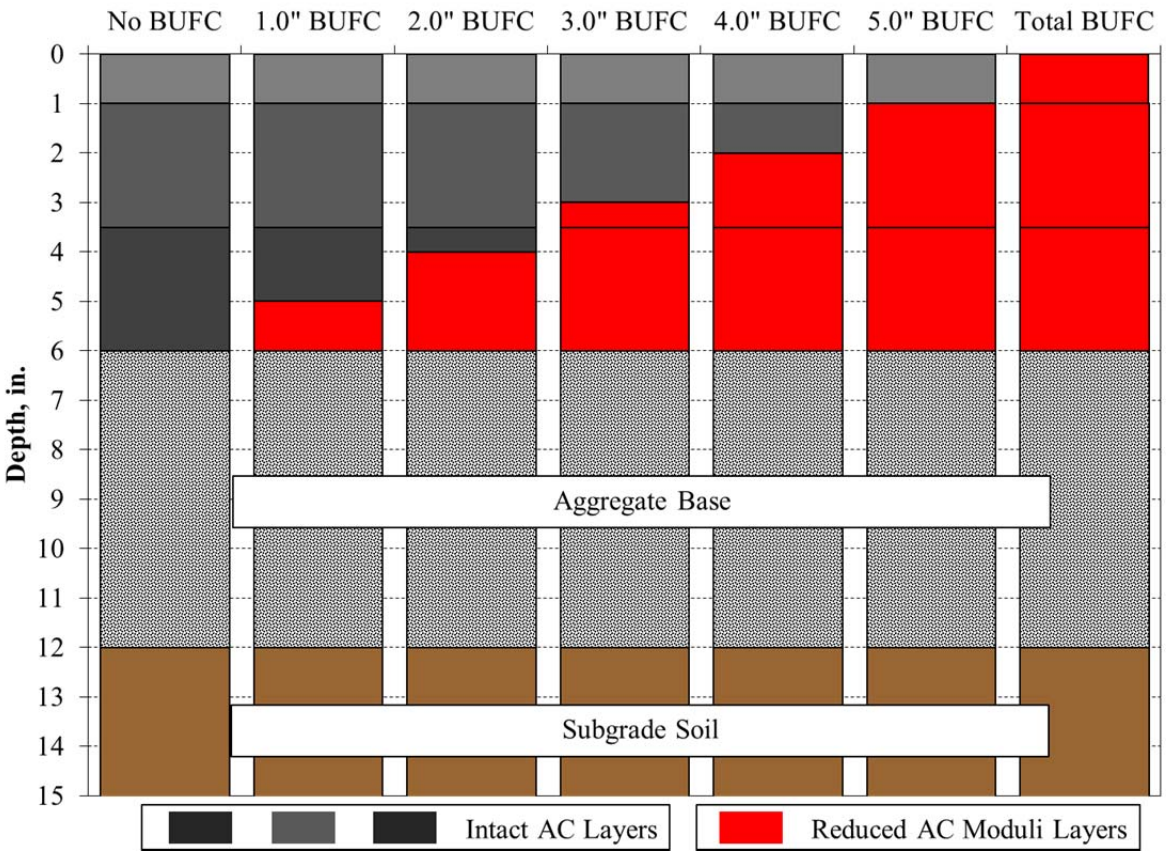

Figure 3.5 – Example cross-sections used to model BUFC.

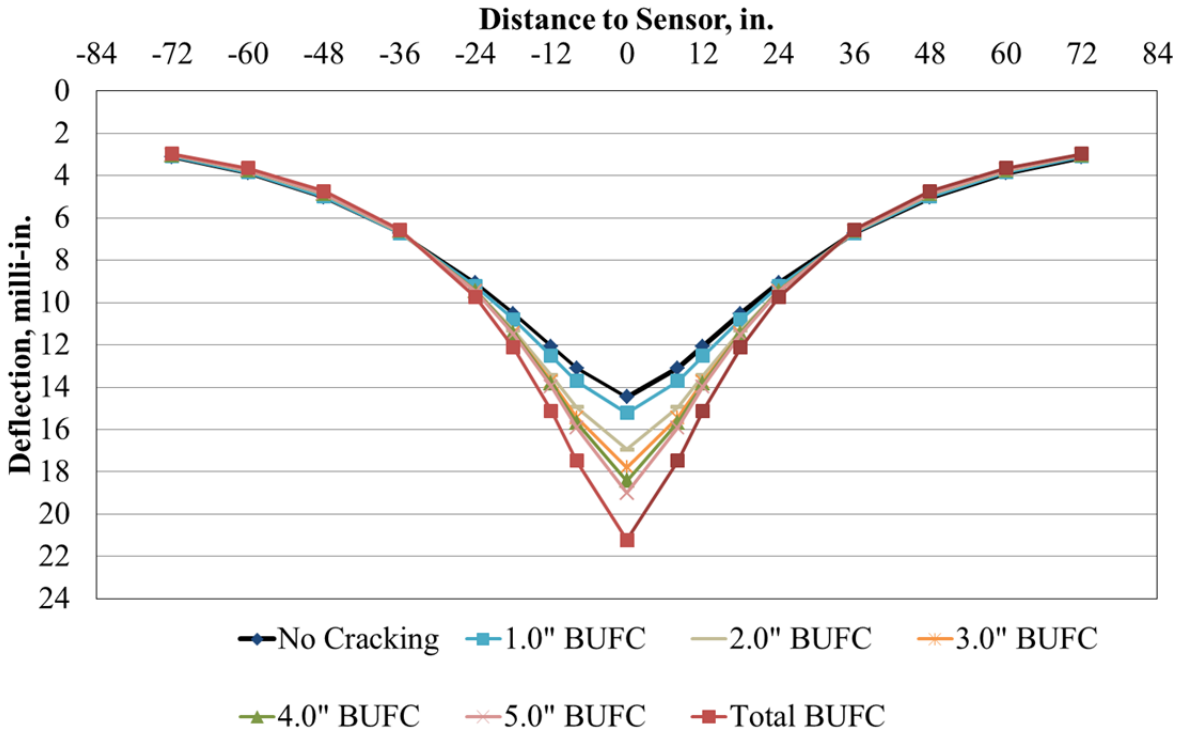

Figure 3.6 – BISAR BUFC simulation (E_{AC}=25%).

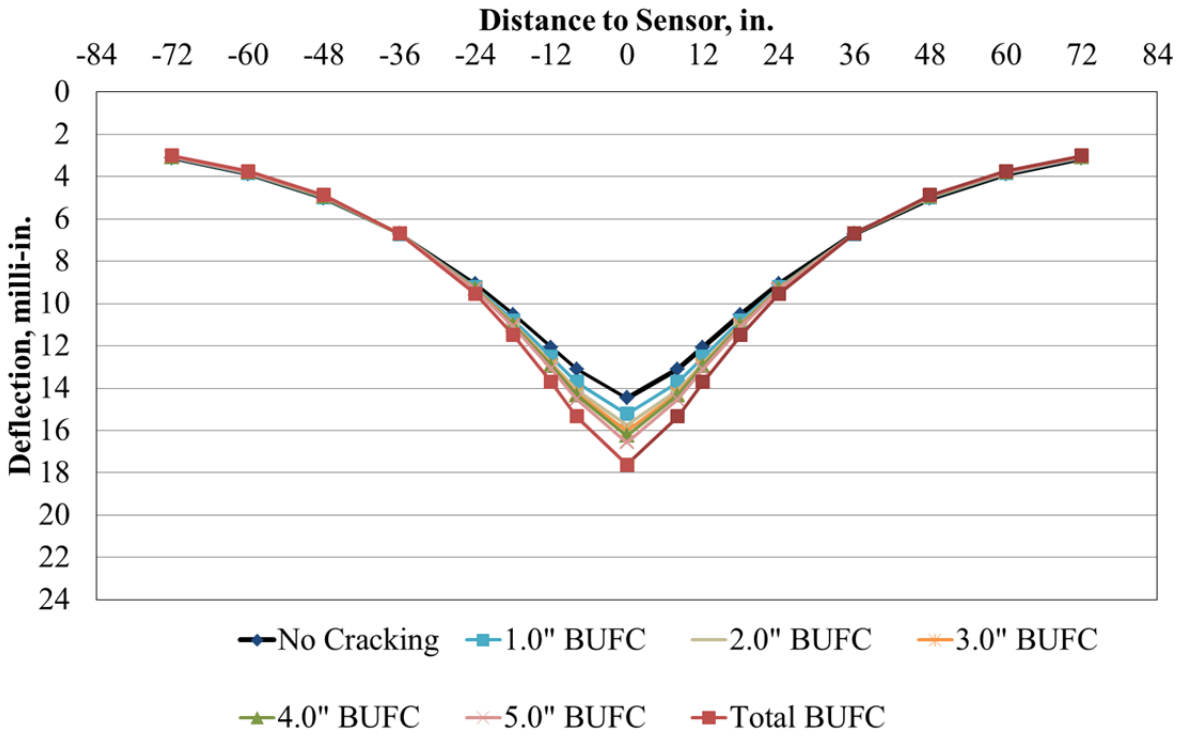

Figure 3.7 – BISAR BUFC simulation (E_{AC}=50%).

3.1.3 Modeling of Top-down Cracking

In a similar fashion as the modeled BUFC, TDC was modeled in BISAR by reducing the modulus of the cracked layer to 50% of the original value. Example cross-sections of the TDC simulations are shown in Figure 3.8. Figure 3.9 shows the simulated deflection basins with increasing propagation of TDC. It can be seen that, as expected, as the cracking propagates down through the structure the resulting deflections increase. The magnitude of the change in deflections with simulated cracking thicknesses is similar for the BUFC and TDC because the same approach was used to simulate the distresses. Further refinement of the TDC model is discussed in the Top-Down Cracking Group Results.

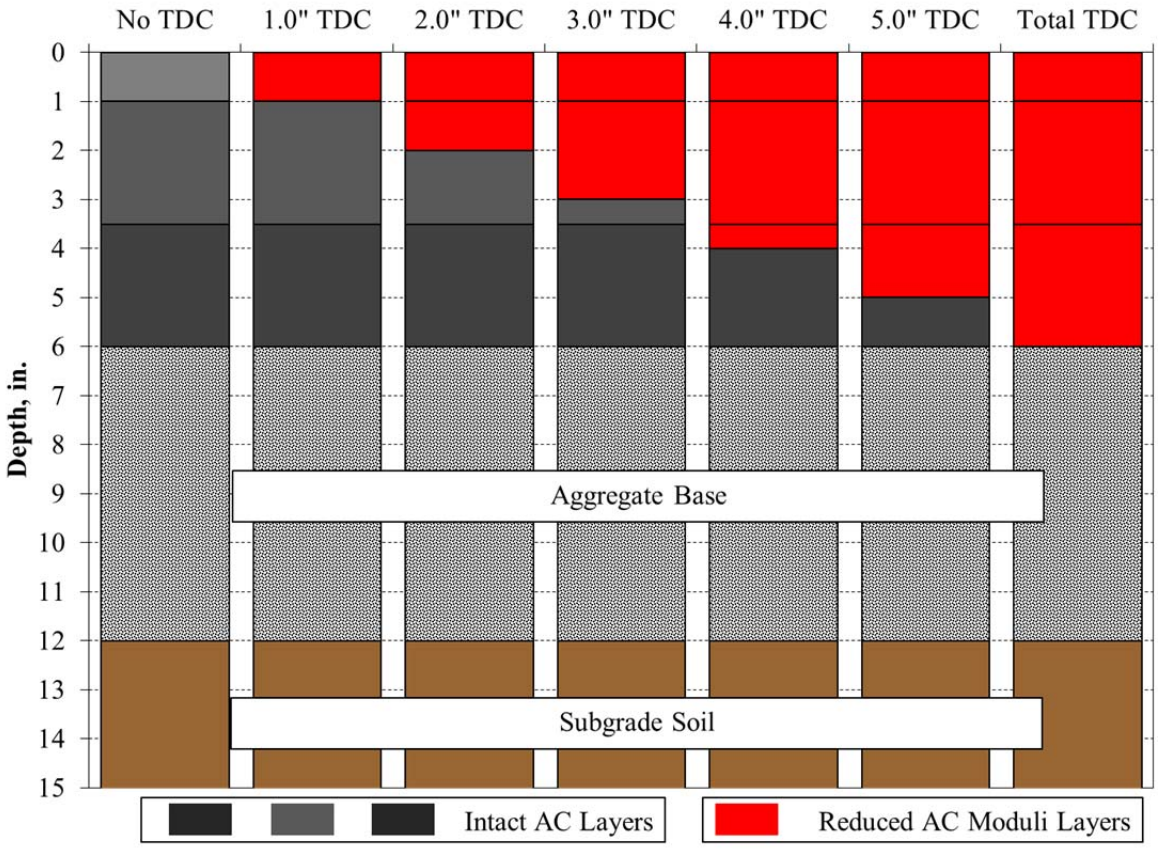

Figure 3.8 – Example cross-sections used to model TDC.

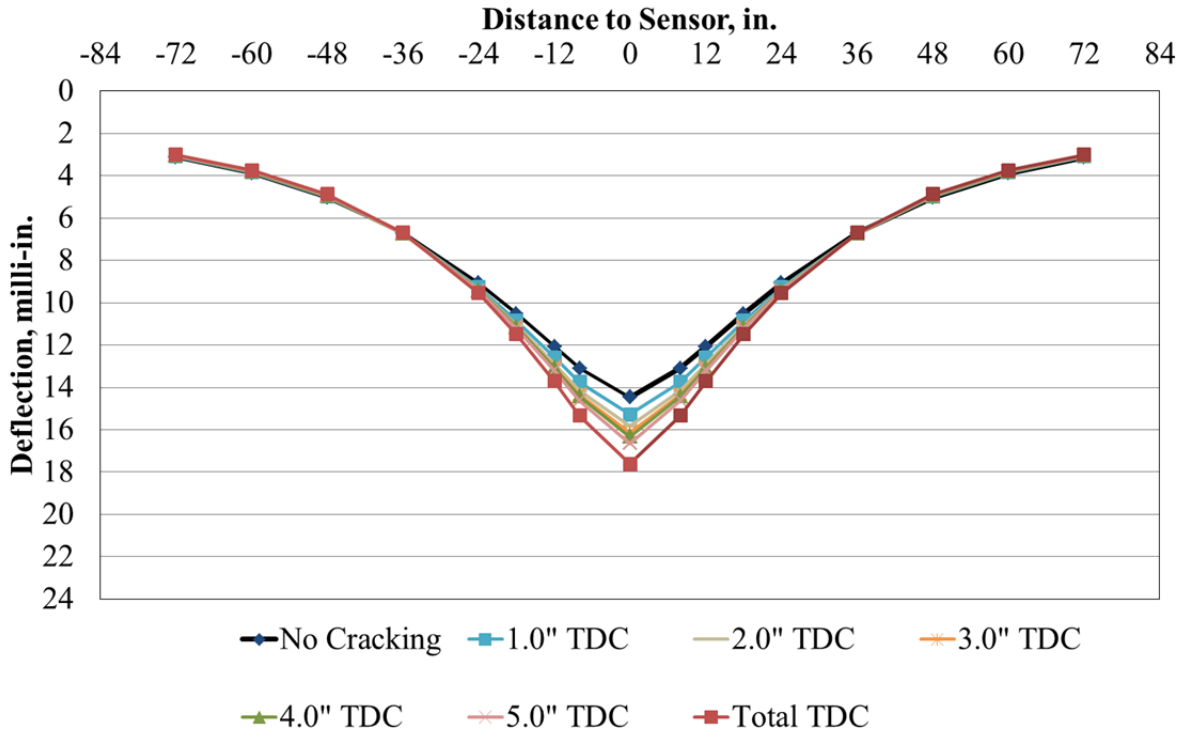

Figure 3.9 – BISAR TDC simulation.

3.1.4 Summary of BISAR Modeling

The overall magnitude of the increase in deflections observed in Figures 3.3 through 3.9 is affected by thickness and material properties used in the simulations; however, a change in the deflections is expected regardless of the simulation inputs (within typical ranges of pavement thicknesses and material properties). As a result, pavement sections of varying thickness and stiffness were included in this work to explore the sensitivity to these inputs. The deflections generated from these simulations were analyzed by calculating DBPs and identifying the DBPs that were sensitive to the change in simulation conditions. In all five figures, the deflections within 18 inches of the center of the load plate captured the greatest change with changes to the

AC inputs. It should be noted that the pavement structure used to generate these consisted of six inches of AC, over six inches of granular base over subgrade soil.

3.2 Deflection Basin Parameters Considered

From the literature review, four DBPs and D_0 were selected to assess their sensitivity to changes in the deflection basins from Delamination, BUFC, and TDC. AREA, AUPP, F_1, SCI, and D_0 have been used effectively in previous research. In addition to these previously used DBPs, two other new DBPs have been developed to take advantage of the FWD sensors located 8 and 18 inches away from the center of the load. The ARE_8 parameter is a derivation of AUPP but instead of using the sensor 36 inches from the center, the 8 inch and 18 inch sensors are used. The AUPP equation is reproduced (Equation 5) and Equation 10 presents the equation for ARE_8. A modified SCI was used and will be referred to as SCI_8. The SCI found in most research will be referred to as SCI_{12}. SCI_8 utilizes D_8 instead of the D_{12}, as shown in Equations 11 and 1, respectively.

$$AUPP = \frac{5D_0 - 2D_{12} - 2D_{24} - D_{36}}{2} \quad [5]$$

$$ARE_8 = \frac{5D_0 - 2D_8 - D_{12} - D_{18} - D_{24}}{2} \quad [10]$$

where: D_0 = center plate maximum deflection

D_8 = deflection measured at 8 inches from load

D_{12} = deflection measured at 12 inches from load

D_{18} = deflection measured at 12 inches from load

D_{24} = deflection measured at 24 inches from load

D_{36} = deflection measured at 36 inches from load

$$SCI_{12} = D_0 - D_{12} \quad [1]$$

$$SCI_8 = D_0 - D_8 \quad [11]$$

The DBPs were calculated for the BISAR generated deflection basins presented in Figures 3.4 through 3.9 and are presented in Tables 3.1 through 3.4. A color gradient (red = greatest change; white = no change) was added to the tables to illustrate the simulation with the greatest change and the most sensitive DBPs. It can be seen in Table 3.1 that, similar to the figures, the largest difference in change in DBPs occurred when the 2/3 interface was completely slipped (α=0.99). There was a much greater maximum percent change when cracking was simulated through the entire AC layers for a moduli reduction to 25% than 50% due to the lower moduli creating higher deflections. Tables 3.2, 3.3, and 3.4 show that there are greater changes in the DBPs as BUFC and TDC increases through the pavement.

Table 3.1 –DBPs from BISAR Simulated Delamination at Interface 2/3

Description	% Change D_0	% Change AREA	% Change AUPP	% Change F_1	% Change SCI_8	% Change SCI_{12}	% Change ARE_8
No Slip α=0.0	0%	0%	0%	0%	0%	0%	0%
2/3 α=.25	1%	1%	3%	3%	7%	6%	4%
2/3 α=.50	3%	2%	9%	8%	17%	14%	12%
2/3 α=.75	8%	5%	22%	18%	36%	33%	27%
2/3 α=.90	16%	8%	43%	33%	63%	60%	52%
2/3 α=.95	23%	11%	59%	42%	81%	79%	70%
2/3 α=.99	37%	13%	87%	54%	107%	107%	98%

Table 3.2 –DBPs from BISAR Simulated BUFC (E_{AC}=25%)

Description	% Change D_0	% Change AREA	% Change AUPP	% Change F_1	% Change SCI_8	% Change SCI_{12}	% Change ARE_8
No Cracking	0%	0%	0%	0%	0%	0%	0%
1.0" BUFC	9%	3%	19%	12%	21%	22%	21%
2.0" BUFC	17%	7%	38%	25%	46%	46%	42%
3.0" BUFC	23%	9%	54%	35%	73%	70%	62%
4.0" BUFC	27%	11%	67%	45%	103%	92%	80%
5.0" BUFC	31%	13%	78%	52%	128%	110%	95%
Total BUFC	47%	17%	113%	70%	175%	154%	136%

Table 3.3 –DBPs from BISAR Simulated BUFC (E_{AC}=50%)

Description	% Change D_0	% Change AREA	% Change AUPP	% Change F_1	% Change SCI_8	% Change SCI_{12}	% Change ARE_8
No Cracking	0%	0%	0%	0%	0%	0%	0%
1.0" BUFC	5%	2%	11%	7%	12%	12%	12%
2.0" BUFC	9%	3%	19%	13%	23%	23%	21%
3.0" BUFC	11%	5%	25%	17%	32%	31%	28%
4.0" BUFC	12%	5%	29%	20%	41%	38%	34%
5.0" BUFC	15%	6%	34%	23%	50%	45%	40%
Total BUFC	22%	8%	49%	32%	69%	63%	57%

Table 3.4 –DBPs from BISAR Simulated TDC

Description	% Change D_0	% Change AREA	% Change AUPP	% Change F_1	% Change SCI_8	% Change SCI_{12}	% Change ARE_8
No Cracking	0%	0%	0%	0%	0%	0%	0%
1.0" TDC	6%	2%	11%	7%	13%	12%	12%
2.0" TDC	9%	3%	19%	12%	23%	22%	21%
3.0" TDC	12%	4%	24%	15%	32%	29%	27%
4.0" TDC	13%	5%	28%	18%	41%	36%	33%
5.0" TDC	15%	6%	34%	22%	49%	44%	39%
Total TDC	22%	8%	49%	32%	69%	63%	57%

The BISAR distress simulations and DBP analysis clearly indicated that the changes in pavement structural response with simulated distress can be captured with the DBPs. In this research, the change in DBPs from modeling was compared to the changes in DBPs measured by the FWD over time.

3.3 Field Data

Sections from the NCAT Test Track were selected to apply and further refine this methodology. The NCAT Test Track is a 1.7 mile closed-loop flexible pavement testing facility located in Opelika, Alabama. The track is divided into 46 research sections that are designed to address the research needs of the section sponsor. Beginning operation in 2000, track research has investigated numerous flexible pavement and construction factors including mix-design properties, structural responses, and surface characteristics. The track operates in three-year research cycles including two years of heavy-truck traffic applied with triple-trailer trucks, as shown in Figure 3.10. Truck traffic was applied to the pavement sections five days a week, resulting in approximately 10 million equivalent single axle load (ESAL) applications over the two-year trafficking portion of the research cycle. Performance of the sections was monitored on a weekly basis for cracking, rutting, and roughness. Pavement responses were monitored on structural sections, located on the tangents, with embedded pressure plates and strain gauges. Regular FWD testing was also conducted on the structural sections. From previous structural sections, FWD and cracking data were scrutinized. The following sub-sections discuss the datasets and how they were prepared for comparison.

Figure 3.10 – Triple-Trailer on NCAT Test Track West Curve.

3.3.1 FWD Data

FWD testing was routinely conducted using a Dynatest 8000 model on the test sections as part of the performance monitoring. The testing was done at 12 fixed locations (referred to as "stations" in this document) within each section, at three transverse offsets at four random longitudinal locations, as shown in Figure 3.11. The first and last 25 feet of each section were transition zones between sections and were excluded from analysis. The remaining 150 feet of the sections were divided into three 50 foot sub-sections. Within each sub-section, a randomly determined testing location was established (RL#1-3). RL#4 was located in the middle of the instrumentation array within each section. Stations 1, 4, 7, and 10 were located in the inside wheel path (IWP). Stations 2, 5, 8, and 11 were located between wheel paths (BWP) and stations 3, 6, 9, and 12 were located in the outside wheel path (OWP).

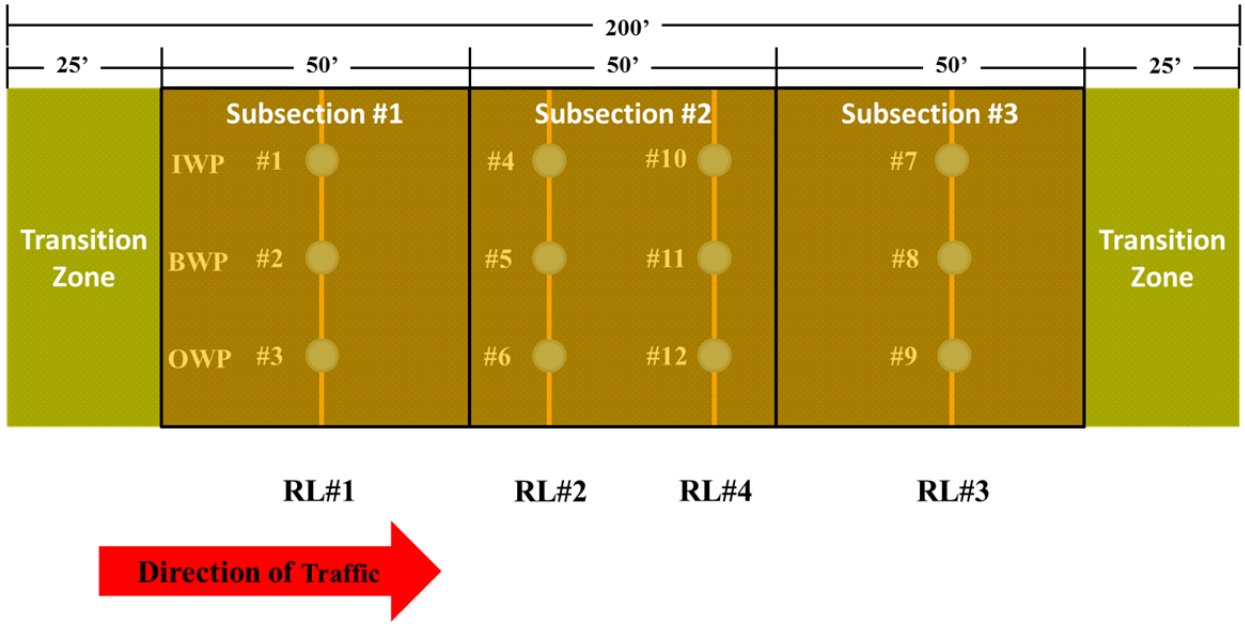

Figure 3.11 –FWD Testing stations within Test Track sections.

Nine sensors were used to capture the deflection basin from each load at distances of 0, 8, 12, 18, 24, 36, 48, 60, and 72 inches away from the center of the load plate, as shown previously in Figure 1.2. FWD testing was conducted at target load levels of 6,000, 9,000, 12,000, and 15,000 lbs. At each of these four load levels, the deflection basins from three replicate drops were recorded at each station on a given testing day. Thus, at each station, on a given day, a total of 12 deflection basins were generated.

The FWD testing protocol used at the NCAT Test Track followed AASHTO and ASTM testing procedures (ASTM D4694, ASTM D4695, and AASHTO T295). The testing protocol and sensor orientation is similar to the requirements for FWD measurements for the Long Term Pavement Performance (LTPP) database (Schmalzer, 2006). The FWD testing for LTPP sites also requires nine sensors to measure deflection, but requires a sensor located 12 inches behind the center of the load plate. Thus, the LTPP sensor setup has sensors at 0, 8, 12, 18, 24, 36, 48,

60, and -12 inches away from the center of the load plate. Another slight difference between the LTPP requirements and the Test Track FWD protocol is that four drops are required at each load level for LTPP sites, instead of the three drops per load level used on the Test Track.

3.3.1.1 Load Correction

FWD deflection basins are influenced by load magnitude, climate, and pavement condition (Huang, 2004). Therefore, to analyze deflection basins to capture changes in the structure from delamination, BUFC, or TDC, the effects of load and climate must be removed. The magnitude of the FWD load has a large influence on the resulting deflection basin. As an example, Figure 3.12 shows the deflections at various testing load levels from the full set of 12 drops at a given station. The R^2 values from the linear trendlines indicate that there is a strong linear relationship between load level and the resulting deflection. Sensors D_0, D_{24}, and D_{72} are displayed to show that there was a strong linear relationship between load and deflection for all sensors regardless of the distance away from the load.

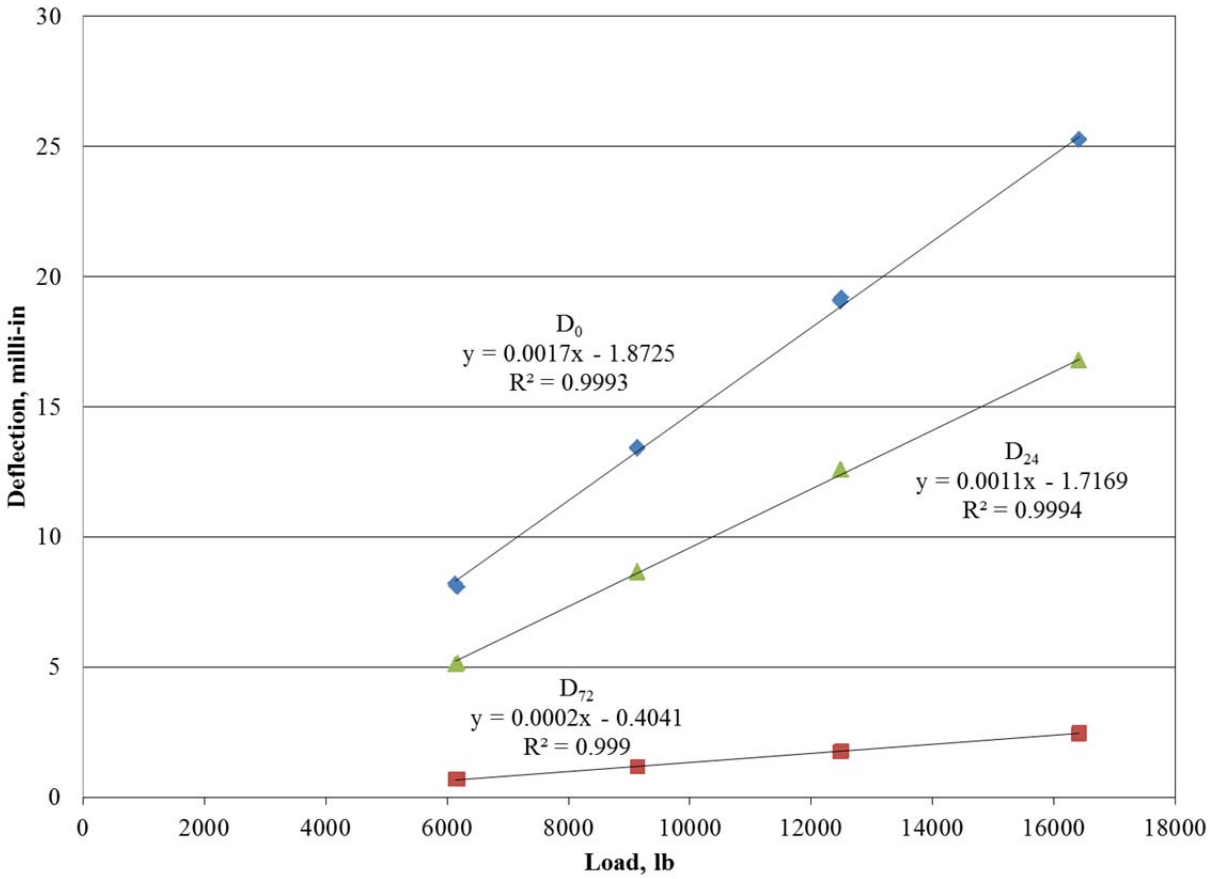

Figure 3.12 – Linear relationship between load and deflection.

A linear regression equation was computed at each testing station, for each sensor, and each set of 12 drops, similar to the equations shown in Figure 3.12. Thus, for a given testing day 108 (12 stations x 9 sensors) linear regression equations were used to normalize the deflection basins to a reference load level of 9,000 lbs. Using a linear regression equation for each sensor, the set of 12 drops (and 12 resulting deflection basins) was reduced to a single equivalent deflection basin at a load level of 9,000 lb. Deflections from all sensors ($D_0 - D_{72}$) were equated to their response at 9,000 lbs. to create a deflection basin in which all sensors were treated the same.

3.3.1.2 Temperature Correction

The modulus of asphalt pavements is influenced by temperature; therefore, the resulting deflection basins are influenced by temperature as well. One of the unique advantages of this research over the projects discussed in the literature review is that mid-depth pavement temperatures were recorded at the time of FWD testing. Thus, it was possible to account for the effect of temperature on the measured deflection basins. Figure 3.13 shows load corrected deflection values versus mid-depth pavement temperature. The effect of temperature diminishes as the sensor distance from the load increases. As discussed previously in the literature review and shown with modeling, the responses from sensors farther away from the load are attributed to the granular layers beneath the AC which are not sensitive to temperature. It should be noted that the R^2 values were lower for this dataset because it includes data from each FWD testing station within one section taken over the entire 2012 research cycle. In addition to spatial variability, temperature, and testing date variability were included in this data, as well as the effect of damage from traffic on the pavement response.

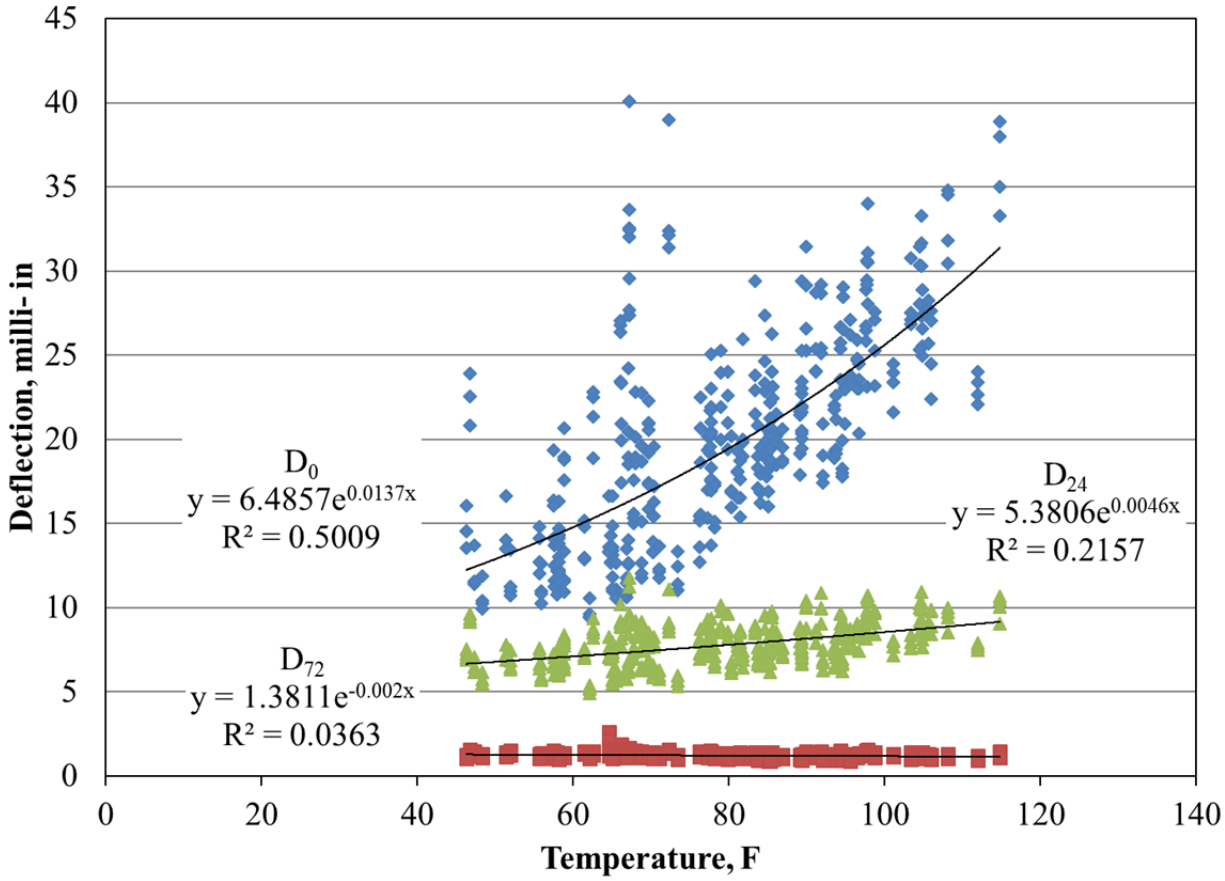

Figure 3.13 – Load corrected deflection versus temperature.

Using the exponential regression equations similar to the ones shown in Figure 3.13, the deflections values from sensors D_0 – D_{36} were corrected to a reference temperature of 68° F. A reference temperature of 68° F was chosen because it is the standard reference temperature used in the AASHTO 1993 Design Guide (AASHTO, 1993). To account for spatial variability, the temperature correction was conducted for each individual station. It was decided to correct deflections up to D_{36}, because these deflections are included in the DBPs that were analyzed to identify the impact of damage on the pavement response from FWD testing. The extremely low R^2 values in Figure 3.14 indicate that the effect of temperature has been removed from this dataset. By comparing Figure 3.13 with Figure 3.14, it can be seen that deflections at

temperatures below 68° F were increased and deflections at temperatures above 68° F were decreased.

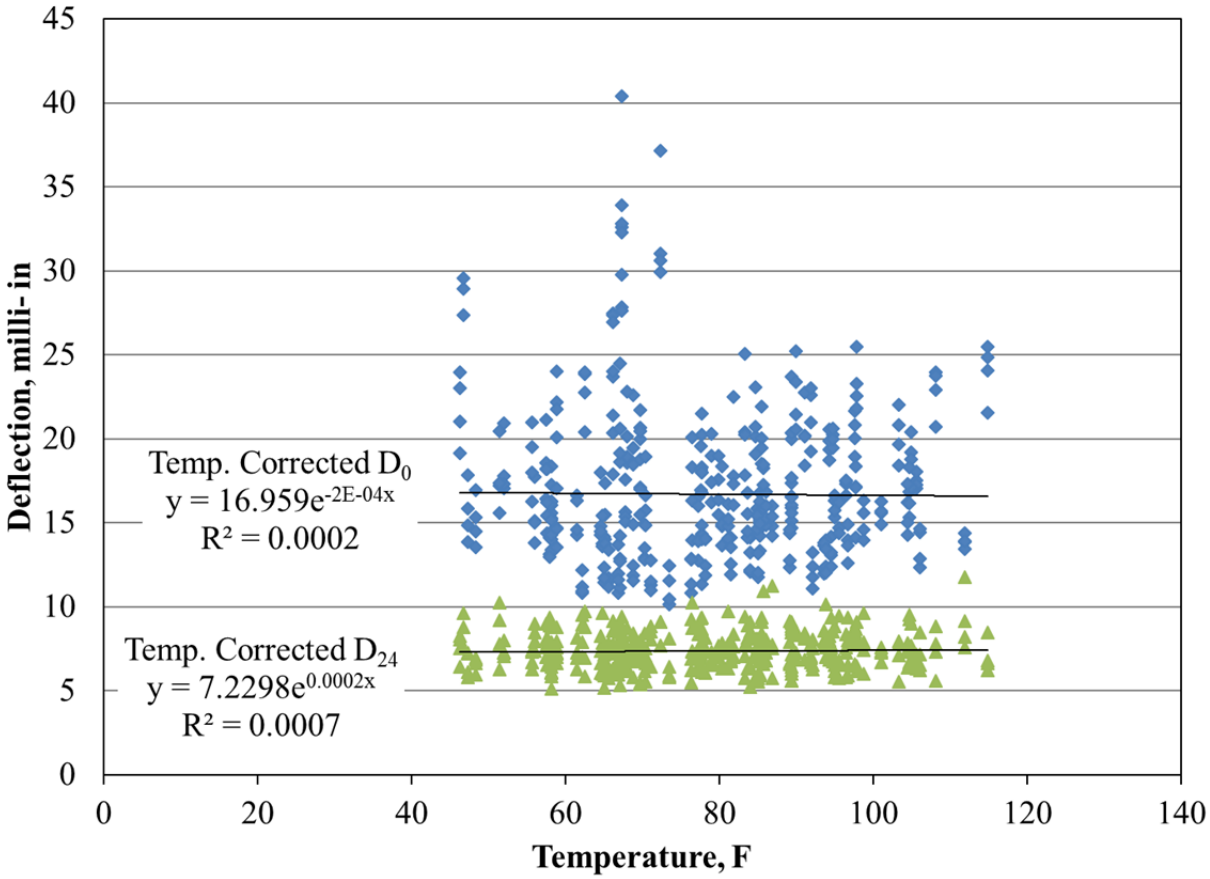

Figure 3.14 – Load and temperature corrected deflection versus temperature.

3.3.2 Investigation of FWD Sensitivity to Orientation and Discontinuitiest

3.3.2.1 Background

As discussed previously, the FWD is a commonly used tool to measure in-situ pavement structural integrity and operates by dropping a weight onto the pavement surface and measuring the corresponding surface deflections at various distances away from the load. From a theoretical

perspective, the deflection basin generated is circular and uniform in all directions. However, despite widespread implementation of the FWD, no documentation of a field validation of this assumption could be found in literature, especially with regard to discontinuities (e.g., cracking) in the AC.

This sub-investigation was conducted to provide a better understanding of how discontinuities were impacting measured deflection basins. In particular, it was necessary to determine at what distance away from the FWD load plate that a crack in the AC began to influence the deflection basin and determine if that distance is the same in all directions.

3.3.2.2 Objectives and Scope

The objectives of this investigation were to determine whether the orientation of FWD sensors (upstream and downstream from load plate) influence measured deflection basins and to assess the effect of a discontinuity on the measured deflection basin. To meet these objectives deflection basins from FWD testing on the same location with sensors located up/downstream from the load plate were compared. Comparisons were also made with respect to orientation and distance after the pavement was cut to replicate a severe discontinuity (e.g., severe cracking).

3.3.2.3 Testing Setup and Experimental Plan

An entrance road to the NCAT facility in Opelika, AL was selected for this investigation because it was in good condition (no visible cracking or rutting), was representative of typical pavements in the area, and could be cored and cut (to simulate discontinuity). The pavement was constructed in 2001 and the surface condition can be seen in Figure 3.15. Two testing sites on this road were chosen and the same testing plan was conducted at each site. Cores taken after completion of the testing verified consistent AC thickness at each testing site. Site 1 had an AC

thickness of 5.7 inches and site 2 had an AC thickness of 4.9 inches. These thicknesses are similar to the thicknesses of some of the Test Track sections that were analyzed. Coring also confirmed that the AC was in good condition without cracks or signs of delamination.

Figure 3.15 - Surface condition of pavement.

At each site, there were seven FWD testing locations spaced at one foot increments between the wheel paths of the outbound lane, as shown in Figure 3.16. The sequence of testing was determined to minimize the amount of time spent aligning the FWD trailer over each testing location. Thus, Location 1 was first tested in Orientation A (Figure 3.16 (a)), followed by Locations 2 through 7 (Figure 3.14 (b)). The FWD trailer was then turned around 180° and the locations were tested in reverse order (Orientation B), 7 (Figure 3.14 (c)) through 1 (Figure 3.16 (d)).

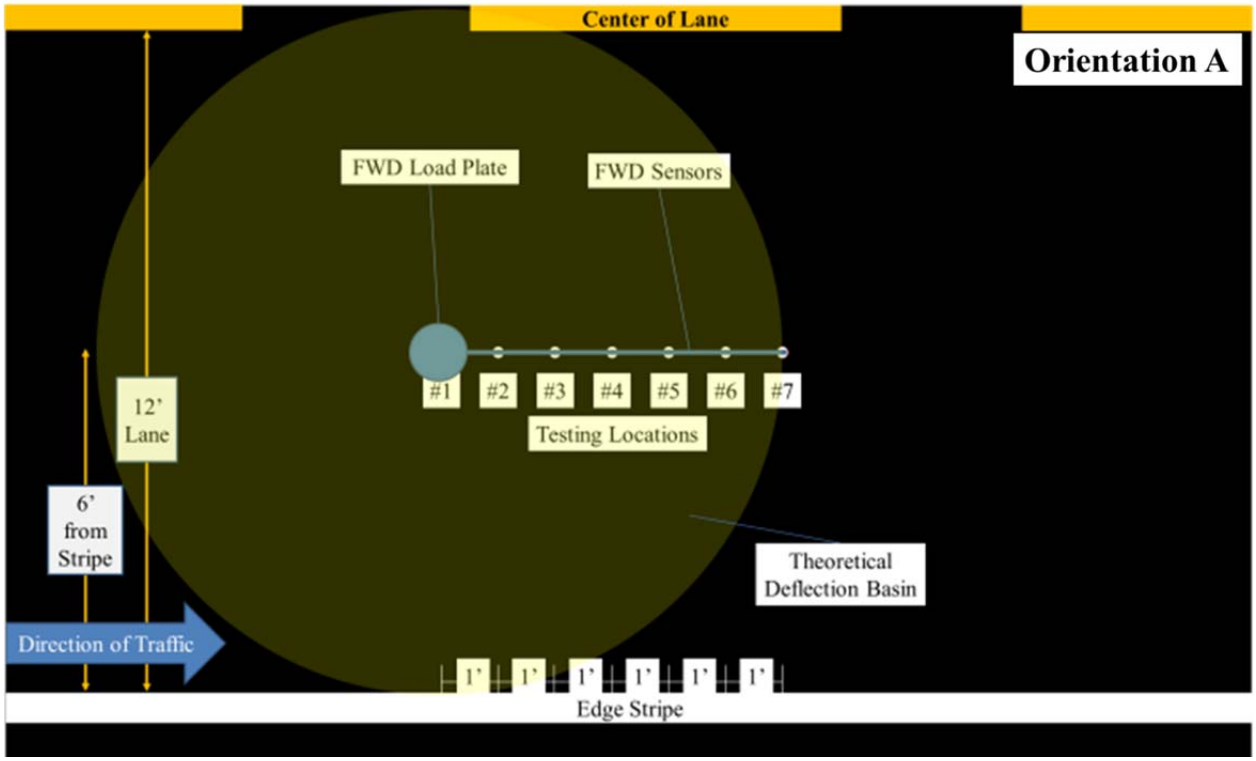
Center of Lane
Orientation A
FWD Load Plate
FWD Sensors
#1
#2
#3
#4
#5
#6
#7
Testing Locations
12'
Lane
6'
from
Stripe
Theoretical
Deflection Basin
Direction of Traffic
1'
1'
1'
1'
1'
1'
Edge Stripe

(a)

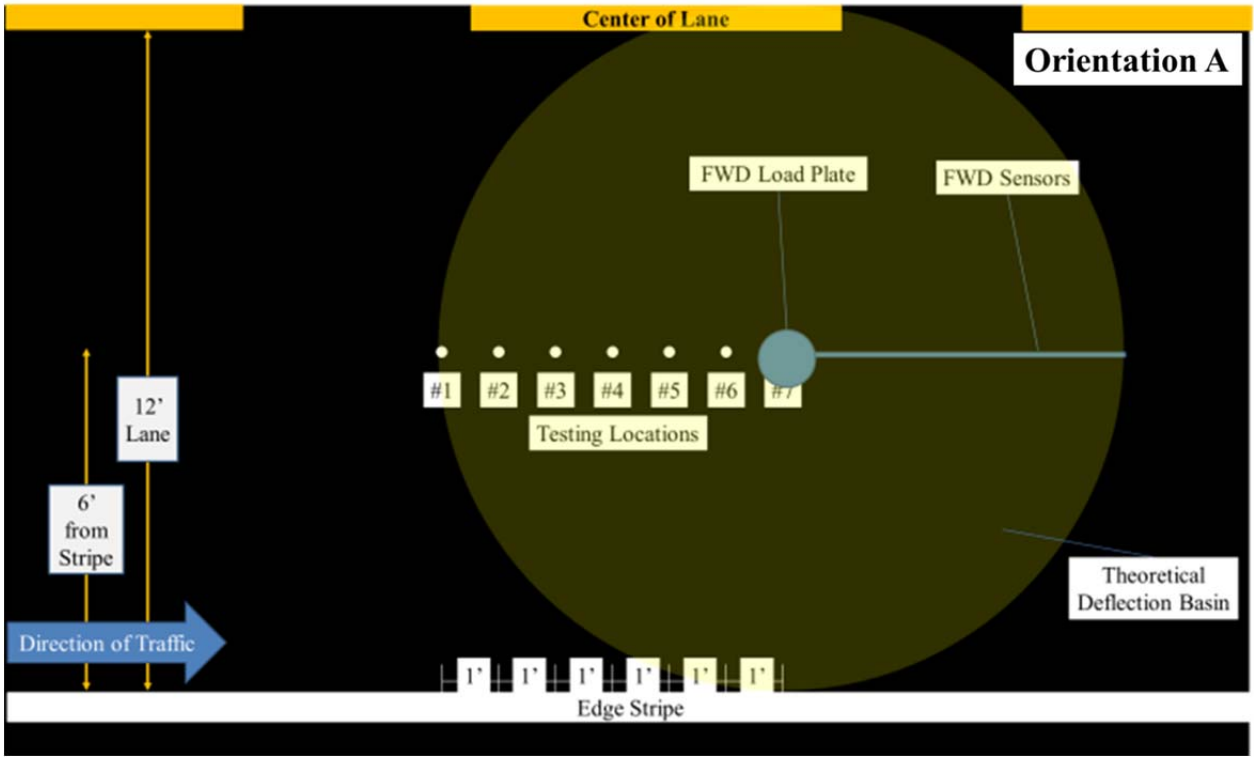
Center of Lane
Orientation A
FWD Load Plate
FWD Sensors
#1
#2
#3
#4
#5
#6
#7
Testing Locations
12'
Lane
6'
from
Stripe
Theoretical
Deflection Basin
Direction of Traffic
1'
1'
1'
1'
1'
1'
Edge Stripe

(b)

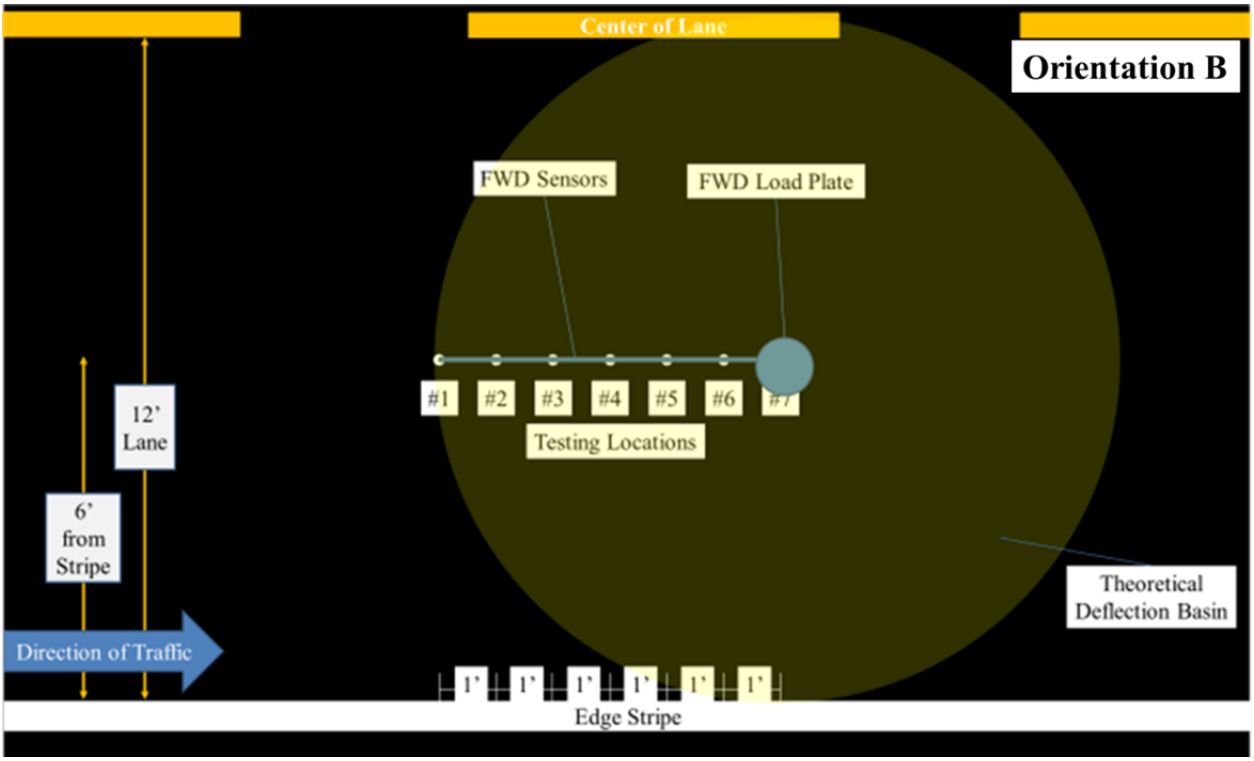

(c)

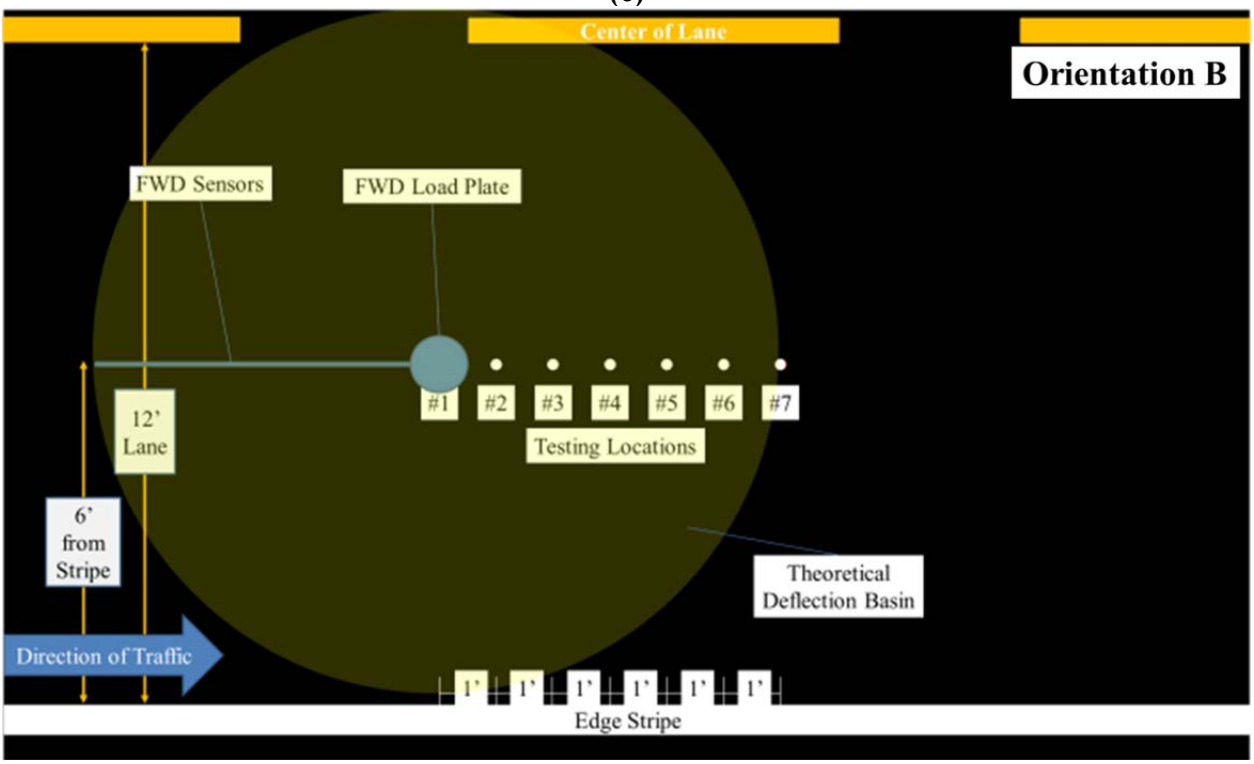

(d)

Figure 3.16 - Plan view of FWD testing procedure.

To minimize the amount of pavement temperature change, the testing protocol was developed to test the seven locations in each site in the least time possible. Thermocouples were installed at mid-depth of the pavement to monitor the temperature during testing. This was done by drilling halfway through the pavement, inserting a thermocouple into the hole, and then filling the hole with roofing asphalt. The thermocouples were installed approximately 20 feet away from each testing site to ensure that they were not influencing the measured deflection basins but were close enough to have the same amount of sun/shade.

Following completion of FWD testing at both locations, a transverse discontinuity was cut through the entire AC layer at location 1 of each site. A picture of FWD testing over the saw cut is presented in Figure 3.17. On the following day, the same FWD testing protocol was initiated once the mid-depth pavement temperature reached the same value recorded during testing on the previous day. This is shown schematically in Figure 3.18.

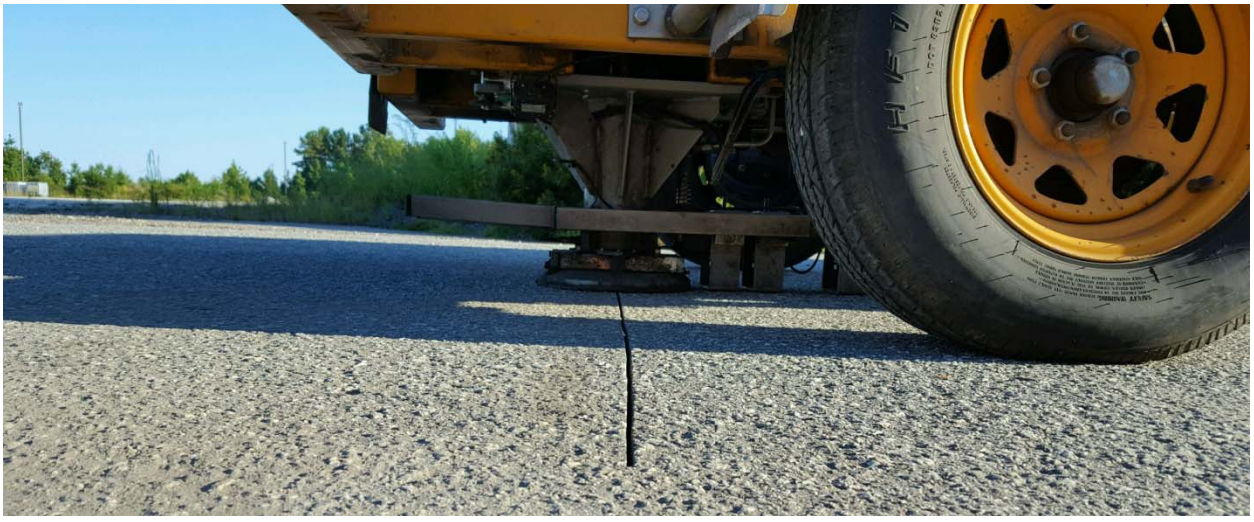

Figure 3.17 – FWD testing over saw-cut discontinuity.

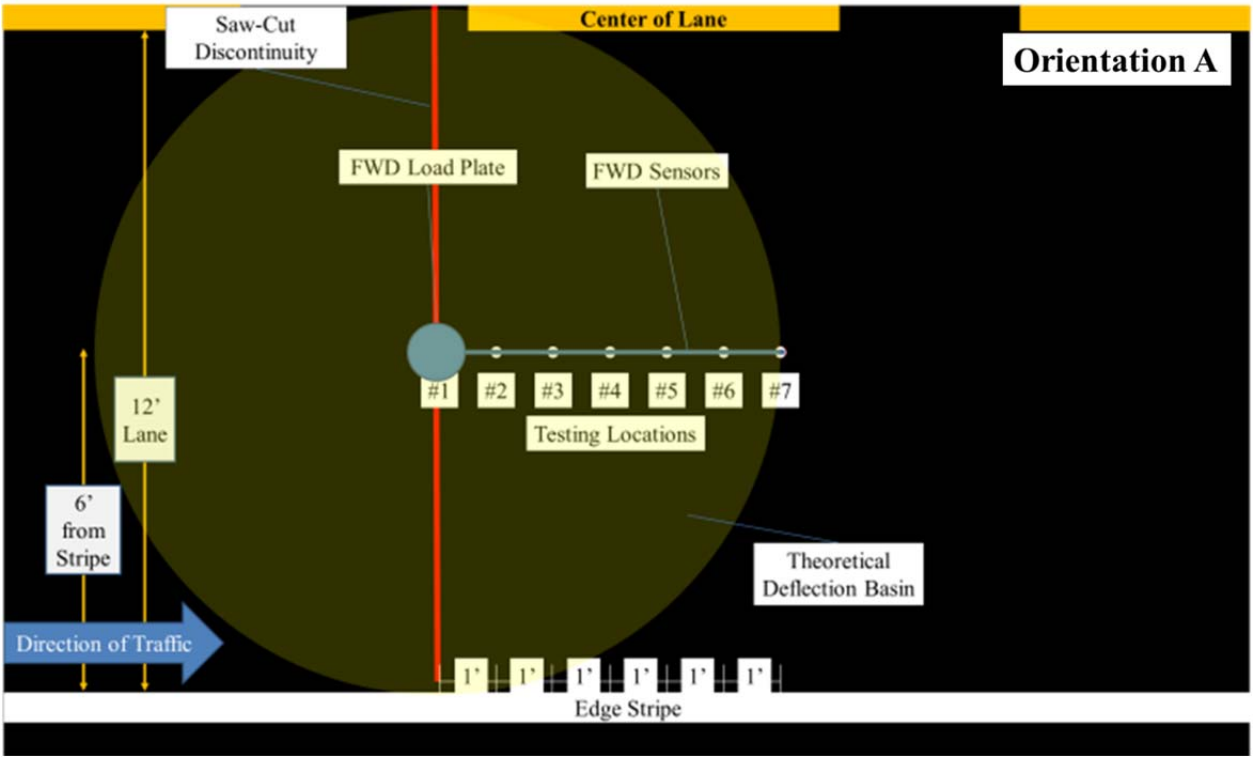
Saw-Cut Discontinuity
Center of Lane
Orientation A
FWD Load Plate
FWD Sensors
#1
#2
#3
#4
#5
#6
#7
Testing Locations
12' Lane
6' from Stripe
Theoretical Deflection Basin
Direction of Traffic
1'
1'
1'
1'
1'
1'
Edge Stripe

(a)

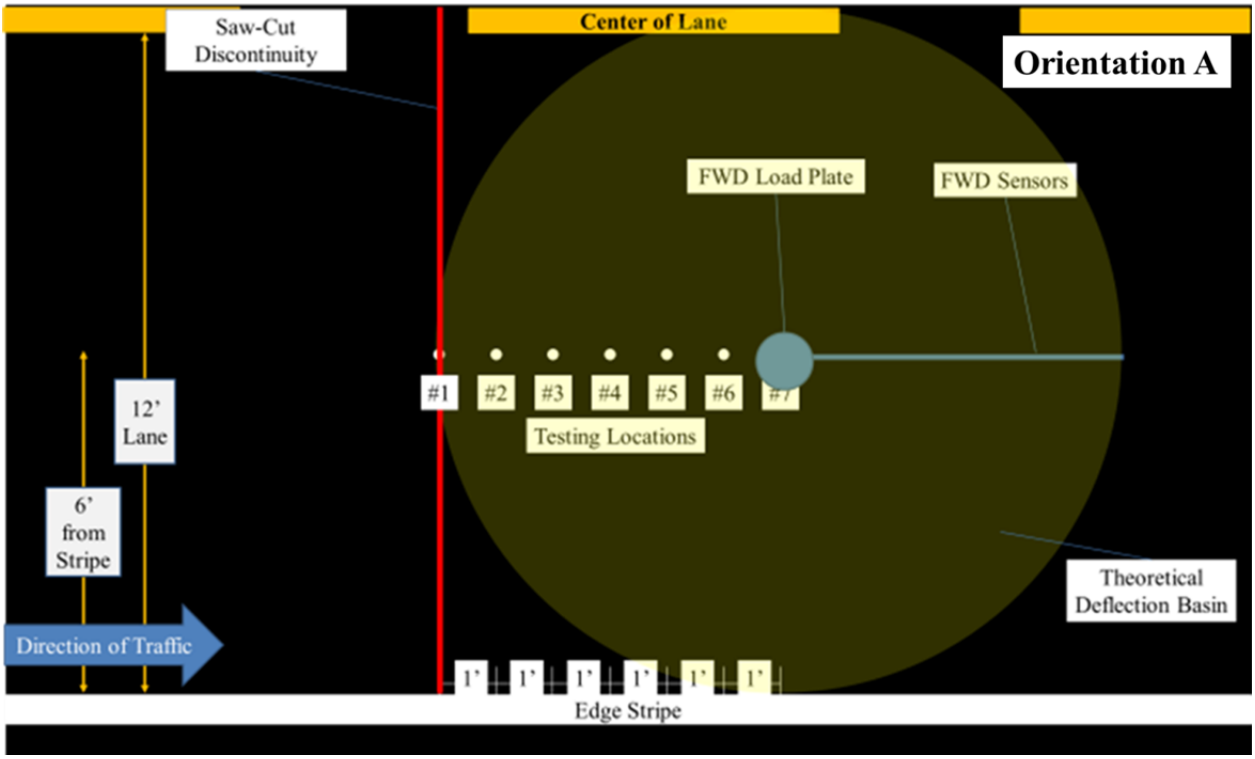
Saw-Cut Discontinuity
Center of Lane
Orientation A
FWD Load Plate
FWD Sensors
#1
#2
#3
#4
#5
#6
#7
Testing Locations
12' Lane
6' from Stripe
Theoretical Deflection Basin
Direction of Traffic
1'
1'
1'
1'
1'
1'
Edge Stripe

(b)

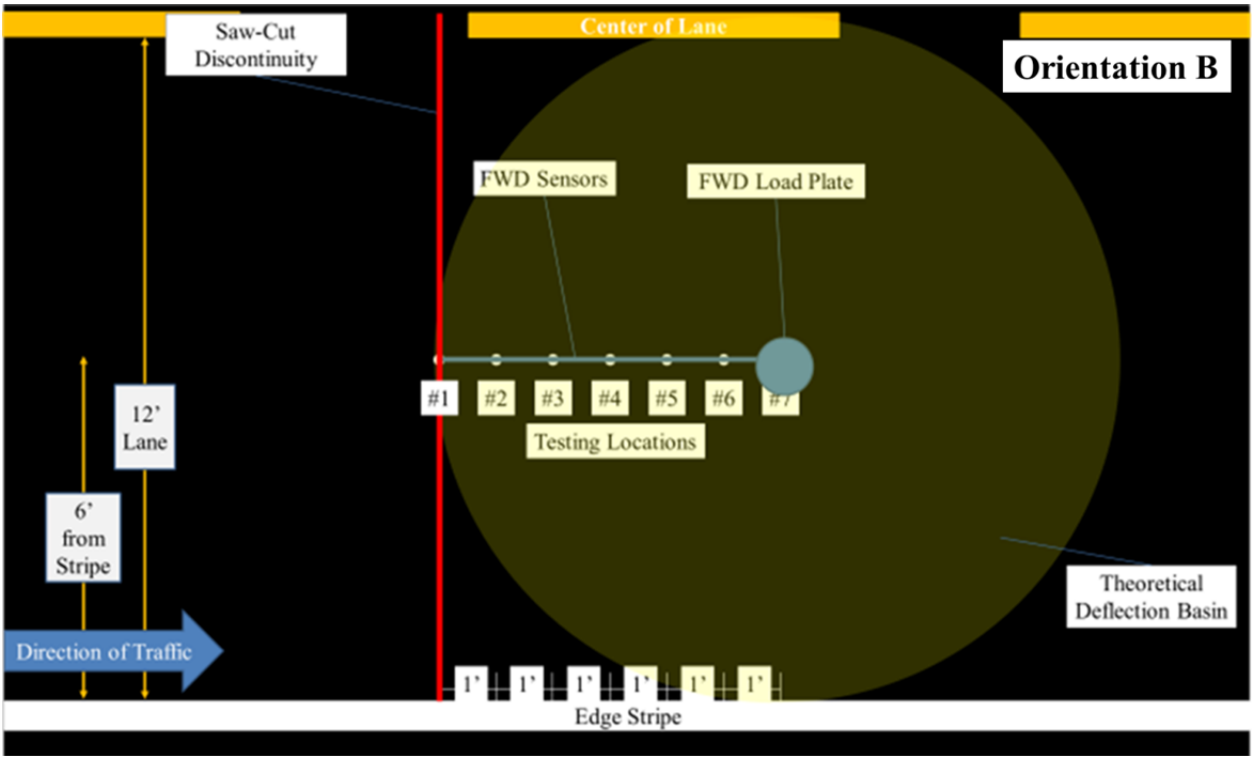

(c)

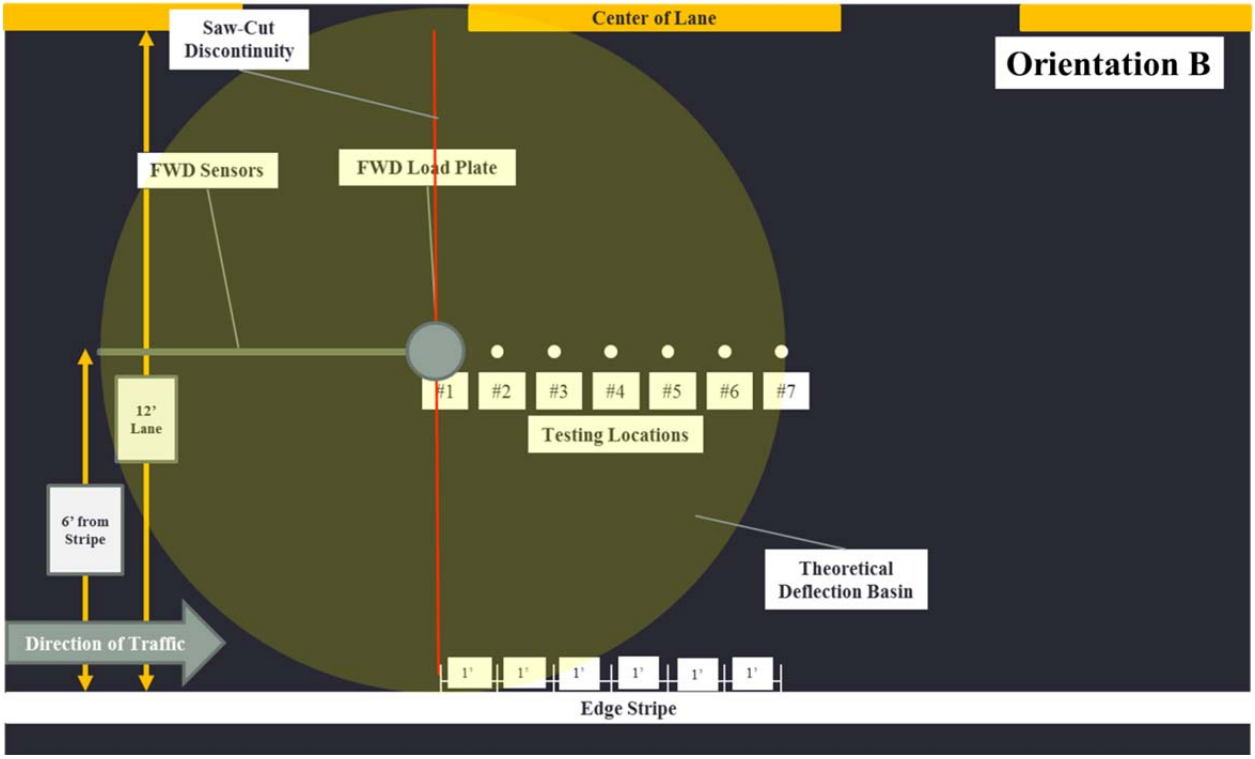

(d)

Figure 3.18 - Plan view of FWD testing procedure with discontinuity.

Testing at each site was completed in less than 33 minutes for all cases. Table 3.5 shows the time to complete testing at each site and the temperature change that occurred over that time. The time completed is the time between testing at location 1 in Orientation A and in Orientation B. All other locations had smaller changes in time and temperature. Over this time the pavement temperatures increased. Site 2 in the cut condition had a significantly higher temperature change during testing due to a slight delay from a software problem and the daily high temperature being greater that day (testing started at the same temperature as the first day but temperature increased faster).

Table 3.5 - Pavement Temperatures during FWD Testing

Site	Condition	Time Elapsed (min)	Start Temperature (F)	Finish Temperature (F)	Temperature Change (F)
1	Uncut	27	84.0	86.0	2.0
1	Cut	33	85.8	86.4	0.6
2	Uncut	22	88.5	90.5	2.0
2	Cut	28	88.7	93.6	4.9

At each location, the FWD testing protocol consisted of eight total drops. The first two were seating loads. Then two drops at target load levels of 6,000, 9,000, and 12,000 lbs. were conducted and the resulting deflections basins recorded. Linear regression was then used to determine the equivalent deflection at exactly 9,000 lbs. for each sensor. Thus, one deflection basin per location, orientation, and condition was generated for comparison.

3.3.2.4 Results

It was necessary to first determine if the orientation of the FWD sensors impacted the deflection basin prior to investigating the impact of the vertical discontinuity. The effect of FWD orientation was assessed by comparing the measured deflection with the FWD sensors in Orientation A to measured deflections in the Orientation B (comparing Figure 3.16 (a) with

Figure 3.16 (d) and Figure 3.16 (b) with Figure 3.16 (c). The results of this comparison are shown in Figure 3.19 in which all FWD sensors and locations are compared for both orientations. It can be seen that overall there is good equivalency between the two orientations as the slope of the linear trendline is 0.9774, with 1 representing perfect agreement. The smaller deflections are along the line of equality but as the deflections increased the Orientation B deflections become slightly larger. This is likely attributed to the temperature increase that occurred from testing Orientation then Orientation B. As the temperature increases, the AC becomes less stiff resulting in increased deflections.

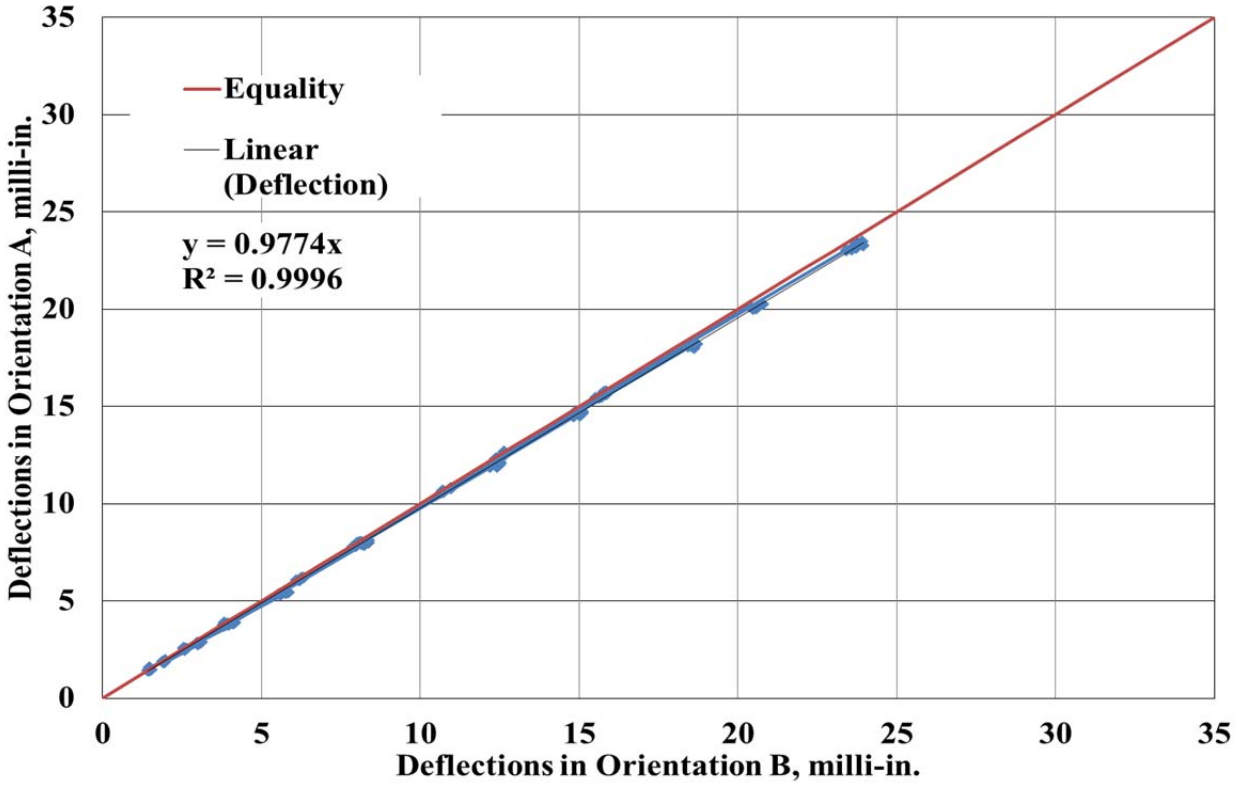

Figure 3.19 - Comparison of FWD orientation on uncut pavement.

After establishing that the orientation of the FWD trailer did not affect the measured deflections in an uncut condition, it was necessary to determine if this held true for pavements

with a vertical discontinuity. Similar results can be observed for comparisons of orientation at each location after the pavement was cut, shown in Figure 3.20. It can be seen that the overall magnitude of the deflections has increased with a severe discontinuity in the testing region and that the slope of the linear trendline has slightly decreased from the uncut section to 0.9734. Visually, it appears that more of the deflections are higher than the line of equality for Orientation B. This may be attributed to the largest temperature increase at a specific location being included in this dataset. Overall, this agreement is very good considering that in Orientation B the sensors are directly over the vertical discontinuity whereas in Orientation A the sensors are in the opposite direction and away from the discontinuity.

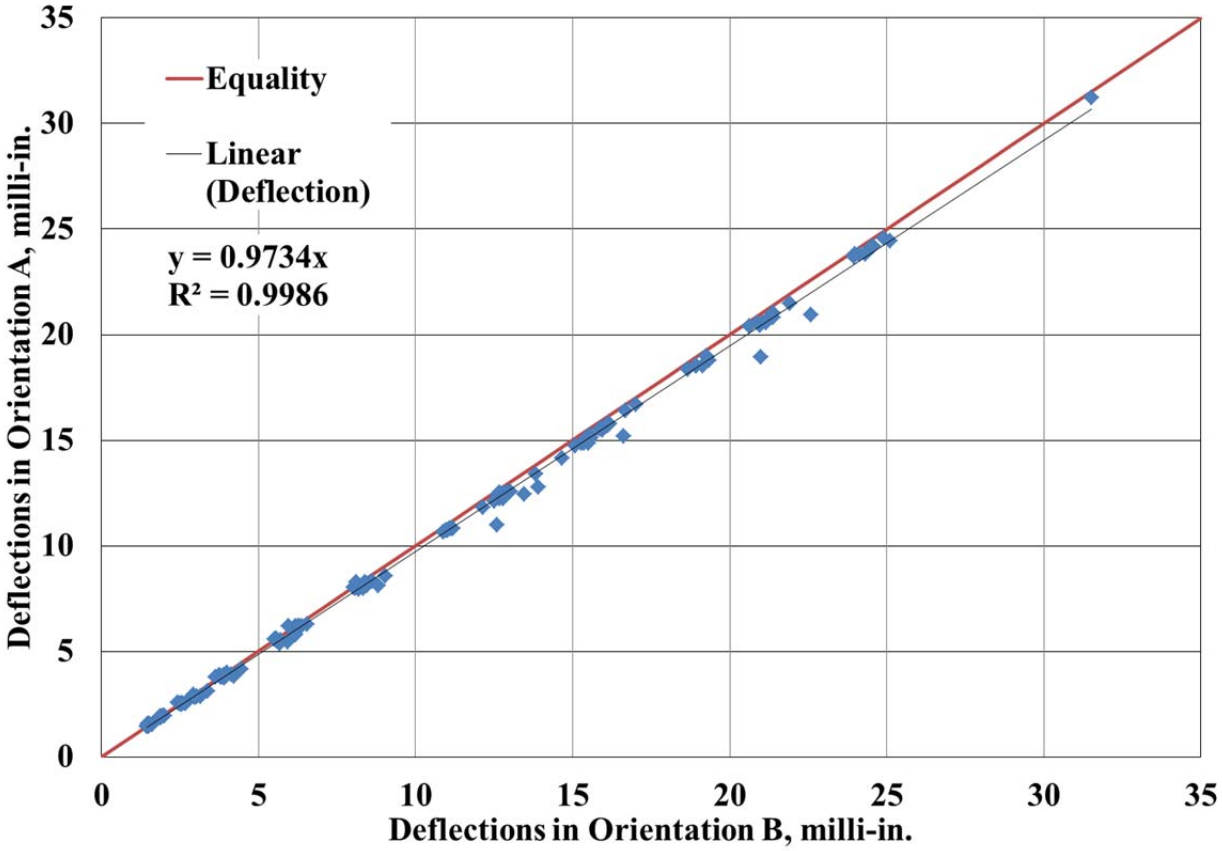

Figure 3.20 - Comparison of FWD orientation on cut pavement.

Next, it was necessary to determine how the deflection basin changed after the discontinuity was cut into the pavement. Figure 3.21 shows a comparison of uncut deflections with deflections measured at the same locations after the pavement was cut. It is apparent in Figure 3.21 that most of the data points are slightly to the right of or along the line of equality; however there are several data points that are a further away from equality. Further inspection indicated that these data points are from location 1 of each site. Thus, Figure 3.21 was split into multiple plots to directly compare deflections measured at each location in the cut and uncut condition.

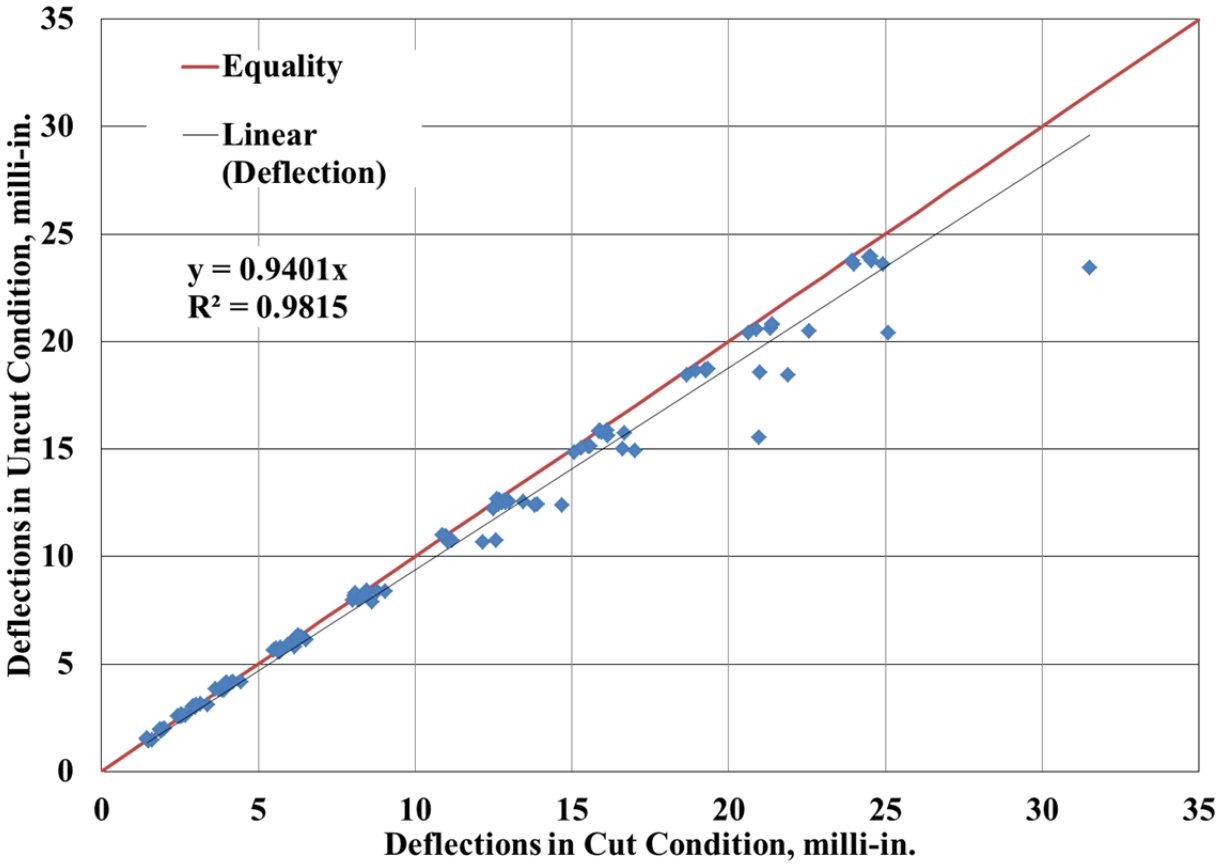

Figure 3.21 - Comparison uncut/ cut pavement deflections.

Figure 3.22 (a) through (f) shows the cut/ uncut comparison for locations1 through 6 of site 1. In the comparison for location 1 (Figure 3.22 (a)), the distance between the line of equality and the data points increases as the deflections increase. As illustrated earlier, the saw-cut discontinuity was cut through location 1. Thus, when the FWD load plate is placed directly over the vertical discontinuity there is a large increase in deflections for both FWD orientations. At location 2 (Figure 3.22 (b)), where the FWD load plate is centered 1 foot away from the vertical discontinuity, there is still increased deflections after the pavement was cut. There is a greater increase with the FWD in Orientation B in which the sensors are spanning over the discontinuity than in Orientation A. When the FWD load plate is centered 2 feet away from the discontinuity at location 3(Figure 3.22 (c)), the data points are only slightly greater than the line of equality and the slope of the trendlines are similar to the slopes observed from comparisons of the intact sections shown previously. In Figures 3.22 (d) through (f) the slopes of the trendlines continue to approach equality as the center of the FWD load is moved away from the discontinuity. A similar trend was observed for the testing on site 2 and the comparison plots from this site are presented in the appendix.

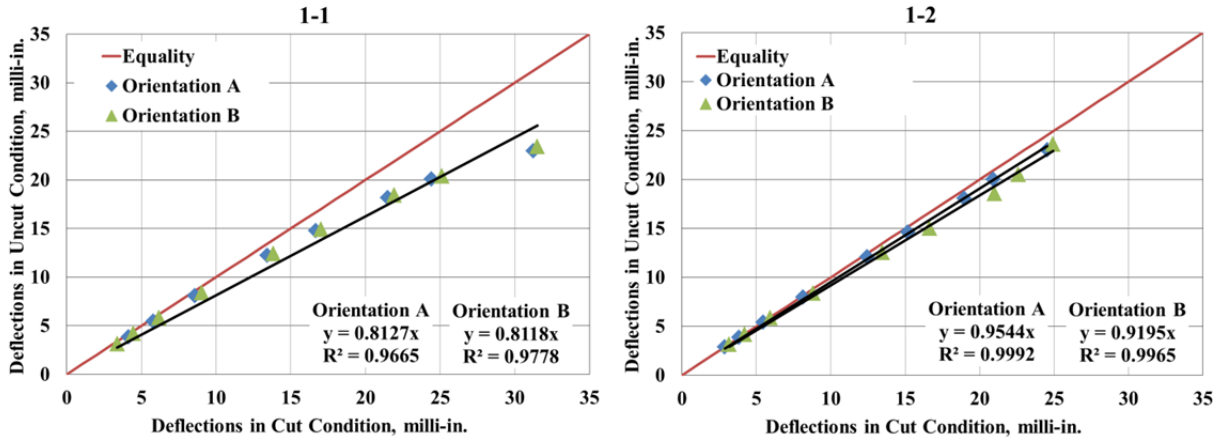

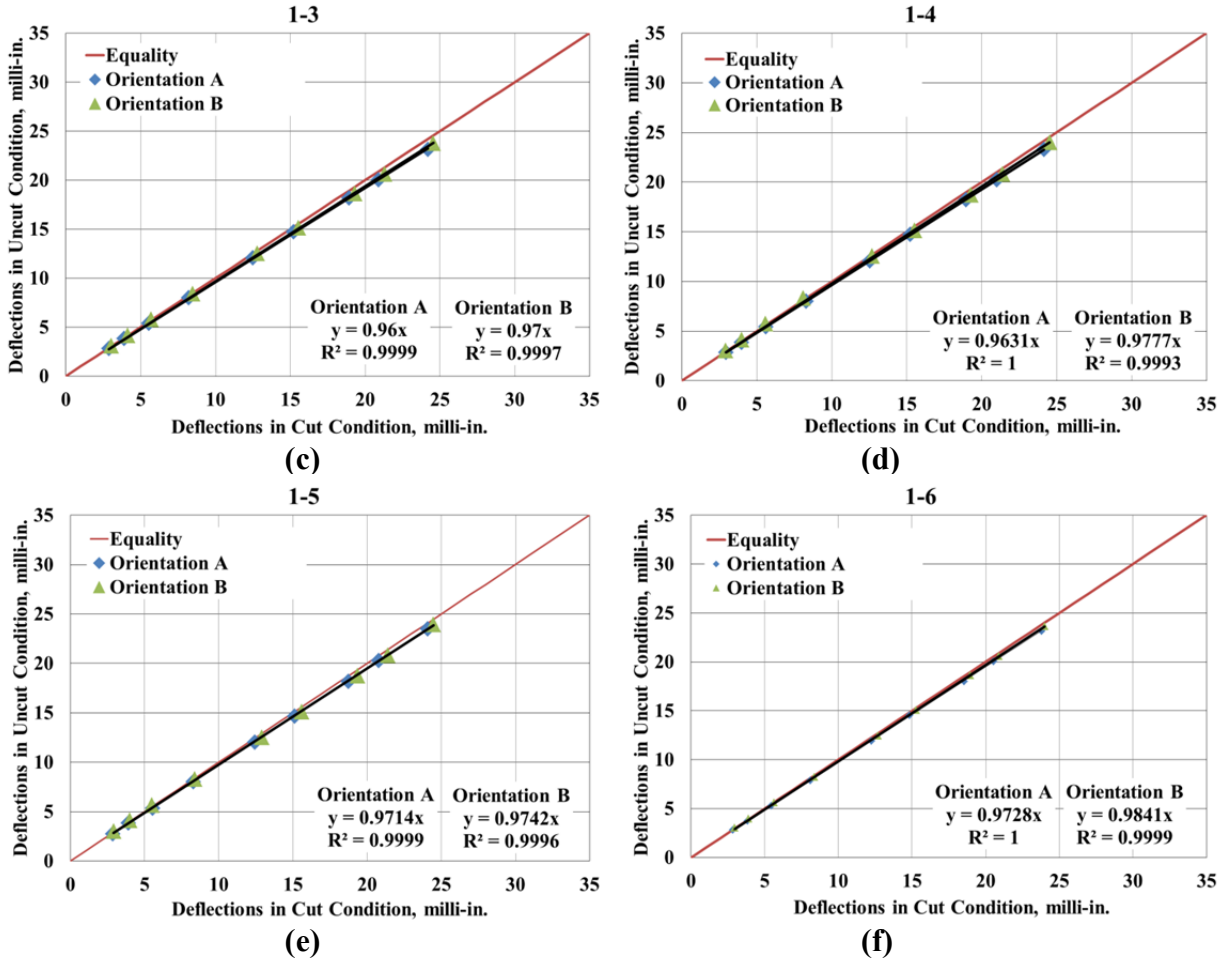

Figure 3.22 - Comparison uncut/ cut pavement deflections by location in Site 1.

A summary of the slopes for each trendline from each location in each orientation is presented in Figure 3.23. It can be seen that as the center of the FWD load plate moves further away from the saw-cut discontinuity, the deflections begin to approach equality. After a distance of 2 feet from the discontinuity the slope increase is less dramatic with distance. Thus for the temperature and pavement conditions used in this study, the discontinuity has an impact on the deflection basin when the load plate is within 1 foot of the discontinuity, regardless of trailer orientation.

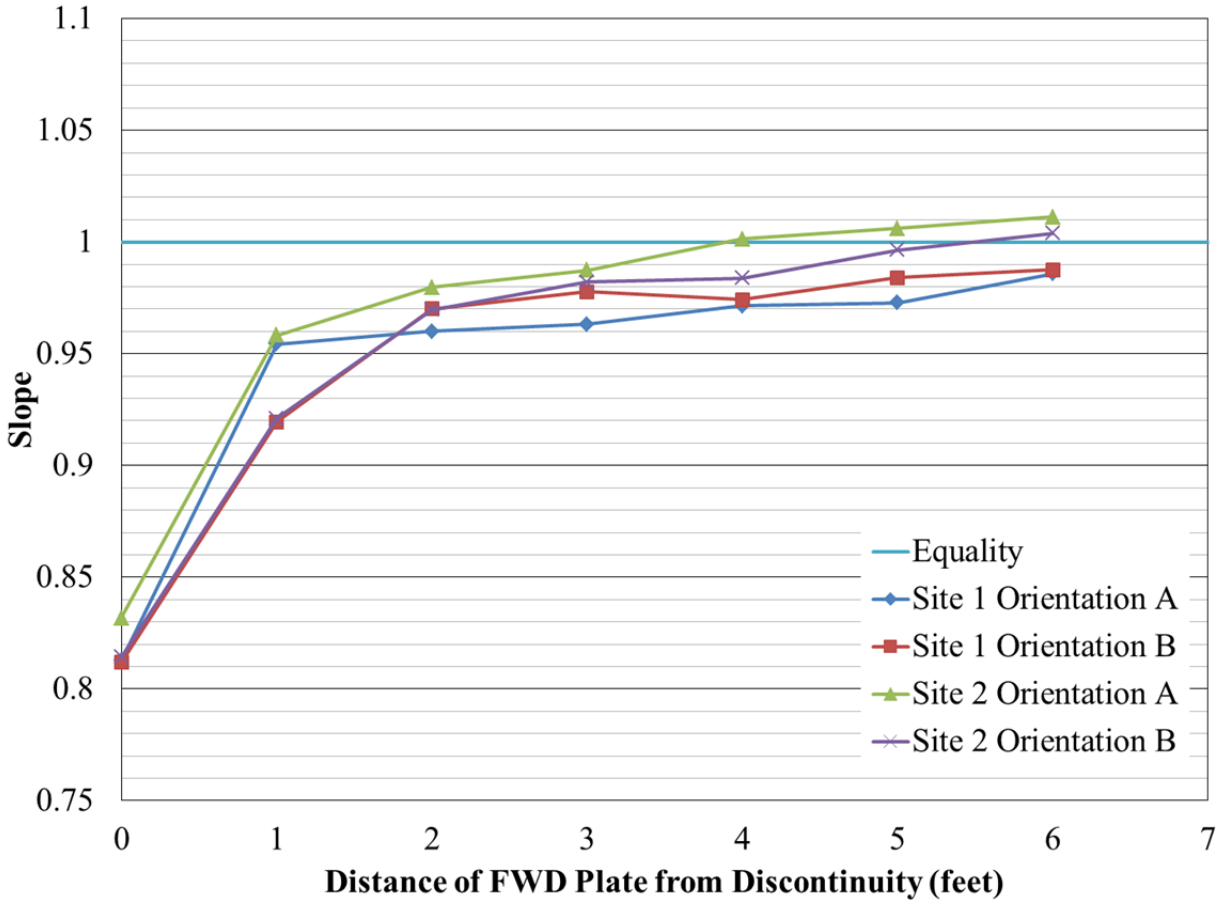

Figure 3.23 - Summary of slopes from uncut/ cut comparisons.

3.3.2.5 Summary and Conclusions

An investigation of FWD sensor orientation was undertaken to determine the impact of a discontinuity on deflection basins. FWD testing was conducted at the same location with the sensors located opposite orientations. A discontinuity was saw cut into the pavement and the FWD testing was repeated the following day once the equivalent pavement temperature had been reached. Multiple comparisons were made with respect to orientation and distance from the vertical discontinuity. From the testing results, the following conclusions have been drawn.

- The reduced FWD testing protocol at each station of two drops at three load levels was implemented to minimize the amount of time between testing each location (and the resulting change in temperature). This protocol was effective in producing repeatable deflection basins at different load levels in a reduced amount of time.
- Orientation of the FWD sensors had little to no impact on the measured deflection basin. The slight difference observed in deflections measured at the same location with different orientations are likely attributed to the minor increase in temperature that occurred over the testing time, as evident by the higher deflections occurring in Orientation B which was tested at higher temperatures.
- A distinguishable difference in the deflection basin from a vertical discontinuity was only observed when the center of the FWD load plate was located within 1 foot of the discontinuity, regardless of orientation. Although there was a greater difference in deflections when the load plate was 1 foot away from the discontinuity and the FWD sensors were spanning over the discontinuity (Orientation B), there was still a noticeable difference in deflections when the FWD was in the opposite orientation (Orientation A). When the center of the FWD load plate was located 2 feet away from the discontinuity there was only a slight difference in deflections. The difference in deflections continued to decrease as the distance from the FWD load plate to the discontinuity increased.
- Thus, for the purpose of assessing the condition of FWD testing locations over time, locations with surface cracks located within 1 foot (in any direction) were considered "cracked". FWD locations without cracking within 1 foot were considered "uncracked".

3.3.3 Cracking Data

Pavement sections were visually inspected for cracks on a weekly basis as part of the performance monitoring routine at the Test Track. As cracks were found, they were traced in white paint so they could be recorded with a camera mounted on a vehicle and the progression over time could be archived. Video recordings, panoramic pictures, or crack maps (depending on availability) were scrutinized to determine the extent of cracking at each of the 12 FWD stations. Each location was classified as either "cracked" or "uncracked". Based on the investigation presented previously, any location that had cracking within 1 foot (in any direction) of the center of the FWD load plate was classified as cracked. It was originally planned to classify cracking in greater detail based on proximity and severity but there was a lot of subjectivity to that approach. To make the cracking classification as transparent and repeatable as possible, it was decided to classify each station as "cracked" or "uncracked". Once a location was cracked there should be a noticeable change in the deflection basin. Examining each location prior to being cracked enabled the objective of detecting cracking prior to it appearing on the surface to be assessed.

As an example of how the condition was determined from video recordings, Figure 3.24 (a) shows a typical random location line as distress began to appear in the section. In the IWP there was a large cracked area and in the OWP there were several cracks. A circle with a 1 foot radius was superimposed over each FWD location (orange dots along white line) to determine if cracks were within 1 foot, as shown in Figure 3.24 (b). Both the IWP and OWP were classified as "cracked" despite the increased severity of the IWP because there were cracks within 1 foot of the FWD testing locations. This process was repeated for all FWD locations and testing dates. These data were summarized over time and an example summary from the 2012 Green Group –

Control RAP Section is shown in Table 3.6. Tables similar to Table 3.6 were generated for each section analyzed.

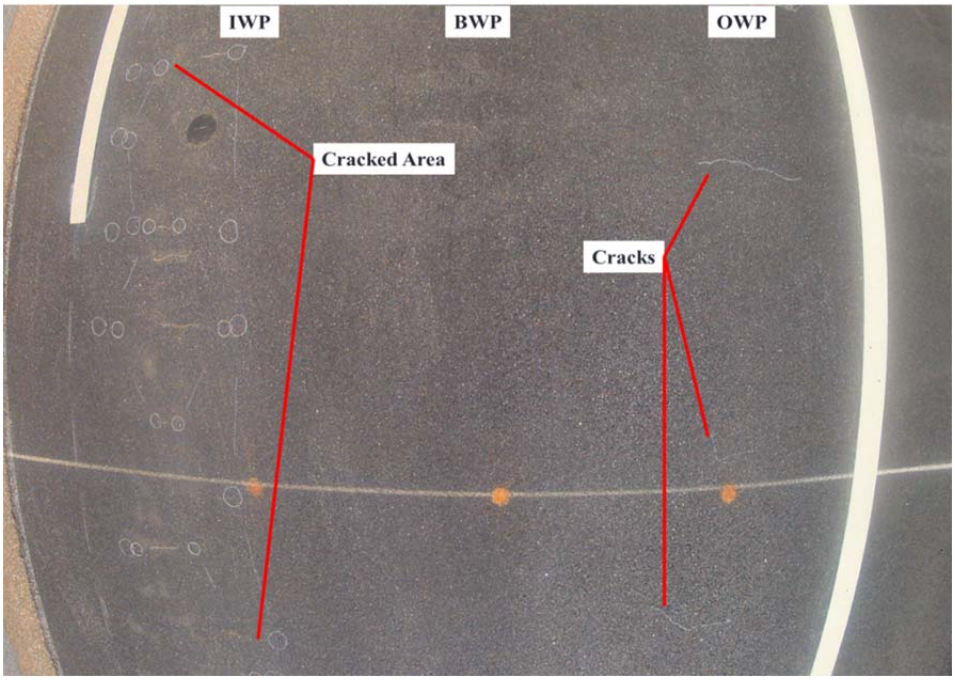

(a)

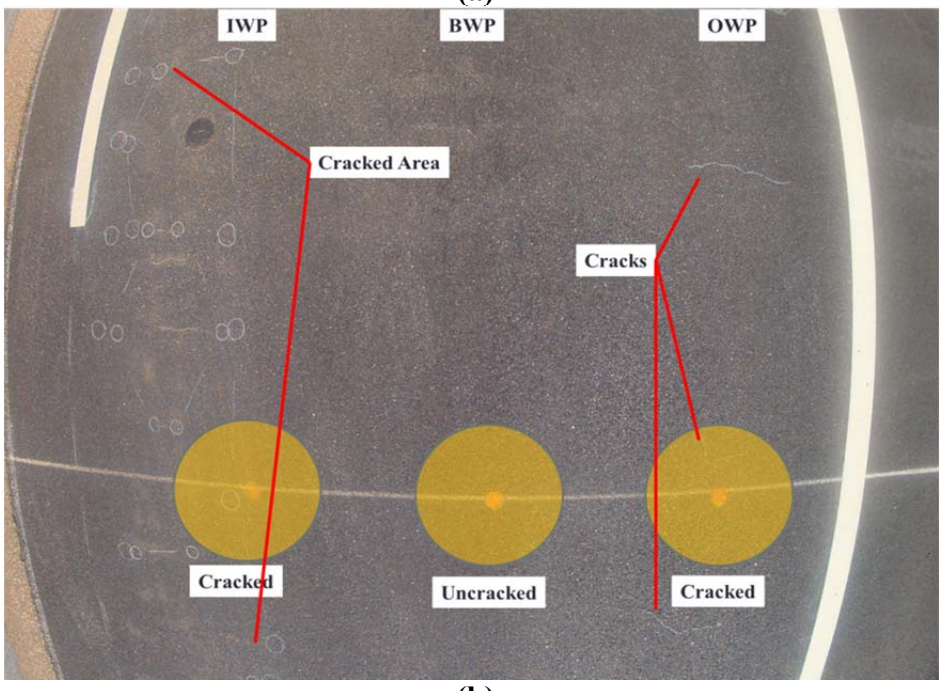

(b)

Figure 3.24– Cracking classification example.

Table 3.6 – Cracking with Date Summary Example

FWD Station	"Cracked" Date
N5-1	5/6/2013
N5-2	Uncracked
N5-3	5/13/2013
N5-4	8/19/2013
N5-5	Uncracked
N5-6	6/17/2013
N5-7	Uncracked
N5-8	Uncracked
N5-9	5/13/2013
N5-10	Uncracked
N5-11	Uncracked
N5-12	6/17/2013

3.4. Sections to be Analyzed

Test Track sections were selected to apply this methodology. The selected sections had a variety of documented failure mechanisms, including AC layer delamination, BUFC, and TDC, along with sections that did not have significant distress. Furthermore, the sections were chosen to include a broad range of AC thicknesses. In all sections assessed, significant rutting or problems with the granular layers were not factors in the failure.

3.4.1 2012 Green Group Sections

The Green Group (GG) experiment was conducted during the 2012 NCAT Test Track research cycle to improve overall pavement performance and sustainability by incorporating recycled materials. Reclaimed asphalt pavement (RAP), recycled asphalt shingles, and ground-tire rubber (GTR) were featured in research sections and compared to a section with typical levels of RAP. The four GG sections investigated are shown in Figure 3.25. The High RAP

section had a large amount of cracking much earlier than anticipated due to delamination and was reconstructed. Both the original and reconstructed High RAP sections were included in this investigation. The GTR section was not included in this study because it was believed to have cracked due to shear in the intermediate lift, a distress mechanism that was not considered in this work. BUFC was identified as the cracking mechanism in the Standard RAP Section. Layer delamination at the AC interface 2/3 was observed in the Original High RAP and the RAP/RAS sections; however, the time of on-set and rate of progression varied greatly between these two sections. The wide variety of cracking mechanisms and rates from the four sections made them ideal for further investigation in this research.

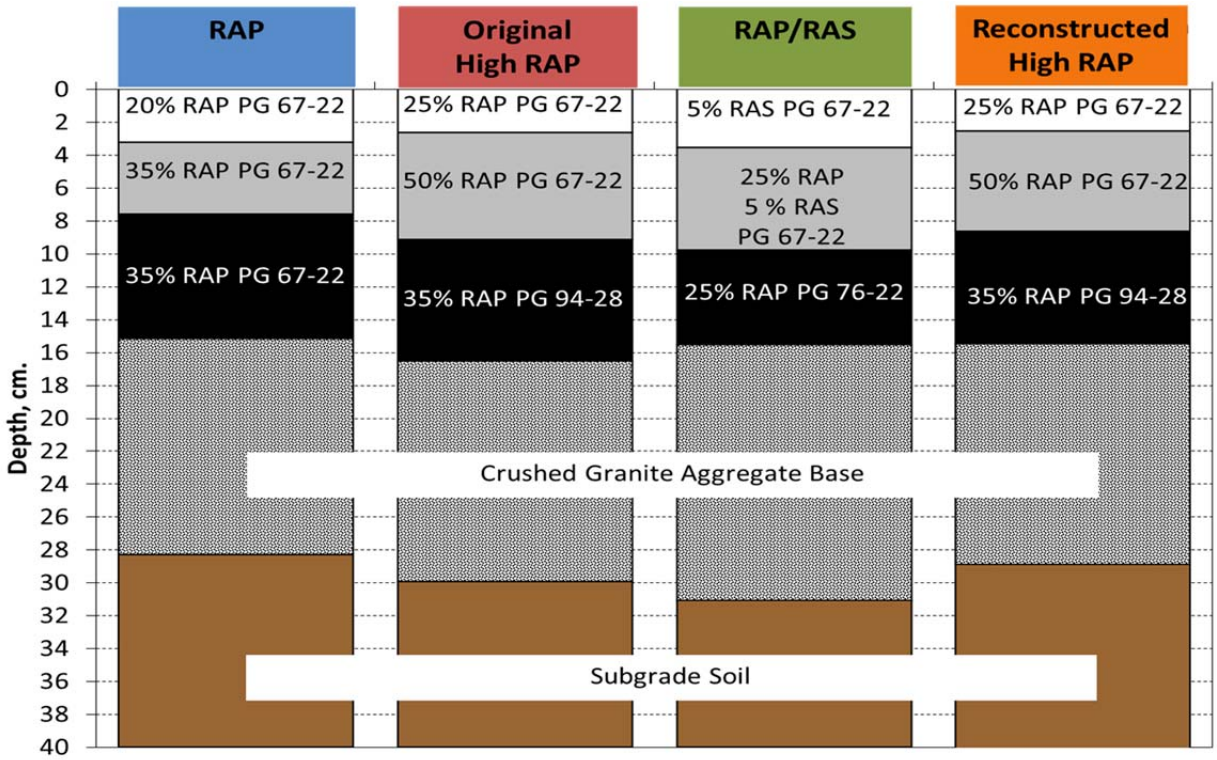

Figure 3.25 – Cross-section of 2012 Green Group (Vrtis and Timm, 2016).

3.4.2 2009 Group Experiment

The 2009 Group Experiment (GE) was initiated to evaluate the performance of sustainable technologies including warm mix asphalt (WMA), high RAP mixes, and porous friction courses (PFCs) (Vargas and Timm, 2013). Six structural sections were constructed on the Test Track during the summer of 2009. Each of the sections was designed to have seven inches of AC over six inches of aggregate base. The as-built cross-sections for the GE are shown in Figure 3.26. Three of the sections featured WMA technologies – foamed WMA, additive WMA, and foamed WMA with 50% RAP. The remaining three sections did not feature WMA – control, PFC, and 50% RAP.

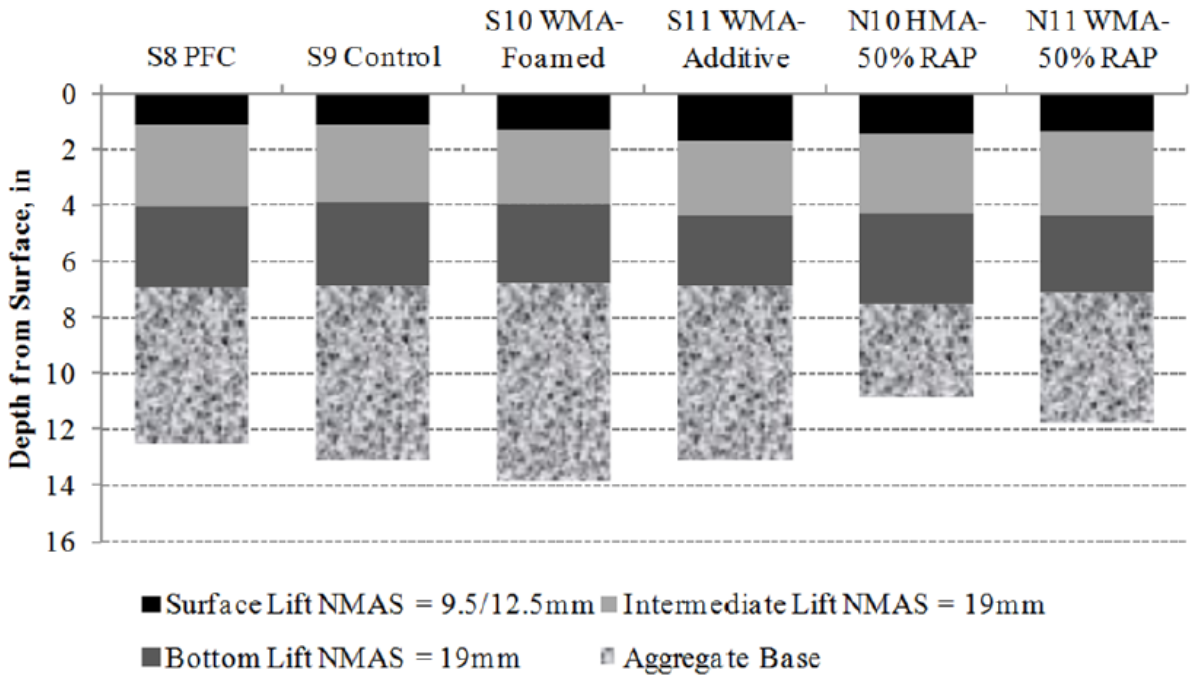

Figure 3.26 – Cross-sections of 2009 Group Experiment (Vargas and Timm, 2013).

There was no cracking observed during the 2009 research cycle and all rutting values were below the 12.5 mm experiment threshold. Traffic was continued through to the 2012

research cycle in which cracking did occur and some sections surpassed the experiment threshold requiring maintenance to be applied. The inclusion of the GE sections provided pavement sections that could be assessed over a longer duration and that performed well for several years before developing cracking.

3.4.2 2006 Florida Energy Ratio Study

The Florida Department of Transportation (FDOT) sponsored two structural research sections during the 2006 Test Track research cycle to validate the energy ratio (ER) concept developed at the University of Florida (Timm, et al., 2009). As shown in Figure 3.27, the only difference between the two sections was the binder grade used in the top two AC lifts. The difference in binder grade led to a large difference in the ER between the two sections, as shown in Figure 3.28. The greater the ER, the more resistance the mix has to TDC.

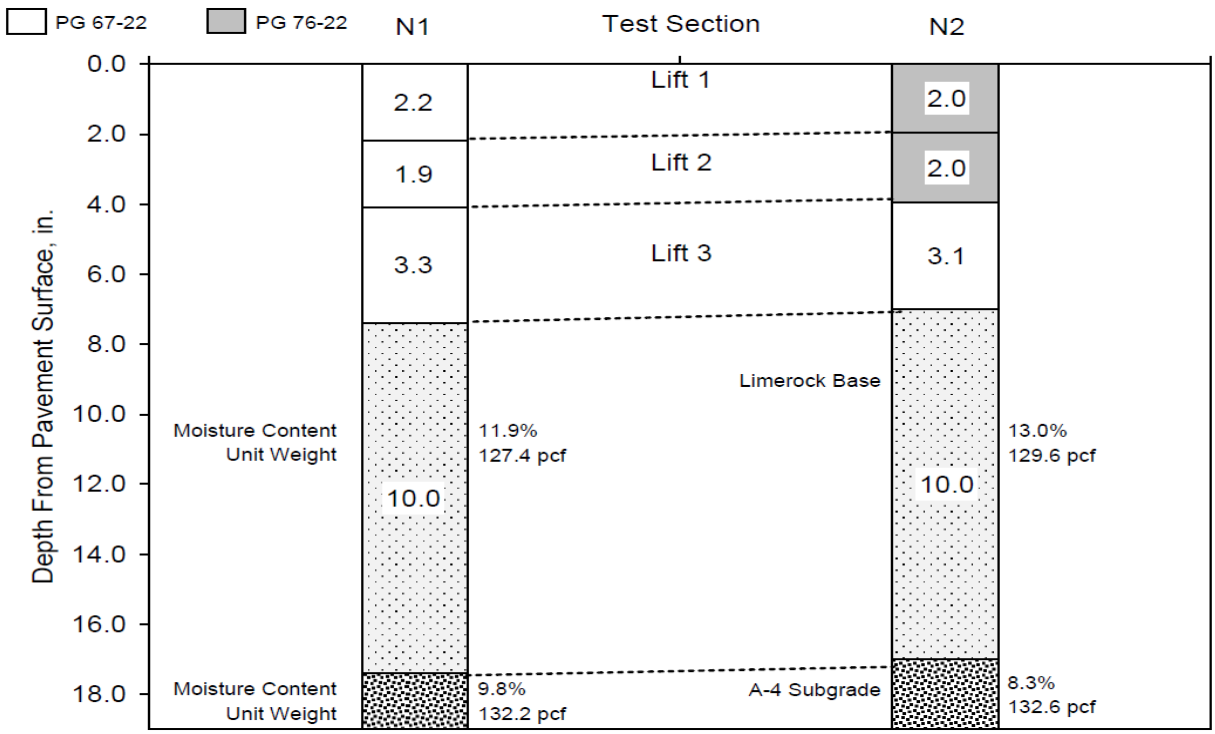

Figure 3.27 – Cross-sections of Florida ER Study Sections (Timm, et al., 2009).

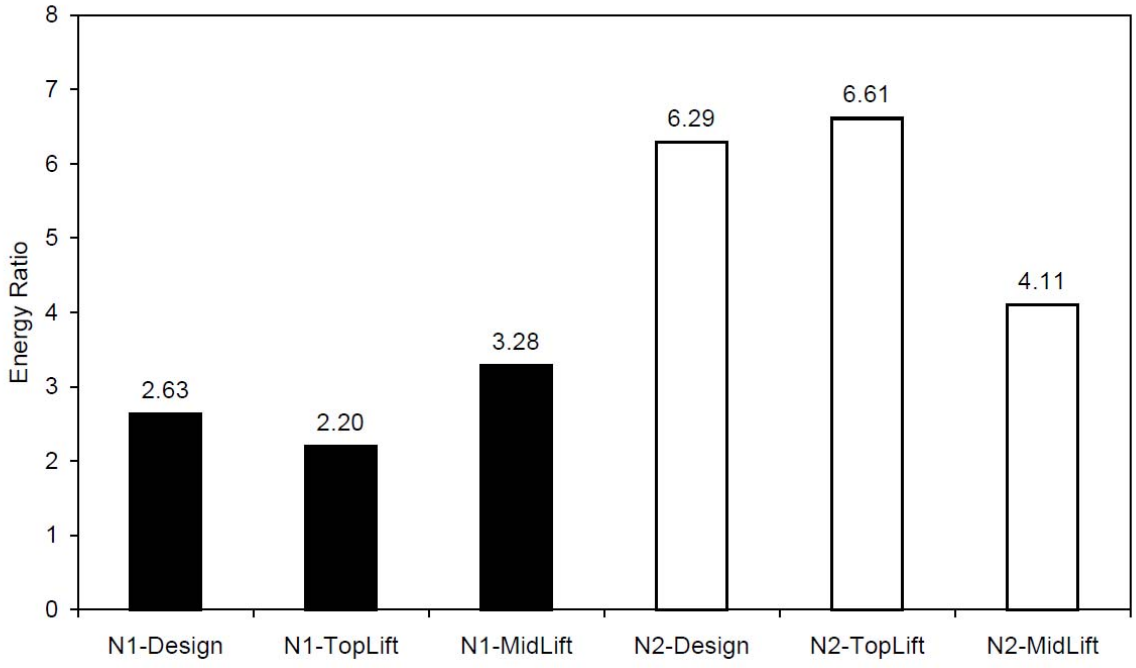

Figure 3.28 – ER Comparison of Florida ER Study Sections (Timm, et al., 2009).

Cracking was observed in section N1, the section with the lower ER, much sooner than in section N2. After cracking appeared in N1, it rapidly deteriorated to the point where a shallow mill and inlay was necessary. Forensic investigation of the sections verified that TDC was the primary distress mechanism and that the section with the higher ER was more resistant to TDC. Including the Florida ER sections in this research allowed the effect of TDC on FWD deflections to be assessed from field data. It provided an indication of whether or not DBPs can be used to assess the depth and nature of the cracks visible at the surface.

3.4.3 2003 Test Track Structural Sections

The structural experiment from the 2003 NCAT Test Track was selected for further evaluation in this research because it featured three AC thicknesses (5, 7, and 9 inch), had monthly FWD testing, and had a wide-range of documented performance, including AC layer delamination and BUFC. The experiment was initiated to investigate the effect of AC thickness and binder modification. An additional section (N8) was built to assess the effectiveness of a rich-bottom layer at improving the fatigue resistance of the AC. As seen in Figure 3.29, sections using unmodified and modified binder were constructed at each AC thickness (N1-N6). Companion sections N7 and N8 had an SMA surface layer and N8 had the rich-bottom AC layer (Timm et al., 2005).

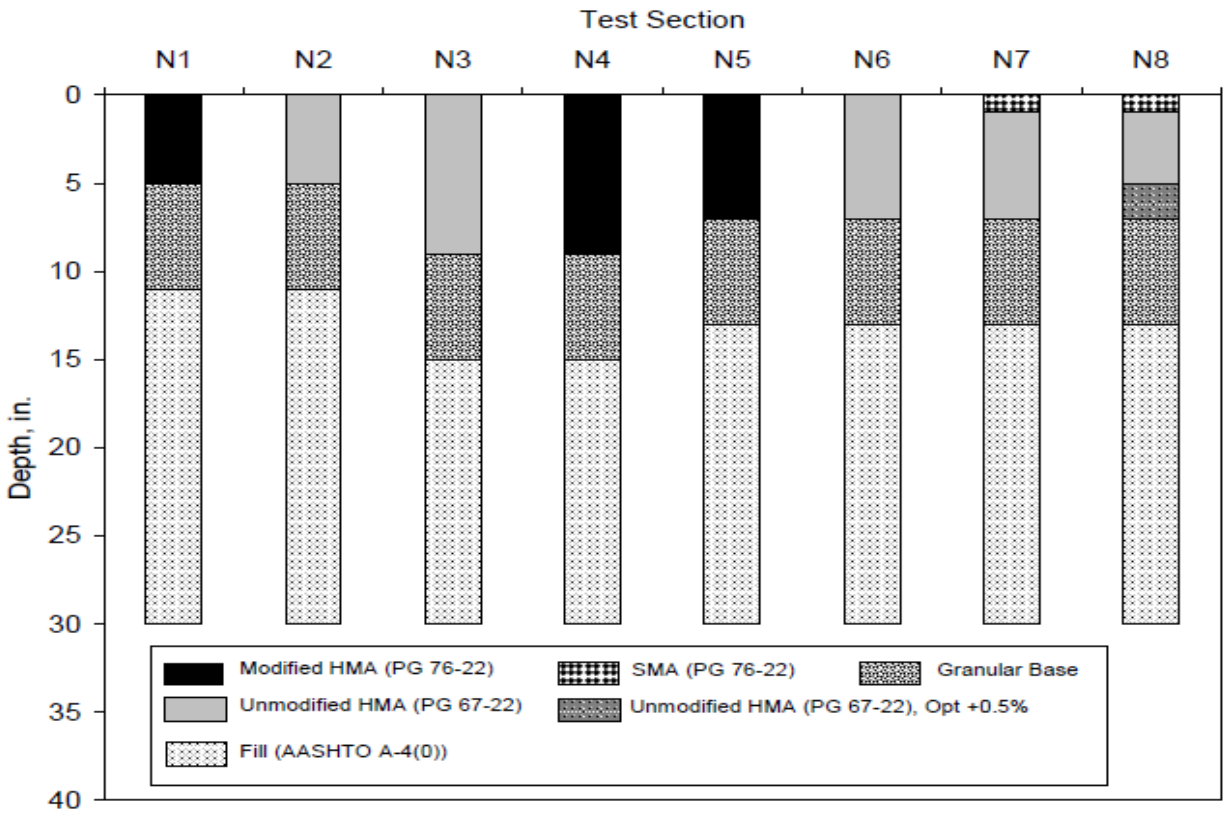

Figure 3.29 – Cross-sections of 2003 NCAT Test Track Structural Experiment sections (Timm et al., 2005).

Three sections (N1, N2 and N8) exceeded the cracking threshold of cracking in more than 20% of the lane area. Cores taken from the sections verified that the cracking in N1 and N2 was due to bottom-up fatigue. Further forensic investigation of N8 determined that layer delamination above the rich-bottom layer resulted in middle-up cracking (Willis and Timm, 2007). Sections N5, N6, and N7 all had some transverse cracking in the wheel path but the level of cracking did not surpass the experiment threshold. The thickest sections (N3 and N4) did not have any cracking observed at the surface in the research cycle.

It must be noted that the FWD testing done during this research cycle was conducted by the Alabama Department of Transportation and had seven sensors to measure deflection, instead

of the nine discussed previously. FWD testing was not conducted as frequently as later cycles. It was also not conducted on RL #4 or on BWP stations, therefore there were six stations available for analysis instead of the 12 available for later cycles. Surveyed layer thicknesses were not available for these sections. Therefore, design thicknesses were used in the BISAR simulations. Cracking at each station was determined from crack maps instead of video or photographs. These limitations provided an assessment of the sensitivity of the methodology to the reduced datasets and its ability to be applied by a broader audience.

3.4.5 Development / Validation Grouping

The sections discussed above were divided into development and validation groups, as shown in Table 3.7. The Development Group was analyzed first and used to identify critical DBP's and fine-tune the modeling procedures for each distress type. Particularly this group was used to determine the most appropriate modulus reduction percentage for BUFC and TDC. After completion of analysis of the Development Group, the methodology and modeling procedure was set before analyzing the Validation Group. Thus, the Validation Group was carefully selected to include sections of each design thickness and that had no distress, delamination, TDC, and BUFC.

Table 3.7 –Developmental and Validation Groups

Failure Mechanism	Group	Cycle	Section	Design Thickness (in.)
Delamination	Developmental	2012	S5	6
	Developmental	2012	S6	6
	Validation	2003	N8	7
TDC	Developmental	2006	N1	7
	Validation	2006	N2	7
BUFC	Developmental	2012	N5	6
BUFC	Developmental	2012	S5'	6
BUFC / TDC	Developmental	2009	N10	7
BUFC / TDC	Developmental	2009	N11	7
BUFC / TDC	Developmental	2009	S9	7
BUFC	Developmental	2009	S10	7
BUFC	Developmental	2009	S11	7
BUFC	Developmental	2003	N1	5
No Distress	Developmental	2003	N3	9
NA	Developmental	2003	N5	7
NA	Developmental	2003	N6	7
NA	Developmental	2003	N7	7
BUFC	Validation	2009	S8	7
BUFC	Validation	2003	N2	5
No Distress	Validation	2003	N4	9

3.5 Summary of Methodology

This chapter discussed the various datasets that were utilized in this work and explained how they were prepared to facilitate a comparison of field and theoretical deflections over time. The approaches taken to simulate the theoretical impact of delamination, BUFC, and TDC were described and the changes in DBPs from each simulated distress were presented. The FWD testing protocol at the NCAT Test Track was outlined and the corrections of measured deflections for load and temperature were documented. The sub-investigation used to determine the influence of cracking on FWD deflection basins was presented as background for the

criterion used to classify cracking at each FWD station. Lastly, the Test Track sections that were utilized were introduced and grouped for analysis of each type of cracking assessed.

CHAPTER 4. DELAMINATION GROUP RESULTS

Three Test Track sections had delamination between AC layers that was verified by forensic investigations. Two sections from the 2012 GG, S5-High RAP and S6-RAP/RAS, were used as developmental sections to refine the procedure to evaluate DBPs over time presented in Chapter 3. Methodology. The third section, 2003 N8-Rich Bottom, was used to independently validate the procedure finalized by the developmental group. The pavement structure of these sections is presented in Figure 4.1 and the documented delaminated interface is highlighted with a dashed-red line.

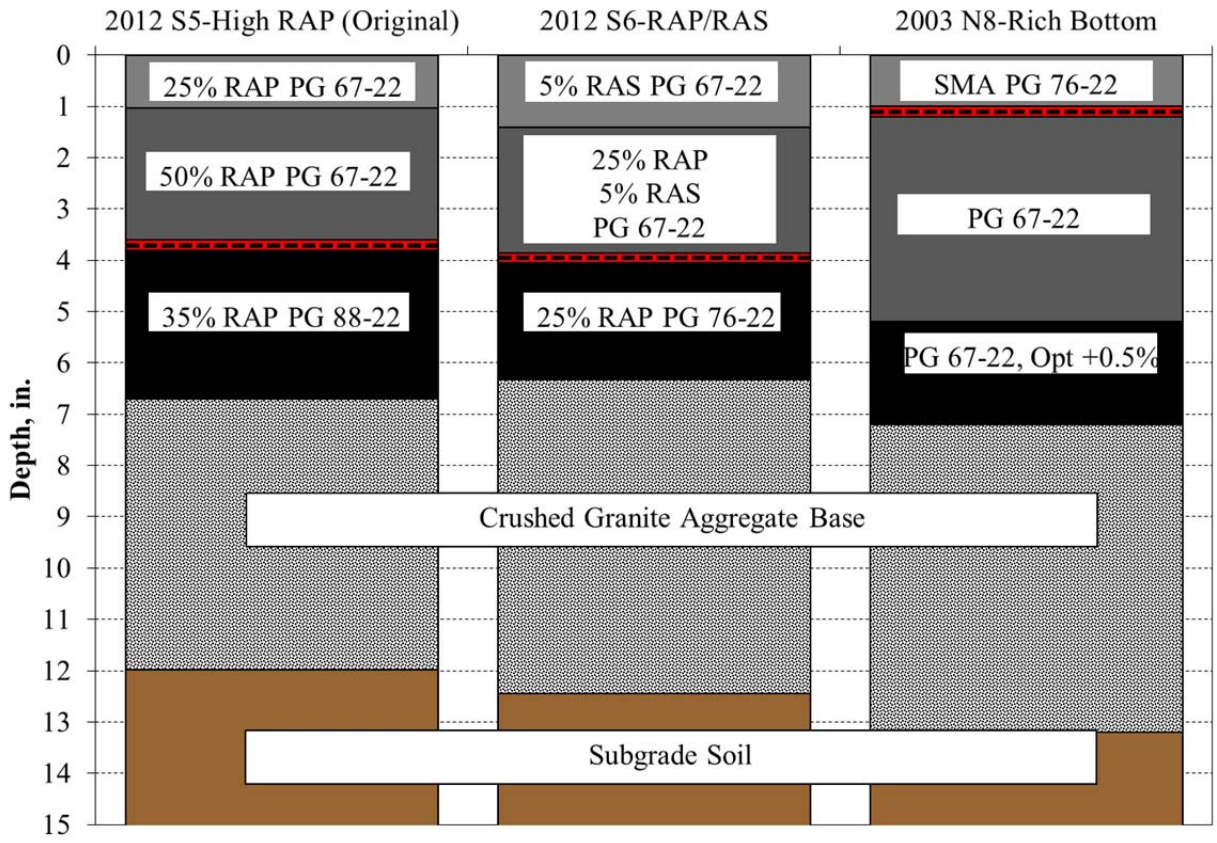

Figure 4.1 – Cross-sections of Delamination Group with delaminated interface in red.

4.1 Delamination Developmental Group

BISAR simulations were conducted for delamination of each interface (1/2 and 2/3) and delamination of both interfaces simultaneous, as shown in Figure 4.2. The largest increase in deflections was observed when both interfaces were delaminated. When the upper interface was delaminated there was less change in deflection than when the lower interface was delaminated. The percent change of DBPs generated from BISAR simulations were compared with the change of DBPs over time from measured FWD data.

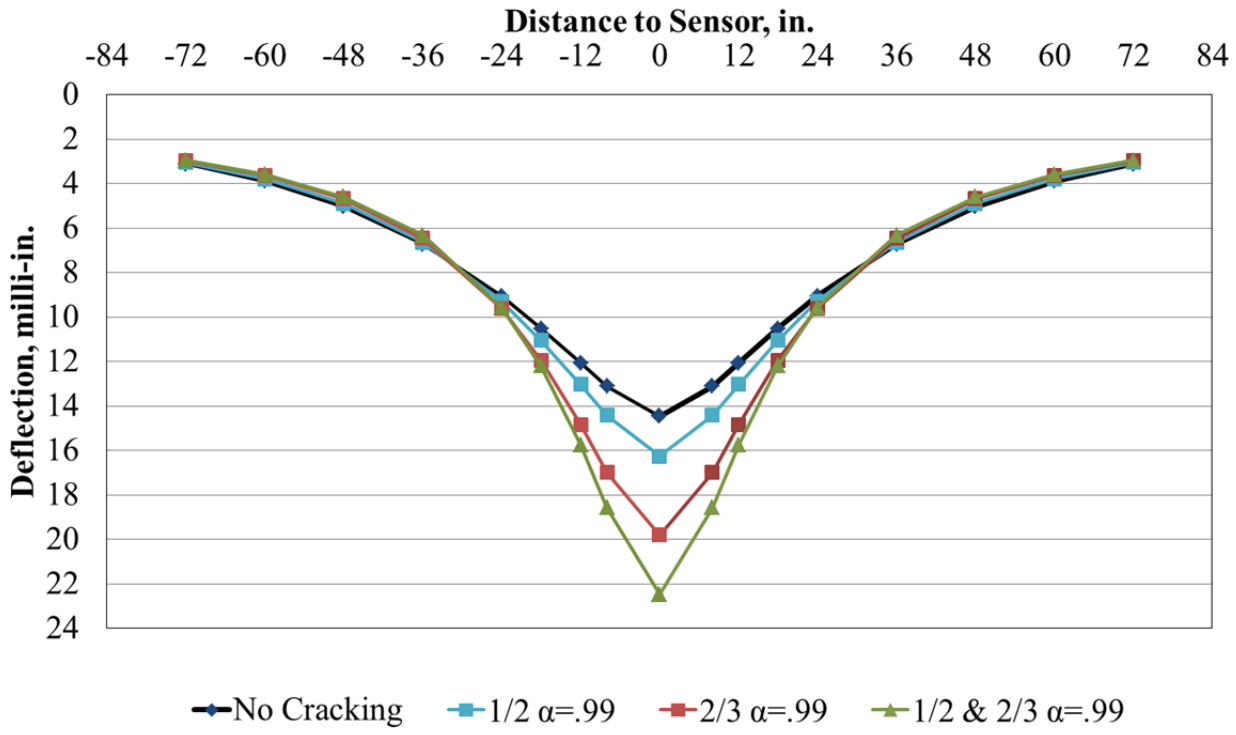

Figure 4.2 – BISAR simulated deflections from various delamination locations.

4.1.1 2012 GG S5-High RAP (Original)

Section S5 was designed to incorporate a high amount of RAP into six inches of AC. The section was constructed during the summer of 2012 with Test Track traffic beginning in October 2012. Cracking was first observed on April 8, 2013 and by April 22, 2013 the cracking had progressed past the predefined failure limit of cracking in 25% of the total lane area. The full depth of the AC was milled and the section was repaved on May 22, 2013. Although the thickness of the GG sections was selected to develop distresses within the three year Test Track research cycle, the rapid onset and progression of cracking was not expected. A forensic investigation was initiated and delamination of the 2/3 interface was identified as the origin of the distress development. Figure 5.3 shows cores taken during the forensic investigation. On core #1, the interface between lifts is apparent. In core #2, debonding at the lower interface can be seen. In core #3, a crack has developed out of this interface and in core #4 the crack has progressed to the surface. In core #5, the cracking has extended through the entire AC structure. Section S5 from the 2012 GG will be discussed in greater detail than other sections to provide the necessary background for the plots and tables that will be used to assess the effectiveness of the DBPs for each section.

(a) Cores taken from Original High RAP section

(b) Cores taken from Original High RAP section with cracking and delamination highlighted.

Figure 4.3 – Photographs of 2012-S5 at time of failure (Vrtis and Timm, 2015).

4.1.1.1 Modeling

The cross-section for S5, shown in Figure 4.1, was modeled in BISAR under a 9,000 lb. load with various levels of slip (α =0.00, 0.25, 0.50, 0.75, and 0.99) at the 2/3 interface. It can be seen in the BISAR simulation results, Figure 4.4, that there is a substantial increase in the deflections within 18 in. from the center of the load plate. The corresponding DBPs from these BISAR simulations are presented in Table 4.1. A color gradient is used in Table 4.1 to show the DBP's sensitivity to varying slip conditions (red = greatest change; white = no change). The

largest percent change from the fully bonded condition occurred in the full slip condition (α=0.99) and the SCI_8, SCI_{12}, ARE8, and AUPP were the most sensitive to the change.

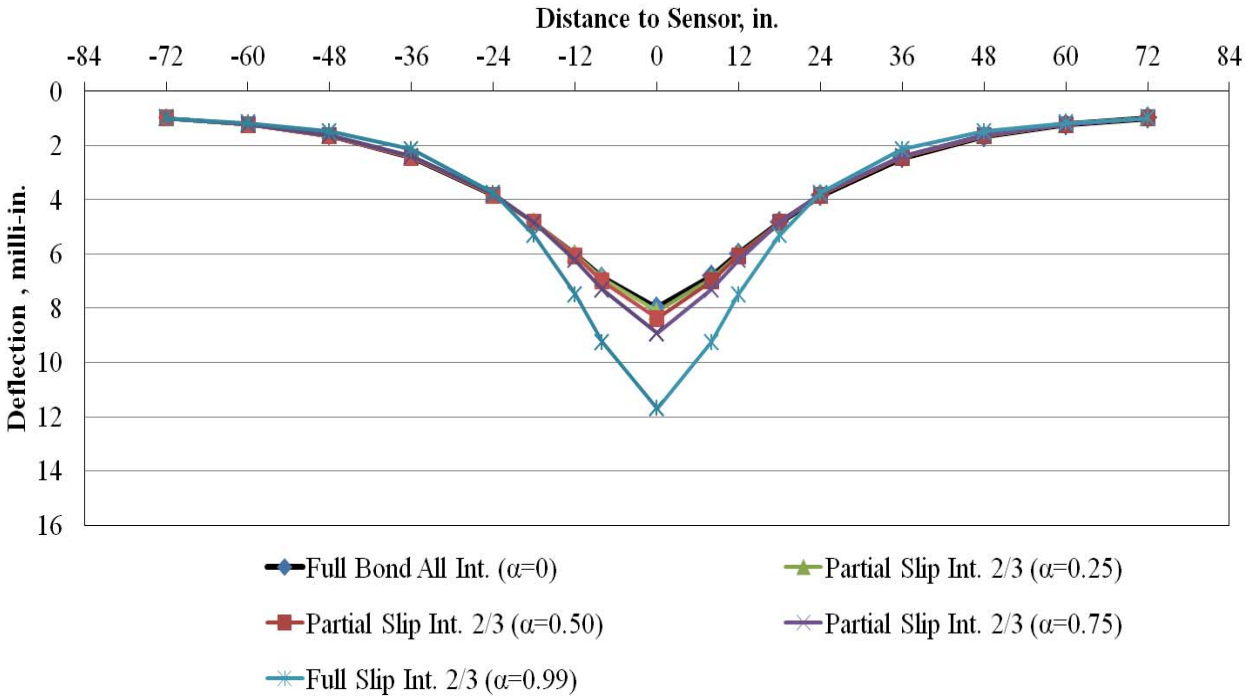

Figure 4.4 – BISAR simulation of 2012-S5 delamination with varying interface 2/3 conditions.

Table 4.1 – Change in DBPs from BISAR Simulation of 2012-S5

Description	% Change D_0	% Change AREA	% Change AUPP	% Change F_1	% Change SCI_8	% Change SCI_{12}	% Change ARE_8
No Slip (α=0.0)	0%	0%	0%	0%	0%	0%	0%
2/3 α=0.25	2%	1%	4%	3%	7%	6%	5%
2/3 α=0.50	5%	3%	11%	9%	18%	16%	13%
2/3 α=0.75	12%	7%	25%	20%	39%	36%	31%
2/3 α=0.99	47%	18%	90%	53%	110%	112%	102%

4.1.1.2 Field Data

Prior to April 1, 2013, there was not any cracking visible on the surface of this section. Cracking was first observed in the section on April 8 but not within one foot of any FWD station where routine testing was conducted. After April 22, 2013, the cracking failure threshold was exceeded and truck traffic began routing around the section to not damage the vehicles or create vertical dynamic forces (bouncing) that would impact the loading of sections downstream. The last date that cracking levels were recorded before reconstruction was also April 22, 2013. Table 4.2 shows the cracking levels at each FWD station. By April 22, eight of the twelve stations had cracking present. All BWP stations (2, 5, 8, and 11) did not have cracking within 1 foot of the FWD stations.

Table 4.2 – Cracking with Date Summary for 2012-S5

FWD Station	3/25/2013	4/8/2013	4/22/2013
		Condition	
S5-1	Uncracked	Uncracked	Cracked
S5-2	Uncracked	Uncracked	Uncracked
S5-3	Uncracked	Uncracked	Cracked
S5-4	Uncracked	Uncracked	Cracked
S5-5	Uncracked	Uncracked	Uncracked
S5-6	Uncracked	Uncracked	Cracked
S5-7	Uncracked	Uncracked	Cracked
S5-8	Uncracked	Uncracked	Uncracked
S5-9	Uncracked	Uncracked	Cracked
S5-10	Uncracked	Uncracked	Cracked
S5-11	Uncracked	Uncracked	Uncracked
S5-12	Uncracked	Uncracked	Cracked

The DBPs for station S5-10 are presented in Table 4.3 and the percent change of each DBP from its initial value is shown in Table 4.4. It is apparent from the color gradient in Table 4.4 that most of the parameters were sensitive to the documented delamination. Similar to the BISAR results shown in Table 4.1, SCI_8 and SCI_{12} had the greatest percent change in DBPs and AREA had the least. The comparison of the simulated DBPs with the DBPs generated from the field data for S5-10 is shown graphically in Figure 4.5. From the plot it can be inferred that delamination likely occurred prior to February 2013 because in early February the measured DBPs begin to exceed their values from the simulated delamination. The red "X" on each line indicates the date that the individual DBP surpassed the theoretical value (presented in Table 4.1)

and did not return below it. A dashed line was used to track the DBP after it surpassed the theoretical change threshold. Although there are dates in which the DBPs decrease from the previous testing date, none of the DBPs returned to below the threshold. This reduction from one point to the next was considered testing variability. It is likely that after delamination occurred, cracks generated at the layer interface propagated to the surface over the next month. Similar trends were found for the other IWP stations (S5-1, S5-4, and S5-7). At these stations the DBPs were capable of identifying delamination before cracking appears on the surface with D_0 and SCI_8 being the first DBPs to surpass simulated values for complete delamination.

Table 4.3 –FWD DBPs from 2012-S5-10

Date	D_0	AREA	AUPP	F_1	SCI_8	SCI_{12}	ARE_8
11/5/2012	14.815	21.352	18.084	0.784	1.721	3.665	11.253
11/26/2012	18.568	19.840	25.005	0.910	3.228	5.744	16.770
12/10/2012	17.117	20.652	21.893	0.849	2.594	4.747	14.314
01/14/2013	20.338	20.552	26.182	0.857	2.978	5.686	16.994
02/04/2013	23.984	20.025	31.929	0.894	3.799	6.988	20.926
02/18/2013	29.578	19.036	41.813	1.020	5.687	9.672	28.294
03/18/2013	27.349	19.305	38.049	0.986	4.943	8.715	25.509
04/01/2013	29.803	18.801	42.716	1.020	5.626	9.804	28.920
04/22/2013				“Cracked”			
04/22/2013	33.914	18.027	50.794	1.105	6.704	11.957	34.657

Table 4.4 – Percent Change of FWD DBPs from 2012-S5-10

Date	% Change AREA	% Change AUPP	% Change F_1	% Change SCI_8	% Change SCI_{12}	% Change ARE_8
11/05/2012	0%	0%	0%	0%	0%	0%
11/26/2012	6%	35%	16%	78%	50%	43%
12/10/2012	3%	21%	8%	50%	29%	27%
01/14/2013	4%	46%	9%	70%	54%	50%
02/04/2013	6%	76%	14%	114%	87%	82%
02/18/2013	12%	141%	30%	237%	174%	161%
03/18/2013	10%	110%	23%	183%	136%	125%
04/01/2013	12%	137%	30%	223%	166%	155%
04/22/2013	16%	181%	41%	285%	224%	206%

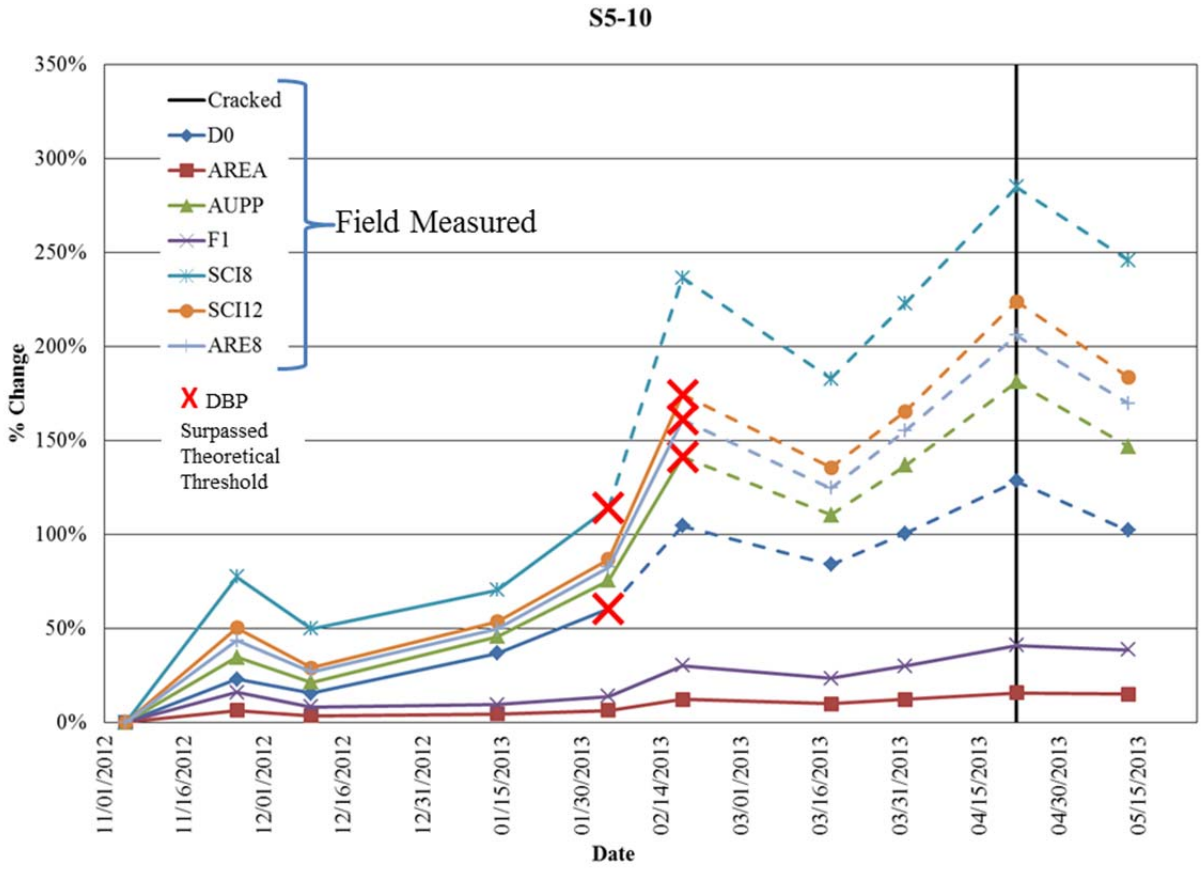

Figure 4.5 – Percent change in DBPs over time for 2012-S5-10.

Station S5-2 did not have any surface cracking. Table 4.5 presents DBPs from this station and the percent change of each is shown in Table 4.6. The same color gradient was used for Table 4.6 as previous tables; however, there is no distinguishable trend with time in Table 4.6. The highest percent change for the DBPs of S5-2 is SCI_8 at 78% which is less than the value from the simulated delamination of 110%. Thus, the DBPs do not indicate that complete delamination has occurred at this station. The DBP values are closer to the values obtained at the intermediate α values from the BISAR simulation. Thus, DBPs were capable of distinguishing between locations with and without distress. These results can be seen graphically in Figure 4.6.

Table 4.5 – FWD DBPs from 2012-S5-2

Date	D_0	AREA	AUPP	F_1	SCI_8	SCI_{12}	ARE_8
11/5/2012	12.430	22.640	13.838	0.681	1.413	2.707	8.499
11/26/2012	14.180	21.762	16.825	0.741	2.013	3.586	10.796
12/10/2012	13.731	22.443	15.513	0.688	1.741	3.149	9.737
01/14/2013	14.219	22.902	15.520	0.656	1.501	3.002	9.437
02/4/2013	14.123	23.005	15.295	0.635	1.664	3.091	9.578
02/18/2013	16.629	22.403	18.842	0.685	2.188	3.904	11.934
03/18/2013	15.491	22.987	16.799	0.654	1.934	3.387	10.594
04/01/2013	16.653	22.463	18.786	0.700	2.217	3.868	11.981
04/22/2013	13.966	23.723	14.288	0.614	1.445	2.783	8.768
05/13/2013	18.009	21.910	21.145	0.737	2.509	4.414	13.427

Table 4.6 – Change in DBPs from 2012-S5-2

Date	% Change AREA	% Change AUPP	% Change F_1	% Change SCI_8	% Change SCI_{12}	% Change ARE_8
11/05/2012	0%	0%	0%	0%	0%	0%
11/26/2012	3%	19%	9%	38%	29%	24%
12/10/2012	0%	10%	1%	20%	14%	13%
01/14/2013	1%	11%	4%	4%	9%	9%
02/04/2013	3%	5%	7%	6%	5%	5%
02/18/2013	0%	32%	1%	46%	37%	35%
03/18/2013	2%	20%	4%	32%	22%	22%
04/01/2013	1%	36%	36%	56%	42%	40%
04/22/2013	4%	4%	10%	3%	3%	3%

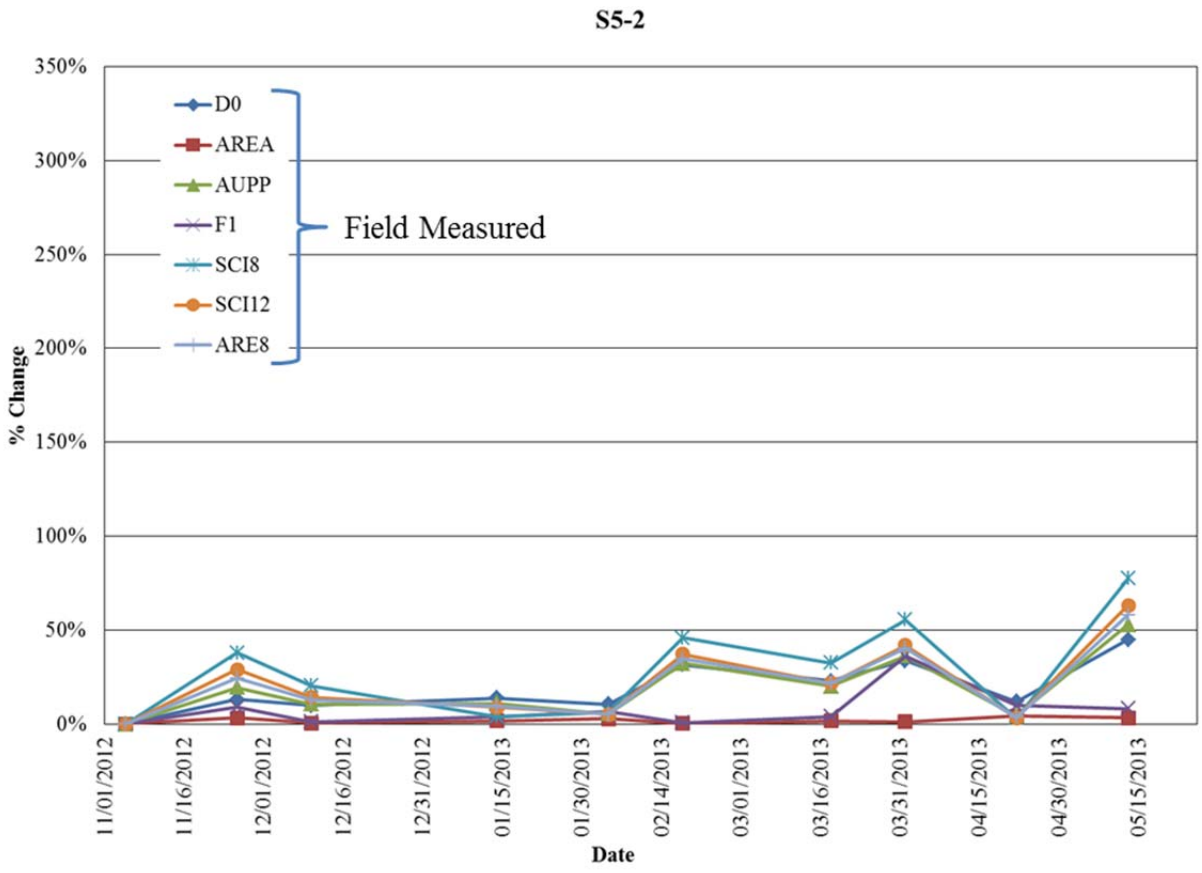

Figure 4.6 – Percent Change in DBPs over time for 2012-S5-2.

The other three BWP stations (S5-5, S5-8, and S5-11) had DBPs surpass the theoretical values for delamination despite being uncracked, which will be referred to as a False Positive. A False Positive was considered an inconclusive result in this research because it could not be definitively determined that cracking would have occurred at the station or if it was an error. Figure 4.7 is a plot of the change in DBPs over time for S5-8. Based on a comparison of Figures 4.7 and 4.5 and on the simulations, it is likely that cracking would have occurred at a later date given more time and traffic before reconstruction.

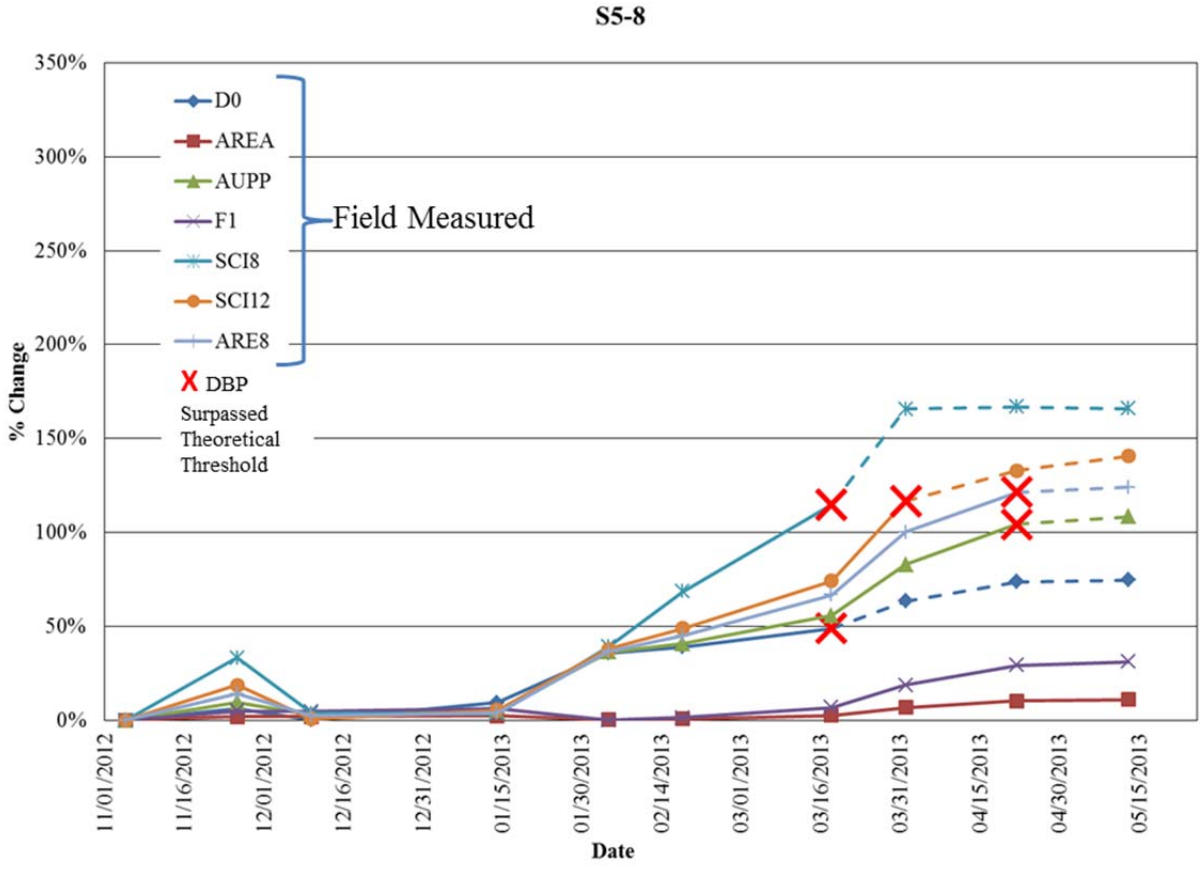

Figure 4.7 – Percent Change in DBPs over time for 2012-S5-8.

There were three stations that the DBPs did not surpass the theoretical values for complete delamination prior to cracking. These stations (S5-3, S5-6, and S5-12) were all located in the OWP. Stations S5-6 and S5-12 had D_0 exceed its theoretical threshold on the last day of testing as shown in Figure 4.8 and were classified as Late Predictions. It can be seen that despite the generally increasing trend over time none of the DBPs had a change greater than 50% until the last testing date. Station S5-3 did not have any DBPs exceed their thresholds. This was classified as a False Negative and is shown in Figure 4.9. False Negatives are troublesome because they indicate that this approach to predict cracking did not work. The reason for the False Negative was unknown but it is interesting that all the Late Predictions and the False Negatives were all in the OWP.

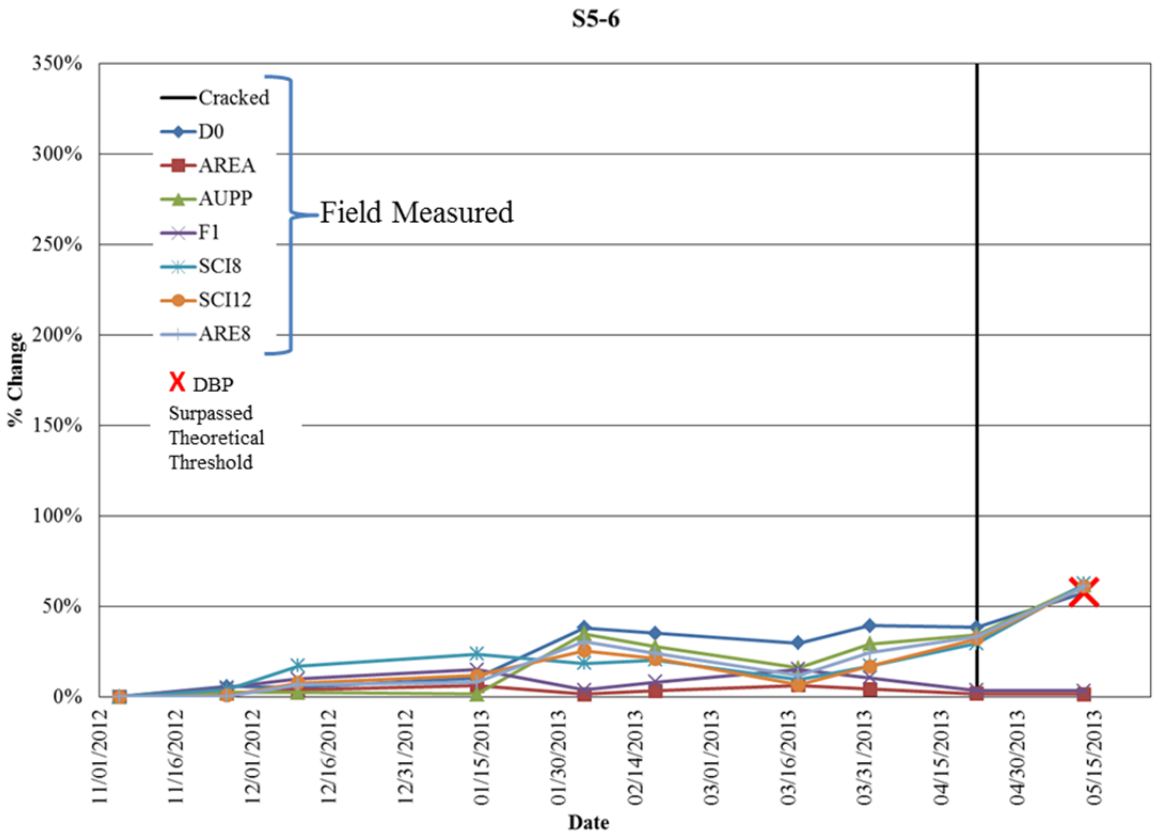

Figure 4.8 – Percent Change in DBPs over time for S5-6.

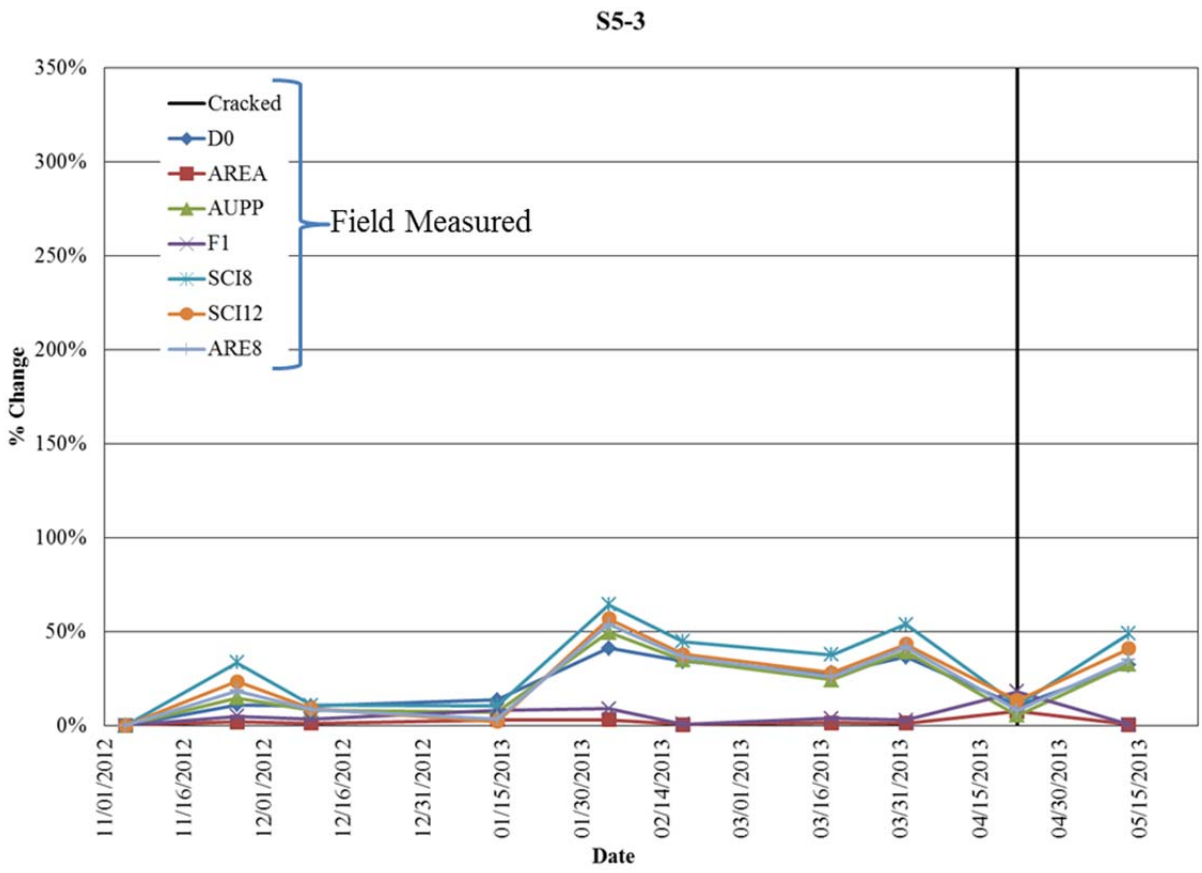

Figure 4.9 – Percent Change in DBPs over time for S5-3.

Each station assessed in this research was classified based on the change of the field DBPs compared to the its theoretical change as either "Early Prediction", "Late Prediction", "False Positive", "False Negative", or "No Cracking Observed No Cracking Predicted (NCO NCP)". The bullets below explain each of these classifications that were used throughout this research.

- Early Prediction – used when the change in DBPs from FWD testing exceeded its theoretical change prior to cracking being observed at that station. This was considered a successful result.

- No Cracking Observed No Cracking Predicted (NCO NCP) – used when the change in DBPs from FWD testing did not exceed its theoretical change and the station did not have any cracking observed. This was considered a successful result.
- False Positive – used when the change in DBPs from FWD testing exceeded its theoretical change but no cracking was observed at that station. This was considered an inconclusive result because it is unknown whether the station would have had cracking given more time and traffic.
- Late Prediction – used when the change in DBPs from FWD testing did not exceed its theoretical change until after cracking was observed at that station. This was considered an unsuccessful result but still shows some merit of DBPs capturing structural changes due to cracking.
- False Negative – used when the change in DBPs from FWD testing did not exceed its theoretical change at a station that had cracking. This was considered an unsuccessful result and was the worst of the classifications as it indicates that the DBPs were not able to capture the structural changes from cracking at any point during the timeframe analyzed.

A summary of the DBP's ability to predict cracking at each station in 2012-S5 is shown in Table 4.7. Stations S5-5, S5- 8, and S5-10 were False Positives in which the accuracy of the DBPs could not be assessed because it is unknown whether those stations would have had surface cracking if the section was not reconstructed but the DBPs indicate that it likely would have cracked. Not including those stations, the DBPs were successful at predicting the cracking performance for six stations and not successful for three stations. Of the three unsuccessful

stations, two had DBPs that surpassed after cracking (Late Predictions) and one (S5-3) had no DBPs surpass at all (False Negative). Again, it should be pointed out that the three stations in which the DBPs did not surpass theoretical values prior to cracking were all in the OWP. Overall, the results indicate that the DBPs were successful in capturing the changes due to delamination prior to cracking for this section. The best performing DBPs was D_0 because it was often the first DBP to exceed its respective theoretical value before cracking appeared.

Table 4.7 – Summary of DBP Prediction for Each Station in 2012 – S5

FWD Station	D_0	AREA	AUPP	F_1	SCI_8	SCI_{12}	ARE_8	1st Predictor	Classification
S5-1	Early	Never	Late	Never	Early	Late	Late	D_0, SCI_8	Early
S5-2	Never	Never	Never	Never	Never	Never	Never	NA	NCO NCP
S5-3	Never	Never	Never	Never	Never	Never	Never	NA	False Negative
S5-4	Early	Never	Early	Never	Early	Early	Early	D_0	Early
S5-5	Early	Never	Early	Never	Early	Early	Early	D_0	False Positive
S5-6	Late	Never	Never	Never	Never	Never	Never	D_0	Late
S5-7	Early	Late	Early	Late	Early	Early	Early	D_0	Early
S5-8	Early	Never	Early	Never	Early	Early	Early	D_0, SCI_8	False Positive
S5-9	Early	Never	Never	Never	Never	Never	Never	D_0	Early
S5-10	Early	Never	Early	Never	Early	Early	Early	D_0, SCI_8	Early
S5-11	Early	Never	Late	Never	Late	Late	Late	D_0	False Positive
S5-12	Late	Never	Never	Never	Never	Never	Never	D_0	Late
Summary: 5 Early, 3 False Positive, 1 NCO NCP, 1 False Negative, 2 Late									

4.1.2 2012 GG S6-RAP/RAS

Section 2012-S6 also had a design AC thickness of six inches. It was constructed during the summer of 2012 and Test Track traffic began in October 2012. Cracking was first observed on June 29, 2013. In October 2013 the right wheel path was patched toward the end of the section covering the BWP and OWP stations of RL#3 and RL#4 (S6-8, S6-9, S6-11, and S6-12).

The cracking threshold (cracking in 25% of the total lane area) was surpassed in December 2013. In early April 2014, the top 1.75 inches of the entire section was removed and replaced with a highly polymer modified binder mix. Cores taken from the section in September 2013 are shown in Figure 4.10. The middle core was removed delaminated at the 2/3 interface. It is not known whether the split was a result of the torque applied by the coring rig or previously split but it was an indication of a very weak interface either way. In the cores that were removed in one piece, the same interface was easily distinguishable and showed signs of cracking and flushing.

Figure 4.10 Cores taken from 2012-S6 in September 2013 (Vrtis et al., 2015).

4.2.1 Modeling

The theoretical change in DBPs for increasing values of α are presented in Table 5.8. The results are similar to those of S5, shown previously in Table 4.1, in which the highest change was seen for SCI_8 and SCI_{12} and the lowest change was for the AREA parameter.

Table 5.8 – Change in DBPs from BISAR Simulation of 2012-S6

Description	% Change D_0	% Change AREA	% Change AUPP	% Change F_1	% Change SCI_8	% Change SCI_{12}	% Change ARE_8
No Slip α=0.0	0%	0%	0%	0%	0%	0%	0%
2/3 α=0.25	1%	1%	3%	2%	5%	4%	4%
2/3 α=0.50	4%	2%	8%	6%	14%	12%	10%
2/3 α=0.75	9%	6%	19%	15%	30%	27%	23%
2/3 α=0.99	38%	15%	72%	44%	88%	89%	81%

4.2.2 Field Data

Although the first crack in this section was found on June 29, 2013, there was not cracking at any of the FWD stations until July 29, 2013. A table similar to the one shown for S5 in which the condition at each station on each available date was used in analysis but due to the larger date range of distress progression in S6, a summary table is provided instead. The dates that each section was first determined to be "cracked" are presented in Table 4.9. Stations S6-8 and S6-11 were patched prior to cracking appearing within 1 foot of the stations; therefore their "cracked" dates are labeled "Patched".

Table 4.9 – Summarized Cracked Dates for 2012-S6

FWD Station	"Cracked" Date
S6-1	2/17/2014
S6-2	11/4/2013
S6-3	8/26/2013
S6-4	9/30/2013
S6-5	2/17/2014
S6-6	10/21/2013
S6-7	8/26/2013
S6-8	Patched
S6-9	8/26/2013
S6-10	11/18/2013
S6-11	Patched
S6-12	7/29/2013

The DBPs did a better job of predicting cracking for this section than for 2012-S5. Table 4.10 shows the summary of DBP predictions. Overall, the percent change of the DBPs from FWD testing accurately matched the theoretical percent change for delamination of the 2/3 interface for 10 of 12 stations and no False Negatives occurred. Figure 4.11 shows the change in DBPs over time for station S6-3 which was typical for most of the stations in this section. The two stations that were not cracked prior to patching did not have changes in their DBPs that exceeded the theoretical changes. Again, D_0 was the most accurate and earliest predictors.

Table 4.10 – Summary of DBP Predication for Each Station in 2012–S6

FWD Station	D_0	AREA	AUPP	F_1	SCI_8	SCI_{12}	ARE_8	1st Predictor	Classification
S6-1	Early	Early	Early	Early	Early	Early	Early	D_0	Early
S6-2	Late	Never	Late	Never	Late	Late	Late	D_0, AUPP, SCI_8, SCI_{12}, ARE_8	Late
S6-3	Early	Late	Early	Late	Early	Early	Early	D_0	Early
S6-4	Early	Early	Early	Early	Early	Early	Early	D_0	Early
S6-5	Early	Early	Early	Early	Early	Early	Early	D_0, SCI_8, SCI_{12}, ARE_8	Early
S6-6	Early	Early	Early	Early	Early	Early	Early	D_0	Early
S6-7	Late	Never	Late	Never	Early	Early	Late	SCI_8	Early
S6-8	Never	Never	Never	Never	Never	Never	Never	NA	NCO NCP
S6-9	Early	Early	Early	Early	Early	Early	Early	D_0	Early
S6-10	Late	Never	Late	Never	Late	Late	Late	D_0, SCI_8, SCI_{12}, ARE_8	Late
S6-11	Never	Never	Never	Never	Never	Never	Never	NA	NCO NCP
S6-12	Early	Late	Early	Late	Late	Early	Early	D_0, SCI_{12}, ARE_8	Early
Summary: 8 Early, 2 NCO NCP, 2 Late									

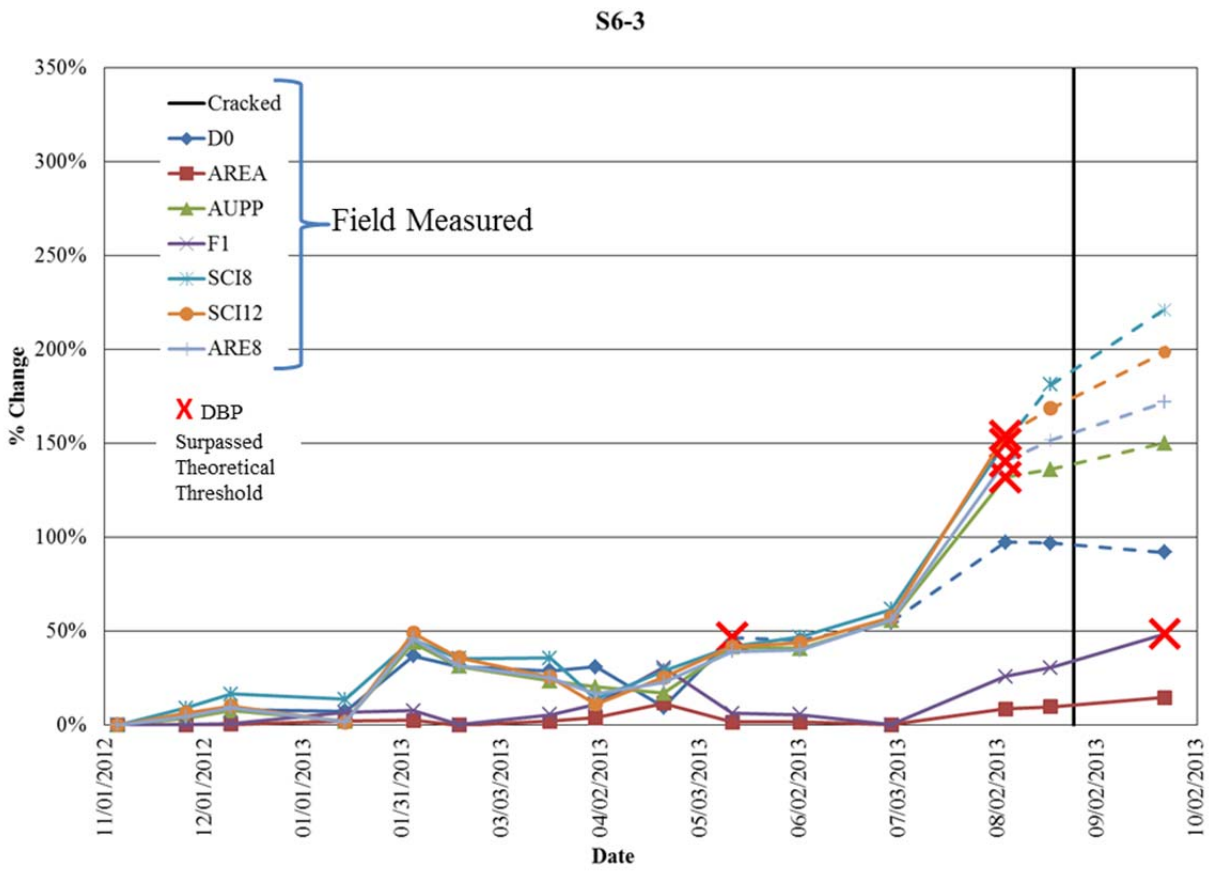

Figure 4.11 – Percent Change in DBPs over time for S6-3.

There were two stations (S6-2 and S6-10) that had DBPs exceed after cracking was observed. However, they had their theoretical values surpassed on the next FWD testing date. There was a month long gap in FWD testing and the date each section was cracked was in the middle of the FWD testing gap. Therefore, the FWD may have exceeded the theoretical change if FWD testing was conducted more frequently prior to cracking, thus improving the overall results of the section. Figure 4.12 shows the DBP trend observed in S6-2 and S6-10. It can be seen that on April 22, 2013 AUPP, SCI_8, SCI_{12}, and ARE_8 all exceeded the theoretical change for delamination. This was considered a testing anomaly because the theoretical change was not exceeded continuously.

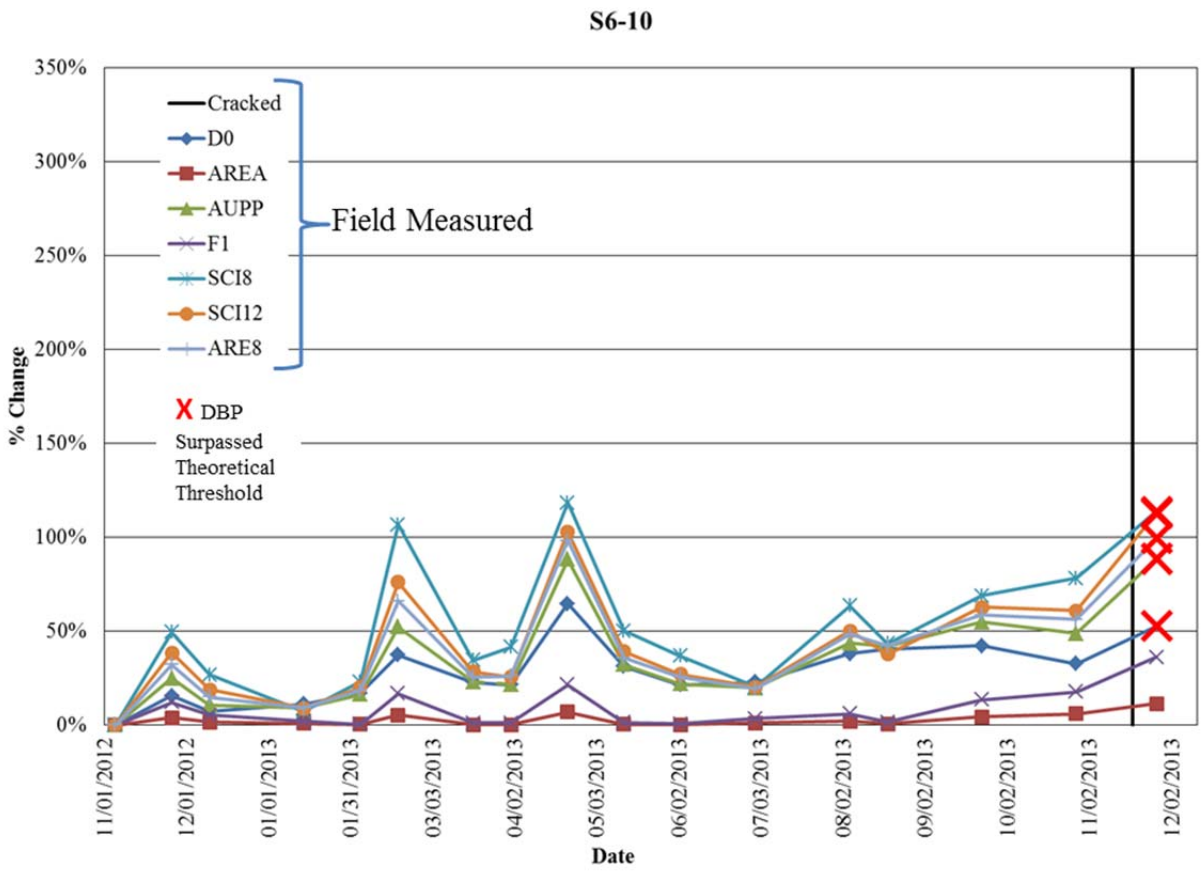

Figure 4.12 – Percent Change in DBPs over time for S6-10.

4.2 Summary of Developmental Group Delamination Sections

Overall, the methodology of comparing the percent change of DBPs measured over time to the theoretical percent change from delamination of the 2/3 interface worked effectively for both sections and in the majority of stations scrutinized. DBPs exceeded their theoretical values for delamination in 13 of the 18 stations that cracked. The DBPs were also successful in distinguishing between cracked and uncracked stations. Four of the six uncracked stations did not have any DBPs exceed their theoretical values. The two False Positives, stations that were uncracked and had at least one DBP exceed its theoretical value, were deemed inconclusive

because cracks may have propagated to the surface if there was more time before the sections were rehabilitated. The ineffectiveness of the methodology on the OWP stations in S5 was not observed in S6, indicating that there was not an underlying ineffectiveness for OWP stations. No change in the proposed procedure was necessary for the delamination group based on the developmental results.

4.3 Validation Group

4.3.1 2003 N8-Rich Bottom

Section 2003-N8 was part of the 2003 Test Track Structural Experiment and was designed to test the "rich-bottom layer" concept. This concept is part of the perpetual pavement design philosophy that carefully designs each layer to optimize the performance of the structure. In perpetual pavement design the surface lift is designed to be abrasion and rut resistant while the intermediate lift is a stiff layer intended to reduce the strains on the bottom lift and also provide rutting resistance. Finally, the bottom lift is intended to be a fatigue tolerant layer that can resist the tensile strain generated as the pavement flexes under a wheel load. The fatigue resistance in the bottom lift can be increased by designing the mix to have a lower air void content or by increasing the binder content to above the optimal binder content determined in the mix-design process. The asphalt content in the bottom layer of 2003-N8 was increased by 0.5% and thus is referred to as a "rich-bottom." The section had a total AC thickness of seven inches, as shown previously in Figure 4.1.

Section N8 was designed to withstand 7 million ESALs prior to cracking but did not perform as expected. The section had significantly more cracking than other comparable sections in the 2003 Structural Experiment that had seven inches of AC, including 2003-N7 which was a companion section to 2003-N8 except 2003-N7 did not have the rich-bottom layer. A forensic

study was initiated to determine if the poor performance of 2003-N8 was due to the rich bottom layer. The investigation determined that a loss of bond between AC layers caused the cracking. Several trenches were cut into the section and cores were taken. An example of what was observed in the trenches is shown in Figure 4.13. Cracks originated along the interfaces, particularly the 1/2 interface, and propagated towards the surface, then throughout the AC structure. Shear testing was conducted on the cores and the 1/2 interface was found to have significantly lower shear strength (Willis and Timm, 2009).

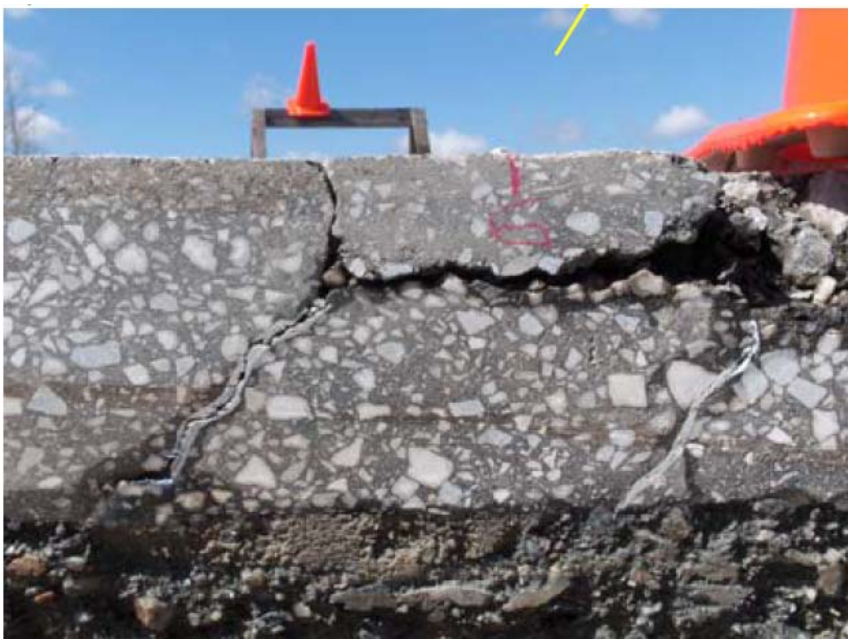

Figure 4.13 – Trench face in N8 showing cracks originated from delamination at 1/2 (Willis and Timm, 2009).

4.3.1.1 Modeling

The delamination distress observed in N8 was modeled in BISAR. Simulations were conducted for varying levels of delamination at the 1/2 interface and for delamination of both layers. As discussed in Chapter 3. Methodology, surveyed layer thicknesses were not available

for the 2003 research cycle; design thicknesses were used. The theoretical percent change of DBPs for the delamination in N8 is presented in Table 4.11.

Table 4.11 – Change in DBPs from BISAR Simulation of 2003-N8

Description	% Change D_0	% Change AREA	% Change AUPP	% Change F_1	% Change SCI_8	% Change SCI_{12}	% Change ARE_8
No Slip α=0.0	0%	0%	0%	0%	0%	0%	0%
1/2 α=0.25	1%	1%	3%	3%	5%	4%	4%
1/2 α=0.50	4%	2%	8%	7%	12%	12%	10%
1/2 α=0.75	9%	5%	18%	14%	26%	25%	22%
1/2 α=0.99	13%	6%	24%	15%	28%	28%	26%
2/3 α=0.99	33%	13%	61%	36%	67%	70%	66%
1/2 & 2/3 α=0.99	56%	20%	108%	63%	132%	134%	122%

4.3.1.2 Field Data

Less field data from the 2003 Track cycle were available than the later cycles. FWD testing was only conducted in the wheel paths and at three random locations within each section. Thus, there were six FWD stations available for DBP comparison over time. At each FWD station, only two drops at a target load level of 9,000 lbs. were conducted. Therefore, the FWD data could not be normalized to an equivalent load level as done with data from other cycles. Exponential regression was used to normalize all deflections to their equivalent response at 68° F. The FWD testing was conducted at longer intervals than the later cycles and temperature data were not recorded on all testing FWD testing dates. For IWP stations of Section N8 (N8-1, N8-4, and N8-7), FWD data from 10 dates were available and for OWP stations (N8-3, N8-6, and N8-9) 12 dates were available. The last available FWD date for this section was February 2, 2005. FWD testing was conducted on four dates later in the cycle but testing time or temperature was not available and those dates could not be used.

Cracking at each FWD station was assessed from crack maps. It is believed that this method resulted in more error in the cracking data because the random locations were superimposed on the crack maps instead of using an image with RLs and cracks painted on the pavement. There were several instances where the crack locations slightly shifted on the crack maps and those were discarded from analysis. Only consistent cracking information was used but this limited that amount of cracking over time data available. Nine dates of cracking were used to capture the distress over two years of traffic.

It was reported that by August 2, 2004 the section had 0.69% cracking (Willis and Timm, 2006). The cracking was localized and in the outside wheel path. Cracking was not observed on any FWD stations until June 2005. The cracking results for each FWD station are presented in Table 4.12. Section N8-6 may have cracked earlier but no cracking data were available from 12/13/2004 through 6/16/2005.

Table 4.12 – Summarized Cracked Dates for 2003-N8

FWD Station	"Cracked" Date
N8-1	Uncracked
N8-3	7/18/2005
N8-4	Uncracked
N8-6	6/16/2005
N8-7	Uncracked
N8-9	7/18/2005

As a result of the limited FWD and cracking data available, analysis of this section was difficult. However, some useful interpretation of the data was still viable. A summary of the DBP comparison for each station is shown in Table 4.13. All of the IWP stations were uncracked and did not have DBPs continuously exceed their theoretical values for delamination of interface 1/2.

In two of these sections D_0 exceeded its threshold on two non-consecutive dates but returned to below the threshold for multiple dates thereafter. This was attributed to the relatively low threshold of D_0 (13%) also influenced by the lack of load normalization on this dataset. Conclusions were difficult to draw for the OWP stations which were cracked, but cracking was observed over five months after the last available FWD date. In general, the OWP stations had more DBPs intermittently exceed their thresholds. Figure 4.14 is a plot of DBPs from N8-6 over time. All DBPs exceeded their theoretical values on the last available FWD date, February 2, 2005. Thus, the theoretical changes were observed within the structure before cracking was visible on the surface. Figure 4.15 is a plot of D_0 over time. Horizontal lines have been added to show the thresholds for D_0 for the delamination scenarios considered. It can be seen that D_0 intermittently exceeded the threshold for full slip on the 1/2 interface (dashed line). D_0 exceeded the threshold for delamination of the 2/3 interface (dotted line) on February 2, 2005 and is likely to have surpassed the delamination of both layers threshold (dash-dot line) if more FWD data were available prior to cracking. No False Negatives occurred in this section. Overall, the validation was successful but more useful analysis could have been conducted if more high quality data were available.

Table 4.13 – Summary of DBP Prediction for Each Station in 2003–N8

FWD Station	D_0	AREA	AUPP	F_1	SCI_{12}	1st Predictor	Classification
N8-1	Never	Never	Never	Never	Never	NA	NCO NCP
N8-3	Early	Never	Early	Never	Early	D_0, AUPP, SCI_{12}	Early
N8-4	Never	Never	Never	Never	Never	NA	NCO NCP
N8-6	Early	Early	Early	Early	Early	D_0	Early
N8-7	Never	Never	Never	Never	Never	NA	NCO NCP
N8-9	Early	Never	Early	Never	Early	D_0	Early
Summary: 3 Early, 3 NCO NCP							

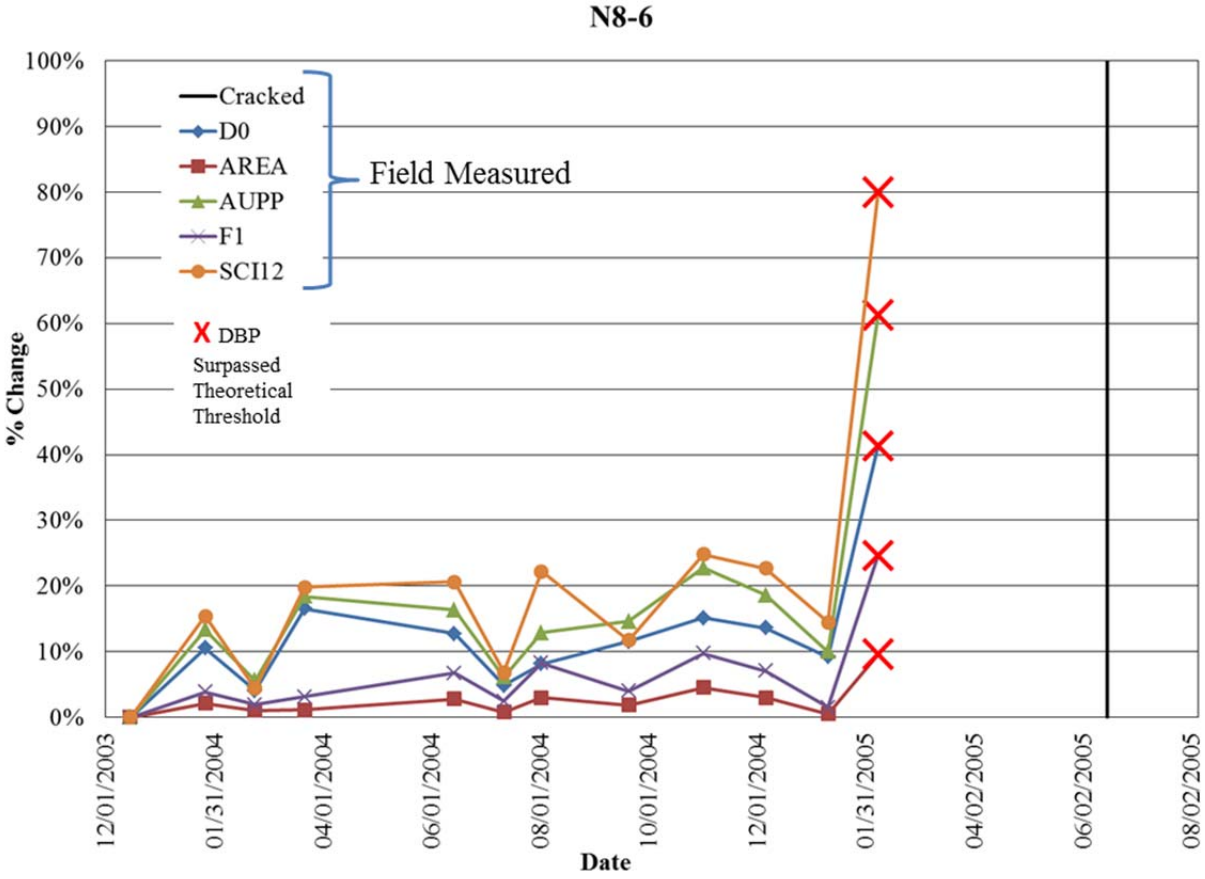

Figure 4.14 – Percent change in DBPs over time for 2003-N8-6.

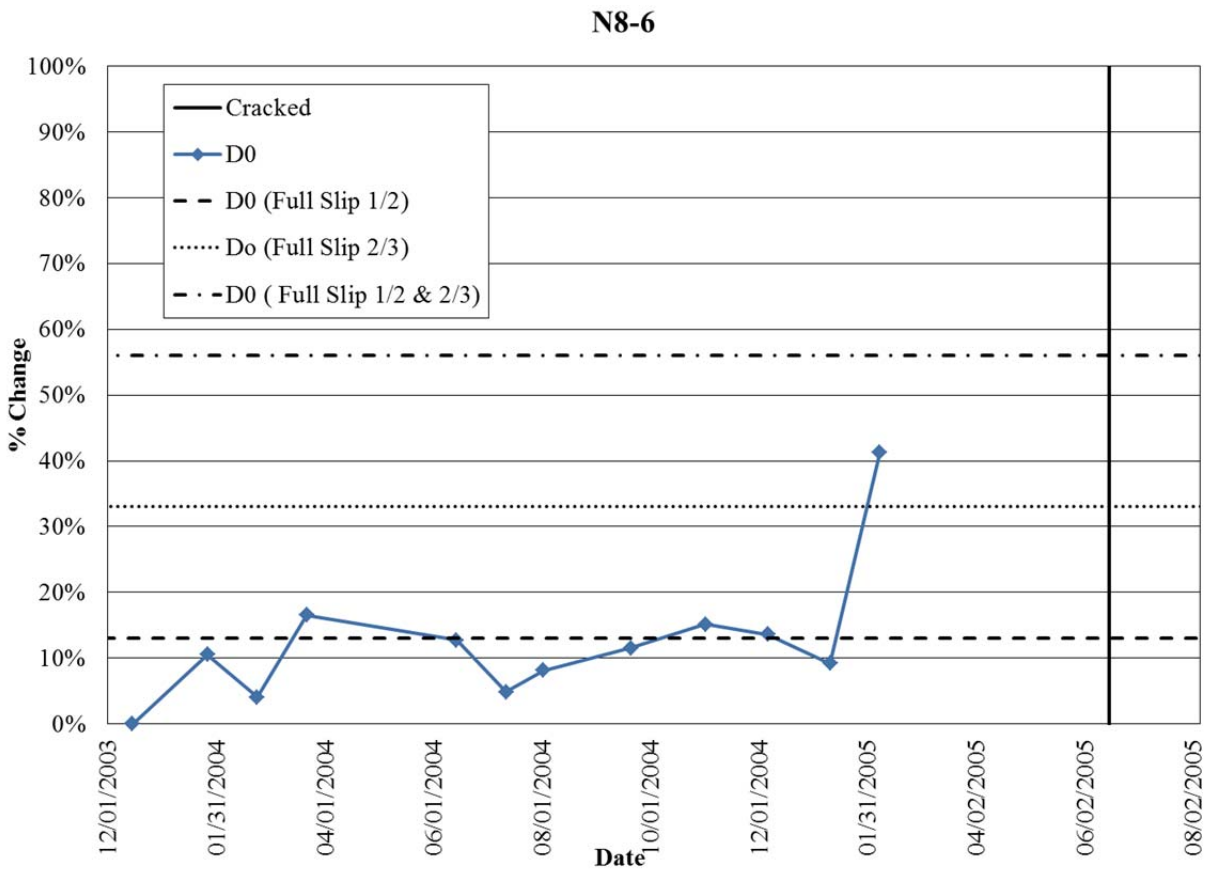

Figure 4.15 – Percent change in D_0 over time for 2003-N8-6.

4.4 Summary and Conclusions from Delamination Group

The DBPs were successful in characterizing the AC structure with respect to cracking in all three delamination sections. A summary of the effectiveness at individual stations is presented in Table 4.14 and Figure 4.16. It can be seen that the change in DBPs were early predictors of cracking (exceeding their theoretical change for delamination) at 16 stations. At six stations the DBPs did not exceed the theoretical change and no cracking was observed (NCO NCP). The DBPs exceeded the theoretical change after cracking was observed at three stations (Late Predictions). The DBPs did not exceed the theoretical change at one station that was cracked

(False Negative). The DBPs exceeded at three stations that did not have cracking (False Positives). Again, the False Positives are inconclusive results because it unknown whether the stations would develop cracking with more time and traffic. False Negatives are problematic because they indicate the cracking that appeared on the surface was not detected in the DBPs. It can be seen in the percentages shown in 4.16 that the DBPs were successful for 74% (Early Prediction and NCO NCP). The False Negative only accounted for 3% of the dataset.

Table 4.14 – Summary of All Delamination Group Stations

Group	Section	Successful?	Early Prediction	NCO NCP	Late Prediction	False Negative	False Positive
Dev.	2012-S5	Successful	5	1	2	1	3
	2012-S6	Successful	8	2	2	0	0
Validation	2003-N8	Successful	3	3	0	0	0
Total		Successful	16	6	4	1	3

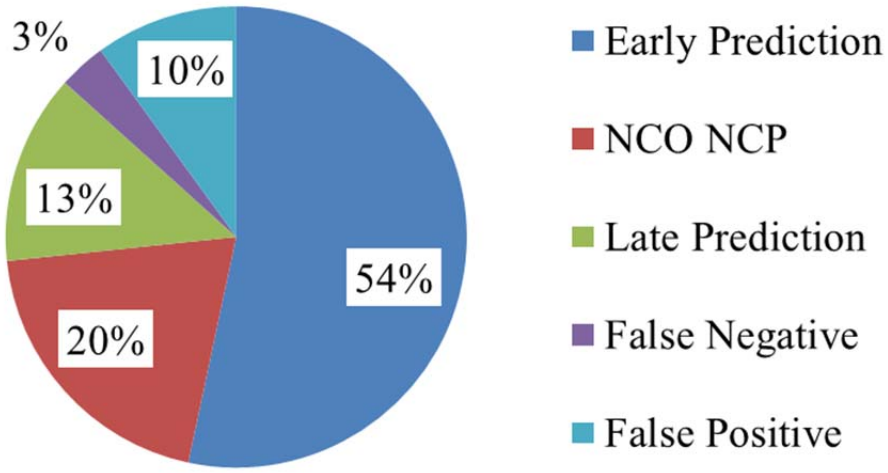

Figure 4.16 – Delamination Group summary of station classification.

The data summarized in Table 4.14 is broken down by individual DBP performance at each station in Figure 4.17. In this figure, the x-axis is the number of days until cracking was observed at each station and the y-axis is the number of days until the change in each DBP exceeded its theoretical percent change. Data points to the right of the line of equality were considered Early Predictions because they surpassed their theoretical change prior to cracking appearing. Data points to the left of the line of equality were considered Late Predictions because they did not exceed theoretical thresholds until after cracking was observed. False Negatives were along the x-axis because they never exceeded the theoretical threshold (zero days until DBP exceeded) but had cracking. False Positives were along the y-axis because they exceeded the threshold but did not yet have any cracking (zero days until cracking). The data points labeled "NCO NCP" were uncracked stations that did not have the DBP threshold exceeded.

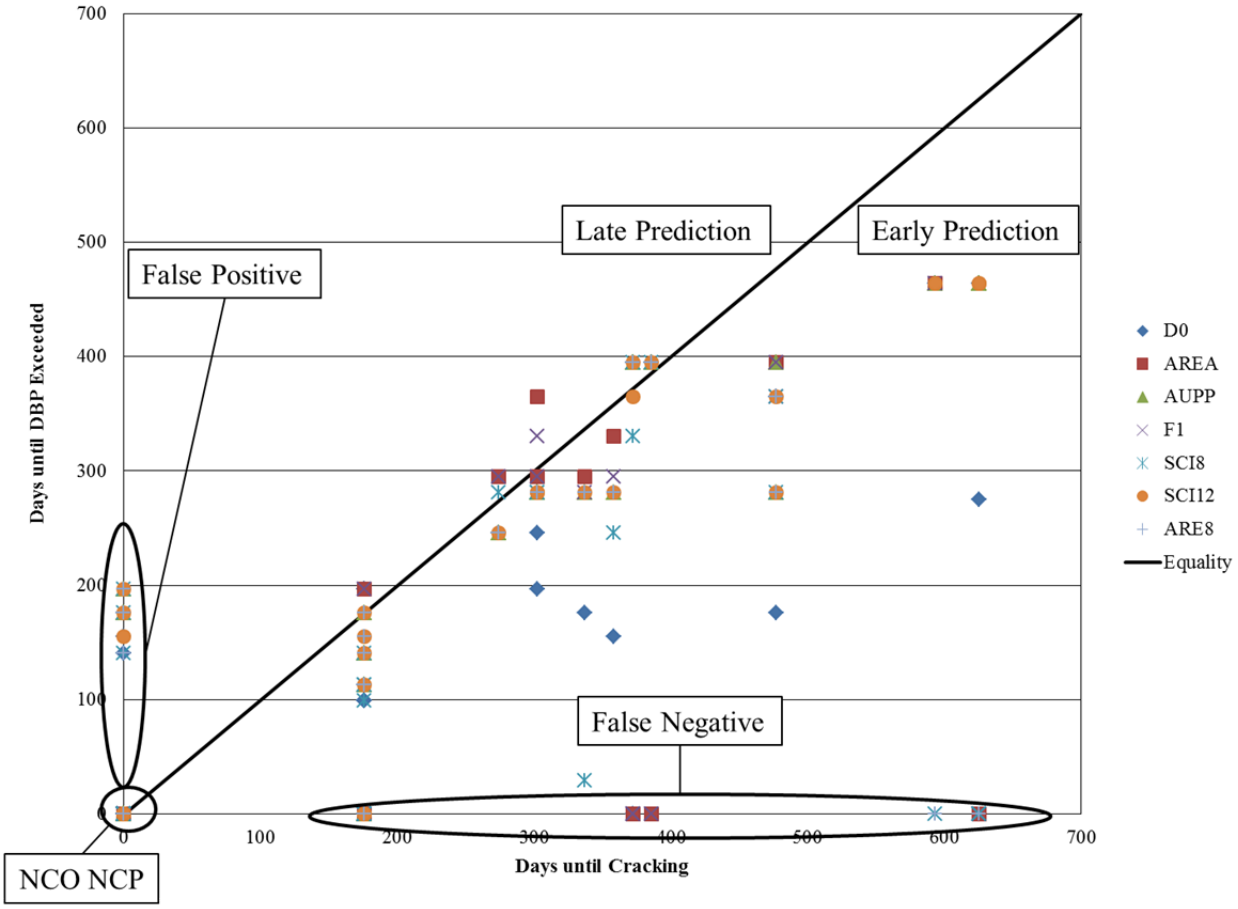

Figure 4.17 – Delamination Group summary of DBPs at each station.

Similar plots to Figure 4.17 were used to evaluate the effectiveness of each DBP. Figure 4.18 shows individual plots for each DBP and Figure 4.19 summarizes the total number of classifications for each DBP. Generally, each DBP in this group was able to successfully capture the structural change due to delamination. It can be seen that AREA (Figure 4.18 (b)) and F_1 (Figure 4.18 (d)) did not have any False Positives and are grouped closer to the line of equality, which may be an indication that they are less sensitive to the early stages of delamination and are not as useful as early predictors. AUPP (Figure 4.18 (c)) and SCI_{12} (Figure 4.18 (f)) were considered the best predictors because they had the fewest amount of False Negatives. SCI_8 and

ARE_8 were included in this work with the belief that they may provide additional insights into the AC performance because they include the response from D_8 which is between D_0 and D_{12}. However, no improvement can be seen in the results of SCI_8 and ARE_8 compared to SCI_{12} and AUPP. Due to the fact that not all FWDs have the D_8 sensor and the lack of additional insights, SCI_8 and ARE_8 may not be necessary for future application of this work. It is recommended to include either F_1 or the AREA parameter, despite their lower prediction ability, because they provide an assessment of the granular base layer which is useful to include to show that the distress was not a result from a base layer issue (none of the sections assessed in this work were reported to have problems with the granular layers).

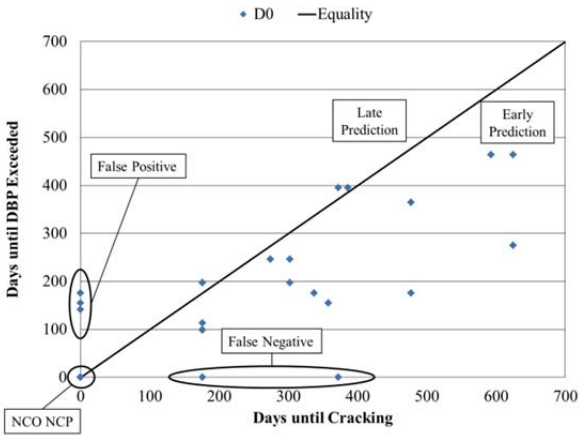

(a) D_0

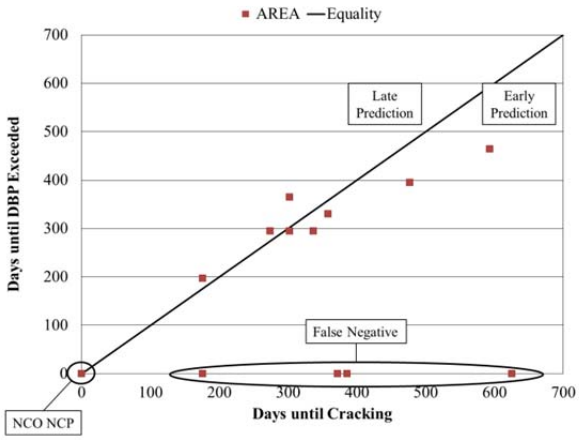

(b) AREA

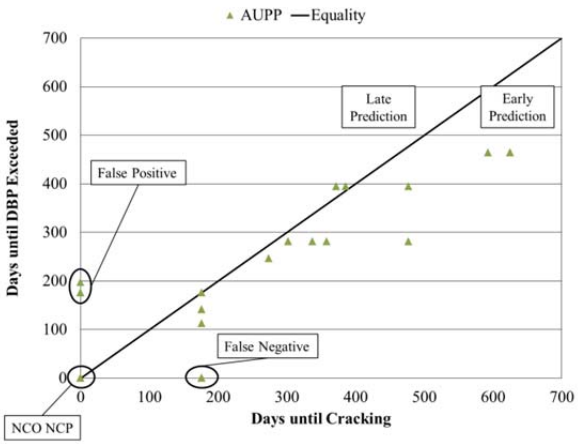

(c) AUPP

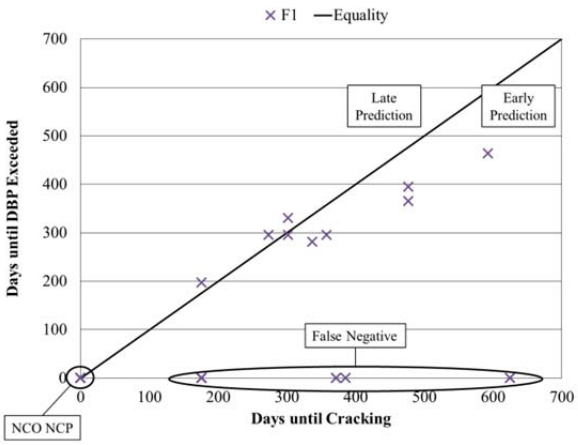

(d) F_1

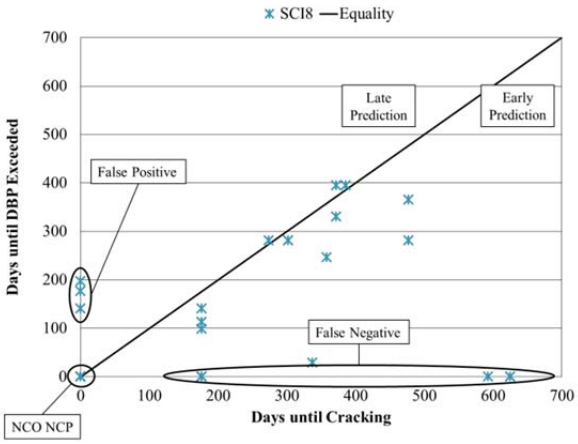

(e) SCI_8

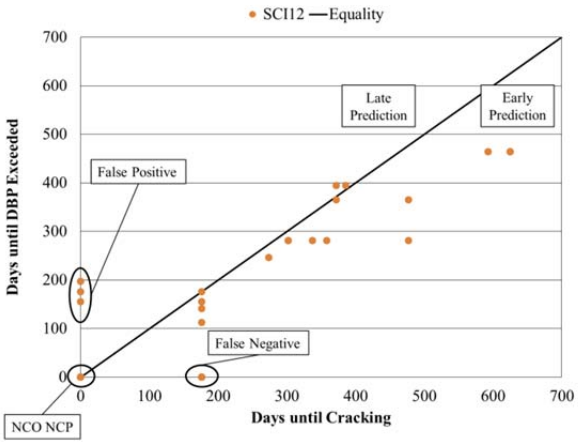

(f) SCI_{12}

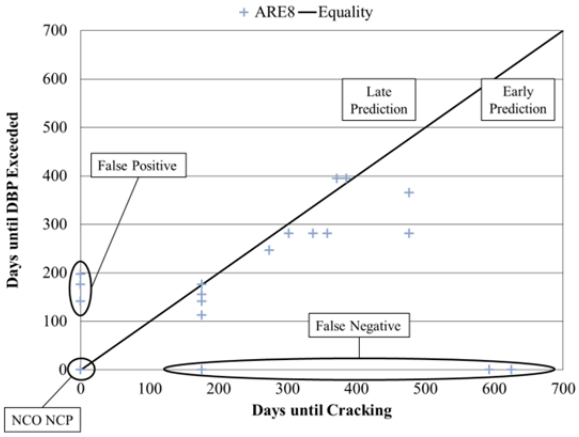

(g) ARE_8

Figure 4.18 – Delamination Group summary for individual DBPs at each station.

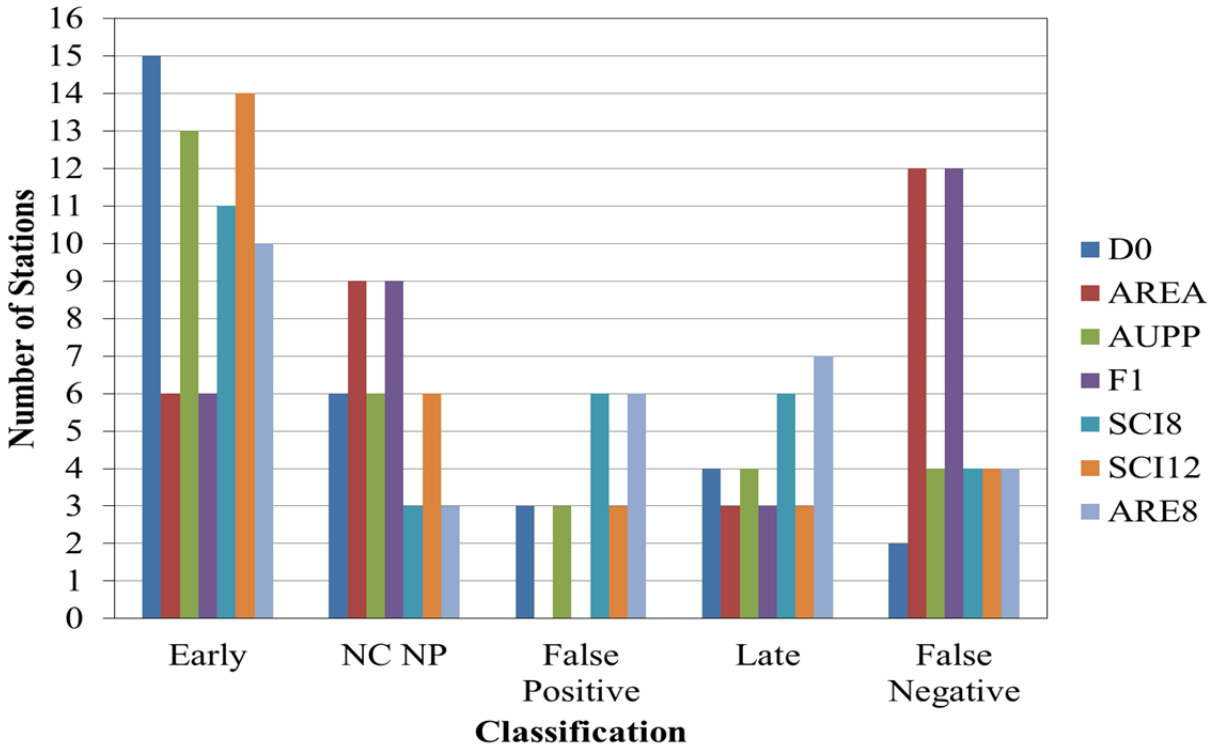

Figure 4.19 – Summary of individual DBP classification for Delamination sections.

The proposed methodology was shown to work for both developmental and validation sections. These results should be further verified with a larger dataset that has a wider range of AC thicknesses. The validation group section highlighted the challenges of working with sparse amounts of data but was still effective in confirming the applicability of the methodology to delamination at the upper interface.

CHAPTER 5. TOP-DOWN CRACKING GROUP RESULTS

Two Test Track sections were constructed as part of the 2006 research cycle to assess the ability of the Energy Ratio (ER) laboratory testing procedure to identify an AC mixture's resistance to TDC. In this dissertation, these two sections were used to develop (2006-N1) and validate the (2006-N2) the methodology to identify TDC from FWD deflection basins. The cross-sections of the two pavement structures are shown in Figure 5.1. In the ER concept, a mixture with a higher ER is more resistant to TDC. Section N2 used a polymer modified binder to achieve a higher ER. Confirming the ER concept, N2 withstood more traffic before TDC initiated and developed significantly less cracking than N1 during the research cycle (Timm et al., 2009). Cores taken from each section verified that the observed cracking was TDC. It is also important to note that these two sections were built on a limerock base material that was significantly different than the typical crushed granite base used in the other sections evaluated in this research.

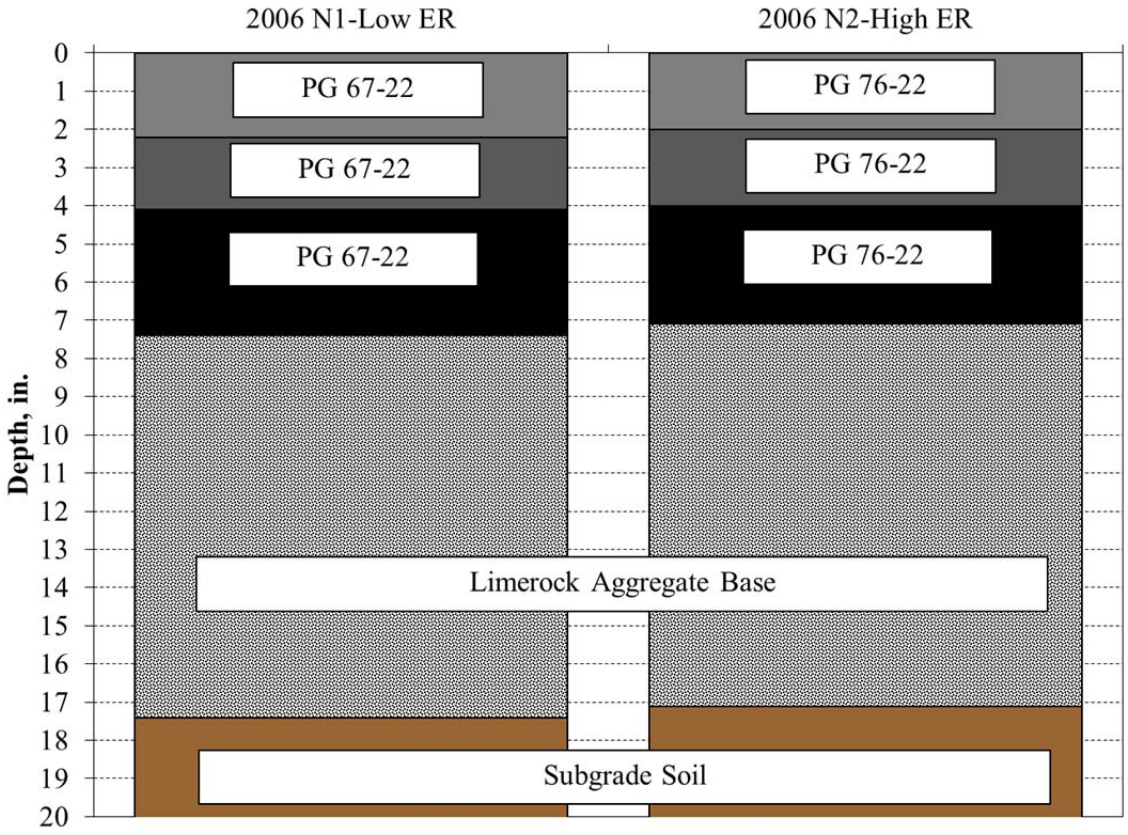

Figure 5.1 – TDC cross-sections.

5.1 Top-down Cracking Developmental Group

The analysis methodology for TDC was fundamentally different than BUFC or delamination. It was expected that at the initial onset of TDC there would not be great changes in the FWD deflections nor the resulting DBPs. The intact pavement structure was simulated in BISAR and then cracking was simulated by lowering the moduli of the AC for cracked layers starting at the top of the structure, as shown previously in Figure 3.8. The AC moduli of the cracked layers were reduced to 50% of their input values. Figure 5.2 shows the simulated deflection basins for 2006-N1 in the intact condition (No Cracking), at the onset of cracking

(1.0” TDC), and after the entire AC structure has been cracked (Total TDC). It can be seen that there was very little change in deflection between the intact condition (No Cracking) and at the onset of cracking (1.0” TDC). As expected, there is a much greater change in the deflections after cracking was simulated through the entire structure (Total TDC). The simulation of cracking through the entire pavement structure was used as the threshold to compare to DBPs. However, the DBPs from the TDC sections were expected to stay under the threshold until after cracking was visible because TDC does not immediately affect the entire AC structure. Thus, for an accurate comparison of theoretical and field DBPs, the change in a DBP over time needed to stay under the theoretical change from the no cracking to total cracking condition.

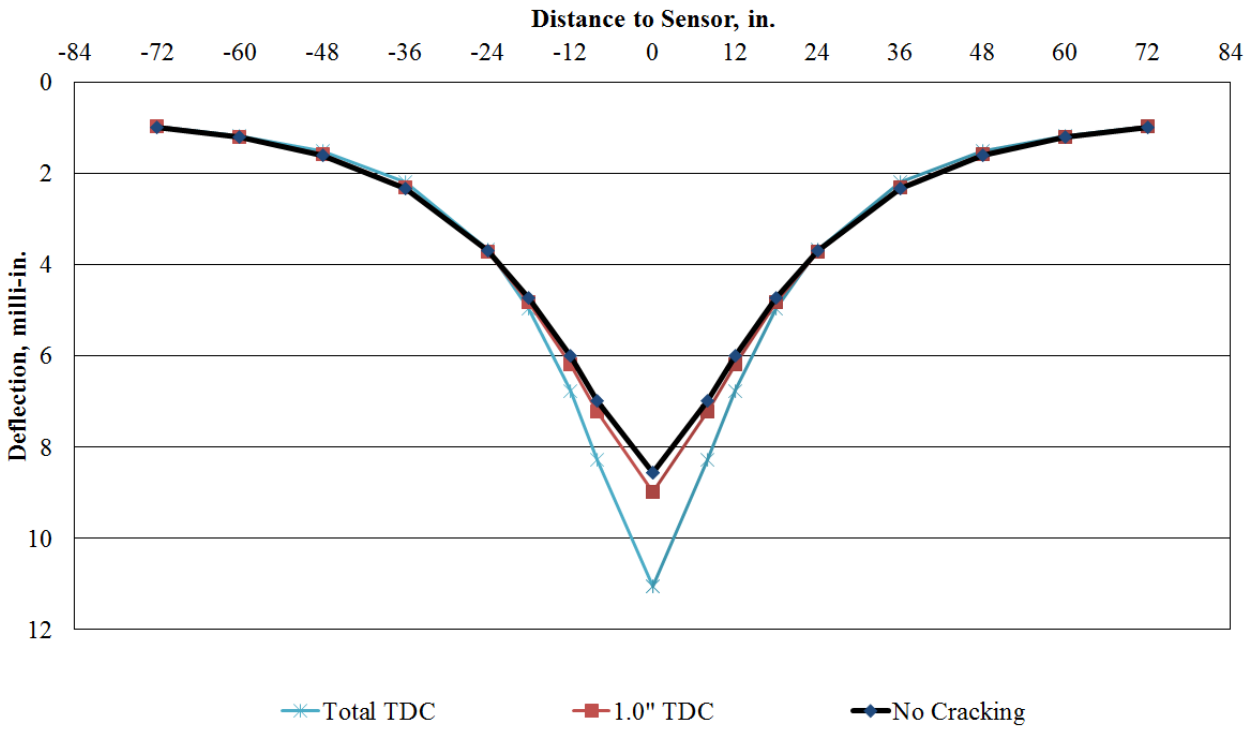

Figure 5.2 – BISAR simulated TDC deflection basins.

5.1.1 2006 Florida Energy Ratio-N1

Section 2006-N1 used an unmodified PG 67-22 binder resulting in a lower ER. Significantly more cracking was observed in N1. Forensic coring verified that the observed cracking was top-down. It can be seen in the photographs of cores taken from N1, shown in Figure 5.3, that cracking originated at the surface.

Figure 5.3- Cores from 2006-N1 showing TDC (Timm et al., 2009).

5.1.1.1 Modeling

The results from the BISAR simulation of TDC are presented in Table 5.1. It is apparent that as the depth of the simulated cracked layers increases, the percent change of the DBPs also increases. “Total TDC” is the condition in which TDC has been simulated through the entire AC by reducing all AC moduli values. The percent change for the “Total TDC” was used as the threshold and the change in DBPs from FWD testing was expected to stay below this threshold.

Table 5.1 – Change in DBPs from BISAR Simulation of 2006-N1

Description	% Change D_0	% Change AREA	% Change AUPP	% Change F_1	% Change SCI_8	% Change SCI_{12}	% Change ARE_8
No Cracking	0%	0%	0%	0%	0%	0%	0%
1.0" TDC	5%	2%	8%	5%	10%	9%	9%
2.0" TDC	8%	4%	14%	9%	20%	17%	16%
3.0" TDC	12%	5%	20%	13%	30%	25%	23%
4.0" TDC	14%	7%	25%	17%	39%	32%	30%
5.0" TDC	17%	8%	31%	21%	48%	41%	37%
6.0" TDC	20%	9%	36%	25%	56%	48%	43%
Total TDC	29%	13%	53%	35%	74%	67%	61%

5.1.1.2 Field Data

As discussed previously, the condition at each FWD station (cracked or uncracked) was assessed using crack maps. The crack maps were generated from regularly conducted visual surveys of the section. The random locations were superimposed over the crack maps to determine if cracks were within 1 foot of an FWD station. This method inherently had more variability than directly using images or video of the pavement to evaluate cracking. There were some inconsistencies found in the cracking data and those crack maps were excluded. A summary of the date that cracking was observed at each station is presented in Table 5.2. Cracking was first observed in the section on April 9, 2007 but not at an FWD station until April 23, 2007 when cracking was observed at N1-7. The majority of the FWD stations had cracking observed on June 4, 2007. Two of the IWP stations, N1-4 and N1-10, did not have cracking until October 15, 2007. By January 28, 2008 the section was reported to be 100% cracked.

Table 5.2 –Summarized Cracked Dates for 2006-N1

FWD Station	"Cracked" Date
N1-1	6/4/2007
N1-2	6/4/2007
N1-3	6/4/2007
N1-4	10/15/2007
N1-5	6/4/2007
N1-6	6/4/2007
N1-7	4/23/2007
N1-8	6/4/2007
N1-9	6/4/2007
N1-10	10/15/2007
N1-11	6/4/2007
N1-12	6/4/2007

After correcting the FWD data for load, a large amount of scatter was noticed in the dataset. Figure 5.4 shows the deflections D_0 and D_{12} versus temperature after being normalized to a 9,000 lb. load. It can be seen in Figure 5.4 that as the temperature increases the deflection also increases and the R^2 for both sensors indicated a reasonable fit of the trendlines. Figure 5.5 shows the same deflections after normalizing to a reference temperature of 68° F. Low R^2 values for the exponential trendlines verified that the regression was performing properly (at least mathematically) and the effect of temperature on deflection was removed. As discussed in Chapter 3. Methodology, a unique temperature correction was applied to each station. Thus, this trend was seen at all stations.

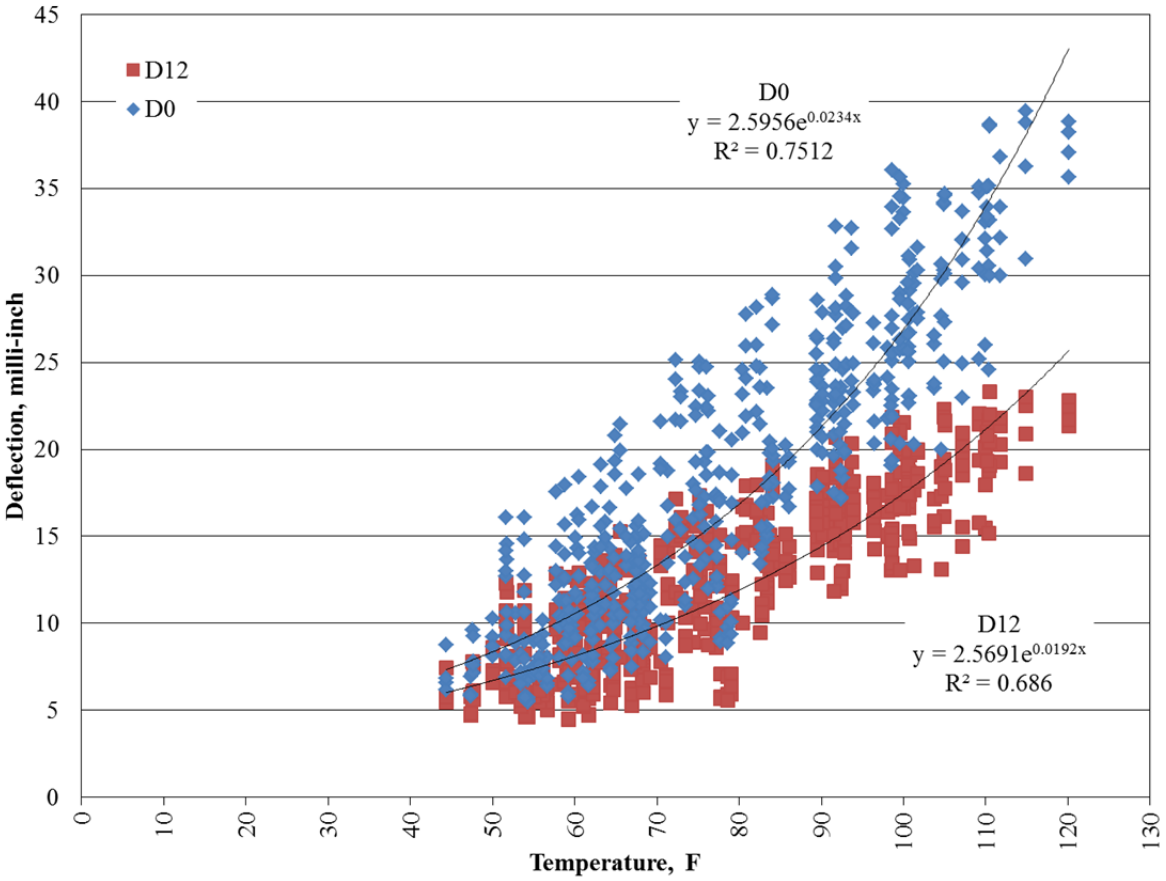

Figure 5.4 – Load corrected D_0 and D_{12} versus temperature for 2006-N1.

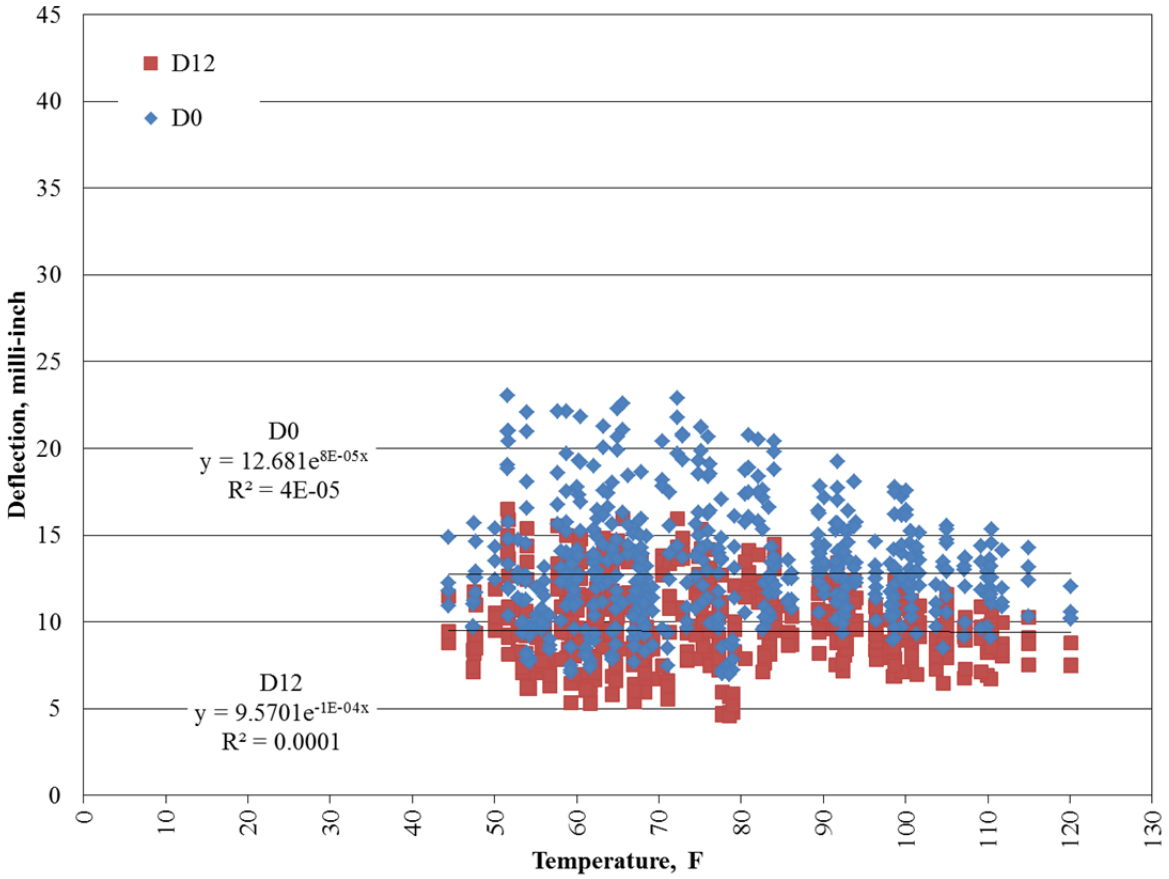

Figure 5.5 – Load and temperature corrected D_0 and D_{12} versus temperature for 2006-N1.

After the normalized deflections were plotted over time, it appears that the normalization was unrealistically adjusting the deflections. Figure 5.6 shows the load and temperature corrected D_0 and D_{12} over the research cycle. The solid black line shows the temperature measured during testing. On a given date three temperatures were recorded, one for each wheelpath. The normalized deflections were highest in the coldest months of the second year, which was opposite of the expected seasonal variation, even after temperature correction. In other research cycles a slight seasonal trend could still be observed in the deflections over time and matched the expectation that higher deflections occurred during the months with higher temperatures.

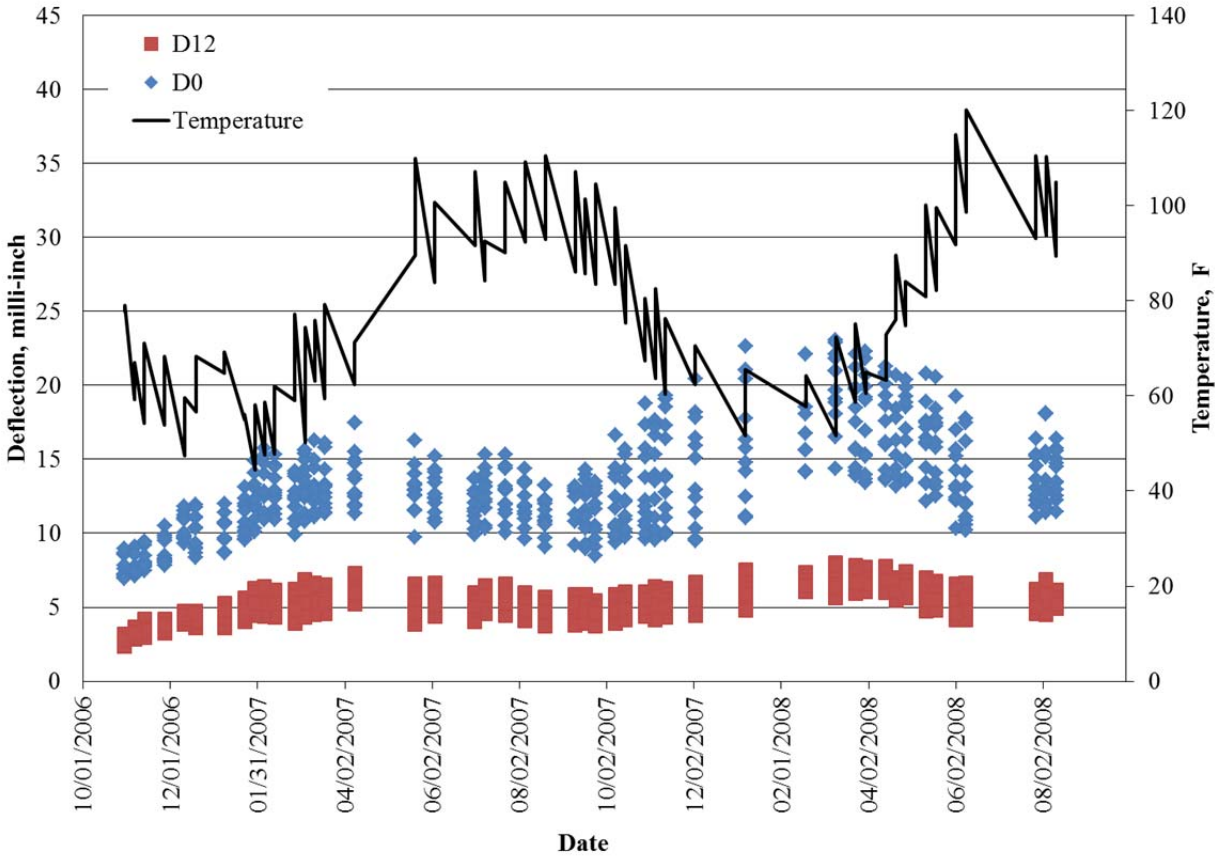

Figure 5.6 – Load and temperature corrected deflections and temperature over time for 2006-N1.

Closer inspection of the dataset prior to temperature normalization revealed a general increasing trend in deflection over time. Figure 5.7 shows load corrected deflections (same data as Figure 5.4) over the research cycle. The deflections followed the seasonal trend with temperature but were still generally increasing over time. When the temperature returned to below 60° F during the second winter of the research cycle, the deflections were not as low as they were the previous year. It is believed the issue with the temperature correction is due to damage developing in the section. During February 2007, the deflections were as high or higher than they were initially despite being measured at lower temperatures.

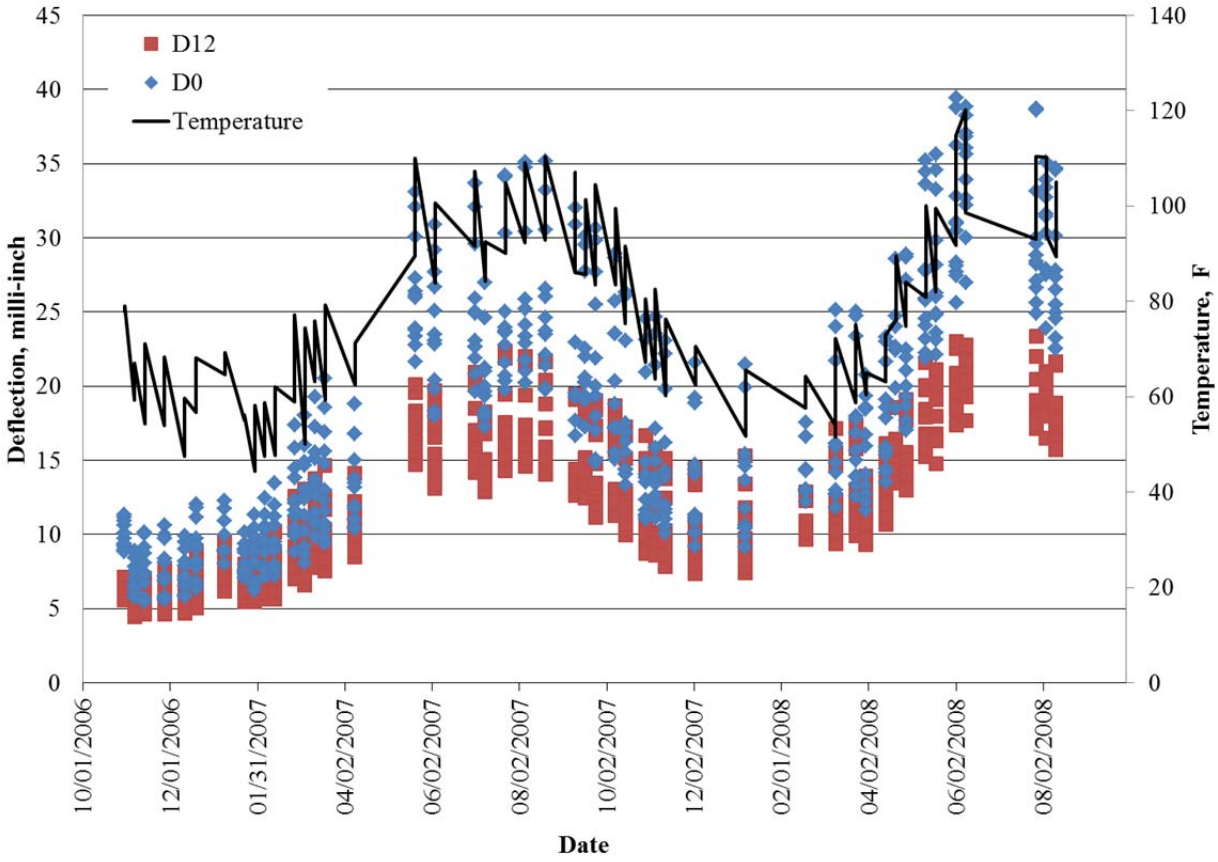

Figure 5.7 – Load corrected deflections and temperature over time for 2006-N1.

Exhaustive effort was placed into attempting to explain, fix, or circumvent the issue with temperature correction but improved results were not obtained. Conducting temperature corrections based on deflections prior to any cracking in the section was investigated but the idea was discarded because the temperature did not exceed 79° F and thus was deemed inappropriate to correct deflections measured at excess of 115° F. Using only deflections measured at temperatures between 63° and 73° F (±5° of 68° F), and not applying a temperature correction was considered but was discarded because it excluded any FWD testing conducted between April 9, 2007 and before October 29, 2007, the critical time when cracking was occurring in the section. Limiting the dataset analyzed was also attempted but did not yield better results. Figure

5.8 shows D_0 and D_{12} after temperature correction using only data obtained prior to cracking being observed at all stations (October 15, 2007). The same effect can be observed in which higher deflections occur in January through April than in July and August.

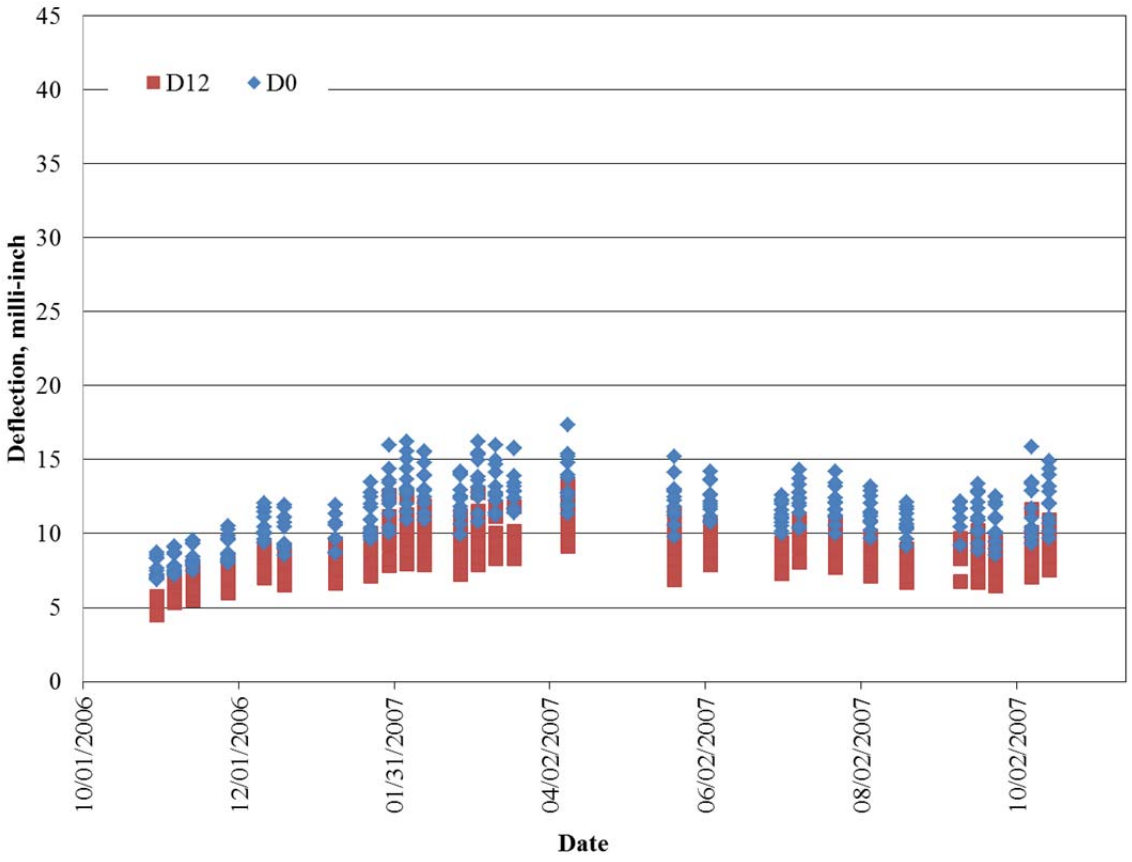

Figure 5.8 – Load and temperature corrected deflections over time using data prior to cracking at all station for 2006-N1.

DBPs were not calculated for this section because it can be observed in Figures 5.6 and 5.8 that the DBPs would have large changes early in the research cycle. The change in DBPs would decrease slightly over the months with higher temperatures and then have larger changes

again. The same trend was observed in the N2 data, as shown in Figure 5.9. Therefore, the methodology to assess DBPs from these TDC could not be developed or validated.

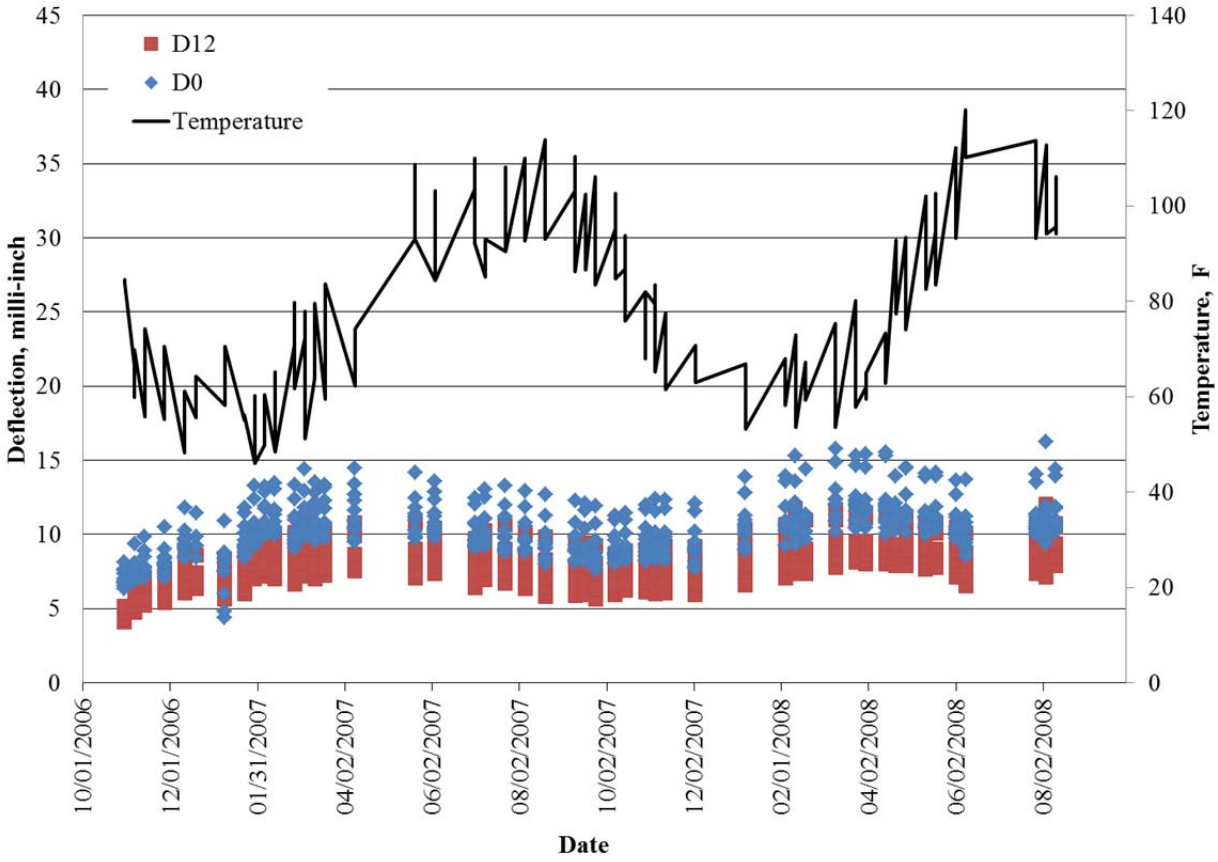

Figure 5.9 – Load and temperature corrected deflections and temperature over time 2006-N2

CHAPTER 6. BOTTOM-UP FATIGUE CRACKING GROUP RESULTS

Bottom-up fatigue cracking (BUFC) was the most common distress observed in the structural sections on the Test Track and therefore is the largest group available for analysis. This group also contains sections that did not have any cracking and sections with a combination of TDC and BUFC. Of the 15 sections that did not have documented delamination or exclusively TDC, 12 were placed in the BUFC Developmental Group and three in the BUFC Validation Group.

6.1 Bottom-up Fatigue Cracking Developmental Group

The pavement structure for each section in the BUFC Developmental Group is shown in Figure 6.1. All sections shown in Figure 6.1 were constructed over a crushed-granite granular base that was placed over the track subgrade soil.

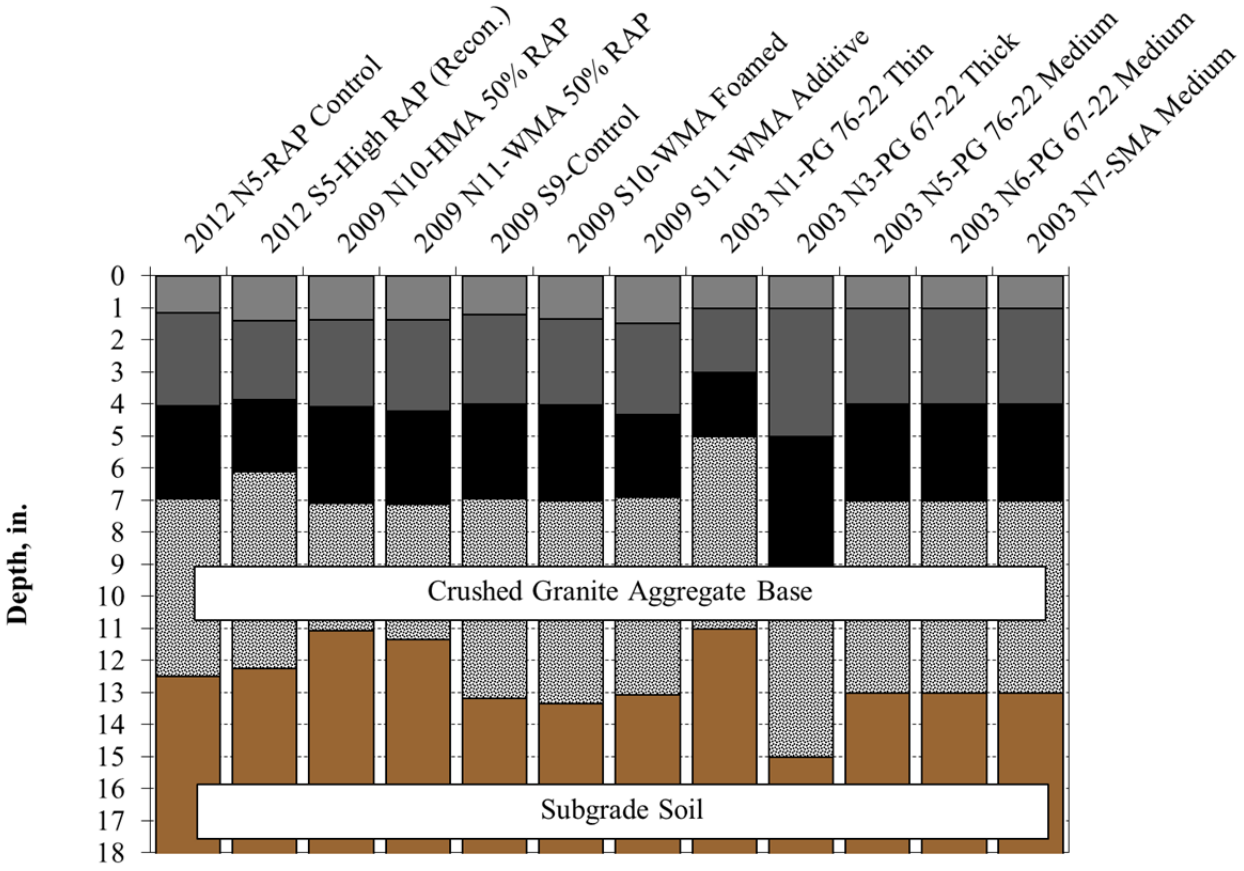

Figure 6.1 – Cross-sections of BUFC Developmental Group.

Each of the pavement sections will be discussed in a manner similar to the delamination sections presented previously, in which the theoretical change in DBPs will be presented and then compared to the DBPs measured during the research cycle. As discussed in Chapter 3. Methodology, fatigue cracking was simulated in BISAR by reducing the moduli of the cracked AC layers starting at the bottom of the AC and propagating up in one inch increments. The BUFC Developmental Group was used to determine the appropriate amount of modulus reduction and to determine how data from each cycle would be handled. No guidance could be found in literature as to the amount of reduction that was appropriate for simulating cracked layers in linear elastic analysis. Therefore, 25 and 50% percent of the original modulus values

were both used for all BUFC Developmental Group sections. It can be seen in Figure 6.2, as expected, that there is a much greater change in the theoretical deflection basins of a fully cracked AC structure simulated with AC moduli of 25% than AC moduli of 50%.

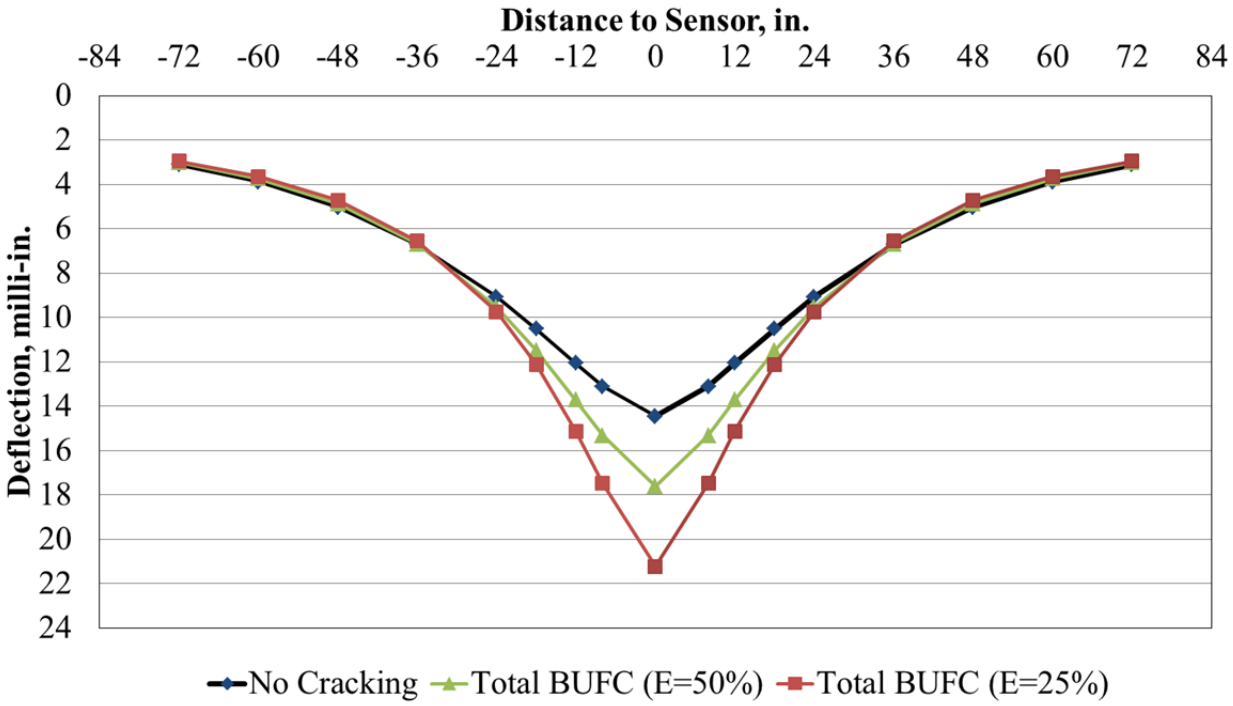

Figure 6.2 – BISAR simulated BUFC deflection basins.

6.1.1 2012 Green Group RAP Control-N5

Section N5 was designed as the control section for the 2012 GG study and featured conventional levels of RAP in the AC. PG 67-22 binder was used in all AC layers. The as-built thickness of the AC was 5.9 inches and the granular base was 5.2 inches. Traffic was initiated on the section in October 2012. The first crack was observed in April 2013 after 2.4 million ESALs were applied. In June 2013, a patch was applied to the beginning of the section (over RL #1) and the failure threshold was reached on August 19, 2013.

6.1.1.1 Modeling

The cross-section was modeled using linear-elastic analysis in BISAR for increasing amounts of BUFC. As discussed previously, BUFC was simulated by lowering the modulus of the cracked portion of the pavement. The change in DBPs, for 25 and 50% of the original AC moduli, is shown in Table 6.1 and 6.2, respectively. It can be seen that, as expected, there is a much greater percent change when the cracked AC moduli is 25% of its original value than when it is 50%. In both cases SCI_8 had the largest percent change with the simulated cracking. It was necessary to compare the simulated and observed percent changes to determine the most appropriate reduction because if the change is too small then the location will be assumed cracked when it is not (False Positive) and if the change is too great then the location will be cracked before it is noticed in the FWD analysis (False Negative).

Table 6.1 – Change in DBPs from BISAR Simulation of 2012-N5 (E_{AC}= 25%)

Description	% Change D_0	% Change AREA	% Change AUPP	% Change F_1	% Change SCI_8	% Change SCI_{12}	% Change ARE_8
No Cracking	0%	0%	0%	0%	0%	0%	0%
1.0" BUFC	13%	5%	22%	14%	25%	26%	24%
2.0" BUFC	24%	10%	43%	26%	51%	52%	48%
3.0" BUFC	33%	14%	62%	39%	83%	80%	72%
4.0" BUFC	40%	16%	76%	49%	113%	103%	90%
5.0" BUFC	45%	18%	87%	56%	138%	121%	106%
Total BUFC	64%	23%	125%	76%	192%	171%	151%

Table 6.2 – Change in DBPs from BISAR Simulation of 2012-N5 (E_{AC}= 50%)

Description	% Change D_0	% Change AREA	% Change AUPP	% Change F_1	% Change SCI_8	% Change SCI_{12}	% Change ARE_8
No Cracking	0%	0%	0%	0%	0%	0%	0%
1.0" BUFC	7%	3%	13%	8%	14%	14%	14%
2.0" BUFC	12%	5%	21%	13%	24%	24%	23%
3.0" BUFC	14%	7%	26%	17%	34%	33%	30%
4.0" BUFC	16%	8%	31%	20%	43%	40%	36%
5.0" BUFC	19%	9%	36%	24%	52%	47%	42%
Total BUFC	28%	12%	51%	32%	71%	66%	59%

6.1.1.2 Field Data

The first cracking that was observed within 1 foot of an FWD station occurred on May 6, 2013 in the IWP of RL#1 (FWD Station N5-1). The summarized cracking results for this section are shown in Table 6.3. All of the BWP sections were uncracked before maintenance was applied.

Table 6.3 – Summarized Cracked Dates for 2012-N5

FWD Station	"Cracked" Date
N5-1	5/6/2013
N5-2	Uncracked
N5-3	5/13/2013
N5-4	8/19/2013
N5-5	Uncracked
N5-6	6/17/2013
N5-7	Uncracked
N5-8	Uncracked
N5-9	5/13/2013
N5-10	Uncracked
N5-11	Uncracked
N5-12	6/17/2013

Plots similar to those utilized to assess delamination were utilized to assess the change in DBPs over time. Figure 6.3 shows the results for the first station to crack, FWD station N5-1. A red "X" is used to designate the point that the DBP exceeds its simulated value for AC moduli of 50% of the original and a black "X" is used to designate when the DBP exceeds its simulated value for AC moduli of 25%. It can be seen that at 50% all DBPs exceeded the simulated change before cracking was observed in the section. The 25% AC moduli thresholds were exceeded later for all DBPs except AREA and F_1.

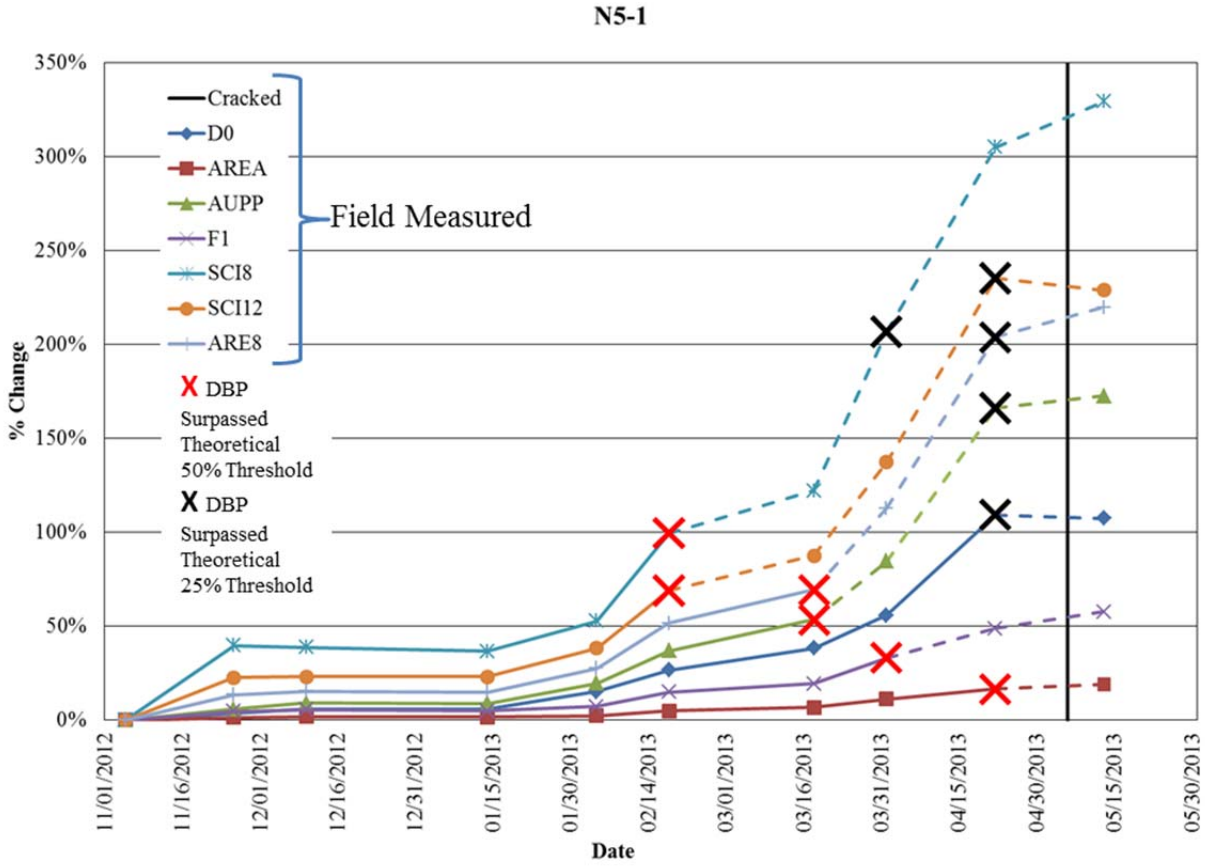

Figure 6.3 – Percent Change in DBPs over time for 2012-N5-1.

The results for the theoretical DBP comparison to field data are presented in Tables 6.4 and 6.5 for modulus values of 25% and 50%, respectively. The same classifications that were used for the delamination sections are used here (discussed in Section 4.1). Again, False Positives occurred when the change in field DBPs exceeded the simulated change but no cracking was observed at that station. This occurred six times when the moduli were 50% their original values and five times at 25% AC moduli.

Late Predictions occurred for comparisons with the AC moduli reduction to 25% in all the OWP stations which did not have any DBPs exceed the simulated values prior to cracking. This was an indication that the simulated modulus reduction to 25% was too great and was not sensitive to the changes in the structure that led to cracking.

Table 6.4 - Summary of DBP Prediction for Each Station in 2012 – N5 (E_{AC}=25%)

FWD Station	D_0	AREA	AUPP	F_1	SCI_8	SCI_{12}	ARE_8	1st Predictor	Classification
N5-1	Early	Never	Late	Never	Early	Early	Early	SCI_8	Early
N5-2	Never	Never	Never	Never	Never	Never	Never	None	NCO NCP
N5-3	Late	Never	Late	Never	Late	Late	Late	D_0, AUPP, SCI_8, SCI_{12}, ARE_8	Late
N5-4	Early	Never	Late	Never	Late	Late	Late	D_0	Early
N5-5	Early	Never	Early	Late	Early	Early	Early	D_0	False Positive
N5-6	Late	Never	Never	Never	Never	Never	Never	D_0	Late
N5-7	Early	Never	Early	Never	Early	Never	Early	D_0, AUPP, SCI_8, ARE_8	False Positive
N5-8	Early	Never	Never	Never	Never	Never	Never	D_0	False Positive
N5-9	Late	Never	Late	Never	Late	Late	Late	D_0	Late
N5-10	Early	Never	Early	Never	Early	Early	Early	D_0	False Positive
N5-11	Early	Never	Early	Never	Early	Early	Early	D_0	False Positive
N5-12	Late	Never	Late	Never	Late	Late	Late	D_0, AUPP, SCI_8, SCI_{12}, ARE_8	Late
Summary: 2 Early, 5 False Positive, 1 NCO NCP,4 Late									

Table 6.5 - Summary of DBP Prediction for Each Station in 2012 – N5 (E_{AC}=50%)

FWD Station	D_0	AREA	AUPP	F_1	SCI_8	SCI_{12}	ARE_8	1st Predictor	Classification
N5-1	Early	Early	Early	Early	Early	Early	Early	SCI_8, SCI_{12}	Early
N5-2	Early	Never	Early	Never	Early	Early	Early	SCI8	False Positive
N5-3	Early	Never	Early	Never	Early	Early	Early	D_0	Early
N5-4	Early	Late	Early	Late	Early	Early	Early	D_0	Early
N5-5	Early	Never	Early	Late	Early	Early	Early	D_0	False Positive
N5-6	Late	Never	Late	Never	Late	Late	Late	D_0	Late
N5-7	Early	Early	Early	Early	Early	Early	Early	D_0	False Positive
N5-8	Early	Never	Never	Never	Never	Never	Never	D_0	False Positive
N5-9	Late	Late	Late	Late	Late	Late	Late	D_0	Late
N5-10	Early	Never	Early	Never	Early	Early	Early	D_0	False Positive
N5-11	Early	Never	Early	Never	Early	Early	Early	D_0	False Positive
N5-12	Early	Late	Late	Late	Late	Late	Late	D_0	Early
Summary: 4 Early, 6 False Positive, 2 Late									

As a whole, the DBPs were fairly accurate in capturing the change in the AC structure due to cracking with the 50% AC moduli reduction. The large amount of False Positives were inconclusive results and no False Negatives occurred. Therefore, given only the DBP changes over time, it is reasonable to assume that a practitioner would deem this section to be distressed and in need of repair.

6.1.2 2012 Green Group High RAP (Reconstructed)-S5'

The Green Group High RAP Section was reconstructed on May 22, 2013. The same materials and structural design were used as original construction but the tack rate was doubled at both AC interfaces to prevent the delamination that occurred with the original section. More detail about the forensic investigation and reconstruction has been documented elsewhere (Vrtis and Timm, 2015; Vrtis, et al., 2015). After reconstruction, cracking did not exceed the failure

threshold over the remainder of the cycle (around 7.2 million ESALs). Cracks were first observed on April 7, 2014 and 15.4% of the lane area was cracked at the end of the cycle. Cores taken from the section verified that delamination did not recur and BUFC was the cause of the cracking.

6.1.2.1 Modeling

Section 2012-S5' was modeled in BISAR using laboratory tested modulus values and layer thicknesses surveyed during construction. The theoretical change in DBPs for moduli values of 25 and 50% are presented in Tables 6.6 and 6.7, respectively. Again, there is a much greater change in DBPs when the AC moduli are reduced to 25% of their original value than 50%.

Table 6.6 – Change in DBPs from BISAR Simulation of 2012-S5' (E_{AC}= 25%)

Description	% Change D_0	% Change AREA	% Change AUPP	% Change F_1	% Change SCI_8	% Change SCI_{12}	% Change ARE_8
No Cracking	0%	0%	0%	0%	0%	0%	0%
1.0" BUFC	13%	5%	22%	13%	25%	26%	24%
2.0" BUFC	25%	10%	45%	27%	53%	54%	50%
3.0" BUFC	34%	14%	63%	39%	82%	80%	72%
4.0" BUFC	41%	17%	79%	50%	113%	105%	92%
5.0" BUFC	48%	19%	92%	59%	143%	126%	111%
Total BUFC	66%	24%	129%	78%	197%	176%	155%

Table 6.7 – Change in DBPs from BISAR Simulation of 2012-S5' (E_{AC}= 50%)

Description	% Change D_0	% Change AREA	% Change AUPP	% Change F_1	% Change SCI_8	% Change SCI_{12}	% Change ARE_8
No Cracking	0%	0%	0%	0%	0%	0%	0%
1.0" BUFC	8%	3%	13%	8%	14%	15%	14%
2.0" BUFC	13%	6%	23%	14%	27%	27%	26%
3.0" BUFC	15%	7%	28%	18%	35%	34%	31%
4.0" BUFC	17%	8%	32%	21%	45%	41%	37%
5.0" BUFC	21%	9%	39%	25%	55%	50%	45%
Total BUFC	29%	12%	53%	33%	73%	68%	61%

6.1.2.2 Field Data

A summary of the observed cracking is presented in Table 6.8. Three of the four IWP stations (S5'-1, S5'-4, and S5'-7) had cracking on May 14, 2014. The other IWP station had cracking by June 16, 2014. The only other station to have any cracking was S5'-12 which had cracking observed after the completion of traffic on the last distress survey date.

Table 6.8 – Summarized Cracked Dates for 2012-S5'

FWD Station	"Cracked" Date
S5'-1	5/14/2014
S5'-2	Uncracked
S5'-3	Uncracked
S5'-4	5/14/2014
S5'-5	Uncracked
S5'-6	Uncracked
S5'-7	5/14/2014
S5'-8	Uncracked
S5'-9	Uncracked
S5'-10	6/16/2014
S5'-11	Uncracked
S5'-12	11/6/2014

A summary of the comparison of theoretical changes for 50% moduli values to measured changes of DBPs is presented in Table 6.9. Overall, only one DBP exceeded its theoretical change in one of the cracked stations (D_0 in S5'-10). The other four cracked stations were False Negatives; they had cracking but did not have any DBPs exceed theoretical values. The stations that did not have cracking were accurately characterized by not have their DBPs exceed theoretical changes. A summary of the comparison at AC moduli values of 25% is presented in Table 6.10. It can be seen that no DBPs exceeded their theoretical change, even on sections that were cracked. Thus, there were five False Negative classifications at 25% moduli.

Table 6.9 - Summary of DBP Prediction for Each Station in 2012 – S5' (E_{AC}=50%)

FWD Station	D_0	AREA	AUPP	F_1	SCI_8	SCI_{12}	ARE_8	1st Predictor	Classification
S5'-1	Never	Never	Never	Never	Never	Never	Never	None	False Negative
S5'-2	Never	Never	Never	Never	Never	Never	Never	None	NCO NCP
S5'-3	Never	Never	Never	Never	Never	Never	Never	None	NCO NCP
S5'-4	Never	Never	Never	Never	Never	Never	Never	None	False Negative
S5'-5	Never	Never	Never	Never	Never	Never	Never	None	NCO NCP
S5'-6	Never	Never	Never	Never	Never	Never	Never	None	NCO NCP
S5'-7	Never	Never	Never	Never	Never	Never	Never	None	False Negative
S5'-8	Never	Never	Never	Never	Never	Never	Never	None	NCO NCP
S5'-9	Never	Never	Never	Never	Never	Never	Never	None	NCO NCP
S5'-10	Early	Never	Never	Never	Never	Never	Never	D_0	Early
S5'-11	Never	Never	Never	Never	Never	Never	Never	None	NCO NCP
S5'-12	Never	Never	Never	Never	Never	Never	Never	None	False Negative
Summary: 1 Early, 7 NCO NCP, 4 False Negative									

Table 6.10 - Summary of DBP Prediction for Each Station in 2012 – S5' (E_{AC}=25%)

FWD Station	D_0	AREA	AUPP	F_1	SCI_8	SCI_{12}	ARE_8	1st Predictor	Classification
S5'-1	Never	Never	Never	Never	Never	Never	Never	None	False Negative
S5'-2	Never	Never	Never	Never	Never	Never	Never	None	NCO NCP
S5'-3	Never	Never	Never	Never	Never	Never	Never	None	NCO NCP
S5'-4	Never	Never	Never	Never	Never	Never	Never	None	False Negative
S5'-5	Never	Never	Never	Never	Never	Never	Never	None	NCO NCP
S5'-6	Never	Never	Never	Never	Never	Never	Never	None	NCO NCP
S5'-7	Never	Never	Never	Never	Never	Never	Never	None	False Negative
S5'-8	Never	Never	Never	Never	Never	Never	Never	None	NCO NCP
S5'-9	Never	Never	Never	Never	Never	Never	Never	None	NCO NCP
S5'-10	Never	Never	Never	Never	Never	Never	Never	None	False Negative
S5'-11	Never	Never	Never	Never	Never	Never	Never	None	NCO NCP
S5'-12	Never	Never	Never	Never	Never	Never	Never	None	False Negative
Summary: 7 NCO NCP, 5 False Negative									

The change in DBPs for 2012-S5' was not able to accurately characterize the cracking performance. Looking solely at the DBPs over time and modeling, it would be assumed that cracking did not occur; however, five FWD stations were cracked and over 15% of the lane area was cracked during the 7.2 million ESALs applied. It is not known why the DBP comparisons were worse for this section than the others.

6.1.3 2009 Group Experiment 50% RAP HMA-N10

Section N10 of the 2009 GE featured a 50% RAP mix and was constructed at hot-mix asphalt temperatures. The as-built pavement structure consisted of 7.1 inches of AC over 4.0 inches of crushed-granite granular base. Like all of the GE sections, there was no cracking after the 2009 research cycle and the section was left in place for the 2012 cycle for additional trafficking. The first cracks were observed in the section on November 18, 2013 after over of 15.5 million ESALs had been applied. The section continued to perform well after cracking

originated and the 2012 research cycle was completed with cracking in only 6.1% of the lane area after 20.1 million ESALs. A patch was applied to the transition zone prior to cracking being observed in the section. The patch came within 1 foot of RL#1; therefore DBPs from RL#1 could not be scrutinized and were discarded from this analysis.

6.1.3.1 Modeling

BUFC was modeled on section 2009-N10 in BISAR for AC moduli values of 25% and 50%, shown in Tables 6.11 and 6.12, respectively. Again, there is a much greater change when cracking was simulated by reducing the AC moduli values to 25% of their original values.

Table 6.11 – Change in DBPs from BISAR Simulation of 2009-N10 (E_{AC}= 25%)

Description	% Change D_0	% Change AREA	% Change AUPP	% Change F_1	% Change SCI_8	% Change SCI_{12}	% Change ARE_8
No Cracking	0%	0%	0%	0%	0%	0%	0%
1.0" BUFC	10%	4%	18%	11%	19%	20%	19%
2.0" BUFC	20%	8%	39%	23%	41%	43%	41%
3.0" BUFC	28%	11%	55%	33%	64%	66%	61%
4.0" BUFC	36%	14%	74%	45%	95%	93%	84%
5.0" BUFC	41%	16%	87%	54%	124%	115%	102%
6.0" BUFC	48%	18%	102%	64%	156%	139%	123%
Total BUFC	67%	23%	141%	82%	212%	189%	169%

Table 6.12 – Change in DBPs from BISAR Simulation of 2009-N10 (E_{AC}= 50%)

Description	% Change D_0	% Change AREA	% Change AUPP	% Change F_1	% Change SCI_8	% Change SCI_{12}	% Change ARE_8
No Cracking	0%	0%	0%	0%	0%	0%	0%
1.0" BUFC	6%	2%	11%	6%	11%	12%	11%
2.0" BUFC	11%	4%	20%	12%	21%	22%	21%
3.0" BUFC	13%	5%	25%	15%	28%	29%	27%
4.0" BUFC	16%	7%	31%	20%	39%	38%	35%
5.0" BUFC	18%	8%	35%	23%	48%	45%	41%
6.0" BUFC	21%	9%	42%	27%	59%	54%	49%
Total BUFC	29%	11%	57%	35%	78%	72%	66%

6.1.3.2 Field Data

The cracking at FWD stations in 2009-N10 is summarized in Table 6.13. Figure 6.4 shows the proximity of the patch to RL#4 which limited the ability to assess the DBPs in an intact state and required it to be discarded from this study.

Table 6.13 – Summarized Cracked Dates for 2009-N10

FWD Station	"Cracked" Date
N10-1	Patched
N10-2	Patched
N10-3	Patched
N10-4	8/19/2014
N10-5	Uncracked
N10-6	8/6/2014
N10-7	Uncracked
N10-8	Uncracked
N10-9	3/17/2014
N10-10	Uncracked
N10-11	Uncracked
N10-12	6/16/2014

Figure 6.4 – Patch near RL#1 in 2009-N10

Upon initial inspection of the 2009 GE FWD dataset, it was noticed that there was a continuous increase in deflections over the first few FWD readings. This effect is shown for section N10 in Figure 6.5 for sensors D_0, D_{12}, and D_{36}. To account for the initial conditioning that occurred over the first month, the second FWD testing date was used as the baseline date instead of the first date. Although the argument could be made that the deflections are still increasing after the second date, measured deflections returned to around these values later in the cycle but did not return to the initial values. Also, it was desired to include as much data as possible in this research as copious amounts of regularly tested FWD data was one of the advantages that this work had over others found in literature. Moving the baseline date to a later date would likely have reduced some of the variable encountered in the DBPs but that could be considered over manipulation of the data to match the expected outcomes. The conditioning

effect of initial traffic was observed, to various extents, in all 2009 GE sections, thus the second date of FWD testing was used as a baseline for all 2009 sections.

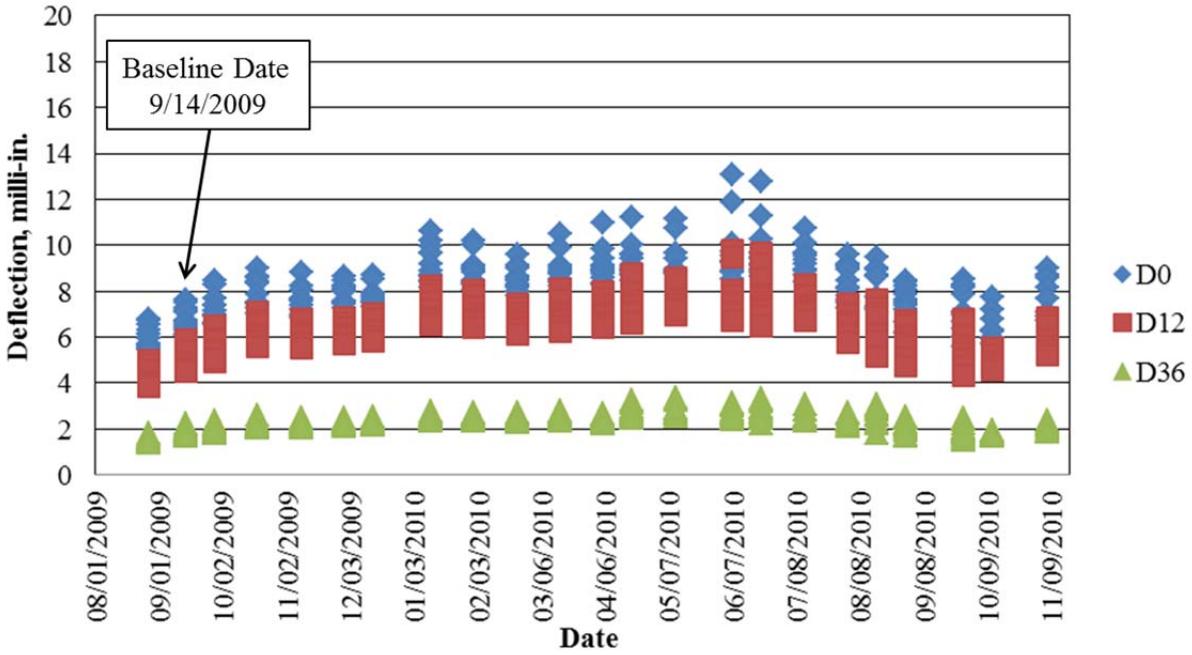

Figure 6.5 – 2009-N10 initial increase in deflections.

All FWD data presented in this work have been normalized for temperature and load following the procedure outlined in the Chapter 3. Methodology. However, slight temperature effects in which the higher deflections occur in the summer months can still be seen in Figure 6.5. It is necessary to view the entire dataset over its six years on the track to verify that the effect of temperature has been mitigated. Figure 6.6 shows the same deflections presented in 6.5 however the x-axis scale has been expanded to include all the FWD testing dates over the two research cycles that the GE was in place. A linear trendline has been applied to D_0 to show that there is very little (<0.2%) slope in the deflection data. The slight slope is attributed damage of the pavement structure and not to seasonal temperature variations.

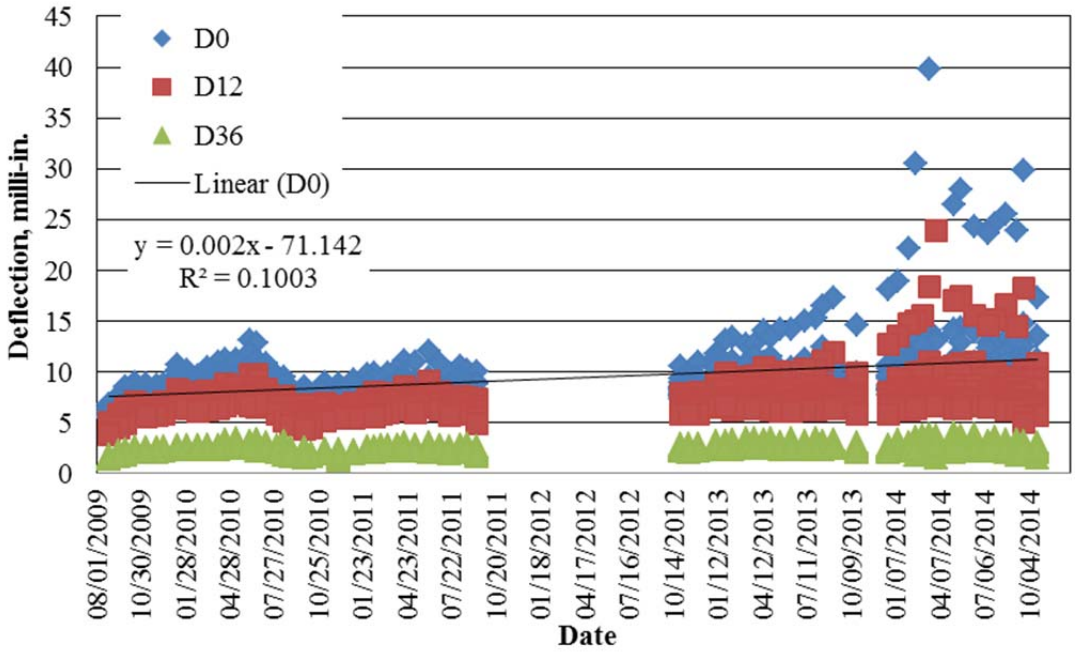

Figure 6.6 – Load and temperature corrected deflections and temperature over time for 2009-N10.

The results of the comparison between field DBPs and their theoretical values are presented in Tables 6.14 and 6.15 for moduli values of 25% and 50%, respectively. With AC moduli values of 25%, no DBPs continuously exceed the theoretical change, including stations that had cracking. Thus, the simulated change in DBPs from a modulus reduction to 25% was greater than the change that actually occurred in the pavement structure that led to cracking. This trend was seen throughout the Developmental Group sections and it was determined that a reduction to 25% was not a realistic approximation. Simulations and comparisons of the 25% AC moduli will no longer be presented for each section. With AC modulus values reduced to 50% in the cracking simulation, D_0 continuously exceeded the theoretical change for all cracked stations. However, D_0 intermittently exceeded the theoretical values throughout the research cycles even at stations that never had cracking within 1 foot of the FWD Test.

Table 6.14 - Summary of DBP Prediction for Each Station in 2009 – N10 (E_{AC}=25%)

FWD Station	D_0	AREA	AUPP	F_1	SCI_8	SCI_{12}	ARE_8	1st Predictor	Classification
N10-4	Never	Never	Never	Never	Never	Never	Never	None	False Negative
N10-5	Never	Never	Never	Never	Never	Never	Never	None	NCO NCP
N10-6	Never	Never	Never	Never	Never	Never	Never	None	False Negative
N10-7	Never	Never	Never	Never	Never	Never	Never	None	NCO NCP
N10-8	Never	Never	Never	Never	Never	Never	Never	None	NCO NCP
N10-9	Never	Never	Never	Never	Never	Never	Never	None	False Negative
N10-10	Never	Never	Never	Never	Never	Never	Never	None	NCO NCP
N10-11	Never	Never	Never	Never	Never	Never	Never	None	NCO NCP
N10-12	Never	Never	Never	Never	Never	Never	Never	None	False Negative
Summary: 5 NCO NCP, 4 False Negative									

Table 6.15 - Summary of DBP Prediction for Each Station in 2009 – N10 (E_{AC}=50%)

FWD Station	D_0	AREA	AUPP	F_1	SCI_8	SCI_{12}	ARE_8	1st Predictor	Classification
N10-4	Early	Never	Never	Never	Never	Never	Never	D_0	Early
N10-5	Early	Never	Never	Never	Never	Never	Never	D_0	False Positive
N10-6	Early	Never	Never	Never	Never	Never	Never	D_0	Early
N10-7	Early	Never	Never	Never	Never	Never	Never	D_0	False Positive
N10-8	Early	Never	Never	Never	Never	Never	Never	D_0	False Positive
N10-9	Early	Never	Never	Never	Never	Never	Never	D_0	Early
N10-10	Never	Never	Never	Never	Never	Never	Never	None	NCO NCP
N10-11	Early	Never	Never	Never	Never	Never	Never	D_0	False Positive
N10-12	Early	Never	Never	Never	Never	Never	Never	D_0	Early
Summary: 4 Early, 1 NCO NCP, 4 False Positive									

An example of the percent change in D_0 intermittently exceeding the theoretical change for BUFC with 50% AC moduli is presented in Figure 6.7. Although there is a general increasing trend in D_0, it can be seen that D_0 first exceeds the threshold in November 2009 but returns below on the subsequent data point. This type of variability dictated that strict rules be established to interpret the data consistently for all sections and stations being assessed. A DBP was not deemed to have surpassed the threshold unless it did so on multiple data points. A single data

point that deviated above or below the threshold with its surrounding data points on the opposite side was considered an anomaly due to testing variability. Thus for this station, it was reported that D_0 surpassed the threshold continuously after January 7, 2013 (despite two data points that non-consecutively returned below the threshold). This set of rules was applied to all sections and stations throughout this research. It must be noted that this variability is believed to be due to the increasing deflections early in the research cycle and most of the other sections and stations did not have this much variability in their data.

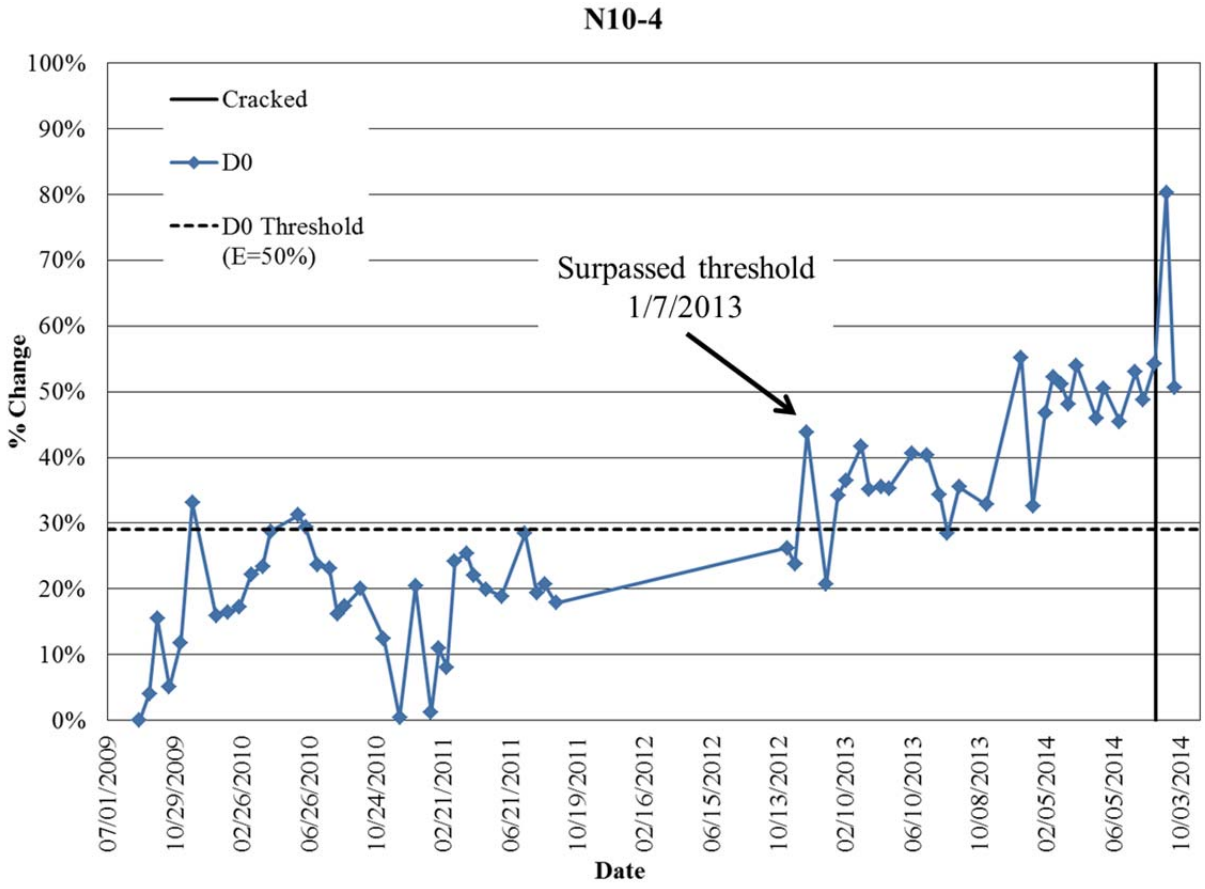

Figure 6.7 – 2009-N10 D_0 over time with E_{AC}=50% threshold.

As shown in the summary at the bottom of Table 6.15, the DBP comparisons were successful for five of the nine stations analyzed. Four were False Positives and there were no False Negatives. Thus, based on only the DBPs over time and the modeling at a 50% AC moduli, one could predict when cracking was likely to occur.

6.1.4 2009 Group Experiment 50% RAP WMA-N11

Section 2009-N11 of the GE was a companion section to 2009-N10 however the section was constructed at warm-mix temperatures, achieved by the foaming method. The as-built pavement structure consisted of 7.1 inches of AC over 4.2 inches of crushed-granite granular base over Test Track subgrade soil. The first cracks in 2009-N11 were observed early in the 2012 cycle (December 3, 2012) but the section never reached the failure threshold. At the end of the 2012 cycle, section 2009-N11 had 16.5% of the lane area cracked.

6.1.4.1 Modeling

The results of the BISAR simulation of BUFC using 50% AC moduli are presented in Table 6.16.

Table 6.16 – Change in DBPs from BISAR Simulation of 2009-N11 (E_{AC}= 50%)

Description	% Change D_0	% Change AREA	% Change AUPP	% Change F_1	% Change SCI_8	% Change SCI_{12}	% Change ARE_8
No Cracking	0%	0%	0%	0%	0%	0%	0%
1.0" BUFC	6%	2%	11%	6%	10%	11%	11%
2.0" BUFC	10%	4%	18%	11%	19%	20%	19%
3.0" BUFC	14%	6%	26%	16%	29%	30%	28%
4.0" BUFC	16%	7%	31%	20%	38%	38%	35%
5.0" BUFC	18%	8%	36%	23%	48%	46%	41%
6.0" BUFC	21%	9%	42%	27%	58%	54%	49%
Total BUFC	29%	12%	57%	36%	77%	71%	66%

6.1.4.2 Field Data

Section 2009-N11 had very little cracking at FWD stations. As shown in Table 7.17, the only FWD station to have cracking within 1 foot was station N11-12. All other stations were uncracked.

Table 6.17 – Summarized Cracked Dates for 2009-N11

FWD Station	"Cracked" Date
N11-1	Uncracked
N11-2	Uncracked
N11-3	Uncracked
N11-4	Uncracked
N11-5	Uncracked
N11-6	Uncracked
N11-7	Uncracked
N11-8	Uncracked
N11-9	Uncracked
N11-10	Uncracked
N11-11	Uncracked
N11-12	11/18/2013

It can be seen in the comparison of the percent change threshold for 50% AC moduli, shown in Table 6.18, that D_0 exceeded the threshold on stations (N11-1, N11-3, N11-7, and N11-10) which did not have cracking. Although D_0 exceeded prior to cracking, creating a False Positive classification, it is important that it exceeded the threshold during the 2012 research cycle and did not continuously exceed during the 2009 research cycle.

Table 6.18 - Summary of DBP Prediction for Each Station in 2012 – N11 (E_{AC}=50%)

FWD Station	D_0	AREA	AUPP	F_1	SCI_8	SCI_{12}	ARE_8	1st Predictor	Classification
N11-1	Early	Never	Early	Never	Never	Never	Never	D_0	False Positive
N11-2	Never	Never	Never	Never	Never	Never	Never	None	NCO NCP
N11-3	Never	Never	Never	Never	Never	Never	Never	None	NCO NCP
N11-4	Early	Never	Never	Never	Never	Never	Never	D_0	False Positive
N11-5	Never	Never	Never	Never	Never	Never	Never	None	NCO NCP
N11-6	Never	Never	Never	Never	Never	Never	Never	None	NCO NCP
N11-7	Early	Never	Never	Never	Never	Never	Never	D_0	False Positive
N11-8	Never	Never	Never	Never	Never	Never	Never	None	NCO NCP
N11-9	Never	Never	Never	Never	Never	Never	Never	None	NCO NCP
N11-10	Early	Never	Never	Never	Never	Never	Never	D_0	False Positive
N11-11	Never	Never	Never	Never	Never	Never	Never	None	NCO NCP
N11-12	Late	Late	Late	Late	Late	Late	Late	SCI_8	Late
Summary: 7 NCO NCP, 4 False Positive, 1 Late									

The DBPs did not exceed the 50% AC moduli simulation values for the cracked station N11-12 but SCI_8 exceeded on the testing date immediately after. A plot of the N11-12's DBPs over time is presented in Figure 6.8. There is a large amount of variability over time that can be seen in the plot but the only point that exceeded the threshold is immediately after cracking and is highlighted with a red "X". The late response of the DBPs for N11-12 might be attributed to the nature of the crack at that station. Figure 6.9 shows that the crack was longitudinal. It was documented in the GE summary report that coring verified that longitudinal cracks were TDC and transverse cracks were BUFC. As discussed in the TDC Group (Chapter 5), TDC is not expected to significantly change the measured deflection prior to cracking occurring. As shown in the summary at the bottom of Table 6.18, comparing the change in field DBPs to their respective theoretical change provided a successful assessment of the cracking performance in this section, especially when considering the nature of cracking (TDC) at the one cracked station.

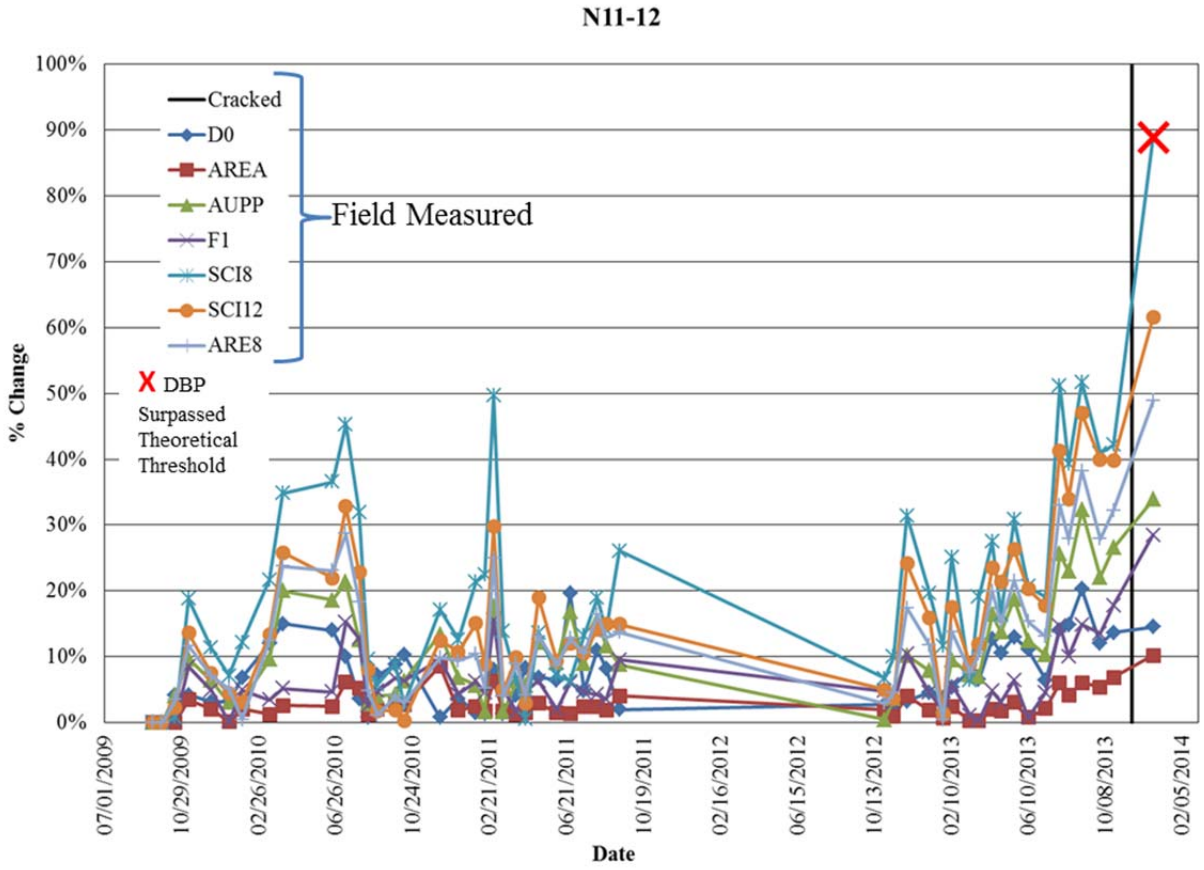

Figure 6.8 – 2009 N11-12 DBPs over time.

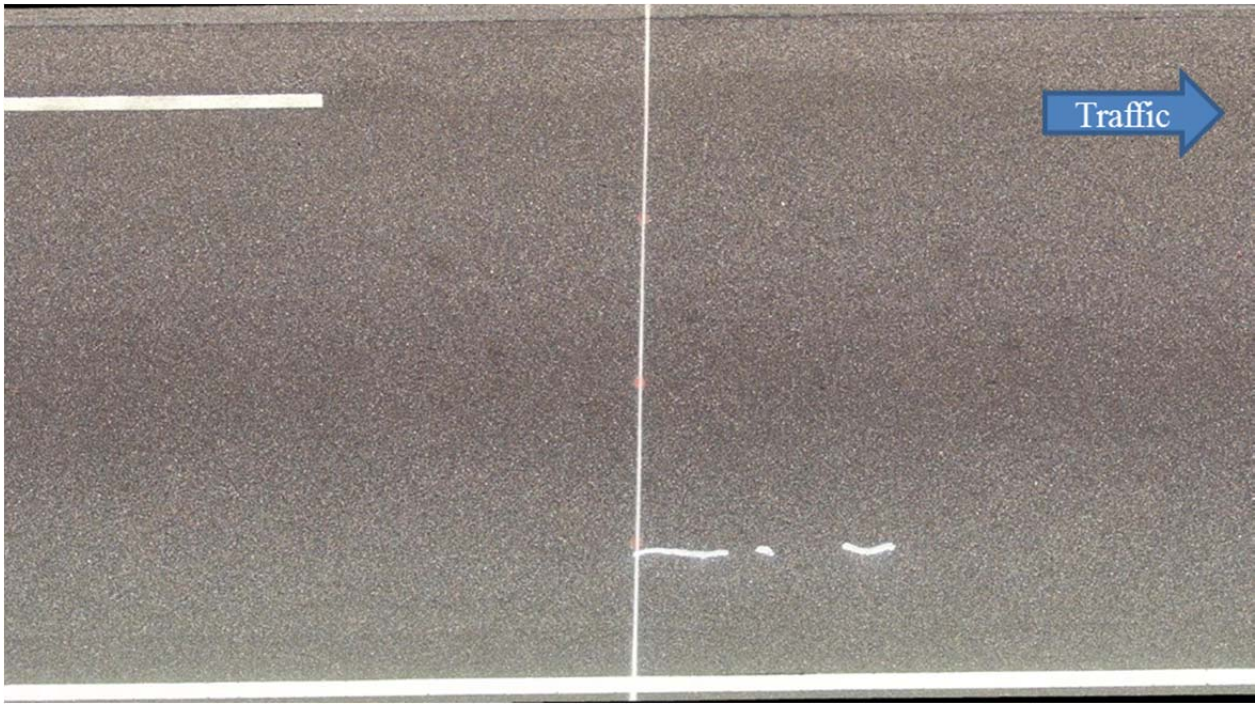

Figure 6.9 – 2009-N11 RL#4 with longitudinal cracks at N11-12.

6.1.5 2009 Group Experiment Control-S9

The control section of the GE did not have RAP and was constructed at HMA temperatures. The as-built pavement structure consisted of 7.0 inches of AC over 6.2 inches of crushed-granite granular base over Track subgrade soil. Cracking was first observed in this section on March 11, 2013 after 11.9 million ESALs.

6.1.5.1 Modeling

BUFC was simulated for the pavement structure of 2009-S9 with the AC moduli reduced to 25% and 50% of its original value. The percent change of the DBPs at 50% reduction is presented in Table 6.19.

Table 6.19 – Change in DBPs from BISAR Simulation of 2009-S9 (E_{AC}= 50%)

Description	% Change D_0	% Change AREA	% Change AUPP	% Change F_1	% Change SCI_8	% Change SCI_{12}	% Change ARE_8
No Cracking	0%	0%	0%	0%	0%	0%	0%
1.0" BUFC	6%	3%	10%	6%	8%	10%	10%
2.0" BUFC	11%	4%	17%	10%	15%	17%	17%
3.0" BUFC	14%	6%	23%	14%	22%	25%	23%
4.0" BUFC	16%	7%	27%	17%	28%	31%	28%
5.0" BUFC	19%	9%	32%	20%	35%	38%	35%
6.0" BUFC	30%	13%	51%	33%	67%	62%	58%
Total BUFC	34%	14%	58%	38%	81%	73%	67%

6.1.5.2 Field Data

Although cracking was first found in 2009-S9 in March 2013 the first crack within 1 foot of an FWD station was not observed until August 19, 2013. A summary of the cracking at each FWD station is shown in Table 6.20. Cracking was observed at only three FWD stations before maintenance was applied to the section at the end of April 2014.

Table 6.20 – Summarized Cracked Dates for 2009-S9

FWD Station	"Cracked" Date
S9-1	Uncracked
S9-2	Uncracked
S9-3	Uncracked
S9-4	Uncracked
S9-5	Uncracked
S9-6	Uncracked
S9-7	Uncracked
S9-8	Uncracked
S9-9	8/19/2013
S9-10	1/27/2014
S9-11	Uncracked
S9-12	11/11/2013

The results of the DBP comparison are presented in Table 6.21 for AC moduli of 50%. Similar to the previous sections, no DBPs exceeded the theoretical values for the BUFC simulation with AC moduli of 25% and therefore it is not presented. D_0 exceeded the theoretical value during the 2012 research cycle in several sections that did not have any cracking (S9-1, S9-4, S9-7, and S9-8). D_0 did not continuously exceed the threshold for any stations during the 2009 research cycle. No DBPs exceeded prior to cracking in any of the cracked sections (S9-9, S9-10, and S9-12). However, closer inspection indicated that this cracking was longitudinal, as shown in Figure 6.10 and 6.11 and therefore likely to be TDC. As discussed previously, TDC is believed to have a much smaller impact of the pavement structure and deflection basin at the time cracking is first observed because the majority of the structure does not have cracking. Figure 6.11 illustrates how cracking was classified for each station. The red line was used to establish the scale of image, since the FWD stations are spaced 3 feet apart. Based on that scale, circles were created with a 1 foot radius. If the cracks were within the circle the station was deemed to be cracked. Thus, S9-10 and S9-12 had longitudinal cracks within 1 foot and S9-11 was uncracked.

Table 6.21 - Summary of DBP Prediction for Each Station in 2009 – S9 (E_{AC}=50%)

FWD Station	D_0	AREA	AUPP	F_1	SCI_8	SCI_{12}	ARE_8	1st Predictor	Classification
S9-1	Early	Never	Early	Never	Never	Never	Never	D_0	False Positive
S9-2	Never	Never	Never	Never	Never	Never	Never	None	NCO NCP
S9-3	Never	Never	Never	Never	Never	Never	Never	None	NCO NCP
S9-4	Early	Never	Never	Never	Never	Never	Never	D_0	False Positive
S9-5	Never	Never	Never	Never	Never	Never	Never	None	NCO NCP
S9-6	Never	Never	Never	Never	Never	Never	Never	None	NCO NCP
S9-7	Early	Never	Never	Never	Never	Never	Never	D_0	False Positive
S9-8	Early	Never	Never	Never	Never	Never	Never	D_0	False Positive
S9-9	Never	Never	Never	Never	Never	Never	Never	None	False Negative
S9-10	Late	Never	Never	Never	Never	Never	Never	D_0	Late
S9-11	Never	Never	Never	Never	Never	Never	Never	None	NCO NCP
S9-12	Never	Never	Never	Never	Never	Never	Never	None	False Negative
Summary: 5 NCO NCP, 4 False Positive, 2 False Negative, 1 Late									

Figure 6.10 – Longitudinal cracking on 2009-S9 RL#3 on 8/19/2013.

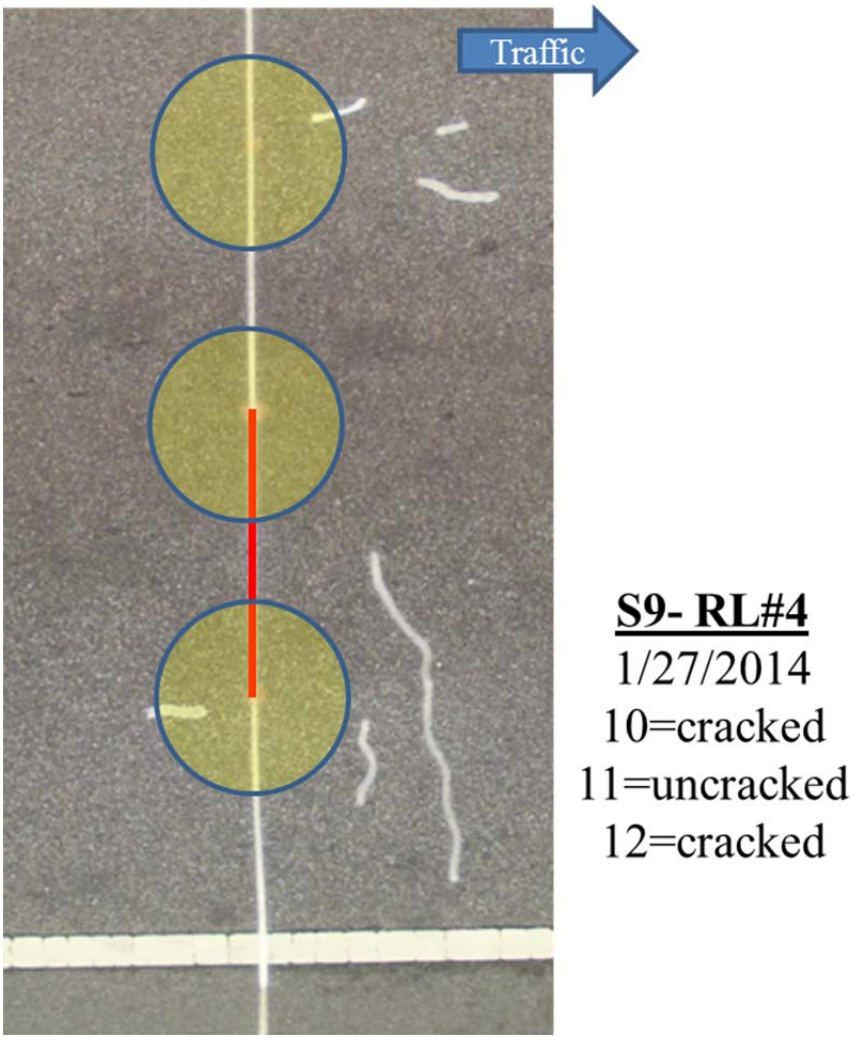

Figure 6.11 – Longitudinal cracking on 2009-S9 RL#4 on 1/27/2014.

The comparison of field and theoretical DBPs was successful in capturing the cracking performance of this section, especially after considering the nature of the cracking (TCD) shown in Figures 6.10 and 6.11.

6.1.6 2009 Group Experiment WMA-Foamed-S10

Section 2009-S10 of the GE used a foamed warm-mix technology to reduce the construction temperature of the AC. The AC layers totaling 7.0 inches were placed over 6.4

inches of granular base. Cracking was first observed early in the 2012 cycle (December 10, 2012) and the experiment was ended on April 21, 2012 when the section was divided to investigate different rehabilitation strategies. At completion of the experiment, the section withstood 17.5 million ESALs with 22.6% of the lane area cracked.

6.1.6.1 Modeling

The theoretical percent change for each DBP with simulated BUFC at AC moduli levels of 50% is presented in Table 6.22.

Table 6.22 – Change in DBPs from BISAR Simulation of 2009-S10 (E_{AC}= 50%)

Description	% Change D_0	% Change AREA	% Change AUPP	% Change F_1	% Change SCI_8	% Change SCI_{12}	% Change ARE_8
No Cracking	0%	0%	0%	0%	0%	0%	0%
1.0" BUFC	6%	3%	10%	6%	10%	11%	11%
2.0" BUFC	10%	4%	18%	11%	19%	20%	19%
3.0" BUFC	15%	6%	26%	16%	30%	30%	28%
4.0" BUFC	17%	8%	31%	20%	39%	38%	35%
5.0" BUFC	19%	9%	35%	23%	48%	44%	40%
6.0" BUFC	23%	10%	42%	27%	60%	54%	49%
Total BUFC	30%	13%	55%	34%	76%	70%	64%

6.1.6.2 Field Data

The FWD station cracking summary for 2009-S10 is presented in Table 6.23. All IWP stations (S10-1, S10-4, S10-7, and S10-1) were cracked. The first station to crack was S10-7 on July 8, 2013.

Table 6.23 – Summarized Cracked Dates for 2009-S10

FWD Station	"Cracked" Date
S10-1	8/19/2013
S10-2	Uncracked
S10-3	7/22/2013
S10-4	8/19/2013
S10-5	Uncracked
S10-6	8/26/2013
S10-7	7/8/2013
S10-8	Uncracked
S10-9	8/19/2013
S10-10	8/19/2013
S10-11	Uncracked
S10-12	Uncracked

Again, the percent change in DBPs for the BUFC cracking simulation using 25% AC moduli was greater than any of the changes in DBPs from the field data and is not shown. The 50% AC moduli simulation comparison is shown in Table 6.24. D_0 was the only DBP that exceeded its threshold prior to cracking and it was successful for all of the cracked stations. It also exceeded in four of the five uncracked stations but did not continuously exceed until February 16, 2014 in those cases. As mentioned previously, the fact that the DBPs did not exceed their thresholds for the vast majority of the two research cycles is an important confirmation that this methodology is effective. It was interesting in this section that D_0 was the only DBP that exceeded its threshold prior to cracking but other DBPs exceeded after cracking. Overall, the comparison of field and theoretical DBPs, especially D_0, was successful in matching the observed cracking performance for this section.

Table 6.24 - Summary of DBP Prediction for Each Station in 2009 – S10 (E_{AC}=50%)

FWD Station	D_0	AREA	AUPP	F_1	SCI_8	SCI_{12}	ARE_8	1st Predictor	Classification
S10-1	Early	Never	Never	Never	Never	Never	Never	D_0	Early
S10-2	Early	Never	Never	Never	Never	Never	Never	D_0	False Positive
S10-3	Early	Never	Late	Never	Late	Late	Late	D_0	Early
S10-4	Early	Never	Never	Never	Never	Never	Never	D_0	Early
S10-5	Early	Never	Never	Never	Never	Never	Never	D_0	False Positive
S10-6	Early	Never	Never	Never	Never	Never	Never	D_0	Early
S10-7	Early	Never	Late	Never	Never	Never	Late	D_0	Early
S10-8	Early	Never	Never	Never	Never	Never	Never	D_0	False Positive
S10-9	Early	Never	Never	Never	Never	Never	Never	D_0	Early
S10-10	Early	Never	Never	Never	Never	Never	Never	D_0	Early
S10-11	Early	Never	Never	Never	Never	Never	Never	D_0	False Positive
S10-12	Never	Never	Never	Never	Never	Never	Never	None	NCO NCP
Summary: 7 Early, 1 NCO NCP, 4 False Positive									

6.1.7 2009 Group Experiment WMA- Additive S11

Section 2009-S11 of the GE used an additive to achieve warm mix temperatures during construction. The as-built pavement structure consisted of 6.9 inches of AC over 6.2 inches of granular base. Although the section was the first of the GE sections to crack, by the end of the experiment it had less lane area cracked than its companion section, WMA-Foamed-S10. At the end of the experiment 14.0% of the lane area was cracked.

6.1.7.1 Modeling

The theoretical changes in DBPs for 2009-S11 are presented in Table 6.25. These values are very close to all of the values presented for the 2009 GE sections. Indicating that although the moduli and thicknesses are changing slightly, the overall amount of change is similar for pavements with similar thicknesses.

Table 6.25 – Change in DBPs from BISAR Simulation of 2009-S11 (E_{AC}= 50%)

Description	% Change D_0	% Change AREA	% Change AUPP	% Change F_1	% Change SCI_8	% Change SCI_{12}	% Change ARE_8
No Cracking	0%	0%	0%	0%	0%	0%	0%
1.0" BUFC	6%	3%	10%	6%	10%	11%	11%
2.0" BUFC	10%	5%	18%	11%	19%	20%	19%
3.0" BUFC	14%	6%	24%	15%	28%	28%	26%
4.0" BUFC	17%	8%	30%	20%	39%	38%	34%
5.0" BUFC	19%	9%	35%	23%	48%	45%	40%
6.0" BUFC	23%	11%	41%	27%	59%	54%	48%
Total BUFC	30%	13%	53%	34%	74%	67%	61%

6.1.7.2 Field Data

The IWP stations (S11-1, S11-4, S11-7, and S11-10) were the only stations to crack in 2009-S11, as shown in the cracking summary presented in Table 6.26. The exact date of cracking for stations S11-7 and S11-9 was not determined because May 6, 2013 was the first date that cracking images were available for this section.

Table 6.26 – Summarized Cracked Dates for 2009-S11

FWD Station	"Cracked" Date
S11-1	4/21/2014
S11-2	Uncracked
S11-3	Uncracked
S11-4	8/19/2013
S11-5	Uncracked
S11-6	Uncracked
S11-7	5/6/2013*
S11-8	Uncracked
S11-9	Uncracked
S11-10	5/6/2013*
S11-11	Uncracked
S11-12	Uncracked

*Unable to verify exact date of cracking

The comparison results for 2009-S11 are presented in Table 6.27. Similar to section 2009-S10, D_0 exceeded the simulated BUFC threshold at 11 of 12 stations, including all of the cracked stations. False Positives occurred from D_0 exceeding its threshold on seven of the eight uncracked stations. The False Positives did not occur until the 2012 portion of the research cycle when distress began to appear in the section, indicating that the False Positives are likely indications of structural changes that will lead to cracking at the surface. There were no False Negatives on this section and it can be concluded that the DBP comparison was successful in capturing the capturing the cracking distress that occurred.

Table 6.27 - Summary of DBP Prediction for Each Station in 2009 – S11 (E_{AC}=50%)

FWD Station	D_0	AREA	AUPP	F_1	SCI_8	SCI_{12}	ARE_8	1st Predictor	Classification
S11-1	Early	Never	Early	Never	Never	Early	Early	D_0	Early
S11-2	Early	Never	Never	Never	Never	Never	Never	D_0	False Positive
S11-3	Never	Never	Never	Never	Never	Never	Never	None	NCO NCP
S11-4	Early	Never	Early	Never	Early	Early	Early	D_0	Early
S11-5	Early	Never	Never	Never	Never	Never	Never	D_0	False Positive
S11-6	Early	Never	Never	Never	Never	Never	Never	D_0	False Positive
S11-7	Early	Never	Early	Never	Early	Early	Early	D_0	Early
S11-8	Early	Never	Never	Never	Never	Never	Never	D_0	False Positive
S11-9	Early	Never	Early	Never	Never	Never	Never	D_0	False Positive
S11-10	Early	Never	Early	Never	Early	Early	Early	D_0	Early
S11-11	Early	Never	Never	Never	Never	Never	Never	D_0	False Positive
S11-12	Early	Never	Never	Never	Never	Never	Never	D_0	False Positive
Summary: 4 Early, 1 NCO NCP, 7 False Positive									

Out of all of the sections analyzed in the BUFC Group, 2009-S11 had the most variability in the DBPs. A longer initial conditioning was observed in this section in which the deflections steadily increased over the first 9 months, as shown in the plot Figure 6.12. The plot shows deflections D_0, D_{12}, and D_{36} that have been normalized to a 9,000 lb. load and to a reference temperature of 68° F. There is an increasing trend from the first test date in August 2009 through May 2010. This long of a conditioning period was not observed in most of the other sections. The cause of the increasing deflection is unknown but it may be attributed to damage accumulation beginning early in the research cycle.

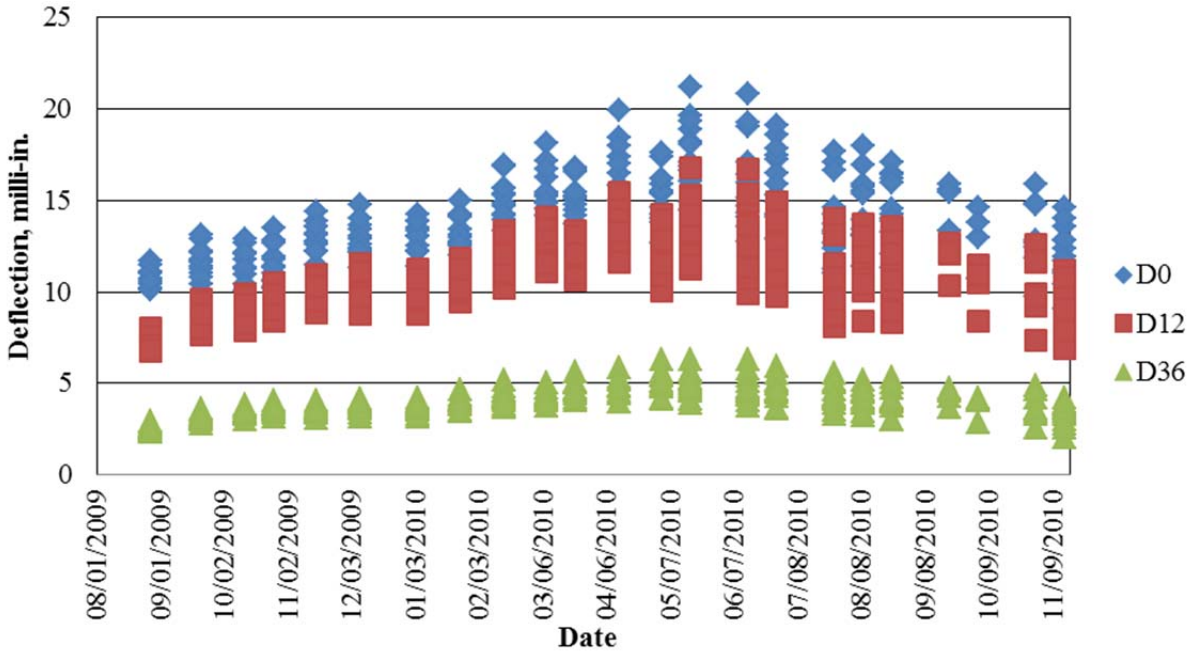

Figure 6.12 – 2009-N11 FWD deflections over time at the beginning of 2009 cycle.

6.1.8 2003 Structural Experiment PG 76-22 Thin-N1

Section N1 of the 2003 Structural Experiment was one of the two sections built with five inches of AC (the thinnest AC ever built on the Test Track). Section 2003-N1 had used a modified PG 77-22 and its companion section 2003-N2 (the other five inch AC section) had an unmodified PG 67-22 binder. This section failed rapidly due to BUFC. Figure 6.13 shows a picture from 2003-N1 of with a large area of fatigue cracks in the wheelpath. Coring verified that the cracking was BUFC.

Figure 6.13 – Fatigue cracking in 2003-N1 (Priest and Timm, 2006)

6.1.8.1 Modeling

The theoretical changes in DBPs for BUFC through the five inch AC structure is presented in Table 6.28 for AC moduli values 50%. Since the FWD used during the 2003 research cycle did not have sensors at 8 and 18 inches (as later research cycles did), the DBPs that consider those sensors were not considered. Surveyed layer thicknesses of the individual AC layers were not available for this research cycle so design thicknesses were used in the simulations.

Table 6.28 – Change in DBPs from BISAR Simulation of 2003-N1 (E_{AC}= 50%)

Description	% Change D_0	% Change AREA	% Change AUPP	% Change F_1	% Change SCI_{12}
No Cracking	0%	0%	0%	0%	0%
1.0" BUFC	8%	4%	13%	9%	16%
2.0" BUFC	14%	7%	22%	15%	28%
3.0" BUFC	17%	8%	27%	19%	36%
4.0" BUFC	19%	10%	32%	23%	43%
Total BUFC	28%	13%	47%	32%	61%

6.1.8.2 Field Data

As discussed in Chapter 3. Methodology, for the 2003 and 2006 research cycles cracking was classified from crack maps instead of videos and images. This was done by superimposing the RLs on the crack maps and evaluating if there were any cracks within 1 foot of each FWD station. This method inherently had more variability than directly assessing images of the pavement. In some cases there were inconsistencies in the crack maps which further limited the useable cracking data because crack maps with inconsistencies were discarded from this evaluation. There were only a limited number of crack maps that were available and some of the stations (N1-6 and N1-9) were already cracked on the first crack map available. A summary of the cracking at FWD stations is provided in Table 6.29.

Table 6.29 – Summarized Cracked Dates for 2003-N1

FWD Station	"Cracked" Date
N1-1	Uncracked
N1-3	10/25/2004
N1-4	Uncracked
N1-6	8/2/2004*
N1-7	8/9/2004
N1-9	8/2/2004*

*Unable to verify exact date of cracking

The FWD testing at each station was more limited during the 2003 research cycle. Deflection basins were measured from two drops targeting 9,000 lbs. instead of the procedure that was used in later cycles in which deflections were measured from 3 drops at several target load levels. As a result of the limited FWD testing procedure, the deflection basins could not be normalized for load. The frequency of FWD testing during the 2003 cycle was more widespread than the later cycles. For most stations in the 2003 cycle there were data from 12 FWD dates that had pavement temperatures available. The deflections were corrected to a reference temperature of 68° F.

The results of the change in field DBPs to theoretical DBPs are presented in Table 6.30. The results were very similar for both AC reduction levels. DBPs exceeded their theoretical values prior to cracking for two of the four cracked stations. DBPs exceeded values at both of the uncracked stations. The large amount of variability in section 2003-N1 and the results in the DBP comparison could be due to a combination of the large amount of distress that was observed on a relatively thin AC structure, the inability to normalize for load, and errors in the crack locations. Despite those concerns, the DBP comparison on this section as a whole was still successful in matching the large amount of distress that occurred.

Table 6.30 - Summary of DBP Prediction for Each Station in 2003 – N1 (E_{AC}=50%)

FWD Station	D_0	AREA	AUPP	F_1	SCI_{12}	1st Predictor	Classification
N1-1	Early	Early	Early	Early	Early	AREA	False Positive
N1-3	Late	Late	Late	Late	Late	D_0, AUPP, SCI_{12}	Late
N1-4	Early	Never	Early	Never	Early	D_0	False Positive
N1-6	Early	Early	Early	Early	Early	AREA, SCI_{12}	Early
N1-7	Late	Never	Late	Never	Never	D_0, AUPP,	Late
N1-9	Early	Early	Early	Early	Early	AREA	Early
Summary: 2 Early, 2 False Positive, 2 Late							

6.1.9 2003 Structural Experiment PG67-22Thick-N3

Section N3 of the 2003 Structural Experiment had nine inches of AC over six inches of granular base. An unmodified 67-22 binder was used in this section. The section performed very well and no cracking was documented.

6.1.9.1 Modeling

BUFC was modeled in BISAR by reducing the AC moduli to 25 and 50% for the cracked portion of the pavement. The results for the 50% AC moduli simulations are presented in Table 6.31. It is interesting that the nine inch pavement structure leads to a greater change in DBPs from the uncracked to cracked simulations than the thinner sections. Thus, in a thicker pavement structure, greater changes in DBPs can be expected.

Table 6.31 – Change in DBPs from BISAR Simulation of 2003-N3 (E_{AC}= 50%)

Description	% Change D_0	% Change AREA	% Change AUPP	% Change F_1	% Change SCI_{12}
No Cracking	0%	0%	0%	0%	0%
1.0" BUFC	5%	2%	8%	4%	8%
2.0" BUFC	9%	3%	15%	8%	15%
3.0" BUFC	12%	4%	22%	12%	23%
4.0" BUFC	15%	5%	28%	16%	30%
5.0" BUFC	17%	7%	33%	20%	38%
6.0" BUFC	20%	8%	39%	25%	47%
7.0" BUFC	22%	9%	45%	29%	56%
8.0" BUFC	26%	10%	52%	32%	65%
Total BUFC	32%	12%	64%	38%	78%

6.1.9.2 Field Data

N3 did not have any cracks during the 2003 research cycle, as shown in the summary table, Table 6.32.

Table 6.32 – Summarized Cracked Dates for 2003-N3

FWD Station	"Cracked" Date
N3-1	Uncracked
N3-3	Uncracked
N3-4	Uncracked
N3-6	Uncracked
N3-7	Uncracked
N3-9	Uncracked

In the comparison of theoretical DBPs to field DBPs, both moduli reduction levels performed accurately. That is, no DBPs continuously exceeded their threshold values. No DBPs exceeded the change for 25% AC moduli for any of the stations. At 50% AC moduli, only one DBP exceeded the threshold on one date (N3-1 on January 26, 2004). Since this only occurred on

one date and returned to below the threshold it was deemed an outlier. The success on the comparison on this section is an important result because it indicates that this methodology works well for intact pavements. The fact that there were no False Positives on this section, which was a pavement that was known to have performed well, is a strong indication that most of the False Positives observed in other sections were not erratic results but early indicators of distress. Also, it is noteworthy that this worked without normalization for load.

Table 6.33 - Summary of DBP Prediction for Each Station in 2003 – N3 (E_{AC}=50%)

FWD Station	D_0	AREA	AUPP	F_1	SCI_{12}	1st Predictor	Classification
N3-1	Never	Never	Never	Never	Never	None	NCO NCP
N3-3	Never	Never	Never	Never	Never	None	NCO NCP
N3-4	Never	Never	Never	Never	Never	None	NCO NCP
N3-6	Never	Never	Never	Never	Never	None	NCO NCP
N3-7	Never	Never	Never	Never	Never	None	NCO NCP
N3-9	Never	Never	Never	Never	Never	None	NCO NCP
Summary: 6 NCO NCP							

6.1.10 2003 Structural Experiment PG 76-22 Medium-N5

Section N5 of 2003 Structural Experiment used a modified PG 76-22 binder in seven inches of AC that was built over six inches of granular base (design thicknesses). Some cracking was observed in the section but it did not reach the predefined failure threshold for this cycle of cracking in 20% of the lane area.

6.1.10.1 Modeling

The results of the BUFC simulations in BISAR are presented in Tables 6.34. The results are very similar to those presented previously for the 2009 GE sections that also had seven inches of AC.

Table 6.34 – Change in DBPs from BISAR Simulation of 2003-N5 (E_{AC}= 50%)

Description	% Change D_0	% Change AREA	% Change AUPP	% Change F_1	% Change SCI_{12}
No Cracking	0%	0%	0%	0%	0%
1.0" BUFC	6%	3%	10%	6%	11%
2.0" BUFC	11%	4%	19%	11%	21%
3.0" BUFC	15%	6%	26%	16%	30%
4.0" BUFC	17%	8%	31%	20%	39%
5.0" BUFC	20%	9%	36%	24%	46%
6.0" BUFC	23%	10%	42%	27%	54%
Total BUFC	30%	12%	56%	35%	70%

6.1.10.2 Field Data

The cracking summary for 2003-N5 is presented in Table 6.35. The only cracking at the FWD stations occurred at RL#1 (stations N5-1 and N5-3). All other stations were uncracked.

Table 6.35 – Summarized Cracked Dates for 2003-N5

FWD Station	"Cracked" Date
N5-1	8/15/2005
N5-3	12/13/2004
N5-4	Uncracked
N5-6	Uncracked
N5-7	Uncracked
N5-9	Uncracked

A summary of the DBP comparison at AC moduli of 50% is presented in Table 6.36. The DBPs did not exceed their thresholds for station N5-1 which had cracking recorded on August 15, 2005. It should be noted that the last FWD date was over six months earlier on February 7, 2005. The DBPs did not exceed theoretical values for N5-3 until April 18, 2005 despite cracking being observed on December 13, 2004. Again, the poor results may be attributed to the inability

to normalize for load or errors in the cracking data; however, careful inspection of the last crack map available from August15, 2005 indicates that cracking may have been longitudinal. Figure 6.14 shows the crack map from August 15, 2005. The x-axis shows the distance from the end of the section and the y-axis is the distance from the centerline. Traffic is moving right to left on the map. The random locations have been superimposed over the crack map. The IWP is at a y-axis offset of 3 feet and the OWP is at an offset of 9 feet. It can be seen that the majority of the cracks are in the longitudinal direction. Based on the theoretical results of the TDC group and the 2009 GE sections, the lack of change in the DBPs may be an indication of TDC and not a False Negative result. Confirmation that the cracking in N5 was TDC was found in a later report and an image of the cracking at a RL is provided in Figure 6.15 (Timm, 2009). After consideration of the TDC, it is apparent that the comparison of field and theoretical DBPs was successful for this section.

Table 6.36 - Summary of DBP Prediction for Each Station in 2003 – N5 (E_{AC}=50%)

FWD Station	D_0	AREA	AUPP	F_1	SCI_{12}	1st Predictor	Classification
N5-1	Never	Never	Never	Never	Never	None	False Negative
N5-3	Never	Never	Never	Never	Never	None	Late
N5-4	Never	Never	Never	Never	Never	None	NCO NCP
N5-6	Never	Never	Never	Never	Never	None	NCO NCP
N5-7	Never	Never	Never	Never	Never	None	NCO NCP
N5-9	Never	Never	Never	Never	Never	None	NCO NCP
Summary: 4 NCO NCP, 1 False Negative, 1 Late							

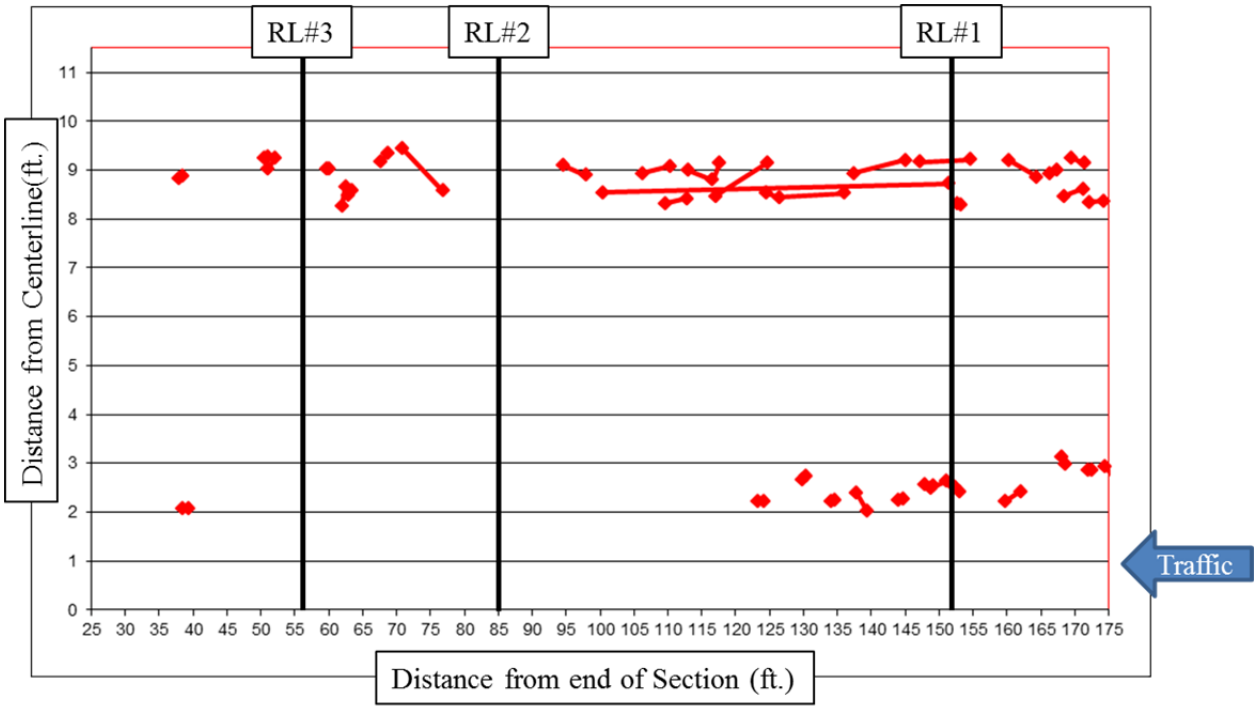

Figure 6.14 – Crack map of 2003-N5 from 8/15/2005

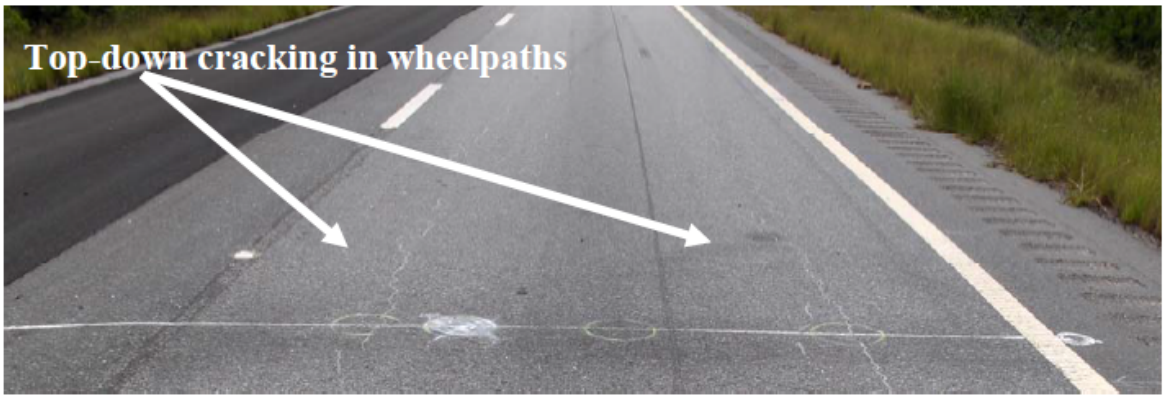

Figure 6.15 – TDC in 2003-N5 (Timm, 2009)

6.1.11 2003 Structural Experiment PG67-22 Medium-N6

Section 2003-N6 also had seven inches of AC over six inches of granular base but used an unmodified PG 67-22 binder. The section was reported to have more cracking than 2003-N5 and areas with interconnected cracks.

6.1.11.1 Modeling

The results of the BISAR simulation of BUFC for N6 are presented in Table 6.37. The results were very similar to the results for 2003-N5 in Table 6.34. Since design thicknesses were used, the same layer thicknesses were input in the simulations of 2003 sections N5-N8 and although different PG grades were used in the two sections, there was very little difference in the moduli values input into the simulations. The surface layer modulus inputs were 5,980 MPa for N5 and 5,930 MPa for N6. The intermediate and bottom layer modulus inputs were 7,320 MPa for N5 and 7,340 for N6. The modulus values were obtained from dynamic modulus (E*) testing at a frequency of 10 Hz. and a temperature of 20° C. The similarity is likely due to the combination of frequency and temperature being in the middle of the E* master-curve resulting in minimal differences from binder grade that would be seen at more extreme combinations of load and temperature. Differences were apparent in the actual deflections generated in BISAR but were within a few milli-inches of each other.

Table 6.37 – Change in DBPs from BISAR Simulation of 2003-N6 (E_{AC}= 50%)

Description	% Change D_0	% Change AREA	% Change AUPP	% Change F_1	% Change SCI_{12}
No Cracking	0%	0%	0%	0%	0%
1.0" BUFC	6%	3%	11%	6%	11%
2.0" BUFC	11%	5%	19%	11%	21%
3.0" BUFC	15%	6%	26%	16%	30%
4.0" BUFC	17%	8%	31%	20%	39%
5.0" BUFC	20%	9%	36%	24%	46%
6.0" BUFC	23%	10%	43%	27%	55%
Total BUFC	30%	12%	56%	35%	71%

6.1.11.1 Field Data

The cracking observed at the FWD stations in 2003-N6 is summarized in Table 6.38. It can be seen that none of the stations had cracking. Although there was more cracked area in this section than in N5, it can be seen in the crack map of N6 from 8/15/2005 (Figure 7.16) that none of the RLs had cracking within 1 foot.

Table 6.38 – Summarized Cracked Dates for 2003-N6

FWD Station	"Cracked" Date
N6-1	Uncracked
N6-3	Uncracked
N6-4	Uncracked
N6-6	Uncracked
N6-7	Uncracked
N6-9	Uncracked

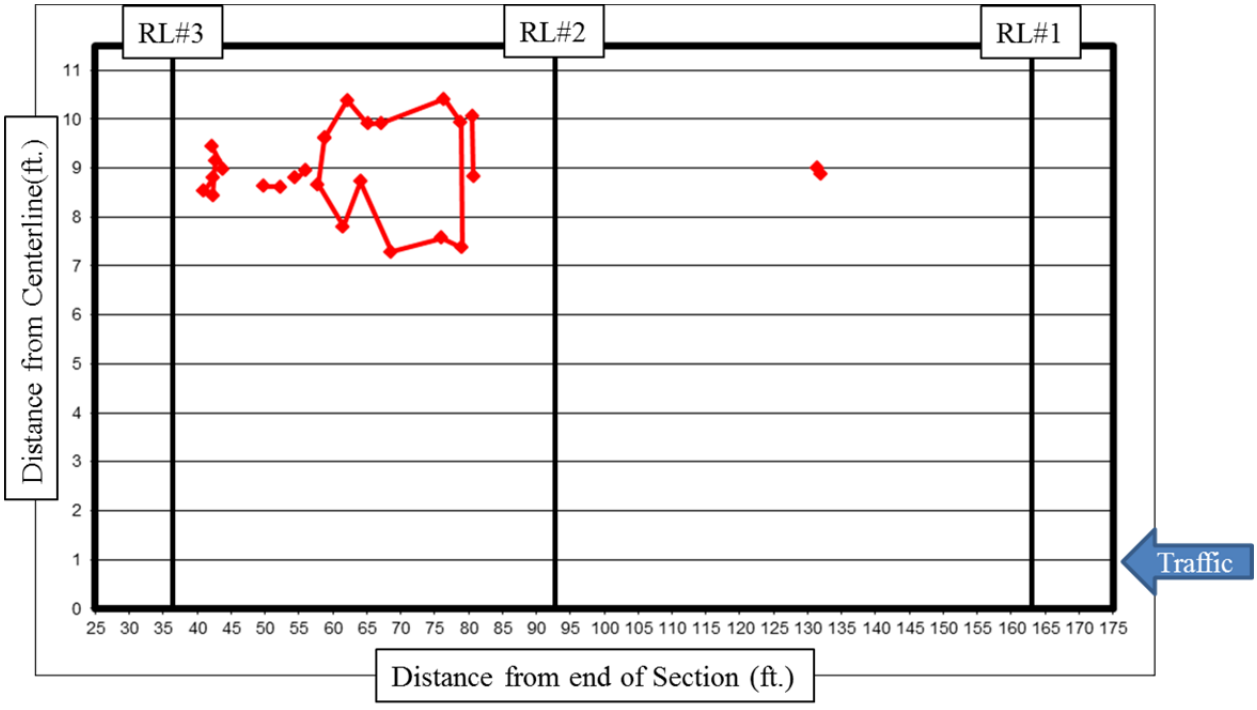

Figure 6.16 – Crack map of 2003-N6 from 8/15/2005

The results of the DBP comparisons for AC moduli of 50% are presented in Table 6.39. None of the stations had any DBPs exceed either their threshold values. Thus, the DBPs successfully matched the documented performance for this section.

Table 6.39 - Summary of DBP Prediction for Each Station in 2003 – N6 (E_{AC}=50%)

FWD Station	D_0	AREA	AUPP	F_1	SCI_{12}	1st Predictor	Classification
N6-1	Never	Never	Never	Never	Never	None	NCO NCP
N6-3	Never	Never	Never	Never	Never	None	NCO NCP
N6-4	Never	Never	Never	Never	Never	None	NCO NCP
N6-6	Never	Never	Never	Never	Never	None	NCO NCP
N6-7	Never	Never	Never	Never	Never	None	NCO NCP
N6-9	Never	Never	Never	Never	Never	None	NCO NCP
Summary: 6 NCO NCP							

6.1.12 2003 Structural Experiment SMA Medium-N7

Section 2003-N7 also had seven inches of AC over six inches of granular base. The one inch surface layer was an SMA mixture. Sections 2003-N7 had an unmodified PG 67-22 binder. It was a companion section 2003-N8 which had the same thickness and mixes except the bottom lift in 2003-N8 had increased binder content. Section 2003-N7 had some cracking that was observed but it did not surpass the cracking failure threshold.

6.1.12.1 Modeling

The results of the BISAR simulations of BUFC are presented in Table 6.40. As discussed previously, the change in DBPs are very similar for all of the seven inch AC section, especially those for the 2003 structural experiment which were simulated with identical design layer thicknesses instead of as-built thicknesses.

Table 6.40 – Change in DBPs from BISAR Simulation of 2003-N7 (E_{AC}= 50%)

Description	% Change D_0	% Change AREA	% Change AUPP	% Change F_1	% Change SCI_{12}
No Cracking	0%	0%	0%	0%	0%
1.0" BUFC	7%	3%	12%	7%	13%
2.0" BUFC	12%	5%	21%	12%	23%
3.0" BUFC	16%	7%	28%	17%	33%
4.0" BUFC	18%	8%	33%	21%	41%
5.0" BUFC	21%	9%	38%	25%	49%
6.0" BUFC	24%	10%	45%	29%	57%
Total BUFC	30%	12%	56%	35%	71%

6.1.12.2 Field Data

Although there was cracking in 2003-N7, none of the cracking was within 1 foot of the FWD stations, as summarized in Table 6.41. A crack map from this section is presented in Figure 6.17. There is cracking close to RL#3 but the closest crack is still over 2 feet away from the station N7-7.

Table 6.41 – Summarized Cracked Dates for 2003-N7

FWD Station	"Cracked" Date
N7-1	Uncracked
N7-3	Uncracked
N7-4	Uncracked
N7-6	Uncracked
N7-7	Uncracked
N7-9	Uncracked

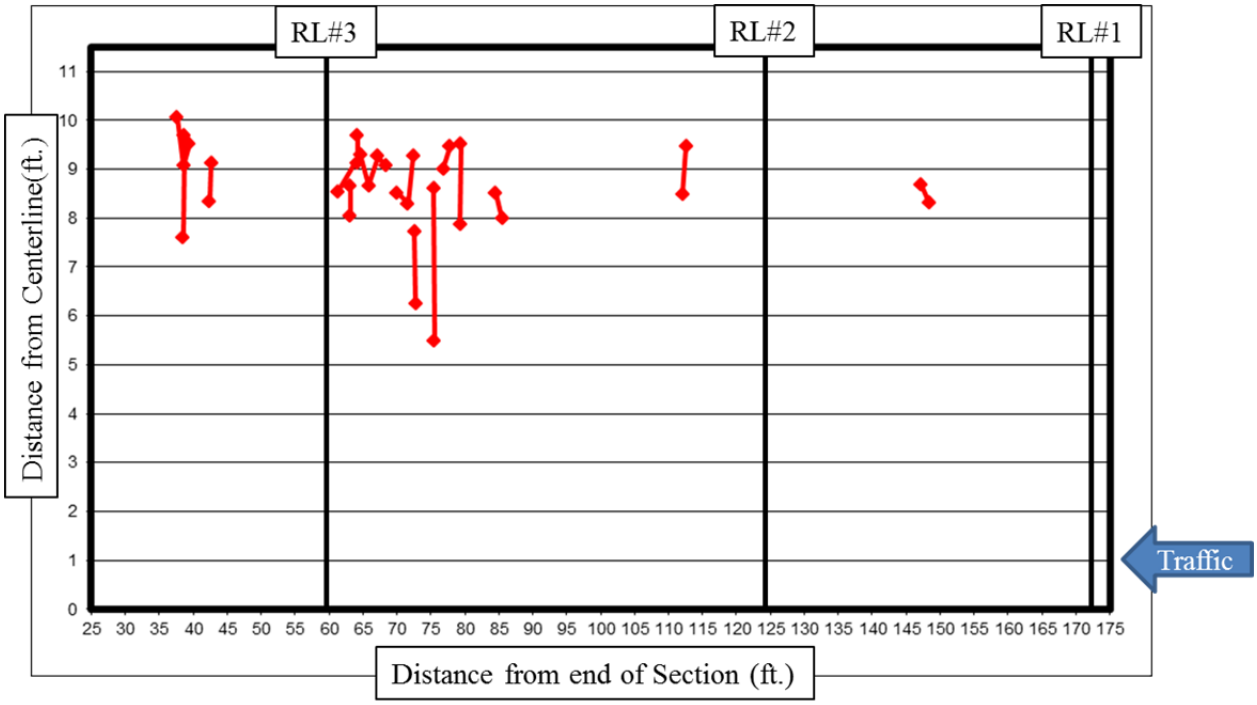

Figure 6.17 – Crack map of 2003-N7 from 8/15/2005

Similar results for both AC moduli levels were again obtained from the comparisons between theoretical and field DBPs. Table 6.42 shows the results for the 50% moduli comparison. D_0 exceeded its threshold of 30% change on the last date of FWD testing at stations N7-6 (D_0=40%) and N7-9 (D_0=34%). Since this occurred on the last date of testing, it is unknown if this was a trend or just an anomaly but it is believed to be an indication of distress within the structure (not an anomaly) because the cracking documented in Figure 6.17 was also in the OWP. Overall, the ability of the DBPs to match the field distress conditions was very good for this section, especially considering the inability to normalize for load.

Table 6.42 - Summary of DBP Prediction for Each Station in 2003 – N7 (E_{AC}=50%)

FWD Station	D_0	AREA	AUPP	F_1	SCI_{12}	1st Predictor	Classification
N7-1	Never	Never	Never	Never	Never	None	NCO NCP
N7-3	Never	Never	Never	Never	Never	None	NCO NCP
N7-4	Never	Never	Never	Never	Never	None	NCO NCP
N7-6	Early	Never	Never	Never	Never	None	False Positive
N7-7	Never	Never	Never	Never	Never	None	NCO NCP
N7-9	Early	Never	Never	Never	Never	None	False Positive
Summary: 4 NCO NCP, 2 False Positives							

6.2 Summary of Bottom-up Fatigue Cracking Developmental Group

The Bottom-up Fatigue Cracking Developmental Group had an array of pavement thicknesses and performance that provided useful guidance in fine-tuning the methodology to be used in the Fatigue Cracking Developmental Group.

It was apparent over the 12 developmental group sections that the BISAR BUFC cracking simulations at an AC moduli at 25% of their original values often predicted too large of a change in the structure because the percent change was not exceed by the change in field DBPs at cracked stations. There were numerous False Negatives in the 25% AC moduli comparisons. A False Negative was deemed to be worse than a False Positive because False Negatives did capture the change that occurred in the structure that led to cracking. False Positives may be an indication of underlying problems in the pavement structure that have not propagated to the surface yet.

The lower percent changes that resulted from the 50% AC moduli simulations were still not exceeded in sections that did not have cracking, such as 2003 N3 or 2009 portions of most of the 2009 GE sections. This was an important confirmation that the simulated changes were not so low that they were exceeded by inherent variability of the data. Moving forward with the

analysis of the Fatigue Cracking Validation Group, BUFC will only be simulated at AC moduli of 50%.

This group also forced rules to be determined to address the challenges of variability and outliers. A single data point that exceeded the threshold once and returned below was not considered to have surpassed and vice versa (after surpassing, if a single data point returned below the threshold one time the DBP was still considered to have surpassed). More variability was observed in the sections that had heavy distress, such as 2003-N1, which was a good indication of the validity of this methodology.

Another issue that was apparent was the initial conditioning that took place in some of the sections as traffic was applied. The second FWD testing date was used as a baseline for comparison in all of the 2009 GE sections. In some sections using the second testing date may not have been necessary, and in some sections using a later date would have provided better results in the comparisons, but to treat all data in each research cycle the same, the second date was used.

The 2003 Structural Sections showed that even with limited data the methodology was still successful. Although deflections at other load levels would have been useful to normalize for load and eliminate a possible source of variability, the performance of the comparisons showed that analysis of other load levels was not essential. More important was the fact that the methodology was still valid with two less FWD sensors and two less DBPs. The sensors at 8 and 18 inches are measuring the responses of the entire pavement structure, including the AC, but they were not absolutely necessary for the functionality of this methodology. Many FWDs do not have the 8 and 18 inch sensors, so the success of the 2003 section was important to show applicability to more testing configurations.

6.3 Bottom-up Fatigue Cracking Validation Group

The Bottom-up Fatigue Cracking Validation Group sections were pre-selected to include each of the AC thicknesses used in the Developmental Group and a variety of distress conditions. The pavement structure of these sections is shown in Figure 6.18. For this group, the change in field measured DBPs was compared with BISAR simulated BUFC using 50% of the AC moduli in cracked layers. Section S8 from the 2009 GE experiment used the second FWD date as the baseline to help mitigate some of the conditioning that was observed in other 2009 GE sections.

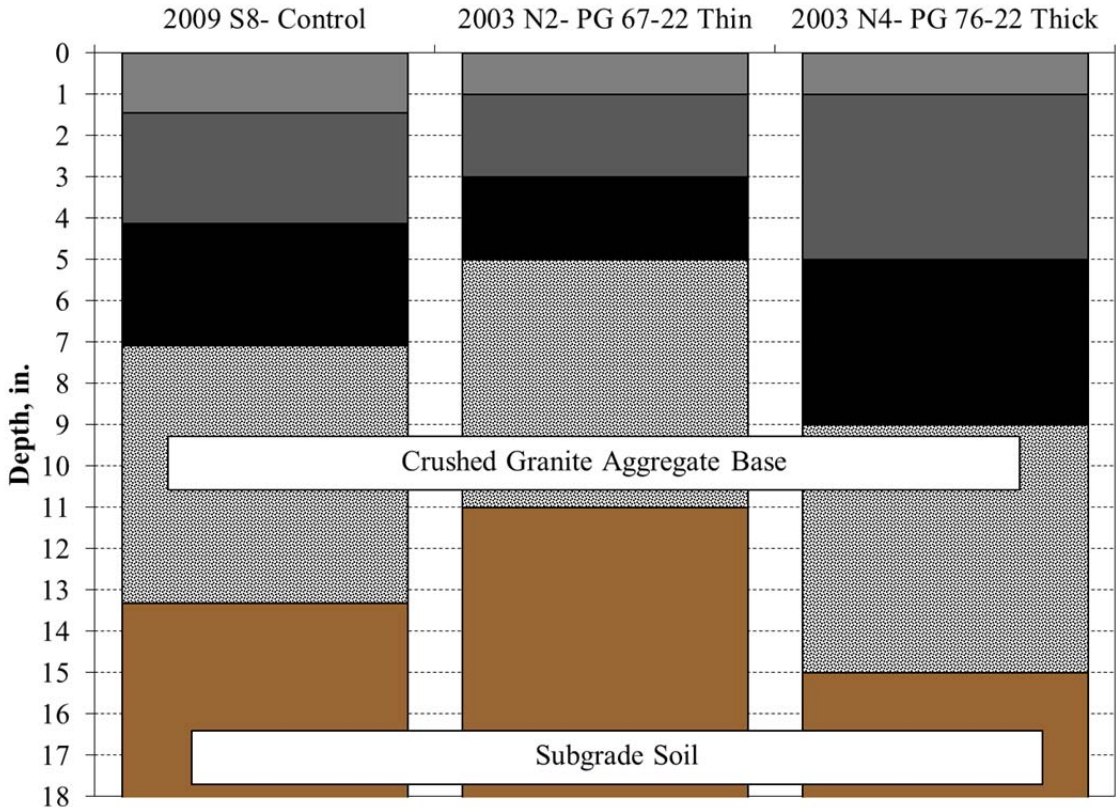

Figure 6.18 – Cross-sections of Bottom-up Fatigue Cracking Validation Group

6.3.1 2009 Group Experiment PFC-S8

Section S8 of the 2009 GE had a seven inch structure including a Porous Friction Course (PFC) surface layer. Although the section did not crack during the 2009 research cycle, significant cracking developed as traffic was continued on the section during the 2012 cycle. The first cracking in the section was observed in March 2013. The cracking failure threshold was exceeded in September 2013 and by March 2014, 36% of the lane area was cracked. On April 24, 2014, the section was converted to a preservation study and treatments were applied. The large FWD dataset from the 2009 GE experiment and the extensive distress observed in 2009-S8 during the 2012 cycle made it ideal to validate the methodology. A successful methodology would show no significant changes in the DBPs during the 2009 cycle and then significant changes during the 2012 portion.

7.3.2.1 Modeling

The BISAR simulation of BUFC in section 2009-S8 is presented in Table 6.43.

Table 6.43 – Change in DBPs from BISAR Simulation of 2009-S8 (E_{AC}= 50%)

Description	% Change D_0	% Change AREA	% Change AUPP	% Change F_1	% Change SCI_8	% Change SCI_{12}	% Change ARE_8
No Cracking	0%	0%	0%	0%	0%	0%	0%
1.0" BUFC	6%	3%	10%	6%	10%	11%	11%
2.0" BUFC	11%	5%	19%	11%	20%	21%	20%
3.0" BUFC	15%	6%	27%	17%	31%	32%	29%
4.0" BUFC	17%	8%	31%	20%	39%	38%	35%
5.0" BUFC	19%	9%	36%	23%	48%	46%	41%
6.0" BUFC	23%	10%	42%	27%	59%	54%	49%
Total BUFC	30%	12%	55%	35%	76%	70%	64%

6.3.2.2 Field Data

The cracking at the FWD stations is summarized in Table 6.44. Stations S8-1, S8-2, S8-8, S8-10, and S8-11 were uncracked when the experiment was converted to a preservation study in April 2014.

Table 6.44 – Summarized Cracked Dates for 2009-S8

FWD Station	"Cracked" Date
S8-1	Uncracked
S8-2	Uncracked
S8-3	7/8/2013
S8-4	8/19/2013
S8-5	2/17/2014
S8-6	5/6/2013*
S8-7	2/3/2014
S8-8	Uncracked
S8-9	8/19/2013
S8-10	Uncracked
S8-11	Uncracked
S8-12	11/11/2013

The results of the theoretical BUFC to field DBP comparison are presented in Table 6.45. During the 2009 research cycle, in which there was no cracking in the section, none of the DBPs exceeded their threshold. Station S8-4 did not have DBPs exceed their thresholds before cracking was observed. Closer inspection of the cracking on this station, shown in Figure 6.19 indicates that cracking was on the outer extent of the one foot radius around the center of the FWD station (shown with yellow circles). The one foot radius criteria was established based on a severe discontinuity in the pavement structure. Therefore, less severe cracks at a distance of one foot may not have the same impact on the deflection basin as the severe discontinuity. Stations S8-8

(after 2/16/2014) and S8-10 (after 7/1/2013) did not have any cracking but D_0 exceeded its theoretical threshold. In station S8-10, AUPP and SCI_8 also exceeded their thresholds after January 27, 2014 and December 23, 2013, respectively. Based on Early Predictions and NCO NCPs occurring at 75% of the stations analyzed, the comparison was successful overall for this section, especially after considering that the DBPs did not surpass their thresholds during the 2009 research cycle when the section was still in good condition. Once distress started occurring in the section during the 2012 cycle, the DBPs began to exceed their threshold values.

Table 6.45 - Summary of DBP Prediction for Each Station in 2009 –S8 (E_{AC}=50%)

FWD Station	D_0	AREA	AUPP	F_1	SCI_8	SCI_{12}	ARE_8	1st Predictor	Classification
S8-1	Never	Never	Never	Never	Never	Never	Never	None	NCO NCP
S8-2	Never	Never	Never	Never	Never	Never	Never	None	NCO NCP
S8-3	Early	Never	Never	Never	Never	Never	Never	D_0	Early
S8-4	Never	Never	Never	Never	Never	Never	Never	None	False Negative
S8-5	Early	Never	Never	Never	Never	Never	Never	D_0	Early
S8-6	Early	Never	Late	Never	Late	Late	Late	D_0	Early
S8-7	Early	Never	Late	Never	Late	Late	Late	D_0	Early
S8-8	Early	Never	Early	Never	Early	Early	Early	D_0, AUPP, SCI_{12}, ARE_8	False Positive
S8-9	Early	Never	Early	Never	Late	Early	Early	D_0, SCI_{12}	Early
S8-10	Early	Never	Early	Never	Early	Never	Early	D_0	False Positive
S8-11	Never	Never	Never	Never	Never	Never	Never	None	NCO NCP
S8-12	Early	Early	Early	Early	Early	Early	Early	D_0, SCI_8, SCI_{12}, ARE_8	Early
Summary: 6 Early, 3 NCO NCP, 1 False Negative, 2 False Positive									

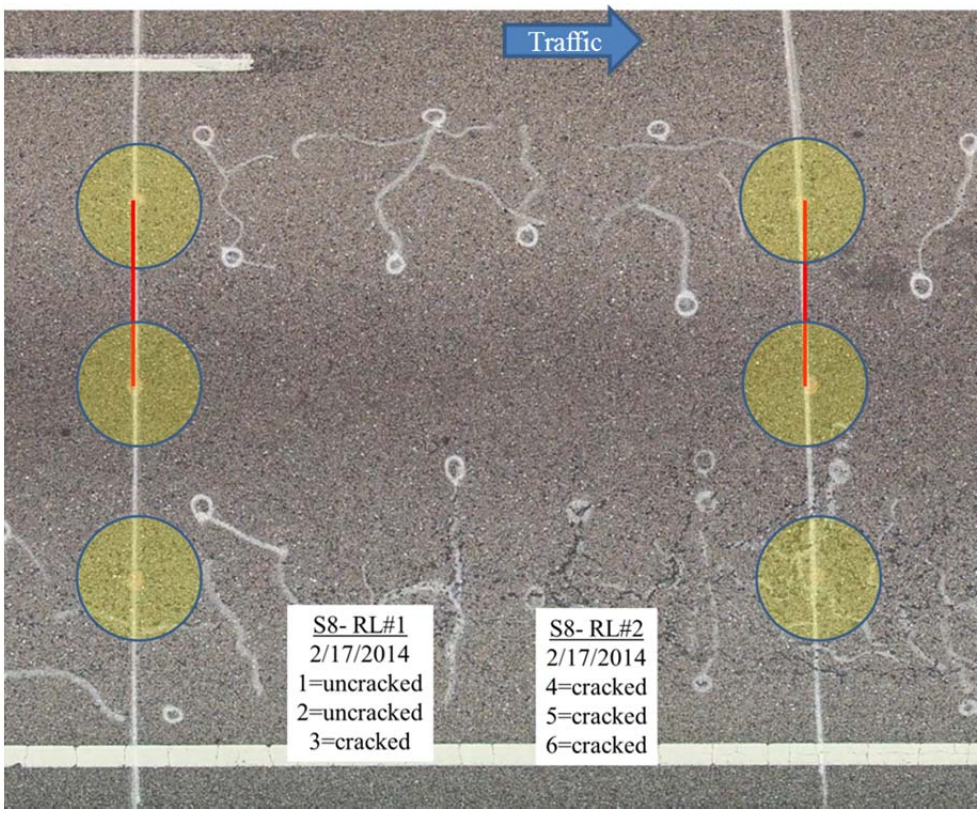

Figure 6.19 –Cracking on 2009-S8 RL#1 and #2 on 2/17/2014.

6.3.3 2003 Structural Experiment PG67-22 Thin-N2

Section N2 of the 2003 Structural Experiment had five inches of AC with an unmodified PG 67-22 binder placed over six inches of granular base. Cracking was first observed in June 2004 after approximately 2.6 million ESALs and the distressed progressed rapidly thereafter. By August 2004, there was interconnected alligator cracking in both wheel paths. It is not surprising that this section reached the failure threshold faster than the other 2003 sections because it had the thinnest AC structure and the lowest binder grade. This section provided an assessment of the applicability of the methodology on a heavily distressed pavement. The main purpose of this work was to capture structural changes in the pavement prior to cracking being visible on the surface and this section was used to assess that phenomenon.

6.3.3.1 Modeling

As with the other sections, BISAR was used to simulate the changes in DBPs due to BUFC. The results of the BISAR simulation are presented in Table 6.46.

Table 6.46 – Change in DBPs from BISAR Simulation of 2003-N2 (E_{AC}= 50%)

Description	% Change D_0	% Change AREA	% Change AUPP	% Change F_1	% Change SCI_{12}
No Cracking	0%	0%	0%	0%	0%
1.0" BUFC	7%	3%	13%	8%	14%
2.0" BUFC	12%	5%	21%	13%	24%
3.0" BUFC	14%	7%	26%	17%	33%
4.0" BUFC	16%	8%	31%	20%	40%
Total BUFC	28%	12%	51%	32%	66%

6.3.3.2 Field Data

All of stations in section 2003-N2 were cracked within a four month span. The date cracking was first observed at each station is presented in Table 6.47.

Table 6.47 – Summarized Cracked Dates for 2003-N2

FWD Station	"Cracked" Date
N2-1	8/23/2004
N2-3	6/28/2004
N2-4	8/30/2004
N2-6	6/28/2004
N2-7	10/25/2004
N2-9	8/30/2004

The comparison of theoretical versus field DBPs is presented in Table 6.48. The DBPs did not exceed their theoretical values for BUFC prior to cracking for station N2-1 however,

cracking was observed on August 23, 2004 and the FWD testing was conducted on June 25, 2004, prior to any cracking in the section. If the station was FWD tested closer to the cracking date it may have been able to capture structural changes that lead to cracking because the FWD testing date after cracking, September 20, 2004, had D_0, AUPP, and SCI_{12} exceed their respective thresholds. The same issue was observed at station N2-4 in which the date that cracking was observed, August 30, 2004 was over two months after the FWD testing prior to cracking on June 25, 2004. Again, on the next FWD date on September 20, 2004 D_0 exceeded its threshold. DBPs exceeded their threshold values prior to cracking in stations N2-3, N2-6, and N2-7. The DBPs did not exceed threshold values prior to cracking in N2-9. Considering the heavy distress that occurred in this section, the lack of more frequent FWD and surface distress measurements, and the inability to normalize for load, the comparison of this section performed well. It was a heavily cracked section and the DBPs were able to capture the change in the pavement structure.

Table 6.48 - Summary of DBP Prediction for Each Station in 2003 –N2 (E_{AC}=50%)

FWD Station	D_0	AREA	AUPP	F_1	SCI_{12}	1st Predictor	Classification
N2-1	Late	Never	Late	Never	Late	D_0, AUPP, SCI_{12}	Late
N2-3	Late	Early	Late	Early	Early	AREA, F_1, SCI_{12}	Early
N2-4	Late	Never	Late	Never	Late	D_0, AUPP, SCI_{12}	Late
N2-6	Early	Early	Early	Early	Early	All	Early
N2-7	Early	Never	Late	Never	Late	D_0	Early
N2-9	Late	Never	Never	Never	Late	D_0, SCI_{12}	Late
Summary: 3 Early, 3 Late							

6.3.4 2003 Structural Experiment PG 76-22 Thick-N4

Section N4 of the 2003Test Track had nine inches of AC with modified PG 76-22 binder placed over six inches of granular base. The section did not have any cracking during the research cycle. This section was used to assess how well this methodology applied to intact pavements that did not develop any visible distress. It was an important check to ensure that DBPs were not exceeding their theoretical limits for structural sound pavements.

6.3.4.1 Modeling

The results of the BUFC BISAR simulation at AC moduli of 50% are presented in Table 6.49. The percent changes were the same for this section as 2003-N3. The actual deflection values differed slightly due to AC moduli changes but the percent changes were the same.

Table 6.49 – Change in DBPs from BISAR Simulation of 2003-N4 (E_{AC}= 50%)

Description	% Change D_0	% Change AREA	% Change AUPP	% Change F_1	% Change SCI_{12}
No Cracking	0%	0%	0%	0%	0%
1.0" BUFC	5%	2%	8%	4%	8%
2.0" BUFC	9%	3%	15%	8%	15%
3.0" BUFC	12%	4%	22%	12%	22%
4.0" BUFC	15%	5%	28%	16%	30%
5.0" BUFC	17%	7%	33%	20%	38%
6.0" BUFC	20%	8%	39%	25%	47%
7.0" BUFC	22%	9%	45%	28%	56%
8.0" BUFC	26%	10%	52%	32%	64%
Total BUFC	32%	12%	64%	38%	78%

6.3.4.2 Field Data

The summary of the cracking at FWD stations is presented in Table 6.50. The comparison of theoretical change in DBPs to the change measured in the field is presented in

Table 6.51. It can be seen from the two tables that no stations were cracked and no DBPs exceeded their thresholds at all for this section. Thus, the methodology proved to be successful because the DBPs did not indicate any structural changes in the pavement section that was known to be intact and well performing.

Table 6.50 – Summarized Cracked Dates for 2003-N4

FWD Station	"Cracked" Date
N4-1	Uncracked
N4-3	Uncracked
N4-4	Uncracked
N4-6	Uncracked
N4-7	Uncracked
N4-9	Uncracked

Table 6.51 - Summary of DBP Prediction for Each Station in 2003 –N4 (E_{AC}=50%)

FWD Station	D_0	AREA	AUPP	F_1	SCI_{12}	1st Predictor	Classification
N4-1	Never	Never	Never	Never	Never	None	NCO NCP
N4-3	Never	Never	Never	Never	Never	None	NCO NCP
N4-4	Never	Never	Never	Never	Never	None	NCO NCP
N4-6	Never	Never	Never	Never	Never	None	NCO NCP
N4-7	Never	Never	Never	Never	Never	None	NCO NCP
N4-9	Never	Never	Never	Never	Never	None	NCO NCP
Summary: 6 NCO NCP							

6.4 Summary and Conclusions from the Bottom-up Fatigue Cracking Group

Similar to the evaluation of the DBPs presented for the Delamination Group, plots were developed that compared the days until cracking at each station with the days until the measured change for each DBP exceeded its theoretical change for BUFC. Figure 6.20 shows all DBPs from all station in the Bottom-up Fatigue Cracking Group.

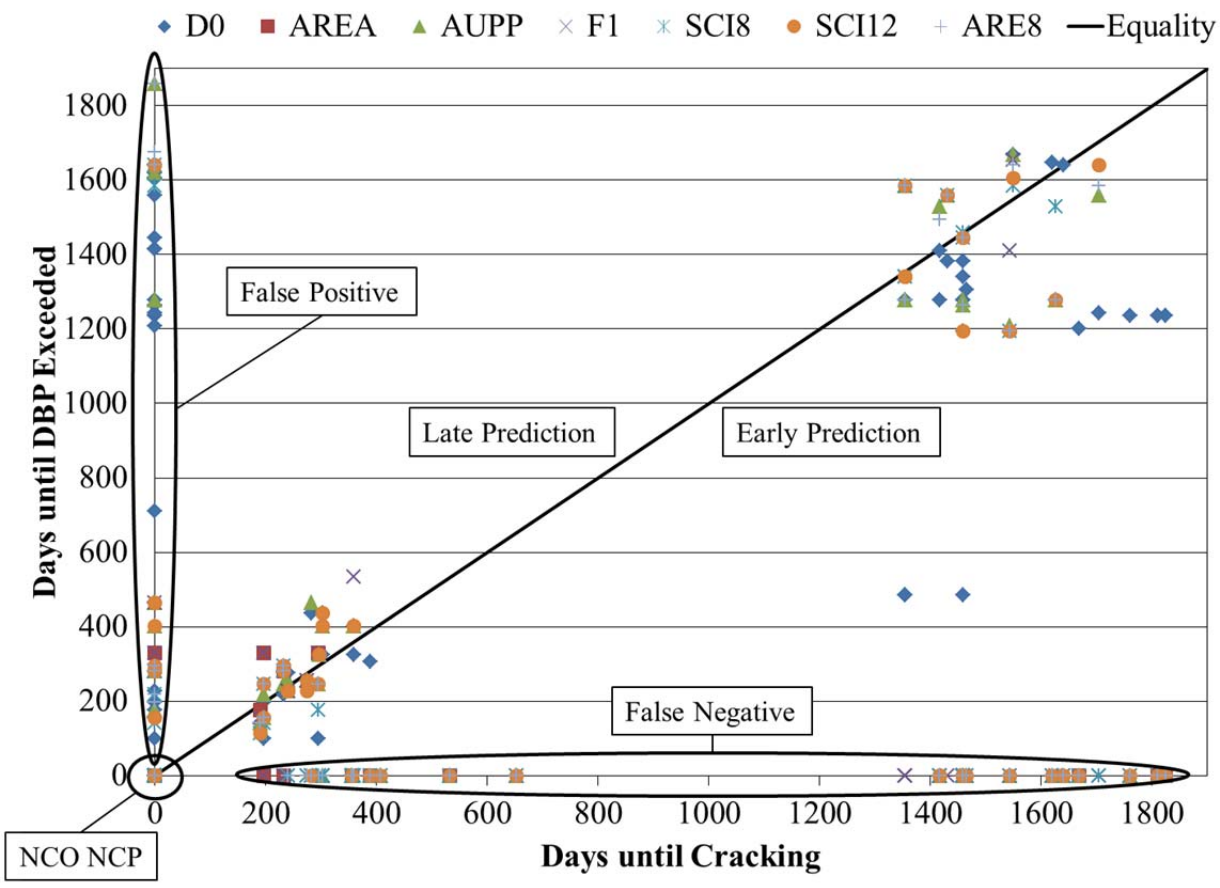

Figure 6.20 – Bottom- up Fatigue Group summary for all DBPs.

As done with the Delamination Group, Figure 6.20 was divided into individual plots to assess the effectiveness of each DBP. Figure 6.21 shows the results for each DBP and Figure 6.22 shows the total number of each classification for each DBP. The D_0 parameter had the fewest amount of False Negatives and the most Early Predictions but it also had the most False Positives. It is not known whether these False Positives were indications of future cracking or over sensitivity of D_0. AREA (Figure 6.21 (b)) and F_1 (Figure 6.21 (d)) were the least sensitive DBP to BUFC. They were early predictors of cracking at only four stations and had a large number of False Negatives, which is likely due to the lower sensitivity of sensors D_{24} and D_{36} that was apparent in the theoretical modeling AREA is the only DBP that utilized the D_{36} sensor. As the distance from the load plate in increased the sensors measure responses of the underlying layers, as shown previously in Figure 2.7. AUPP, SCI_8, SCI_{12}, and ARE_8 all performed very similarly. Similar to the delamination sections, there was no distinguishable benefit gained from the D_8 or D_{18} sensors. It was anticipated that because the D_8 was closer to the load plate it would be more sensitive to the changes in the AC. However, it did not provide any additional benefit to this methodology. SCI_8, and ARE_8 did not provide any unique information that was not captured by one of the other DBPs.

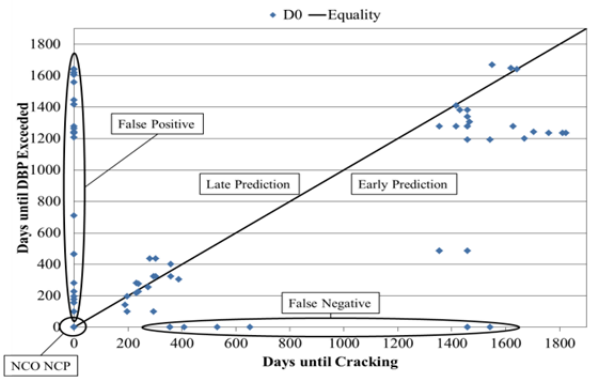

(a) D_0

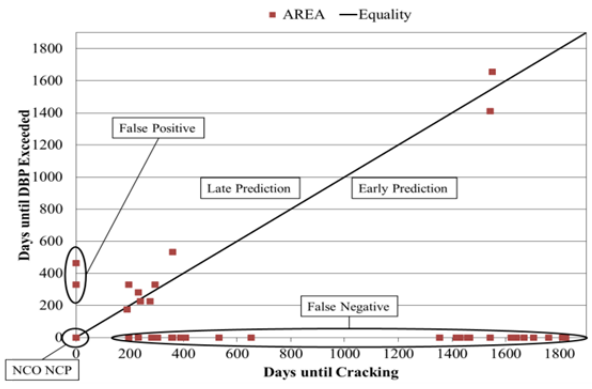

(b) AREA

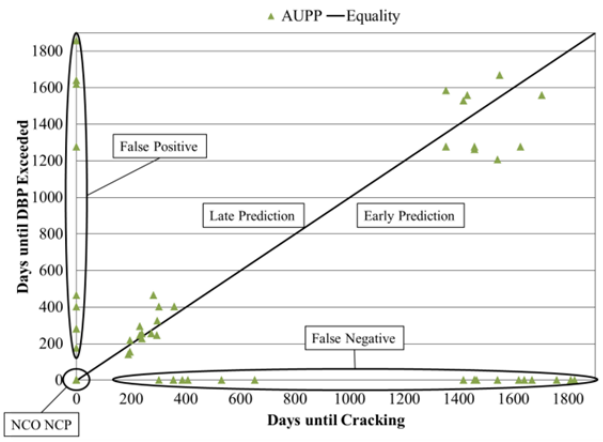

(c) AUPP

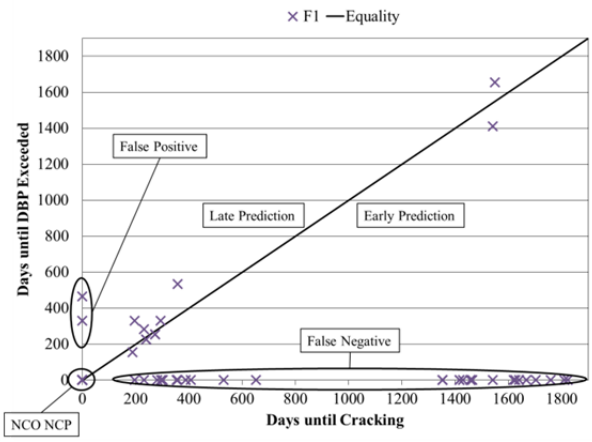

(d) F_1

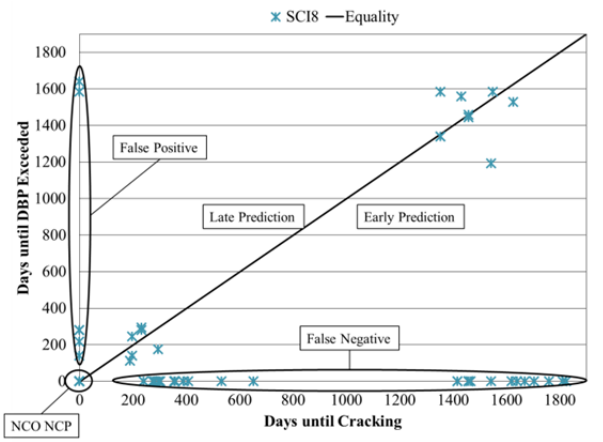

(e) SCI_8

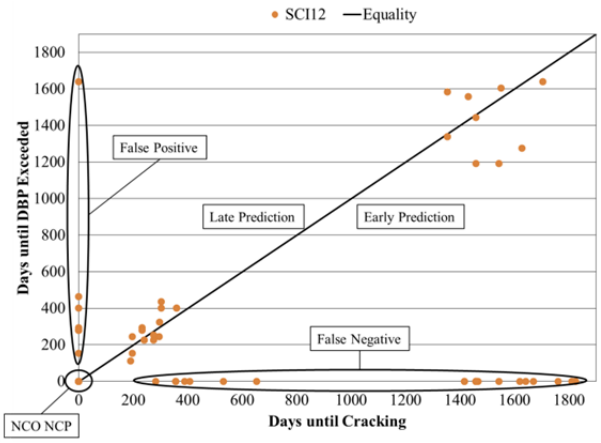

(f) SCI_{12}

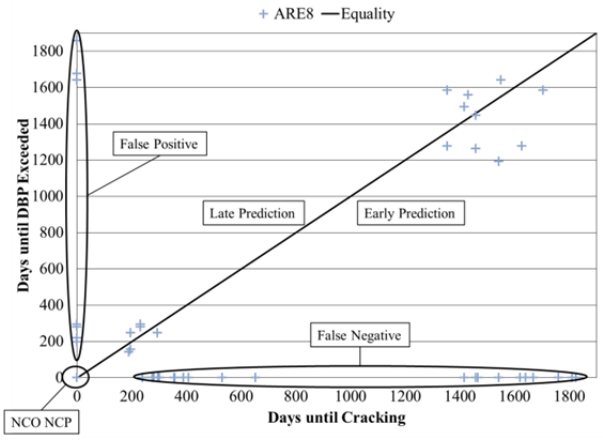

(g) ARE_8

Figure 6.21 – Delamination Group Summary for Individual DBPs.

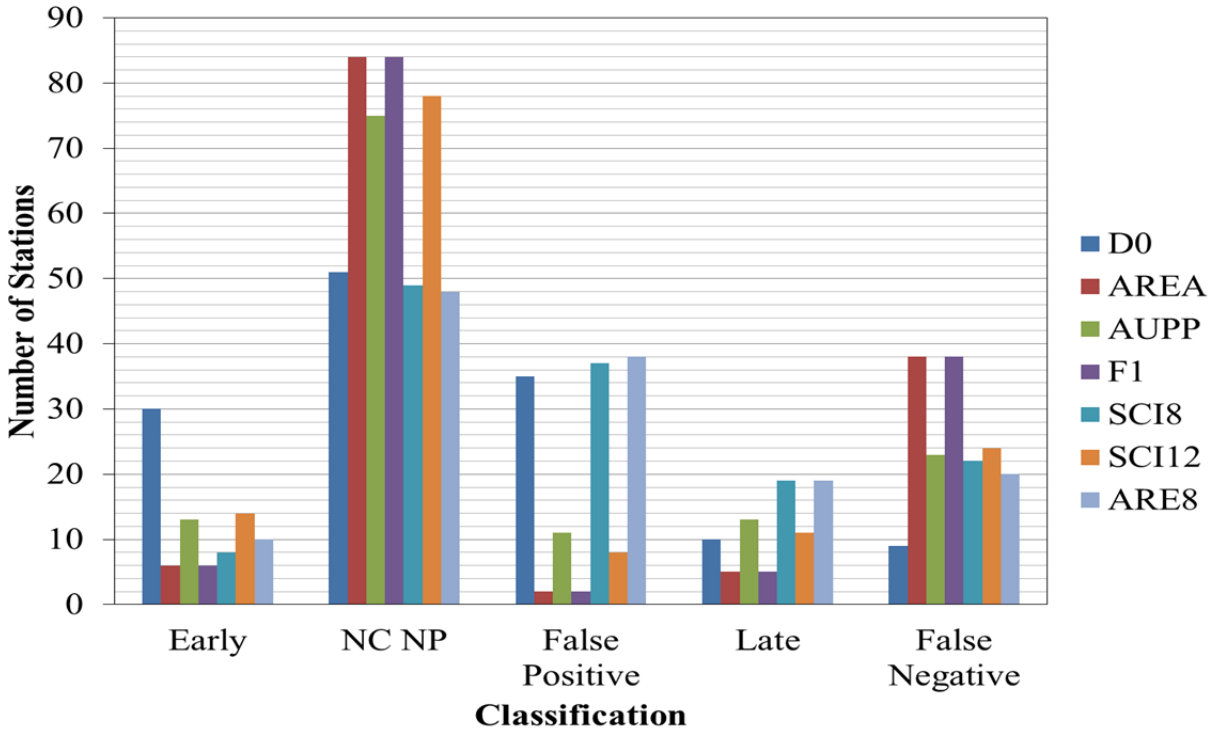

Figure 6.22 – Summary of individual DBP classification for BUFC sections.

The overall success at the DBP comparison on each section in the Fatigue Crack Group is shown in Table 6.52. It can be seen that the comparison of the change in field DBPs to the theoretical DBPs simulated with a 50% AC moduli reduction for cracked layers was successful for 14 out of the 15 sections analyzed. Thus, this type of comparison would be a useful tool to assist in maintenance decisions.

Table 6.52 – Summary of DBP Comparison Performance at each Station.

Section	Accurate
2012-N5	Yes
2012-S5'	No
2009-N10	Yes
2009-N11	Yes
2009-S9	Yes
2009-S10	Yes
2009-S11	Yes
2003-N1	Yes
2003-N3	Yes
2003-N5	Yes
2003-N6	Yes
2003-N7	Yes
2009-S8	Yes
2003-N2	Yes
2003-N4	Yes

The results for each station in the Bottom-up Fatigue Cracking Group are summarized in Figure 6.22. Despite not working perfectly, the BUFC methodology was shown to be successful and would be a useful to for practitioners to help determine sections when cracking was most likely to occur based on FWD data over time. The methodology was proven by the applicability to sections that were known to have performed very well and did not develop any cracking distress. There were no DBPs that exceed their theoretical change on 2003-N3, 2003-N4, and the 2009 traffic portion of the 2009 GE. Thus, the methodology would be very accurate when predicting when no cracking will develop. The results were not as straightforward for the cracked sections. The variability of the DBPs was much higher for sections that developed cracking at some point, which in itself is an indication that distress may be developing. Also, this may be attributed to the normalization for temperature which included deflections from the entire research cycle, regardless of condition. Overall, methodology was accurate for 61% or 83 out of

135 FWD stations (Early Prediction and NCO NCP). The methodology did not work (False Negatives) on 9 stations (7%). The methodology was inconclusive on 34 stations (False Positives). Again it should be noted that the false positives are likely due to changes in the AC that have not manifested to the surface because sections that did not have any observed distress did not have False Positives.

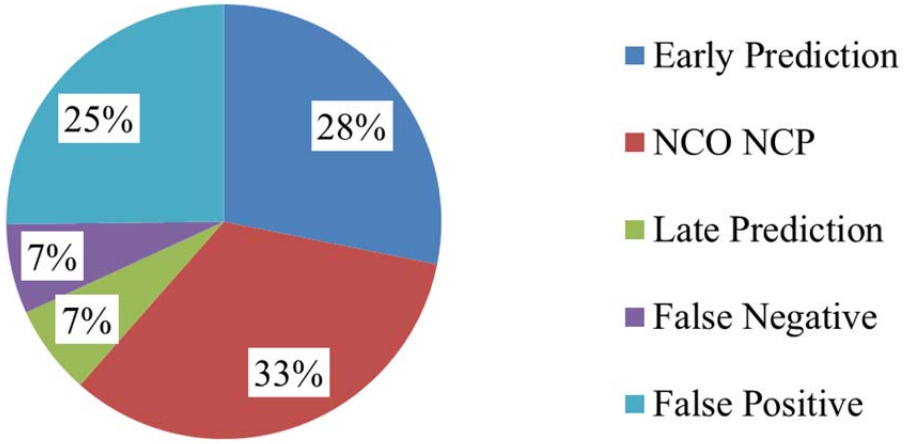

Figure 6.23 –Summary of Bottom-up Fatigue Cracking Group performance.

CHAPTER 7. CONCLUSION

This chapter summarizes the work completed to meet the objectives of identifying structural distress prior to cracking appearing on the surface and determining the mode of cracking after cracking was observed. The overall effectiveness of using the change in deflection basin parameters (DBPs) is discussed and the ability of using DBPs to identify each mode of cracking is examined. Finally, conclusions and recommendations are presented.

7.1 Summary of Theoretical to Field DBP Comparison

The first objective was accomplished by the successful comparison of DBP changes from theoretical modeling and field measured FWD testing. The comparison was successful in distinguishing between distressed and undistressed pavement sections. The comparisons were successful for all three Delamination Group sections and 14 out of 15 bottom- up fatigue cracking (BUFC) Group sections. Comparisons were conducted on the top-down cracking (TDC) Group but looked promising from limited results in the BUFC Group. The performance on a station-by-station basis is summarized in Table 7.1. There were a total of 165 stations from the Delamination and BUFC groups. Only 6% of all stations analyzed had False Negatives, which was the worst result in this work. The late predictions comprised 8% of the 165 stations and could be due to the severe discontinuity that was used to establish the radius of which cracking was considered. A tighter crack is expected to have less of an impact on the deflection basin than the saw-cut. False positives occurred at 22% of the stations. It could not be confirmed if the False Positives were indicators of distress that had not propagated to the surface or inaccurate results. However, based on the progression of DBPs over time at other stations and the sections that did not have distress or changes in DBPs that exceed their thresholds, it is believed that most False Positives were indictors of a structural distress that had not manifested to the surface yet.

The Early Predictions and NCO NCPs comprised 64% of the sections analyzed and were clear indicators of the success of the approach.

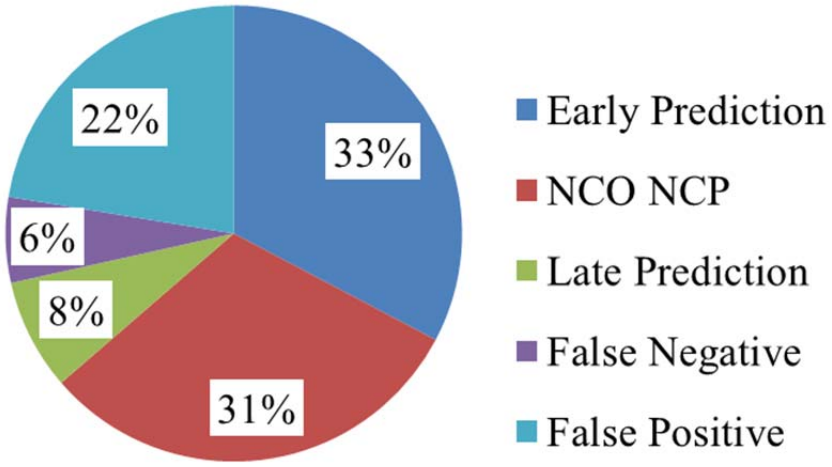

Figure 7.1 – Summary of performance at each station in Delamination and BUFC Group.

7.2 Comparison of Cracking Mechanisms

The other main objective of this work was to use DBPs to identify the type of cracking that was developing in a pavement structure. Table 7.1 summarizes the theoretical change in DBPs, from BISAR simulations, that is anticipated for cracking to be visible on the surface as a result of TDC, BUFC, and delamination mechanisms. These deflection basins, shown in Figure 7.2, and the resulting change in DBPs (Table 7.1) were generated using a six inch AC structure over six inches of granular base over Test Track subgrade soil. This thickness was chosen for the summary because it is a typical thickness of Test Track sections designed to show distress during

the two years of trafficking. As discussed previously, greater changes in DBPs were observed when the AC layers were thicker.

Table 7.1 – Change in DBPs by Distress Type

Description	% Change D_0	% Change AREA	% Change AUPP	% Change F_1	% Change SCI_8	% Change SCI_{12}	% Change ARE_8
No Slip/ No Cracking	0%	0%	0%	0%	0%	0%	0%
1" TDC	5%	2%	11%	7%	12%	12%	12%
Total BUFC	22%	8%	49%	32%	69%	63%	57%
Int. 1/2 Full Slip	12%	5%	29%	20%	36%	35%	32%
Int. 2/3 Full Slip	37%	13%	87%	54%	107%	107%	98%

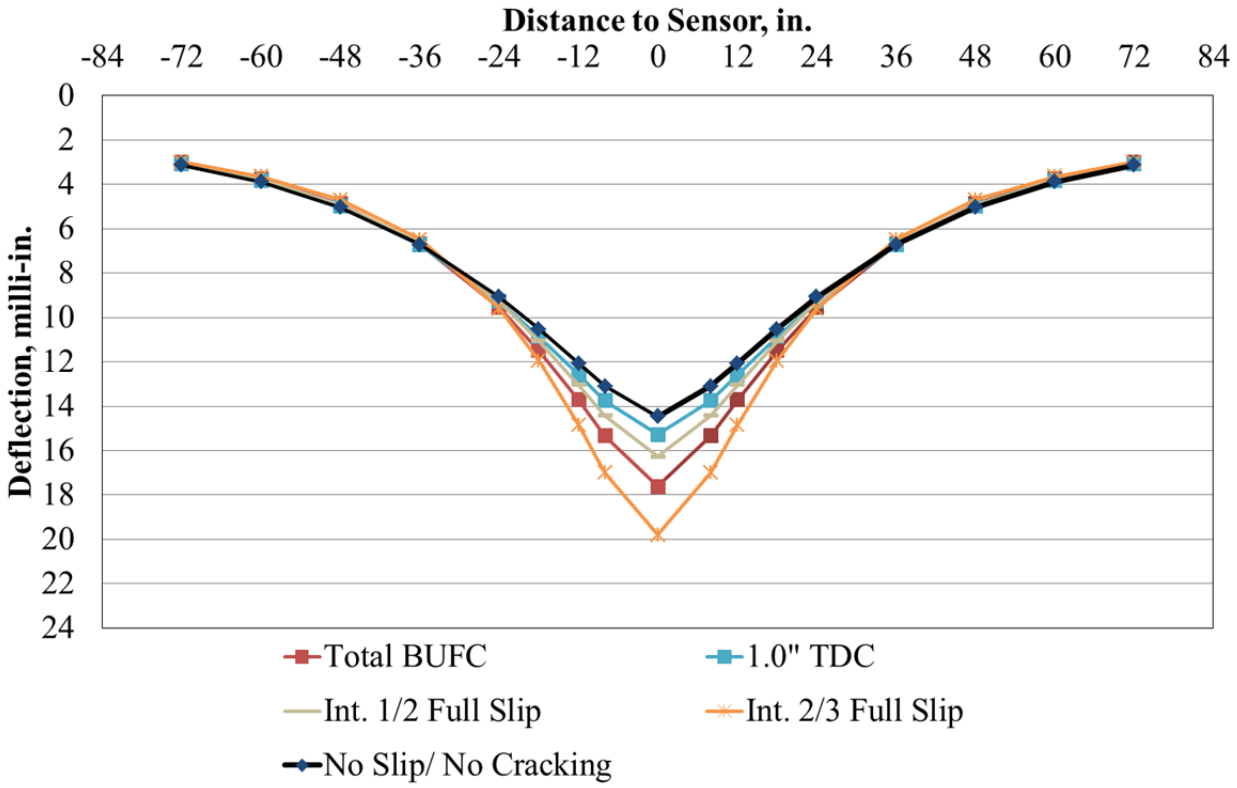

Figure 7.2 – Deflection basins for various distress types.

In both the table and figure, there is only a slight difference between the TDC and the No Slip/ No Cracking simulations as a result of only the top inch of the AC being changed by cracking in the TDC simulation. There are larger differences between the No Slip/ No Cracking simulation and the BUFC and delamination simulations. Thus, evaluation of the change in DBPs after cracking has appeared can distinguish between the cracking mechanisms. This approach could not be developed or validated due to the issues observed in the two sections that were designed to investigate TDC (discussed in Chapter 7 Top-Down Cracking), but it was effective on a limited basis for several sections that had documented TDC. More research is recommended to refine and validate the use of DBPs on TDC sections. The 2015 research cycle at the NCAT Test Track may prove to be particularly useful for the application of this approach. Other accelerated pavement testing (APT) facilities that have a large amount of FWD, material property, and surface performance data, such as MnROAD, are good options to refine the TDC approach.

It was more difficult to distinguish between the BUFC and delamination conditions, especially when looking at the field data. Even though each simulation can be seen in Figure 7.1, the overall magnitude of change should be noted. The changes in DBPs from both delamination conditions and BUFC, were successfully used to capture changes in the AC before cracking appeared on the surface. However, the ability of to discern between delamination and BUFC was not evident.

7.3 Conclusions and Recommendations

This work compared changes in DBPs from theoretical modeling and FWD testing at the NCAT Test Track. Three delamination sections and 15 BUFC sections were scrutinized resulting

in 165 specific locations used for analysis. Based on the work presented in this dissertation the following conclusions were drawn:

- The reduced FWD testing procedure used in the FWD sensitivity to discontinuity investigation was successful in providing repeatable deflections basins that had high R^2 values for the linear trendlines used to normalize for load. Thus, two drops at three load levels was a sufficient FWD testing procedure for this work. This reduced procedure saves time spent at each location and could allow for more locations to be tested on a given day.
- The orientation of the FWD trailer did not have a significant impact on the deflection basins measured, except within 1 foot of the saw-cut discontinuity. There was still a noticeable difference, regardless of orientation, in the deflection basins measured with the load plate 1 foot away from the discontinuity than with the basins measured at greater than 1 foot away. Thus for the pavement thickness considered in this research, a crack within 1 foot of the FWD testing station was expected to affect the resulting deflection basin.
- Comparing the change in DBPs from field testing to theoretical modeling was successfully able to identify structural changes that lead to cracking in all the delamination sections. The approach was valid with delamination at both interfaces in AC pavements with three AC layers. It would be interesting to apply to thicker pavements with more than three lifts but it is expected that DBPs would still be able to identify the structural change prior to cracking occurring as modeling has shown that greater AC thickness leads to greater changes in the DBPs.

- The comparison of field and theoretical DBP changes was successful for all BUFC sections except one. It is recommended that the 50% AC moduli BUFC and delamination between AC layers simulations be implemented immediately at APT facilities that have similar datasets to identify sections that are likely to have structural cracking in the near future. Long-term, this approach could be used on a network level to predict structural cracking once continuous deflection technologies are further implemented.
- The approach to assess TDC could not be verified with field data but appeared promising from theoretical simulations and a limited number of stations in the BUFC group. Further analysis on a greater number of TDC sections is recommended.
- The theoretical DBP change was more sensitive to the input AC thickness than to AC moduli or aggregate base properties. This was especially evident in the simulations from 2003 sections in which design thicknesses were used. Thus, for future application of this work it is more important to have accurate layer thicknesses than modulus values, which is easier to obtain than to conduct modulus testing.
- It was found that the D_8 and D_{18} sensors did not provide any unique information that was not captured by the other sensors. The DBPs utilizing the D_8 sensor, SCI_8 and $ARE_{8,}$ had similar results as SCI_{12} and AUPP but did not provided any additional benefit in identifying distress and are therefore not essential in future applications of this work.

CHAPTER 8. REFERENCES

AASHTO (1993). *AASHTO Guide for Design of Pavement Structures*. American Association of State and Highway Transportation Officials.

AASHTO T 256-01. *Standard Test Method for Pavement Deflection Measurements*. American Association of State and Highway Transportation Officials.

AASHTO TP 79-13.*Standard Test Method for Dynamic Modulus and Flow Number of Hot Mix Asphalt.* American Association of State and Highway Transportation Officials.

Al Hakim, B., Cheung, L. W., & Armitage, R. J. (1999). *Use of FWD Data for Prediction of Bonding between Pavement Layers.* International Journal of Pavement Engineering, *1*(1), pp. 49-59.

ASTM D4694 -09. *Standard Test Method for Deflections with a Falling Weight-Type Impulse Load Device*. ASTM International. (Reapproved 2015).

ASTM D4695 -09. *Standard Guide for General Pavement Deflection Measurements.* ASTM International. (Reapproved 2015).

Brown, E.R., Kandal, P.S., Roberts, F.L., Kim, Y.R., Lee, D.Y., Kennedy, T.W. (2009). *Hot Mix Asphalt Materials, Mixture Design, and Construction.* Third Edition, NAPA Research and Education Foundation.

Chen, D.H. (2009). *Slippage Failure of a New Hot-Mix Asphalt Overlay*. Journal of Performance of Constructed Facilities, 24(3), pp. 258-264.

Gomba, S., Liddle, J., Mehta, Y.A., (2005) *Evaluation of Interlayer Bonding in Hot Mix Asphalt Pavements.* International Journal of Pavements, Volume 4, 13-24.

Gopalakrishnan, K., Thompson, M.R. (2005). *Use of Deflection Basin Parameters to Characterize Structural Degradation of Airport Flexible Pavements*. ASCE Geo-Institute and Geosynthetics 2005 Congress Conference.

Highway Research Board. (1962). *The AASHO Road Test", Report 5, Pavement Research Special Report 61E.* National Academy of Sciences – National Research Council.

Heitzman, M., Maser, K., Tran, N.H., Brown, R., Bell, H., Holland, S., Ceylan, H., Belli, K., Hiltunen, D. (2013). *Nondestructive Testing to Identify Delamination Between HMA Layers.* SHRP2 Renewal Research. REPORT S2-R06D-RR-1.

Horak, E. (1987). *The Use of Surface Deflection Basin Measurements in the Mechanistic Analysis of Flexible Pavements*. Proceedings, Vol. 1, Sixth International Conference Structural Design of Asphalt Pavements, University of Michigan, Ann Arbor, Michigan, USA.

Hoffman, M.S., Thompson, M.R. (1982). *Backcalculating Nonlinear Resilient Moduli from Deflection Data*. Transportation Research Record 852, TRB, National Research Council, pp. 42-51.

Hossain, A.S. M.M., Zaniewski, J.P. (1991). *Characterization of Falling Weight Deflectometer Deflection Basin*. Transportation Research Record 1293, TRB, National Research Council, pp. 1–11.

Huang, Y. H. (2004). *Pavement Design and Analysis*. Pearson/Prentice Hall.

Hu, X., Walubita, L.F. (2010). *Effects of Layer Interfacial Bonding Conditions on the Mechanistic Responses in Asphalt Pavements*. Journal of Transportation Engineering, 137(1), pp. 28-36.

Jung, F.W., Stolle, D.F.E (1992). *Nondestructive Testing with Falling Weight Deflectometer on Whole and Broken Asphalt Concrete Pavements*. Transportation Research Record 1377, TRB, National Research Council, pp. 183-192.

Khweir, K. & Fordyce, D. (2003). *Influence of Layer Bonding on the Prediction of Pavement Life* Proceedings of the Institution of Civil Engineers - Transport 2003 156:2, pp. 73-83.

Kim, Y.R., Lee, Y.C., Park, S., Ranjithan, S.R. (1999) *Interpretation of FWD Data When Pavement Layers Are Not Intact*. No. FHWA-NC-99-002. North Carolina Department of Transportation.

Kim, Y.R., Ranjithan, S.R., Troxler, J.D., Xu, B. (2000). *Assessing Pavement Layer Condition using Deflection Data*. National Cooperative Highway Research Program Project 10-48. Transportation Research Board.

Kruntcheva, M.R., Collop, A.C., Thom, N.H. (2005). *Effect of Bond Condition on Flexible Pavement Performance*. Journal of Transportation Engineering, 131(11), pp. 880-888.

Moore, N.D. (2016). *Evaluation of Laboratory Cracking Tests Related to Top-Down Cracking in Asphalt Pavements.* (Master's Thesis), Auburn University.

Mohammad, L.N., Elseifi, M.A., Bae, A., Patel, N., Button, J., Scherocman, J.A. (2012) *Optimization of Tack Coat for HMA Placement*. National Cooperative Highway Research Program Report 712. Transportation Research Board.

Park, H., & Kim, Y.R. (2003). *Prediction of Remaining Life of Asphalt Pavement with Falling-Weight Deflectometer Multiload-Level Deflections*. Transportation Research Record 1860,TRB, National Research Council, pp.48-56.

Pavement Interactive. Accessed on January 20, 2017.
http://www.pavementinteractive.org/article/Deflection/

Rijkswaterstaat. Accessed on Febraury 28, 2017.
https://beeldbank.rws.nl/Photos/3163/474518.jpg

Romanoschi, S.A., Metcalf, J.B. (2003). *Errors in Pavement Layer Moduli Backcalculation due to Improper Modeling of the Layer Interface Condition*. Proceedings of Transportation Research Board 2003 Annual Meeting CD-ROM.

Shell International Oil Products. (1998). *BISAR 3.0 User Manual*

Schmalzer, P.N. (2006). *LTPP Manual for Falling Weight Deflectometer Measurements, Version 4.1*. Report No. FHWA-HRT-06-132, Federal Highway Administration.

Taylor, A.J. (2008). *Mechanistic Characterization of Resilient Moduli for Unbound Pavement Layer Materials* (Master's Thesis), Auburn University.

Thompson, M.R., Garg, N. (1997). *Mechanistic-Empirical Evaluation of the Mn/ROAD Low Volume Road Test Sections*. Project IHR-535, University of Illinois at Urbana-Champaign.

Timm, D.H., West, R., Priest, A., Powell, B., Selvaraj, I., Zhang, J., Brown, R. (2005). *Phase II NCAT Test Track Results*. NCAT Report 06-05,National Center for Asphalt Technology.

Timm, D., Sholar, G., Kim, J., Willis, J. (2009). *Forensic Investigation and Validation of Energy Ratio Concept*. Transportation Research Record 2127, TRB, National Research Council, pp. 43-51.

Timm, D. H. (2009). *Design, Construction and Instrumentation of the 2006 Test Track Structural Study.* NCAT Report 09-01, National Center for Asphalt Technology.

Vrtis, M.C., Timm, D.H., Willis, J.R. (2015). *Structural and Performance Characterization of Resource Responsible Sections at the NCAT Test Track.* Proceedings of Transportation Research Board 2015 Annual Meeting.

Vrtis, M.C. & Timm, D.H. (2015). *Case Study on Premature Pavement Failure and Successful Reconstruction of a High RAP Section at the NCAT Test Track.* Proceedings of ASCE Transportation and Development Institute 2015 Highway Pavements Conference.

Wang, L.B., Myers, L.A., Mohammad, L.N., Fu, Y.R. (2003). *Micromechanics Study on Top-Down Cracking*. Transportation Research Record 1853, TRB, National Research Council, pp. 121-133.

Willis, J.R., & Timm, D.H. (2007). *Forensic Investigation of Debonding in Rich Bottom Pavement*. Transportation Research Record 2040, TRB, National Research Council, pp. 107-114.

Willis, J.R., & Timm, D.H. (2006). *Forensic Investigation of a Rich-Bottom Pavement*., NCAT Report 06-04, National Center for Asphalt Technology

(a) Xu, B., Ranjithan, S.R., Kim, Y.R. (2002). *New Relationships Between Falling Weight Deflectometer Deflections and Asphalt Pavement Layer Indicators*. Transportation Research Record 1806, TRB, National Research Council, pp. 48-56.

(b) Xu, B., Ranjithan, S.R., Kim, Y.R. (2002). *New Condition Assessment Procedure for Asphalt Pavement Layers Using Falling Weight Deflectometer Deflections*. Transportation Research Record 1806, TRB, National Research Council, pp. 57-69.

Xu, B., Ranjithan, S.R., Kim, Y.R. (2003). *Case Studies: using APLCAP for Asphalt Pavement Layer Condition Assessment*. Transportation Research Record 1860, TRB, National Research Council, pp. 66-75.

Appendix

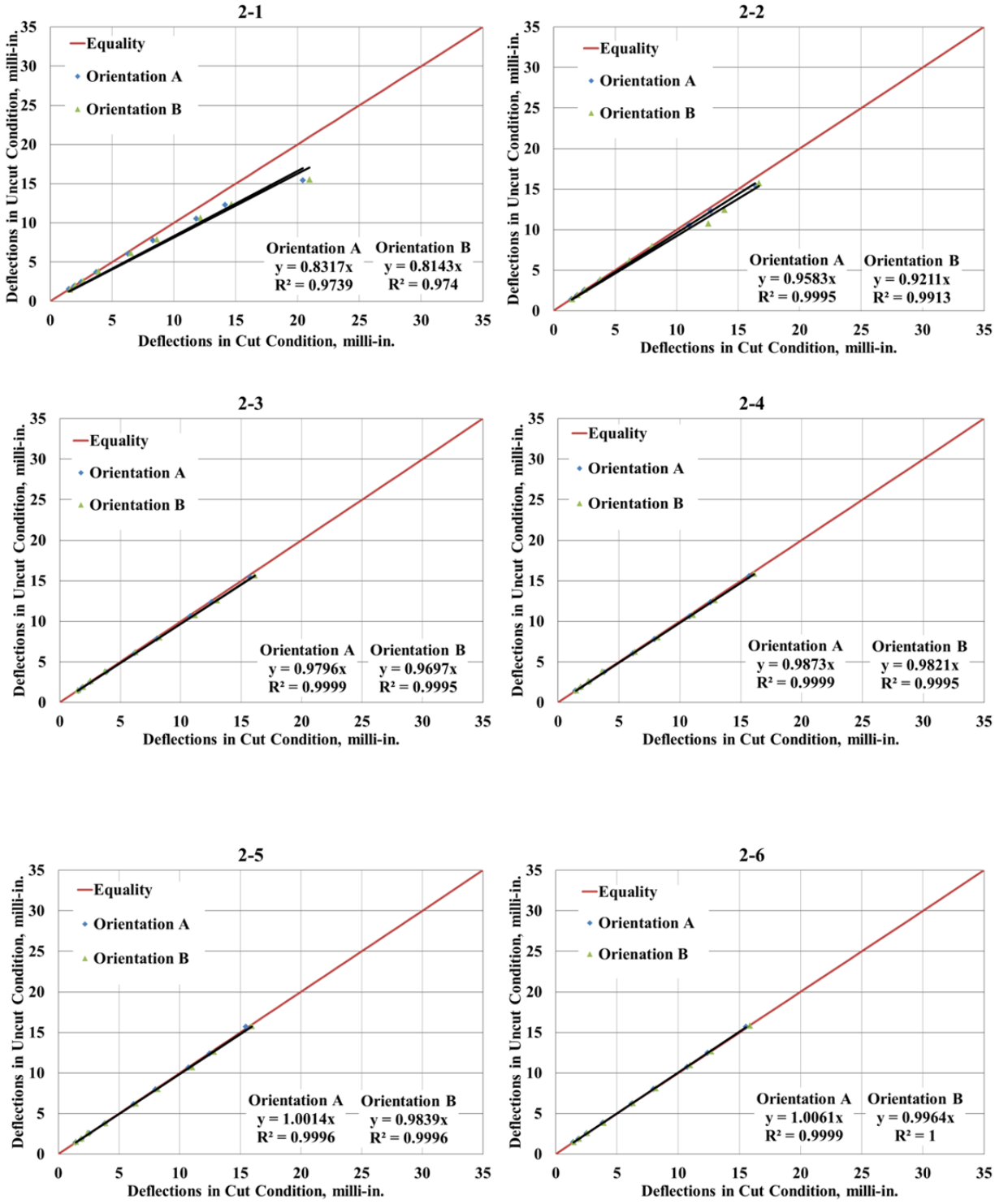

Comparison Uncut/ Cut Pavement Deflections by Location in Site 2

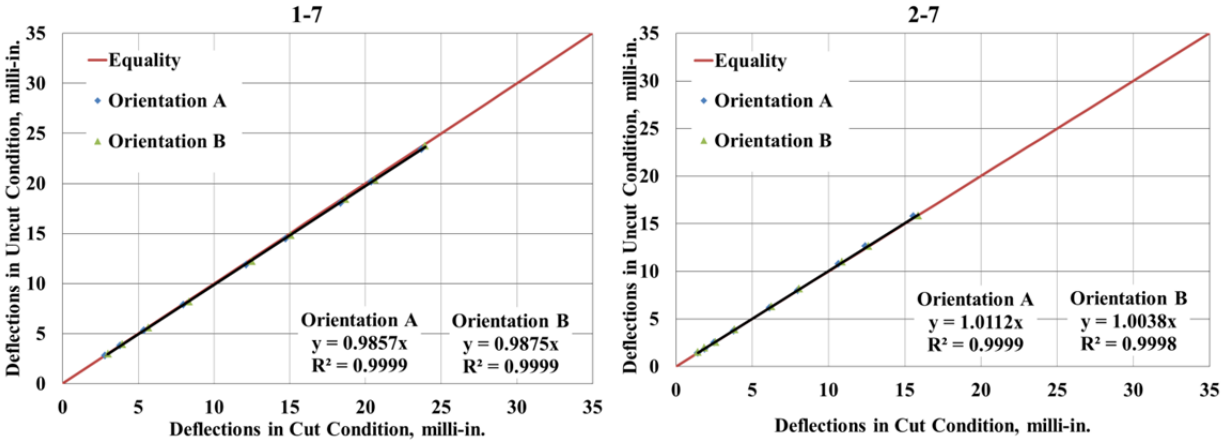

Comparison Uncut/ Cut Pavement Deflections for Location 7